Handbook T-XVI
CIERMMI Women in Science
Engineering and Technology

MARROQUÍN-DE JESÚS, Ángel
OLIVARES-RAMÍREZ, Juan Manuel
VENTURA-OVALLE, Dulce María de Guadalupe
CRUZ-CARPIO, Luis Eduardo   *Coordinators*

ECORFAN®

ECORFAN®

©ECORFAN-México, S.C.

Handbooks

Definition of Handbooks

Scientific Objectives

To support the International Scientific Community in its written production of Science, Technology and Innovation in the CONACYT and PRODEP research areas.

ECORFAN-Mexico, S.C. is a Scientific and Technological Company in contribution to the formation of Human Resources focused on the continuity in the critical analysis of International Research and is attached to the RENIECYT of CONACYT with number 1702902, its commitment is to disseminate research and contributions of the International Scientific Community, academic institutions, agencies and entities of the public and private sectors and contribute to the linkage of researchers who perform scientific activities, technological developments and training of specialized human resources with governments, businesses and social organizations.

To encourage the interlocution of the International Scientific Community with other study centres in Mexico and abroad and to promote a wide incorporation of academics, specialists and researchers to the serial publication in Science Niches of Autonomous Universities - State Public Universities - Federal IES - Polytechnic Universities - Technological Universities - Federal Technological Institutes - Teacher Training Colleges - Decentralised Technological Institutes - Intercultural Universities - S&T Councils - CONACYT Research Centres.

Scope, Coverage and Audience

Handbooks is a product edited by ECORFAN-Mexico S.C. in its Holding with repository in Mexico, it is a refereed and indexed scientific publication. It admits a wide range of contents that are evaluated by academic peers by the double-blind method, on topics related to the theory and practice of the CONACYT and PRODEP research areas respectively with diverse approaches and perspectives, which contribute to the dissemination of the development of Science, Technology and Innovation that allow arguments related to decision-making and influence the formulation of international policies in the field of Science. The editorial horizon of ECORFAN-Mexico® extends beyond academia and integrates other segments of research and analysis outside that field, as long as they meet the requirements of argumentative and scientific rigour, in addition to addressing issues of general and current interest of the International Scientific Society.

Arbitration Committee

Assignment of Rights

By submitting a Scientific Work to ECORFAN Handbooks, the author undertakes not to submit it simultaneously to other scientific publications for consideration. To do so, the author must complete the Originality Form for his or her Scientific Work.

The authors sign the Authorisation Form for their Scientific Work to be disseminated by the means that ECORFAN-Mexico, S.C. in its Holding Mexico considers pertinent for the dissemination and diffusion of their Scientific Work, ceding their Scientific Work Rights.

Declaration of Authorship

Indicate the name of 1 Author and a maximum of 3 Co-authors in the participation of the Scientific Work and indicate in full the Institutional Affiliation indicating the Unit.

Identify the name of 1 author and a maximum of 3 co-authors with the CVU number -PNPC or SNI-CONACYT- indicating the level of researcher and their Google Scholar profile to verify their citation level and H index.

Identify the Name of 1 Author and 3 Co-authors maximum in the Science and Technology Profiles widely accepted by the International Scientific Community ORC ID - Researcher ID Thomson - arXiv Author ID - PubMed Author ID - Open ID respectively.

Indicate the contact for correspondence to the Author (Mail and Telephone) and indicate the Contributing Researcher as the first Author of the Scientific Work.

Plagiarism Detection

All Scientific Works will be tested by the PLAGSCAN plagiarism software. If a Positive plagiarism level is detected, the Scientific Work will not be sent to arbitration and the receipt of the Scientific Work will be rescinded, notifying the responsible Authors, claiming that academic plagiarism is typified as a crime in the Penal Code.

Refereeing Process

All Scientific Works will be evaluated by academic peers using the Double Blind method. Approved refereeing is a requirement for the Editorial Board to make a final decision which will be final in all cases. MARVID® is a spin-off brand of ECORFAN® specialised in providing expert reviewers all of them with PhD degree and distinction of International Researchers in the respective Councils of Science and Technology and the counterpart of CONACYT for the chapters of America-Europe-Asia-Africa and Oceania. The identification of authorship should only appear on a first page, which can be removed, in order to ensure that the refereeing process is anonymous and covers the following stages: Identification of ECORFAN Handbooks with their author occupancy rate - Identification of Authors and Co-authors - PLAGSCAN Plagiarism Detection - Review of Authorisation and Originality Forms-Assignment to the Editorial Board - Assignment of the pair of Expert Referees - Notification of Opinion - Statement of Observations to the Author - Modified Scientific Work Package for Editing - Publication.

ECORFAN CIERMMI Women in Science

Volume XVI

The Handbook will offer volumes of selected contributions from researchers who contribute to the scientific dissemination activity of the Colegio de Ingenieros en Energías Renovables de Querétaro A.C. in their areas of research in Engineering and Technology Sciences. In addition to having a total evaluation, in the hands of the directors of the Colegio de Ingenieros en Energías Renovables de Querétaro A.C., the quality and timeliness of its chapters, each individual contribution was refereed to international standards (RESEARCH GATE, MENDELEY, GOOGLE SCHOLAR and REDIB), the Handbook thus proposes to the academic community, recent reports on new developments in the most interesting and promising areas of research in the Engineering and Technology Sciences.

MARROQUÍN-DE JESÚS, Ángel. PhD
OLIVARES-RAMÍREZ, Juan Manuel. PhD
VENTURA-OVALLE, Dulce María de Guadalupe. MsC
CRUZ-CARPIO, Luis Eduardo. BsC

Coordinators

CIERMMI Women in Science T-XVI Engineering and Technology *Handbooks*

Prologue

The United Nations has affirmed that climate change is "an existential threat to life on the planet", which is why great leaders have put on the table a call in which we must all take action and share responsibility so that this Common Home, as Pope Francis calls it, can survive: "It is necessary to realize that what is at stake is our own dignity. We are the first to be interested in leaving a habitable planet for the humanity that will succeed us" (cf. Laudato Si, May 24, 2015, 160).

In this excellent Handbook, elaborated by CIERMMI and ECORFAN-MEXICO, we will witness the visualization of ten excellent investigations where we will be able to find proposals for solutions to this problem.

The researches show diverse tones ranging from biogas and biodiesel production proposals as low-cost alternative scenarios to improve environmental performance in a workspace or to generate clean energy in a municipality.

To solve the problem of soil contamination by hydrocarbons, polymeric materials are proposed, as well as a green infrastructure that shows accessible solutions.

On the other hand, in the biomedical field we can find articles that show us the progress in the technology of electro-spinning, as well as the mechanical characterization of the lumbar vertebrae that mark the tendency to provide a solution to a more dignified health and respect for life.

In the educational part, there is a proposal for a learning strategy of formative projects that allow the student to develop a new culture for the creation and use of products that benefit humanity, to mitigate climate change that affects everyone.

It is a desire that these works are the beginning of more opportunities for different researchers to shed light on the points where the institutions that make decisions for the common good, can focus their attention to hear proposals for solutions. But also, may it be a space where projects are born that can give hope by promoting education and quality projects giving solutions to the countries.

I congratulate the researchers and their collaborators, as well as the organizers of the CIERMMI for allowing this space to elevate the dignity of the person and with it, to enthuse future generations in the educational, scientific and technological fields, to give concrete answers that will lead to solutions for the benefit of our Common Home.

Ventura-Ovalle, Dulce Maria de Guadalupe
President Querétaro IEEE Section
Santiago de Querétaro, Qro. on November 8, 2021.

Introduction

The Colegio de Ingenieros en Energías Renovables de Querétaro A.C. (CIER-QUERÉTARO), and its chapters of Renewable Energy, Industrial Maintenance, Mechatronics and Informatics, technical sponsors of the International Interdisciplinary Congress on Renewable Energy, Maintenance, Mechatronics and Informatics, CIERMMI 2021 has as general objective to establish a space for discussion and reflection on issues related to the areas of: renewable energy, industrial maintenance, mechatronics and informatics with the participation of students, teachers, researchers and national and international speakers, promoting the formation and consolidation of research networks. Contributing to provide a space for dissemination and discussion of the presentations of students, graduates, academics and researchers, representatives of various higher education institutions, research centers in our country, as well as educational institutions beyond our borders. Promoting the formation of research networks between different institutions. Offering a space for undergraduate, master's, doctoral and postdoctoral students, in which they can present the progress of the research they carry out in their different educational centers. Providing a space in which study groups and members of academic bodies, linked to the curricular program of renewable energy, industrial maintenance, mechatronics and computer science careers, can present the research work developed within their institution and in collaboration with other national or international educational institutions. Establishing a training space for the attendees, through the development of specific lectures and conferences.

This volume, Women in Science T-XVI-2021 contains 8 refereed chapters dealing with these issues, chosen from among the contributions, we gathered some researchers and graduate students from the 32 states of our country. We thank the reviewers for their feedback that contributed greatly in improving the book chapters for publication in these proceedings by reviewing the manuscripts that were submitted.

As first chapter, *Siordia, Villagrán, Mota and Hernández*, present Application of finite automates for the light point trace in a solar tracking positioning system on two axes, as second chapter, *Soto, Bones and Santos*, will talk about Prototype of technical boxes to increase productivity in native bee meliponaria (Scaptotrígona), as third chapter, *González, Soto and Ahuacatitla*, present Value chain design to open a recycling plant in the municipalities of Huauchinango-Xicotepec, Puebla as the fourth chapter, *Becerra, Hernández, Ruiz and Cedano* propose Ion exchange of heavy metals using a modified zeolite filter integrated into a prototype autonomous water purifier (AWP) on a community scale as the fifth chapter, *De Anda, Betanzos, Sánchez and Aguirre*, perform Approach to the optimization of parameters of a truncated cone solar concentrator using the Excel Solver tool, as sixth chapter *Sánchez, Navarro and García*, developed Methodology for processing meteorological and hydrometric data at basin level, as seventh chapter, *Ceron, Ceron, Lara and Martinez*, will discuss Evaluation of the Heavy Metals Levels in PM10 Particles in air of an urban site of Leon City, in the cold dry climatic season 2018, as last chapter, *Suarez, Zarate, Pere and Vazquez* focus on Comparative Study of Inorganic Pollutant (Chromo) in a Surface Body Water in Frontera, Centla, Tabasco.

MARROQUÍN-DE JESÚS, Ángel
OLIVARES-RAMÍREZ, Juan Manuel
CRUZ-CARPIO, Luis Eduardo
VENTURA-OVALLE, Dulce María de Guadalupe

Coordinators

Content   Page

Chapter 1 Application of finite automates for the light point trace in a solar tracking positioning system on two axes

Capítulo 1 Aplicación de autómatas finitos para el rastreo de punto luminoso en un sistema de posicionamiento para seguimiento solar en dos ejes

SIORDIA-VÁSQUEZ, Xóchitl†*´, VILLAGRÁN-VILLEGAS, Luz Yazmín´, MOTA-VALTIERRA, Georgina del Carmen´´ and HERNÁNDEZ-RODRIGUEZ, Isaura Victoria´´´

´Universidad Veracruzana, Engineering and Chemical Sciences Unit, Venustiano Carranza Extension s / n. Col. Revolución, Poza Rica, de Hidalgo, Veracruz, C.P 93390, Mexico.

´´Universidad Autónoma de Querétaro, Faculty of Engineering, Sebastián Camacho No.5, Zona Centro, Santiago de Querétaro, Querétaro, México, Zip Code 91000.

´´´TecNM/CENIDET, Electronic Engineering Department, Interior Internado Palmira S / N, COL. Palmira, Cuernavaca, Morelos, Mexico.

ID 1st Author: *Xóchitl, Siordia-Vásquez* / **ORC ID:** 0000-0002-8472-8001, **CVU CONACYT ID:**1036998

ID 1st Co-author: Luz Yazmín, Villagrán-Valdez / **ORC ID:** 0000-0003-3860-2923, **CVU CONACYT ID:** 96365

ID 2nd Co-author: Georgina del Carmen, Mota-Valtierra / **ORC ID:** 0000-0001-5856-8633, **CVU CONACYT ID:** 173432

ID 3rd Co-author: Isaura Victoria, Hernández- Rodríguez / **ORC ID:** 0000-0003-0384-034X, **CVU CONACYT ID:** 172646

X. Siordia, L. Villagrán, G. Mota and I. Hernández

* xsiordia@uv.mx

Abstract

This article presents the application of finite automata for light point tracking in a two-axis solar tracking positioning system. The finite automaton sets the rules of reactive control when the ultraviolet radiation sensor is activated, estimating the averages of the signals sent by the photoresistors determines the angle of greats light incidence and codes the rules of motion to which the vertical axis and the horizontal axis must conform. The reactive control algorithm for the automaton is programmed in a C++ language and implemented in an Arduino UNO microcontroller. The validation of the results is carried out by manipulating the prototype of a two-axis solar tracking system that uses a photovoltaic solar panel as a collector. The results also show that the application of finite automata solves the problem of deviations between the positioning of the tracking system and the incidence of the sunbeam on the collector since it includes a self-adjustable function that verifies the correct orientation of the positioning system avoiding manual adjustments and mechanical recalibration alignments, this extends the service life of the system monitoring by reducing wear on the servomotors.

Finite automates, Positioning on two axes, Light point trace, Solar tracking

Resumen

Este artículo presenta la aplicación de autómatas finitos para el seguimiento de puntos de luz en un sistema de posicionamiento de seguimiento solar de dos ejes. El autómata finito establece las reglas de control reactivo cuando se activa el sensor de radiación ultravioleta, estimando los promedios de las señales enviadas por las fotorresistencias determina el ángulo de incidencia de la luz grande y codifica las reglas de movimiento a las que deben ajustarse el eje vertical y el eje horizontal. El algoritmo de control reactivo del autómata está programado en lenguaje C++ e implementado en un microcontrolador Arduino UNO. La validación de los resultados se realiza mediante la manipulación del prototipo de un sistema de seguimiento solar de dos ejes que utiliza un panel solar fotovoltaico como colector. Los resultados también muestran que la aplicación de autómatas finitos resuelve el problema de las desviaciones entre el posicionamiento del sistema de seguimiento y la incidencia del rayo solar sobre el colector ya que incluye una función de auto-ajuste que verifica la correcta orientación del sistema de posicionamiento evitando ajustes manuales y alineaciones mecánicas de recalibración, esto alarga la vida útil del sistema de seguimiento reduciendo el desgaste de los servomotores.

Autómata finito, Posicionamiento en dos ejes, Rastreo de punto luminoso, Seguidor solar

1.1 Introduction

Solar tracking systems play an important role in the performance of capture technologies as the amount of solar radiation that is absorbed by the collector determines the output power (Abadi I., 2019). A two-axis solar tracking positioning system allows automatic movements on the azimuth axis, from north to south, producing an elevation that ensures that sunlight always impacts perpendicularly on the top of the solar collector (Jing-Min, 2013).

In the state of the art, two approaches have been extensively researches to achieve a high degree of precision in the action of solar tracking: open loop tracking based on mathematical models that use a formula or a PID control algorithm to model the behavior of the solar tracking to be performed (Blanco Muriel, 2001) (Chong, 2009), the second approach uses loop control closed to adjust the photovoltaic panel towards a bright spot in the sky, (Arenas Rosales, 2017), as illustrated by Figure 1.

The closed loop tracking approach is carried out by means of a feedback control algorithm that adjust the positioning of the collector towards the light point based on the signal emitted from an array of sensors placed on the photovoltaic panel, (Toranzo, 2015), commonly formed by charge-torque (CCD) devices, or light dependent photo resistances (LDR´s), (Bajpai & Kumar, 2011) , these elements are also used to generated a feedback error signal and excite the controller to adjust the positioning system ensuring that the light beam impacts the surface of the photovoltaic panel, (Arturo, 2010), (Berenguel, y otros, 2004).

In this type of closed loop control, it has been reported in the state of art the use of adaptive algorithms with diffuse logic based on human experience or adaptative chronological tracking algorithms with solar trajectory tracking models, the latter offering reactive capabilities to correct the positioning error. Although there is research evidence on correcting the sensor array, (Celso de la Cruz Casaño, 2012), (Rizk J., 2008), and improving the accuracy of the solar tracking algorithms, in all cases, the control law requires the establishment of the initial conditions.

This paper proposes an empirical research approach that presents the application of infinite automata in the design of reactive control law that manages to fit a two-axis solar tracking system without initial conditions requirements.

The rest of this chapter is organized as follows: Section 2 describes rule modeling and the actions that the automaton must perform. Section 3 presents the experimentation that allows to check the performance of the automaton to perform the tracking of the luminous point. Section 4 presents the conclusion of the work carried out and proposals for improvement.

1.2 Metodology

1.2.1 Light point tracking in a two axis- solar positioning system

In the work done by , (Sidek, y otros, 2017), (Gregor, y otros, 2015) y (Fathabadi, 2016) , the control system was regulated by a microcontroller unit and auxiliary devices that included an encoder and a global positioning system GPS, which helped determine the path of the sun. In (Tharamuttam & Ng, 2017), a controller was developed that combined photo resistances with a magnetometer that served as a digital compass to determine azimuth. The authors demonstrated that the positioning system worked smoothly under all climatic conditions.

In addition, in the articles proposed by, (Sidek, y otros, 2017), (Ho, y otros, 2017) , the authors developed a solar tracker with controls based on GPS global positioning sensors and digital compasses, however, several evidences of random factors that cause the loss of the GPS signal such as atmospheric interference have been reported in the literature electromagnetic interference or climatic changes that modify solar activity, (Zhang, Gong, Dimitrovosky, & Li, 2013). Another problem of the electronic compass is the deviation caused by external magnetic interference especially in metallic reflectors, such deviation cannot be modeled numerically or compensated by calibration, (Lee, Kim, Yun, & Lee, 2005). Such a condition indicates that using an electronic compass and global positioning system, GPS, for the solar tracking system not cost-effective, (Jorge Arturo Pelayo López, 2020), (Nurzhigit Kuttybay1, 2020) when comparing the efficiency of tracking and tracking the light point as show in Table 1.1.

Table 1.1 Comparison on efficacy in solar system based on photo resistance

Parameters	Fixed	Developed LDR Solar Tracker	Developed Schedule Solar Tracker
Installation	Easy	Moderate	Moderate
Mechanism	No mechanism	Simple	Simple
Cost	Cheap	Moderate	Moderate
Design	Simple	Moderate	Moderate
Maintenance	Less	Moderate	Moderate
Efficiency at sunny weather	Reference efficiency	57.4% > Fixed system	57.4% > Fixed system
Efficiency at cloudy/rainy weather	Reference efficiency	>32,2 % Fixed system	> 37.7% Fixed system >4.2% than LDR ST

Source: (Nurzhigit Kuttybay1, 2020)

Based on this evidence, this paper proposes to use a light spot tracking system of a hybrid type consisting of an arrangement of 4 photo resistances, a grove type ultraviolet radiation sensor and a control algorithm based on a finite automaton embedded in an Arduino UNO microcontroller. The cellular array of 4 sensors detecting light or LDR photoresistences, are placed on the polycrystalline photovoltaic panel, oriented towards each of the cardinal points and strategically place in each of the corners of a solar panel, cell identifiers are described in the Table 1.2, the sensor that detects ultraviolet radiation is placed in the central part of the upper shaft as seen in Figure 1.1.

Figure 1.1 Sensor array on the photovoltaic panel

90°
North

LDRSI

LDRSD

West

East

135°

45°

LDRII

LDRID

180°

360°

South

270°
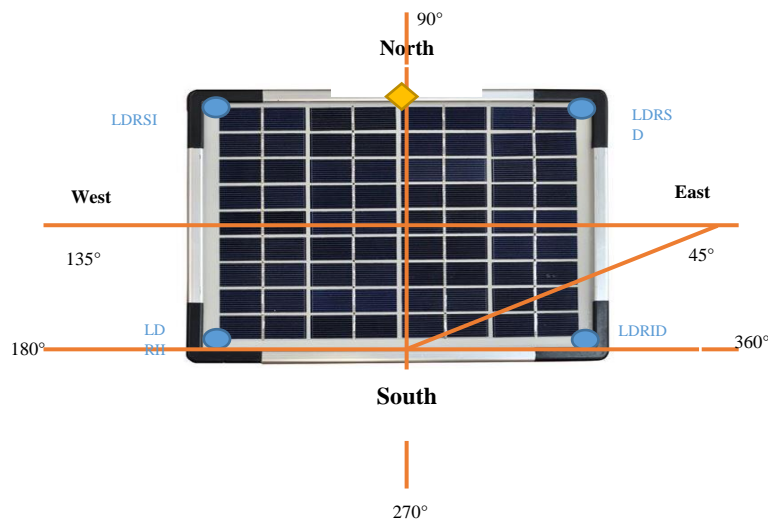
Source: Own elaboration

1.2.2 Description of the automaton modeling and generation of the ruler

The angle of incidence and the information it sent from the ultraviolet radiation sensor establish and adjustment rule so that the two-axis positioning system ensures that the motion of the photovoltaic panel is oriented towards the relative position of the sun, both at azimuth and altitude, a condition that involves controlling two servomotors placed perpendicularly, one on the vertical axis, which adjust the movements to make the tilt of the collector from north to south, and the other placed on the horizontal axis which adjust the movements from east to west, as illustrated in **Figure 1.1**.

Table 1.2 Cell array description

	Position	Identifier
Cell 1	Top left	ldsi
Cell 2	Top right	ldsd
Cell 3	Lower Left	ldii
Cell 4	Lower right	ldid

Source: Own elaboration

The light spot tracking rule is realized by a cellular automaton which is designed as an n-dimensional array of units called cells represented by each of the 4 LDR´s placed on the photovoltaic panel. Each cell has several finite states that interconnect whit each other in a known as described in the **Table 1.2.**

It should be noted that in the absence of a light beam, the cells send a zero-status bit to the data bus of the Arduino UNO microcontroller an in the presence of the light spots they send a status bit 1. The automaton, from the reading of light spots, calculates a series of thresholds and difference values that allow it to make decisions to adjust the movements of the horizontal and vertical servomotors in a neighborhood of 2^4 possible candidate solutions.

El comportamiento del autómata se fundamenta en el cálculo de umbrales que se utilizan para estimar un par de diferencias que regulan el ajuste de los servomotores vertical y horizontal para seguir el patrón de comportamiento que sigue el rayo luminoso durante el día, de acuerdo con el algoritmo de la **Figura 1.2.**

Figure 1.2 Flow chart that models the decision rule
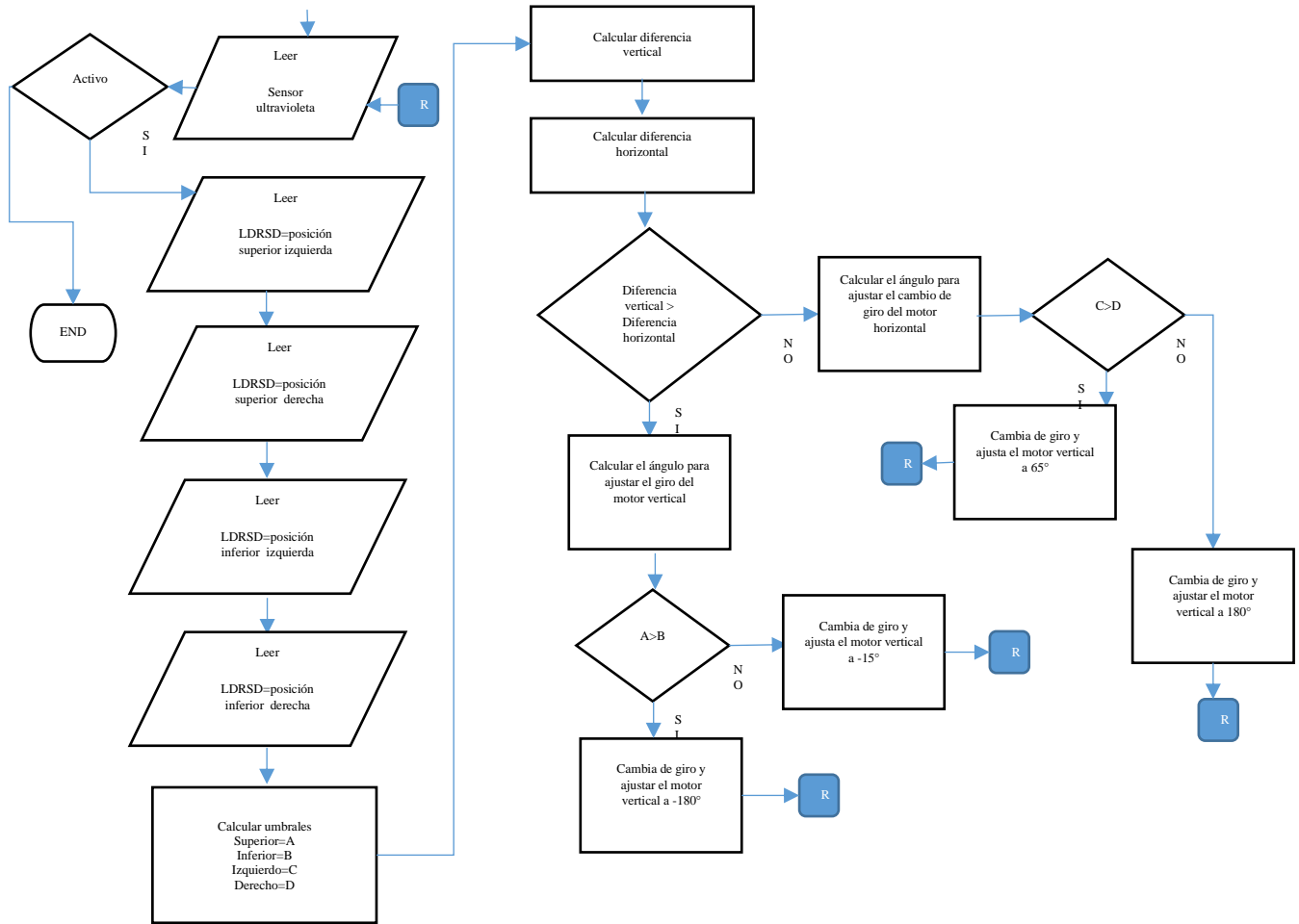
Source: Own elaboration

The control rules are established from 4 thresholds=upper (1), B=lower (2), C=left (3), C=right (4). In these expressions it is observed that the thresholds are expressed by average of two signals sent by cells by the position in which they were placed on the photovoltaic panel where A represent the maximum upper horizontal threshold, B the maximum lower horizontal threshold, C the maximum vertical threshold of the cells placed on the right and D the maximum vertical threshold of the cells placed on the left. Table 1.3 describes the status variables related to the thresholds.

$$A = \frac{ldsi + ldsd}{2} \tag{1}$$

$$B = \frac{ldii + ldid}{2} \tag{2}$$

$$C = \frac{ldsi + ldii}{2} \tag{3}$$

$$D = \frac{ldsd + ldid}{2} \tag{4}$$

Table 1.3 Tresholds and their state variables

Threshold	State Variable	Description
A	00	The light is received by the upper LDRs.
B	01	Light is received by the lower LDRs
C	10	Light is received by the left LDR
D	11	Light is received by the right LDR

Source: Own elaboration

The automaton encodes the thresholds and estimates two difference-based rules, DH=horizontal difference (5), DV=vertical difference(6) to make control action decision and adjust the azimuth angle and altitude, both regulated from the two servomotors. Once the thresholds have been obtained, the control actions whit which the automaton adjust the movements of the left and right servomotor are modelled, according to the state variables defined by the thresholds, as show in **Table 1.4**.

$$DH = (A - B) \tag{5}$$

$$DV = (C - D) \tag{6}$$

Table 1.4 Set of actions to adjust the servomotor

Action	Vertical difference VD	Horizontal Difference HD	Description
q1	00	00	Calibrate the motors to the starting position
q2	01	00	Adjust horizontal motor to 80°
q3	10	00	Adjust vertical motor to 45°
q4	11	00	Change of vertical motor rotation to start 45° and set upper limit to 80° and lower limit to 15°.
q5	00	00	Disables vertical motor
q6	00	01	Adjust horizontal motor to 65°
q7	00	10	Adjust the motor horizontal a 180°
q8	00	11	Cambia de giro el motor horizontal y vuelve a la posición de inicio, 180|° y ajusta el límite superior a 65°.

Source: Own elaboration

Figure 1.3 Modeling the automaton in JFPLAP
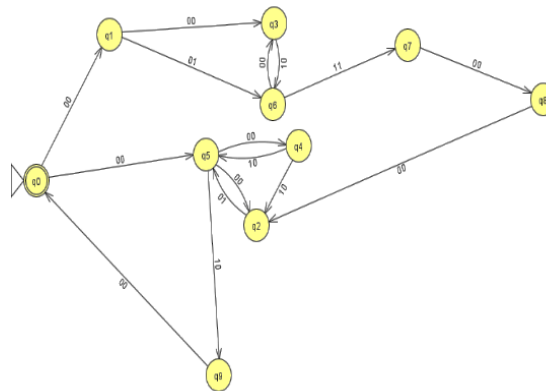
Source: Own elaboration

The modeling of the automaton is illustrated in **Figure 1.3** and JFLAP software was used to check its correct performance, and **Figure 1.4** shows the flow diagram that models the decision rule used by the automaton to track the luminous point.

1.3 Experimental Results

The automaton was programmed in C++ language and implemented in an Arduino UNO microcontroller as illustrates in **Figure 1.4**. The **Figure 1.5** shows the experimental facilities used for the validation of the results. The experiment was carried out at the facilities of Engineering and Chemical Sciences Unit, in the Poza Rica city, Veracruz, México. The purpose was to test performance of automaton to perform light beam tracking.

Figure 1.4 Schematic of the hardware for the implementation of the automaton
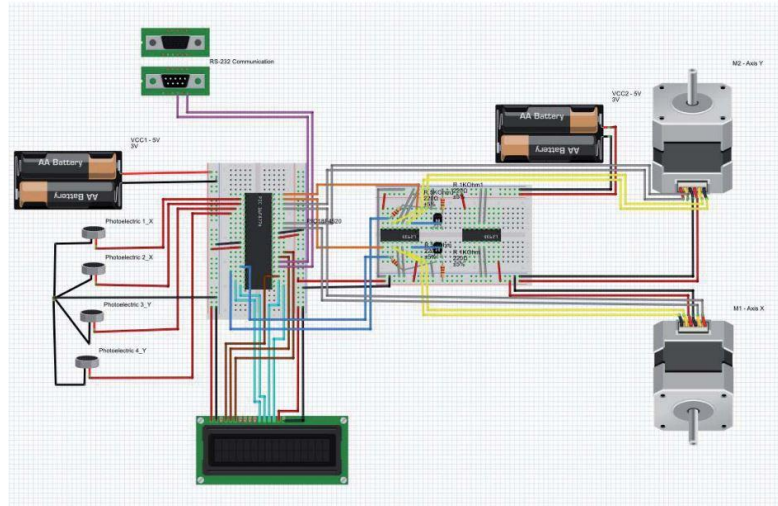
Source: Own elaboration

Figure 1.5 Experimental facilities

Source: Own elaboration

Figure 1.6 Validation of light spot tracking by the automaton
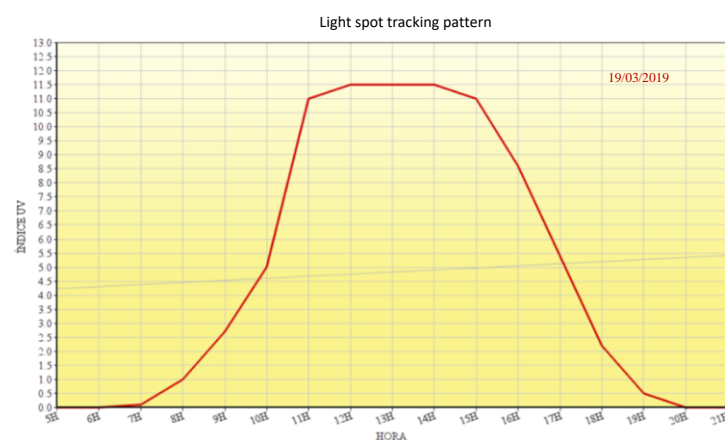
Source: Own elaboration

The results show that the control rules established in the automaton for the tracking of the luminous point manage to carry out precise tracking of the same, as illustrated in **Figure 1.6**, where it is observed that form 8 hours in the morning begins the follow-up of the luminous point and ends at 20 horas. This registry is checked by behavior pattern acquires from the UV radiation sensor.

Figure 1.7 Results validation in sun solar earth tools
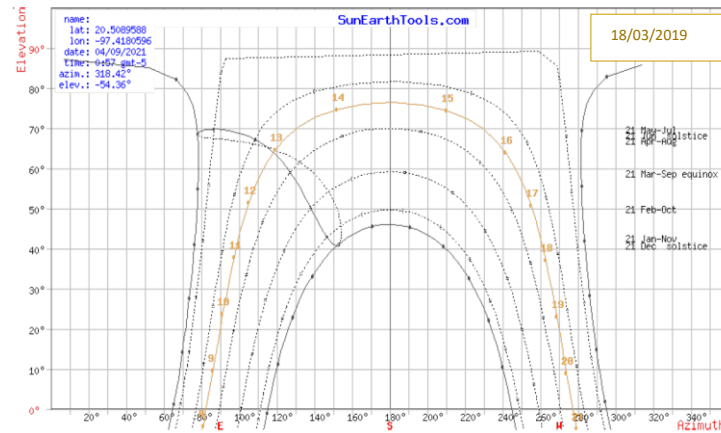
Source: Own elaboration

This behavioral pattern of the luminous beam for the day and the experimental area was checked with software sun solar earth tools, as illustrated in the **Figure 1.7**.

1.4 Conclusions

In this chapter it was show that the use of automata is a useful tool to develop descriptive models of physical system since they can be modeled by means of state variables and simple rules of establishing transition functions.

The use of array of sensors whose signals from behavior patterns that define the control rules minimizes the computation since the automaton manages to make intuitive behavioral decision from the thresholds values also the calculation on the differences determines the incidence where the highest light point is located by adjusting the elevation of the photovoltaic panel trough the coding of the movement of the servomotors, without the need to use initial conditions.

The results also show that the application of finite automata solves the problem of deviations between the positioning of the tracking system and the incidence of the sunbeam on the collector since it includes a self-adjustable function that verifies the correct orientation on the positioning system and avoids manual adjustments and mechanical alignment to recalibrate the system, this extends the service life of the follow-up system as wear is reduced on the servomotors.

To evaluate the performance of automaton in tracking light spots, it´s recommended to extend the experimentation throughout the year under variable weather conditions.

1.5 References

Abadi I., M. A. (2019). Design and Implementacion of Mobile Active Two -Axis Solar Traker with reflector Based on Particle Swarm Fuzzy Controlle. *International Review on Modelling and Simulation IREMOS*, *12 (2)*.

Arenas Rosales, F. M. (Octubre de 2017). Generación fotovoltaica con adición de seguimiento cenital en el centro de méxico. *Pistas Educativas, 39*, 34-55.

Arturo, M. A. (2 de July de 2010). High Precisionsolar traking system. *In Proceedings of the world congress on Engineering*, 844-846.

Bajpai, P., & Kumar, S. (2011). Desing, Develompemnt and performance test of an Automatic Two-Axis solar tracker system. En IEEE (Ed.), *In proceedings of 2011 annual IEEE India Conference*, (págs. 1-6). Hyderabad,India.

Berenguel, M., Rubio, F., Valverde, A., Lara, P., Arahal, M., Camacho, E., & López, M. (2004). An artificial vision based control system for automatic heliostat positioning offset correction in a central receiver soalr power plant. *Solar enenrgy, 76*, 563-575.

Blanco Muriel, M. A. (2001). Computing the solar vector. *Solar Energy, 70*, 431-441.

Celso de la Cruz Casaño, C. L. (2012). Seguidor solar adaptativo bsado en un controlador lógico programable para paneles fotovoltaicos. *Apunt. cienc. soc., 2*(2), 88-100.

Chong, ,. K. (2009). Desing and construcction of non-imaging planar concetrador for concentrador photovoltaic system. *Renewable Energy, 34*, 1364-1370.

Fathabadi, H. (Septiembre de 2016). Npvel higth efficient offline sensor less dual axis solar traker for using in photovoltaic system and solar concentradors. *Renewable Energy*(95), 485-494. doi:https://doi.org/10.1016/j.renene.2016.04.063

Gregor, R., Takase, Y., Rodas, J., Carreras, L., Gregor, D., & López, A. (2015). Biaxial solar tracking system based on the MPPT aproach integrating ICTs for photovoltaic . *J. Photoenergy* , 1-10.

Ho, M., Lai, A., Chong, K., Tan, M., Lim, B., King, Y., & Lee, J. (Diciembre de 2017). Desing and construction of protype mobile sun tracking systemmfor concentrator photovoltaic system. *Energy Procedya, 142*, 736 - 742. doi:https://doi.org/10.1016/j.egypro.2017.12.120

Jing-Min, W. a.-L. (2013). Desing and implmentacion of a sun tracker whith adual-axis single motor for an optical sensor based photovolthaic system sensor. *sensors, 13*, 3157-3168. doi:10.3390/s130303157

Jorge Arturo Pelayo López, C. S. (diciembre 2020). Sistema de seguimiento solar de un eje para aumentar la eficiencia de los sistemas fotovoltaicos bajo distintas condiciones climáticas. (U. A. Yucatan, Ed.) *Ingeniería Revista Académica de la Facultad de Ingeniería Universidad Autónoma de Yucatán, 24*(3), 11-23.

Lee, K., Kim, Y., Yun, ,., & Lee, J. (Mayo de 2005). Magnetic interference free dual elelctric compas . *Sensors and Actuators A: Physical, 120*(2), 441-450. doi:https://doi.org/10.1016/j.sna.2005.01.032

Nurzhigit Kuttybay1, A. S. (Octubre de 2020). Optimized Single-Axis Schedule Solar Trackerin Different Weather Conditions. *Energy, 13*(5226), 2-18. doi:doi:10.3390/en1319522

Rizk J., C. Y. (2008). Solar Traking System: More Efficent use of solar panels. *Engineering and Technology*, 313-315.

Sidek, M., Azis, N., Hasan, W., Ab Kadir, M., Shafie, S., & Radzi, M. (2017). Automated positioning dual axis solar tracking system whith precision elevation and azimut angle control. *Enenrgy, 124*, 160-170.

Tharamuttam, J., & Ng, A. (Diciembre de 2017). Desing and development of an automatic solar tracker. *Enerngy Procedia*(143), 629-634. doi:https://doi.org/10.1016/j.egypro.2017.12.738

Toranzo, M. (2015). Seguidor solar, optimizando el aprovechamiento de la energia solar,. *Aplicaciones Industriales; Ingenieria Energetica, XXXVI*(2), 192-198.

Zhang, Z., Gong, S., Dimitrovosky, A., & Li, H. (2013). Time synchonization attack in smart grid: Impact and analysis. *IEEE Tras. Smart Grid, 4*(13), 87-98. doi:10.1109/TSG.2012.2227342

Chapter 2 Prototype of technical boxes to increase productivity in native bee meliponaria (Scaptotrígona)

Capítulo 2 Prototipo de cajas técnicas para aumentar la productividad en la meliponaria autóctona (Scaptotrígona)

SOTO-LEYVA, Yasmin†*, BONES-MARTÍNEZ, Rosalía and SANTOS-OSORIO, Arturo

Tecnológico Nacional de México / Instituto Tecnológico Superior de Huauchinango, Mexico.

ID 1st Author: *Yasmin, Soto-Leyva* / **ORC ID:** 0000-0003-2652-7065, **CVU CONACYT ID:** 951464

ID 1st Co-author: *Rosalía, Bones Martínez* / **ORC ID:** 0000-0001-8829-9737, **CVU CONACYT ID:** 368744

ID 2nd Co-author: *Arturo, Santos-Osorio* / **ORC ID:** 0000-0003-3643-5770, **CVU CONACYT ID:** 951024

Y. Soto, R. Bones and A. Santos

* yasmin.soto@huauchinango.tecnm.mx

Abstract

Obtaining different products derived from honey has become relevant in recent years in the State of Puebla and considering that Mexico is the fifth largest exporter of honey in the world, the need arises to generate breeding alternatives to improve the productivity of native bees; being the Tetragonisca Angustula bee the domesticated species of the northern region of the State and the main producer of sweet and viscous substances for human consumption. The general objective of this work is based on the design and construction of the physical prototype of a technified box model, making use of materials extracted from the region that are characterized by having various physical and mechanical properties adaptable to environmental conditions to favor the reproduction of the aforementioned native bee and improve the productivity rates of the different hive communities that make up the established meliponaria; The specific objectives are structured in 3 Phases; Phase 1 determines the optimal dimensions of the model considering the different areas that make up the nest, later it was designed using SolidWorks technological software; Phase 2 develops a qualitative study of the properties of the types of wood in the region considering the environmental characteristics for the reproduction of bees, likewise includes a quantitative analysis through a logistical intervention to include the variables that intervene in the generation of costs to acquire materials; Regarding Phase 3, the physical manufacture of the prototype is presented. The technified box will provide the Meliponarians with a means of safe housing, suitable to increase the reproduction of native bees; increased honey productivity in the region and providing a utility model for regional economic growth, based on operations (breeding and management) typical of Meliponiculture.

Meliponiculture, Bees, Prototype, Technified boxes

Resumen

La obtención de diferentes productos derivados de la miel ha cobrado relevancia en los últimos años en el Estado de Puebla y considerando que México es el quinto exportador mundial de miel, surge la necesidad de generar alternativas de crianza para mejorar la productividad de las abejas nativas; siendo la abeja Tetragonisca Angustula la especie domesticada de la región norte del Estado y la principal productora de sustancias dulces y viscosas para el consumo humano. El objetivo general de este trabajo se basa en el diseño y construcción del prototipo físico de un modelo de caja tecnificada, haciendo uso de materiales extraídos de la región que se caracterizan por tener diversas propiedades físicas y mecánicas adaptables a las condiciones ambientales para favorecer la reproducción de la mencionada abeja nativa y mejorar los índices de productividad de las diferentes comunidades de colmenas que conforman la meliponaria establecida; Los objetivos específicos se estructuran en 3 Fases; En la Fase 1 se determinan las dimensiones óptimas del modelo considerando las diferentes áreas que conforman el nido, posteriormente se diseñó utilizando el software tecnológico SolidWorks; En la Fase 2 se desarrolla un estudio cualitativo de las propiedades de los tipos de madera de la región considerando las características ambientales para la reproducción de las abejas, así mismo se incluye un análisis cuantitativo a través de una intervención logística para incluir las variables que intervienen en la generación de costos para adquirir los materiales; En cuanto a la Fase 3, se presenta la fabricación física del prototipo. La caja tecnificada proporcionará a los meliponicultores un medio de alojamiento seguro, apto para incrementar la reproducción de las abejas nativas; aumentando la productividad de la miel en la región y proporcionando un modelo de utilidad para el crecimiento económico regional, basado en operaciones (cría y manejo) propias de la Meliponicultura.

Meliponicultura, Abejas, Prototipo, Cajas tecnificadas

2.1 Introduction

Ramirez and Ortiz (1995) emphasize that the colonies of stingless bees, except for some species, have their nests in hollow tree trunks, the peasants cut them and hang them in the eaves of their houses, the honey extraction processes the performed in a rustic way, thus obtaining smaller amounts of this liquid approximately 600 ml in a period of time of 6 months, the applied system represents a latent risk for the hives due to the lack of the optimal housing infrastructure for the collection of the various products.

The bees that do not contain stinger distinguished as wild or native bees (Scaptotrigona) are mainly reproduced in meliponiculture, among the multiple species that make it up, the Tetragonisca Angustula stands out, which lives in permanent colonies formed by a variable number of young with hives. comprising dozens to one hundred thousand Rasmussen honey flies, 2003), these native individuals are relevant since they act as pollinators in the different ecosystems due to the fact that they make up the majority group of bees in the regions (Roubick. 1989. Slaa, 2006; García-Olivares, 2015).

Meliponiculture is a fruitful activity that means an income opportunity for workers in the northern region of the State of Puebla. However, it is limited by the lack of knowledge of the appropriate techniques for the exploitation, monitoring and strengthening of the hives. Currently there is a great variety in nest structures or hives and they are usually found in natural hollows of logs and rocks, or in constructions made by meliponicultores, these housing buildings are usually improvised and do not have the necessary requirements to protect honey flies from environmental conditions and external organisms, thus contributing to expose beehives to negative factors that cause low levels of productivity, infestation of pests. He honeycomb or hive must be a suitable medium for the reproduction and generation of different derived products, (pollen, propolis, honey, brood foot); Analyzing this requirement, the technified box prototype is created, the applied methodology is divided into 4 phases through which the physical design of a rational model is presented with divisions or rises that strengthen the nest structure using SolidWorks technological software, Subsequently, it is manufactured from thermal wood, seeking to preserve the temperature characteristics that promote an adequate environment for the development of the native bee, considering economic aspects that influence the acquisition of materials, the generation of the prototype provides a utility model suitable for be applied in the meliponarios, of the region at an accessible cost ensuring the reproductive conditions of the bee Tetragonisca Angustula and notably improving productivity levels.

2.1.1 Objectives

2.1.2 General Objective

Design and build a physical prototype of a technified box to improve the productivity of the native species Tetragonisca Angustula Scaptotrigona, making use of materials suitable for the reproduction and protection of the environmental conditions of the meliponarians located in the Sierra Norte of the State of Puebla.

2.1.3 Specific objectives

a)   Determine the ideal dimensions of the box that allow the optimal development of the hive.

b)   Identify the appropriate materials for the manufacture of the prototype and evaluate the costs presented.

c)   Design prototype in SolidWorks design software.

d)   Build physical prototype of technical box.

2.1.4 Justification

Regional economic development is driven by the performance of different activities that are attached to natural resources, the exploitation of these brings with it the contribution of means of subsistence for the economically active population: the Sierra Norte de Puebla is characterized by an extensive catalog from natural environments that promote the development of different species of flora, fauna and vegetation, being the Scaptotrigona bee of the Tetragonisca Angustula species one of the insects that encourages, the activity of the meliponiculture in the region; the productive operations of breeding and management are carried out in the meliponarios established in different parts of the territory making use of improvised hives that do not ensure the ideal productivity of the products derived from honey, causing that the annual profits do not represent positive benefits for the meliponic farmers; considering that there is already an opening for the development of the productive activity described, it is proposed to create a physical prototype of a technified box whose main function is to replace the current nests to adequately preserve reproduction and increase the productivity of the products derived from honey.

Within the various advantages of using the prototype of a technified box for the rearing of bees, we find that the design allows the constant evaluation of the state of the hive considering that a movable structure made up of 3 reproductive areas is handled: nest, super nest, honeycomb; Thus, the extraction of the sweet liquid is also facilitated, the hive is not damaged and it is kept in constant internal review to eliminate the sources that favor pests; in the same way, the thermoregulation of the temperature is maintained by increasing the amount of products that are produced inside pollen, propolis, honey, wax, etc. The economic use through the collection of the aforementioned products is aimed at human consumption and health: generating mixed with honey: dehydrated pollen; use of propolis as an antimicrobial agent and antioxidants in the treatment of bites, infected wounds, respiratory tract infections; production of wax candles and handcrafted figures.

In this way, the prototype manufactured is a utility model to increase the indexes of productivity of honey derivatives and generate higher profits for the meliponic farmers of the Sierra North of the state of Puebla.

2.1.5 Theoretical Framework

To understand the objective of this research, the theoretical foundations that support the formulation, design and manufacture of the prototype are described:

2.1.6 Meliponicultura in Mexico

It is identified as a viable, simple and easily executed economic activity within production systems, environmentally sustainable that allows the provision of environmental services to agroecosystems through pollination and registered products, with great local demand and high price. González (2004) describes meliponiculture as the cultivation of native bees without stinging activity that dates back to times before the arrival of the Spanish, the honey flies of America come from the Meliponini tribe, this group of bees lack stinger and their nests are structured horizontally. They are considered the main group of domesticated honey flies in America, they are characterized by performing social activities within the multiple hives where they multiply; the hierarchical structure is divided into three levels: the queen, workers and drones; these maintain a positive relationship for the improvement and protection of the nests (Harriet, 1999).

The history of meliponiculture in Mexico, was born in the Peninsula of Yucatán, and extends towards the Sierra Norte de Puebla (Cuetzalan). The Huastecas (especially Potosina), Totonacapan in Veracruz; the interest to reproduce this harvesting technique has been awakened among the coffee-producing inhabitants, seeking to take advantage of the different products provided by the species of honey flies (Figure 2.1 Types of melipona bees) that make up the colonies of the meliponarios. It can be seen in the regions of the Mexican tropics distinguished before (except for the Yucatan Peninsula), currently, it is being effecting with another genus of Mexican bee, named in the Nahua language "Pisil Nekmej ", and in Totonac language" Táxkat ". The meliponicultores of the Huasteca collects the qualifier of Yakeme (Manzo 2009). Scaptotrigon bees like Zoogenetic resource contributes to pollination processes; guaranteeing the food security of the region in which they are established.

Figure 2.1 Types of melipona bees

Plebela sp	• Renowned as: Fly bee, it is very small black or gold, it´s nest contains a small wax entrance (piquera).
Lestrimelitta sp	• Renowned as: Cayasán, Lemon bee, it is small black in color and it´s nest contains a small wax entrance (piquera)
Melipona Favosa	• Renowned as: Ererreú, is Medium (10 to 11 mm), black in color and reddish hair, with light stripes on the abdomen, its nests; muddy entrance with radial stripes and covered nests in trees.
Trigona Tetragonista Angustula	• Renowned as: Negrillo, is medium, black, slender, its nest contains a wax entrance, covered in various sites.
Melipona Fulviventris	• Renowned as: Moro-Moro, is medium, dark in color, thorax with reddish hair we and fulvo-colored abdomen, its nest contains a radiated mud entrance with hole for a single bee and nests covered in tree cavities.

Source: Own elaboration with data obtained from Quezada Euan, J. J. (2018). Abejas sin aguijón de México (1st ed.). México: Universidad Autónoma de Yucatán. (Original work published 2018)

2.1.7 Nests of Scaptotrigona of the species Tetragonisca Angustula

The nests of these bees are in any cavity or container that they find available in natural conditions, they prefer cavities in living trees in the same way they make their hives suspended from branches using abandoned bird nests or in the ground, underground. The materials used for the construction of brood combs are propolis and batumen. Propolis is a flexible mixture, composed of wax and vegetable resins, the bathumen is a solidified material made up of clay, vegetable resins and seeds.

2.1.8 Parts of a nest

The parts that make up the nests are different according to the species. For the case analyzed, it is recommended to build as floors that allow the passage of a bee in the entry and exit gate in order to avoid infestations of plagues: nest, supernido, melario and piquera. Internally, the honeycomb must be composed of thin sheets of propolis that surround the brood or nest area. The cells must be cylindrical, arranged from one side to the other in an orderly manner. The food storage compartment is located on the edge of the nest, outside the breeding area, it is made up of propolis cups, which acquire an oval appearance, where the bees collect honey and pollen separately. Similarly, the construction of the waste area must be located outside the breeding and food storage areas.

2.1.9 Prototype

The etymological definition of the term "prototype" is constituted by the Latin prefix of Greek origin "protos" which means "the first" and "types" which means "type, impression, figure or model" (Etymologies, 2016), considering what has been described previously defined as: the first version of a new type of design or model that is built to understand the behavior of the problem and its possible solutions in a real environment (Maner, 2013), this can be perceptible or also a virtual unit, for example, a computer program. The most notable characteristics that represent it are:

1. Limited functionality over a period of time: Nature and purpose manufacturing should be clear during the cycle of use.

2. High degree of user participation which evaluates the operation. provides improvements and specifies requirements.

3. High degree of analysis: Considering that users cannot indicate the requirements to have experience with the system.

2.1.10 Classification of prototypes

Lacalle (2006) and Walter Maner (2013) propose a simple classification, establishing "fidelity" as a measurement indicator that corresponds to the level of similarity of the variables of appearance and functionality of the model (Table 2.1 Prototype classification scheme).

Table 2.1 Prototype classification scheme

Prototype type	Variable	Features
Low fidelity	Appearance	They are quick in their development and use different materials to those of the final product, cheap, simple and easy to produce useful in the early stages of development and during the conceptual design.
High fidelity	Appearance	Similar to the final product, they use the same materials, they provide a detailed idea of the product, including characteristics such as cost, quality and performance.
Exploratory	Functionality	Applied to clarify project goals, identify requirements, examine design alternatives or investigate a large and complex system, it allows initial conceptual ideas to be compared with design expectations and requirements.
Experimental	Functionality	It allows the validation of certain specifications of the product that is being designed and constitutes an intermediate element for the realization of certain pilot tests.
Operational	Functionality	It is iterative, progressively improved and becomes the design final supports applying changes.

Source: Own elaboration with data obtained from La calle (2006) y Walter Maner (2013)

2.1.11 High-tech boxes for bees

The incorporation of the rational boxes through the physical prototype presented in the research facilitates the operational activities in meliponiculture, both the biological material management (colonies) in relation to divisions and production management (efficient harvest) of honey and other goods such as pollen, and propolis. At the present there are multiple models of rational boxes, the boxes with divisions and built with wood with an average thickness of 2.5 cm, are the most used, the different models are described below:

1. Caja Maria: according to Monteiro (2000), it is a box with a simple structure, which shows a fixed central brood chamber and two removable chambers for storing honey and pollen, facilitating harvesting without damaging the nest, built mainly of wood.

2. UTOB box: box developed by the University of Utrecht in Trinidad and Tobago, it consists of two sectors, for the brood chamber and another for the honey and pollen production chamber. The separations of the chambers allow to isolate the food store from the nest, which allows reduce colony stress at harvest time (Sommeijer, 1999).

3. Arturom box: it consists of a base for a brood chamber, divided into two 7.5 cm sections. Tall each separated, a central hole of 5 cm in diameter. Above the brood chamber is placed a rise separated by strips with spaces for the bees to climb and build the honey and pollen pots (Mejia, 2006).

4. Improved Brazilian box: vertical box modified according to the Portugal Araujo design with sections Disassembled, it consists of two compartments for the brood chamber and two risers for the production of honey. The measurements are: brood chamber 14 X 14 X 10 cm and 4 cm thick, the production chamber are 18 X 18 X 8 am and 2 cm thick (Baquero and Stamatti, 2007 and Guzmán et al., 2011).

5.   Simple box (traditional box): consists of an elongated drawer without divisions, with a movable upper part (Mejía, 2006). These boxes are traditionally used in various areas of the South Region, the measurements of this box are variable and can reach up to 100 X 21 X 25 cm.

The importance of the use of these physical means for reproduction is that they provide an optimal space in which zootechnical conditions are not affected by climatic changes and in the same way the colonies are difficult to access for pests and / or enemies. (Baquero & Stamatti. 2007).

2.1.12 Supplier analysis

According to Cameiro (2004) a supplier is a business entity that supplies the company with goods and / or services necessary for its use in the production of goods and / or services of the company. The particularities of a supplier's product, as well as the points of proximity with the value chain of a company, can significantly disrupt costs and thus the differentiation of a company from the competition. Suppliers are responsible for offering supplies efficiently, early and quickly, as well as the possibility of coordination, reduction of traction costs, inventory costs and risks. Suppliers support the suitability of the companies they supply, establish jobs, promote the exchange of products with others, contribute to the multiplicity of the workforce and the economy, and affirm the technological persistence between natural resource processors and the rest of the industry (Torres, 2009).

According to (Hernández, 2014) Once the supply sources have been identified, we proceed to the choice of suppliers that are best suited to the demand, based on a series of criteria, as a result, a list of optimal suppliers is obtained. This process is only carried out for the acquisition of the products that are most commonly purchased, since it has an economic cost and is only profitable if the final savings obtained is greater than the investment made in the search for suppliers for the company. In this sense and considering what is described, logistics interventions are applied for the analysis and selection of suppliers, considering the different costs derived for the purchase and transport of raw materials for the production of technified boxes for the Meliponarians.

2.1.13 Methodology to be developed

The methodological description that allowed the design and manufacture of the presented prototype was developed from 3 phases (Figure 2.2 Phases of the methodological process corresponding to the investigation).

Figura 2.2 Phases of the methodological process corresponding to research
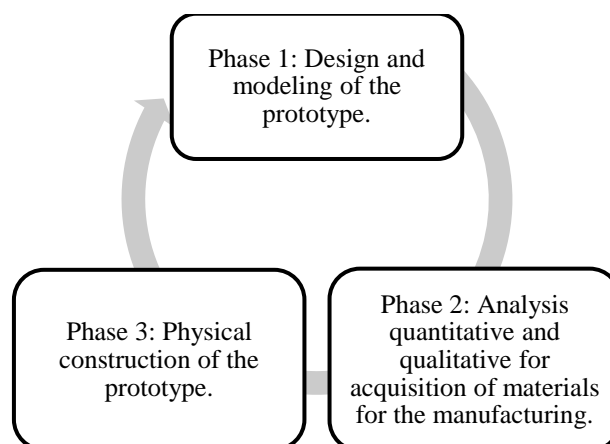
Source: Own Elaboration

2.1.14 Phase 1: Design and modeling of the prototype

Using the theoretical reference consulted, the areas that will make up the technical box are defined in the first instance, following a vertical building superimposed between 7 zones:

1.   Base legs.

2. Base.

3. Nest.

4. Super nest.

5. Melario.

6. Top.

7. Fastener.

The measurements are determined and the characteristics of the different zones are described, specifying the dimensions for further consideration in the scaled design in SolidWorks Software (Table 2.2 Description and dimensions of parts that make up the prototype).

Table 2.2 Description and dimensions of parts that make up the prototype

Part	Features	Dimensions
Base legs	They contribute the stability of the box the contemplating the control of sudden movements.	2 cm x 4 cm x 22 cm.
Base	It allows the colony of bees that inhabit the hive to develop suitable environmental conditions for reproduction.	2 cm x 22 cm x 22 cm
Nest	Contains the hive brood foot.	7.5 cm x 23 x 23 cm
Super nest	This zone allows the separation of the hive into two sections to create a new nucleus or a new hive.	6.5 cm x 23 cm x 23 cm
Melario	In this area is the honey, during the extraction process the analyzed area is slightly detached without being affected.	8 cm x 23 cm x 23 cm
Top	Ensures permeability, protecting the content of the hive, providing ideal environmental characteristics for improving the productivity of bees.	2 cm x 23 cm x 23 cm
Fastener	Allows manipulation and movements to move the hive.	2 cm x 2 cm x 19 cm.

Source: Own elaboration

2.1.15 Phase 2: Quantitative and qualitative analysis for the acquisition of materials for manufacturing.

2.1.16 Qualitative analysis

Making an analysis through the application of exploratory research, we proceeded to determine the different types of wood existing in the Sierra Norte, highlighting those whose thermal properties allow the regulation of environmental conditions in the region. Considering that the natural vegetation is contained in tropical evergreen forests, mountain mesophilic forests, and coniferous and oak forests. (Rzedowski, 1992; INEGI, 2005) (Figure 2.3 Types of concurrent forests in the Sierra Norte de Puebla) a comparative study is carried out between the different woods present in the region and the area of influence, since the aim is to achieve the appropriate environment For the development of melipon bees Tetragonisca Angustula, the physical and mechanical properties that allow the accumulation of heat in the wood are analyzed, the density and moisture content being variable that determine the environment conducive to reproduction (Table 2.3 Qualitative analysis of the characteristics of the different wood models of the region).

Figure 2.3 Concurrent Forest types in the Sierra Norte de Puebla
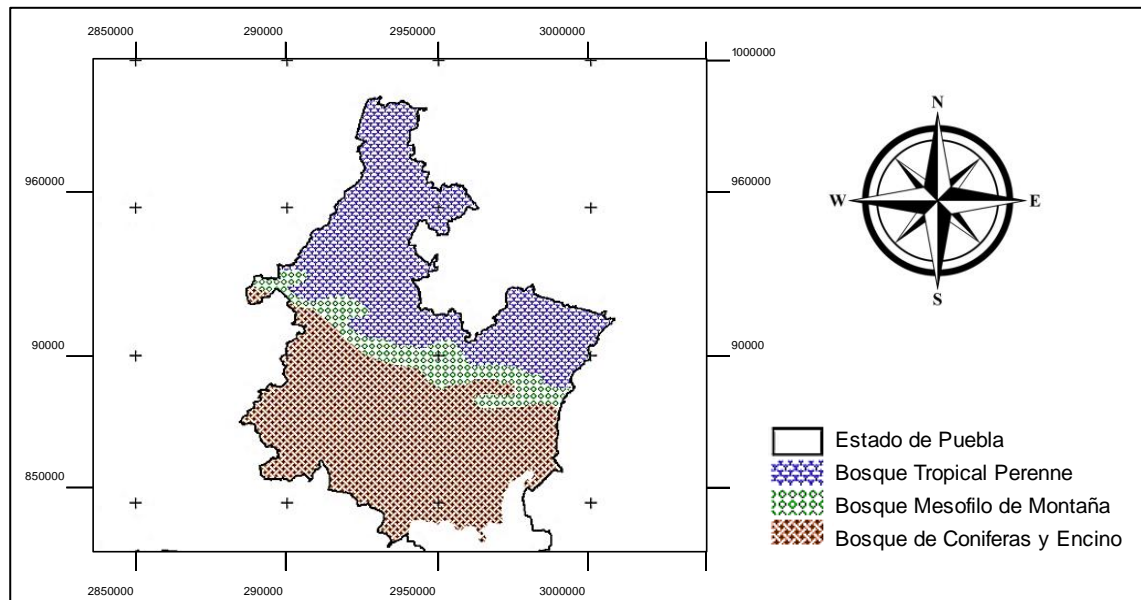
Table 2.3 Qualitative analysis of the characteristics of the different wood models in the region

	Features	Types of wood		
		White Pine	Cedar	Jonote o chaca
Physical properties	Color	White tree and yellow-brown heartwood,	Sapwood from light pink to yellow. Heartwood yellow even to reddish Brown.	Light color
	Defects	It has abundant knots, normally healthy.	Exposure of knots in varying dimensions, with accumulations of resin.	The wood presents knots.
	Fibrous Structure	Straight	Straight, presentation of spaces intertwined.	Straight
	Grain	Half	Half	Thin
	Density	500 kg/m^3	490-520 kg/m^3	560 kg/m^3
	Humidity	12% humidity	12% humidity	12% humidity
	H ardness	1,8 – 2,1 in the test of Monnin.	2 in the test of Monnin.	3,2 in the test of Monnin.
	Durability	Not durable against insects. Perceptive to the aggression of fungi and insects.	Its natural structure is tenacious to the aggression of fungi and insects, it is durable and smells of resin root; so it is considered suitable for exteriors.	Durable against fungi and insects in suitable environmental conditions.
	Dimensional stability.	Volumetric shrinkage coefficient: 0,38%	Volumetric shrinkage coefficient: 0,34%	Volumetric shrinkage coefficient: 0,38%
Mechanical properties.	Compression.	434 kg/cm^2	415 kg/cm^2	490 kg/cm^2
	Static bending.	874 kg/cm^2	753 kg/cm^2	850 kg/cm^2
	Elasticity	90.000 kg/cm^2	90.000 kg/cm^2	103.000 kg/cm2
General	Work ability	Drying process soon. Risk of cracks and imperfections.	Late drying, low probability of blemishes. High risk of amber oozing.	Quick drying, with risk of damage.
	Price	Low to moderate.	Moderate.	Moderate.

The increase in humidity in the composition of the wood influences the specific heat, considering that the caloric capacity of pine is similar to that of brick, however, the density of wood represents 1/3 with reference to brick. (Wood Products, 2018), the density of jonote or chaca wood is higher than the density of pine and cedar, maintaining 12% humidity; This means that the heat content is higher in the jonote material (Figure 2.4 Jonote wood), as well as the mechanical properties: compression, static bending and elasticity, present greater benefits compared to other materials.

Figure 2.4 Jonocote wood

Source: Own elaboration

2.1.17 Quantitative analysis

We proceeded to determine the set of necessary materials (Jonote wood, acetates, wire for meliponiculture, nails) to acquire them, considering that the costs must be feasible for the economy of the region, a logistical intervention was applied for the selection of suppliers considering the variables that directly intervene in the generation of direct indirect costs: fuel performance and price (Km/L), travel distance (Km), annual maintenance cost projection, load unit usage period (min), cost of booths, unit cost of raw materials and supplies, with an insurance cost of 40% with respect to the unit value of the transported cargo (Table 2.4 Logistical intervention for selection of suppliers).

Table 2.4 Logistics intervention for supplier selection

Suppliers	Jonocote wood			Wire for Meliponiculture			Steel nails for Meliponiculture			Acetates		
	Chiconcuautla	Zacatlán	Honey	CDMX	Tulancingo	Zacatlán	Huauchinango Centro	Tulancingo Centro	Huauchinango El Paraíso	Huauchinango Centro	Huauchinango El Potro	Huauchinango Cbtis
Pieces	1	1	1	100	100	100	100	100	100	100	100	100
Fuel efficiency (km/l)	14	14	14	14	14	14	14	14	14	14	14	14
Distance (KM)	38.3	60.5	69	173.6	54.1	60.5	2.8	54.5	4.2	2.8	5.4	6
Annual maintenance cost ($)	$ 1,200	$ 1,200	$ 1,200	$ 2,200	$ 2,200	$ 2,200	$ 879	$ 879	$ 879	$ 400.00	$ 400.00	$ 400.00
Charging unit usage time (MIN)	89	82	400	149	61	82	11	62	14	11	16	20
Booths cost	$ -	$ -	$ -	$ 220.00	$ 73.00	$ -	$ -	$ -	$ -	$ -	$ -	$ -
Unit cost of parts (m², unidades)	$ 240	$ 270	$ 210	$ 6.9	$ 7.5	$ 6.5	$ 2.5	$ 2.8	$ 2.6	$ 7.00	$ 7.20	$ 6.80
Minutes annual	518400	518400	518400	518400	518400	518400	518400	518400	518400	518400	518400	518400
Fuel cost	$ 59.97	$ 94.73	$ 108	$ 2.718	$ 0.847	$ 0.947	$ 0.044	$ 0.853	$ 0.066	$ 0.0438	$ 0.0845	$ 0.0939
Maintenance cost	$ 0.206	$ 0.190	$ 0.926	$ 0.006	$ 0.003	$ 0.003	$ 0.000	$ 0.001	$ 0.000	$ 0.00008	$ 0.00012	$ 0.00015
Toll cost	$ -	$ -	$ -	$ 2.200	$ 0.730	$ -	$ -	$ -	$ -	$ -	$ -	$ -
Insurance cost (40% of unit cost)	$ 96	$ 108	$ 84	$ 2.76	$ 3	$ 2.60	$ 1	$ 1.12	$ 1.04	$ 2.80	$ 2.88	$ 2.72
Total cost	$ 156.17	$ 202.9	$ 193.0	$ 7.68	$ 4.58	$ 3.55	$ 1.04	$ 1.97	$ 1.11	$ 2.84	$ 2.96	$ 2.81

Source: Own elaboration

Using the cost calculation, the supplier selection process was carried out applying a statistical analysis to determine the ideal option for the acquisition of inputs, the results indicate that the supplier for jonote wood is the municipality of Chiconcuautla with a cost of $ 156.17, the wire for meliponicultura will be purchased in the CDMX with a value of $ 3.55, the nails will be purchased at Huauchinango Centro at a cost of $ 1.04, and the acetates will be purchased at Huauchinango Cbtis with a price of $ 2.81 (Figure 2.5 Statistical analysis for selection of suppliers).

Figure 2.5 Statistical analysis for selection of suppliers
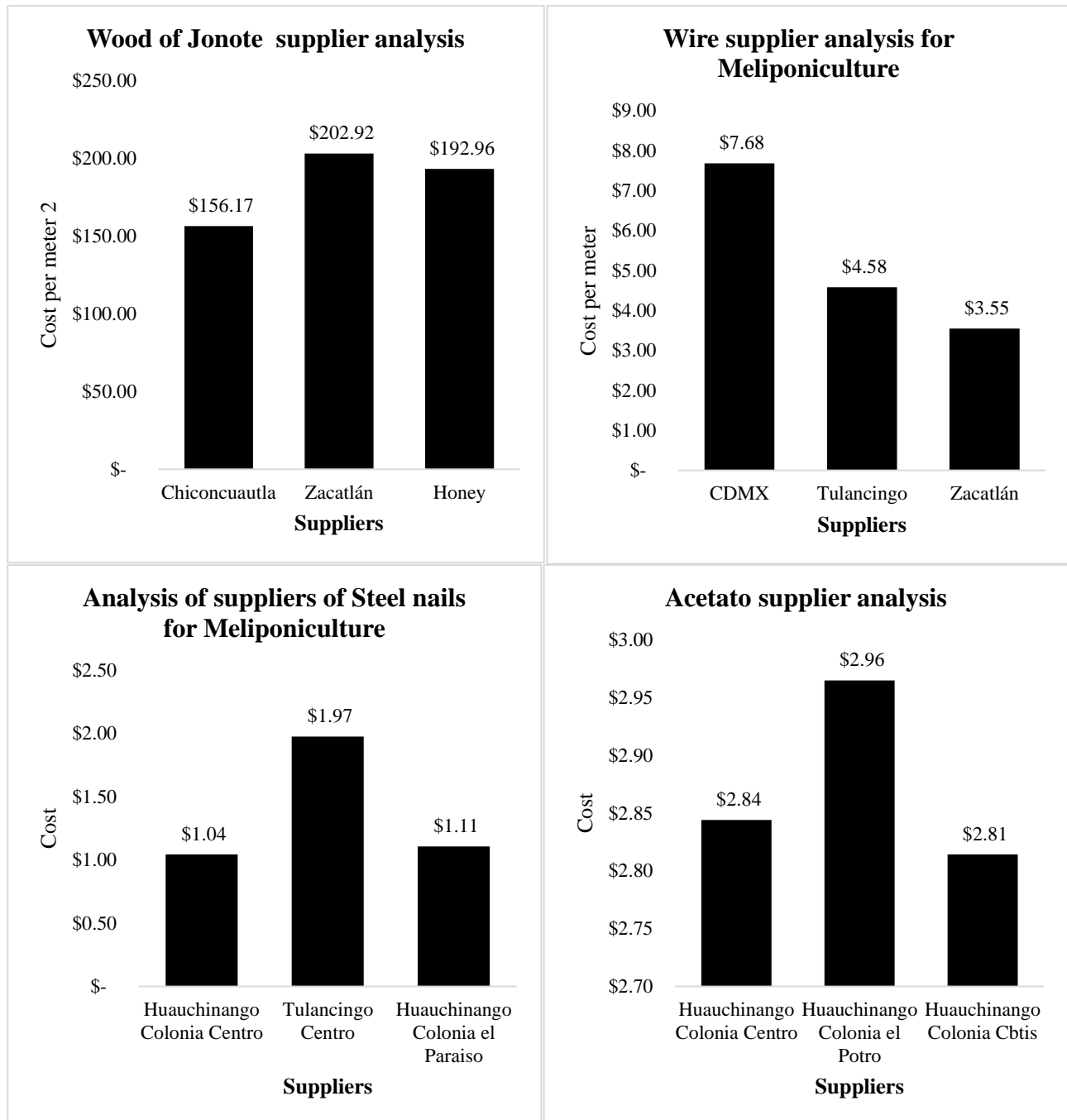
Source: Own elaboration

2.1.18 Phase 3: Physical construction of the prototype

Derived from the design and modeling, as well as the physical acquisition of the materials, we proceed to build the prototype; determining the working method with the creation of the process diagram in which the optimal activities and the standard time for manufacturing were established (Figure 2.6 Process diagram for technified box). Once the optimal work process was established, the model was physically built (Figure 2.7 Physical construction of the prototype).

Figure 2.6 Process diagram for technified box

PROCESS OPERATIONS DIAGRAM			
Manufacturing:	Technified box.	Method:	Actual
Area:	Production.	Total time (min)	248
Operator:	1	Total time (hours)	4.13
Elaboration:	-		

Technified box.

Time	Op.	Description
45 min.	0-1	Wood cutting and preparation.
28 min.	0-2	Base construction.
11 min.	0-3	Leg to base assembly.
35 min.	0-4	Nest building.
25 min.	0-5	Super nest construction.
8 min.	0-6	Placement of acetates in the super nest.
29 min.	0-7	Melario construction.
12 min.	0-8	Placement of wire between honeydew and super nest.
19 min.	0-9	Cap construction.
33 min.	0-10	Box assembly.
3 min.	2	Box inspección.

Source: Own elaboration

Figure 2.7 Physical construction of the prototype

Source: Own elaboration

In the same way, the effectiveness of the design was assessed by subjecting the built prototype to various environmental conditions in a sampling period of 30 days, the recorded observations are recorded below (Table 2.5 Abstract of Recorded Observations):

Table 2.5 Summary of registered observation

Period	Precipitation rainy.	Wind	Sunny	Cloudy	Physical state of the box
Day 1		X			Excellent
Day 2			X		Excellent
Day 3			X		Excellent
Day 4			X		Excellent
Day 5			X		Excellent
Day 6			X		Excellent
Day 16			X		Excellent
Day 17	X				Well
Day 18	X				Well
Day 19				X	Well
Day 24			X		Excellent
Day 25			X		Excellent
Day 26			X		Excellent
Day 27			X		Excellent
Day 30				X	Well

Source: Own elaboration

The statistical analysis corresponding to the observation days shows us that the exposure of the boxes to different environmental conditions categorizes an Excellent condition in 73.33% presenting non-significant changes in the physical structure; Likewise, the condition of Good is presented in 23.33% considering possible changes, with regular criticality that in the long term will cause deterioration in the boxes (Graphic 2.1 Physical status of the prototype).

Graphic 2.1 Physical status of the prototype

Physical Status of the prototype.
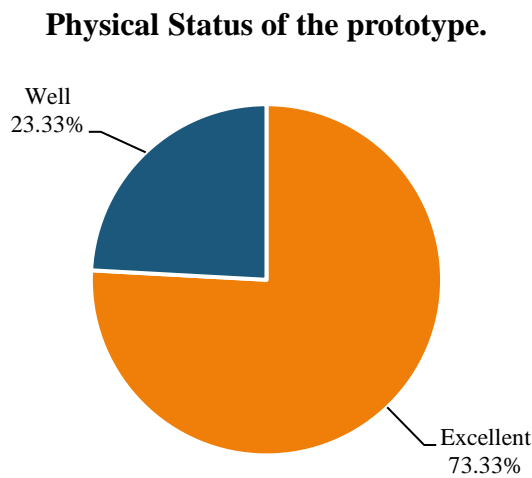
Source: Own elaboration

By means of statistical research, the percentage of influence with respect to the affectation of the physical conditions of the technical box is exposed: the different atmospheric events that are exposed with the study carried out are represented by precipitation and condensation: rain and drizzles (Rainy precipitation), humidity and mist (condensation), as well as sunny and wind weather. The rainy precipitations affect mainly the conditions of the manufactured model (71.43%), followed by the cloudy climate (42.86%), since these climates considerably increase the increase in humidity of the environment and with it the affectation of the box; Thus, it is also deduced that the environmental factors of sunny and wind do not present critical participation (Graphic 2.2 Analysis of the impact of climatic conditions).

Graphic 2.2 Analysis of the impact of climatic conditions
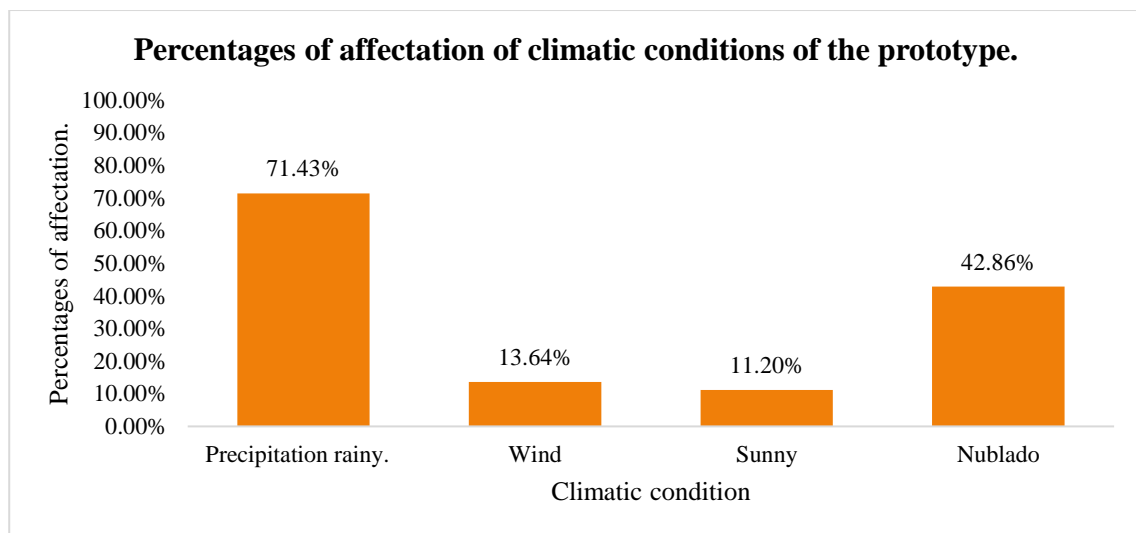
Source: Own elaboration

The information obtained will be useful to us, since it will allow us to formulate an improvement plan for the conservation of the box and thus fully ensure its resistance to weather conditions.

2.2 Results

The results observed in Phase 1 are shown with the scaled design in the SolidWorks software of the proposed prototype, the model exposes each of the parts that make up the hive (Figure 2.8. Technified box model in SolidWorks software):

- Base: The assigned shape is square in order to take advantage of the adaptability of bees: generating a medium that reduces stress levels in the reproduction processes.

- Nest: This area is assigned for the brood foot, placing a circular opening that provides the entry of oxygen.

- Super nest: In order to obtain a greater quantity of breeding for the generation of new nuclei, sectioned elements are included (wire for meliponiculture, acetates); to develop a communication space between nest and super nest.

- Melario: Within this area originates the sweet and sticky substances from which later the honey and some of its derivatives will be extracted.

- Top: Being very necessary to have a closed space for the development of bees, a cover is also included whose main purpose is to regulate the temperature of the created hive. After the design of components, the assembly is carried out to form the prototype full.

After the design of components, the assembly is carried out to form the prototype full.

Figure 2.8 Technified box model in SolidWorks software
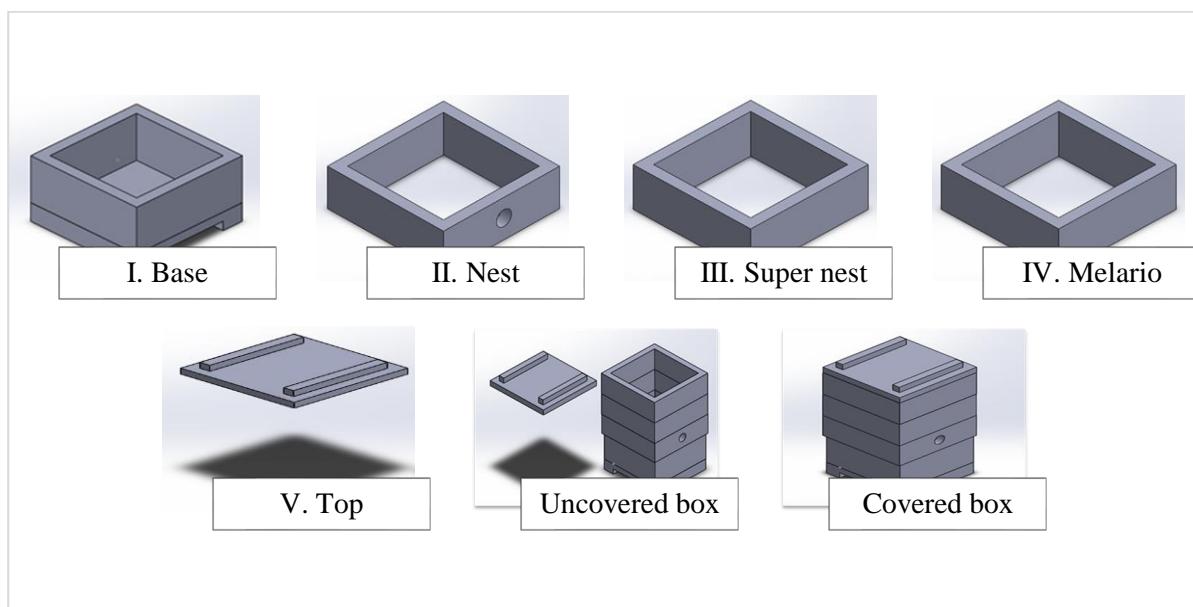
Source: Own elaboration using SolidWorks Software 2017

The effects obtained for Phase 2 according to the qualitative analysis of the types of wood existing in the region and the area of influence allowed us to observe the general, physical and mechanical characteristics, concluding that for jonote wood: the density (Km / m³) is of 560, 12% higher than that of white pine, this factor presents a Monnin index of 3.2, 64% more with respect to white pine, the dimensional stability is equal to the pine indicator; Similarly, there is 13% more understanding (Km / cm²) with respect to the lower index, for the elasticity factor (Km / cm²) it remains 14.4% higher than the 2 elements analyzed (Figure 2.9 Statistical analysis of the general, physical and mechanical characteristics of wood in the región): the aforementioned conditions consider jonote or chaca wood as the optimal acquisition option as the main input to manufacture the prototype.

Using the logistical intervention, we proceeded to determine the optimal suppliers (Table 2.6 Selection of suppliers) to buy the set of required materials, Chiconcuautla being the supplier of jonote wood with a unit price of $ 156.1729, the town of Tulancingo the supplier of wire for meliponicultura with a value of $ 10,652, for nails and acetates Huauchinango was selected with a cost of $ 5,220 and $ 5,628 respectively; accounting for a raw material purchase value of $ 177,673.

Figure 2.9 Statistical analysis of the general, physical and mechanical characteristics of wood in the region
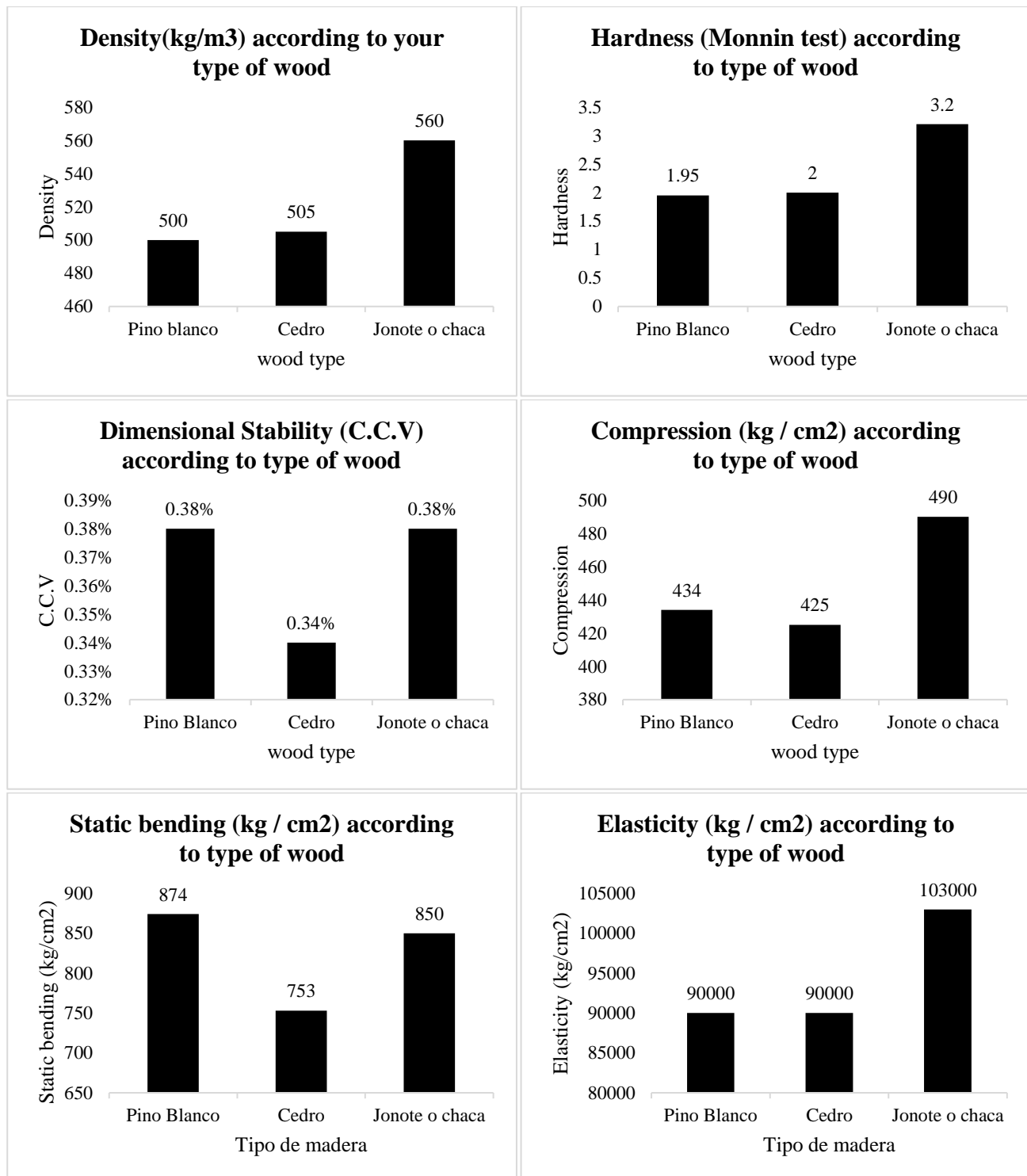
Source: Own elaboration using SolidWorks Software 2017

Table 2.6 Selection of suppliers

Selection of suppliers				
Materials	Supplier	Unit price	Required quantity	Subtotal
Jonote Wood	Chiconcuautla	$ 156.1729	1	$ 156.173
Wire for Meliponiculture	Tulancingo	$ 3.5507	3	$ 10.652
Steel nails for Meliponiculture	Huauchinango Colonia Centro	$ 1.0440	5	$ 5.220
Acetates	Huauchinango Colonia Centro	$ 2.8141	2	$ 5.628
TOTAL				$ 177.673

Source: Own elaboration using SolidWorks Software 2017

The process of elaboration and documentation of the work system for the manufacture of the technified box through the diagram of operations carried out in Phase 3, allows to determine the Standard Time with a total of 248 minutes or 4.13 hours necessary for the construction; If you want to sell the model, you proceed to calculate the cost of sale: raw material cost- $ 177,673 + labor cost $ 36.92 (Salary for Puebla in Mexico 2021) - $ 152.60: the total cost is $ 330,273 considering a margin of 40% profit, the resulting cost of sale is $ 462.3822 comparing the costs of boxes for Melipona bees (Table 2.7 Analysis of brands, models and prices established by the main suppliers of technified boxes for Meliponiculture in México) manufactured Chilpancingo, Guerrero of $ 699.00 and in Lázaro Cárdenas, Quintana Roo of $ 800.00, it is deduced that the cost decreases in an interval from 36.03% to 73.01% respectively; in such a way that the prototype presented is a utility model that satisfactorily meets the quality and cost requirements.

Table 2.7 Analysis of brands, models and prices established by the main suppliers of technical boxes for Meliponiculture in México

Mark	Model	Provider location	Price
Mielguayab	Melipona	Chilpancingo, Guerrero	$ 728.00
Melipona-Scaptotrigona	Melipona	Chilpancingo, Guerrero	$ 699.00
Ana honey	Lamstrong	Comitán De Domínguez, Chiapas	$ 920.00
Madera	Langstroth	Toluca, Estado De México	$ 1,343.56
Mundo Melífero	Langstroth	Mérida, Yucatán	$ 560.00
Na Chab	Langstroth	Ocosingo, Chiapas	$ 989.00
Ingenieria y Ecosistemas	Melipona	Lázaro Cárdenas, Quintana Roo	$ 800.00
Maderas de pino	Tecnificada	Del Bravo, Guerrero	$ 615.00

Source: Own elaboration with data from https://www.mercadolibre.com.mx/

Once the prototype was manufactured and validated (Figure 2.10 Technified box), 15 models were installed within a meliponary of the region (Figure 2.11 Extraction of honey and its derivatives) the results were beneficial, considering an increase in the levels of honey production, contemplating that at the beginning of the analysis an average production of 600 mm was recorded in one period. 6 months; At the end of the first semester after the implementation of the technical boxes, an average of 800 ml per hive was harvested, increasing production by 33.33%, for the second period 975 ml were collected with a benefit of 62%: the production of derived products such as propolis, pollen and wax (Figure 2.11 Extraction of honey and its derivatives). Regarding the internal affectation of the hive, the indices of affectation by external agents were reduced, at the end of the first semester 2 affected hives were detected and for the second period 1 hive with affectation was observed.

Figure 2.10 Technified box

Source: Own elaboration

Figure 2.11 Extraction of honey and its derivatives

Source: Own Elaboration

2.3 Appreciation

To the Higher Technological Institute of Huauchinango and the Industrial Engineering Division for the facilities provided for the preparation of the chapter presented.

2.4 Conclusions

A quantitative and qualitative analysis was carried out by means of which a technified box model for melipon bees was designed, considering the existing theoretical references regarding the breeding of the species of bees. Through exploratory research, variables that make up optimal physical, mechanical and functional characteristics for meliponiculture in the region were analyzed, determining that the appropriate wood for the construction of the technified box is jonote or chaca wood. Identifying the foregoing, the economic requirements of the materials were established, taking into account the acquisition and transportation values of each one, with this the total cost of the box was calculated without considering the cost of labor, being $ 177,673 (Mexican pesos). Next, the prototype was physically built, in reference to what was obtained in the scale design of the SolidWorks design software, it is relevant to mention that to obtain the total cost of the prototype, the standard time of the process was calculated through the diagram of process operations, in this way it is concluded with a cost of sale of $ 462.3822 being a lower value with respect to other boxes currently marketed with similar characteristics and functionality. Finally, the resistance and effectiveness of the box was validated, exposing it to a sampling of 30 days under climatic conditions of the region, the result of this statistical analysis indicates that the greatest affectation is contributed by rainy precipitations, the above generated the formulation of proposals improvement for the location of this prototype in open or closed environments.

The physical development of the technified box brought multiple benefits that are reflected in the increase in the productivity of honey and its derivatives, as well as the decrease in the levels of affectation by pests, preserving in a safe way the native bee species Tetragonisca Angustula de la Sierra Norte del Estado de Puebla: in the same way, an efficient work system was created for the physical construction of the model that, by presenting a competitive cost, would create a new source of employment to promote the economic and sustainable development of the región.

2.5 References

CONAFOR. (2007). Fichas técnicas tecnológicas y usos de maderas comercializadas en México (Vol. II). Retrieved from https://www.conafor.gob.mx/biblioteca/catalogo-maderas-tomo2.pdf

G. Quesada-Euan, J. J. (2019). *Stingless Bees of Mexico: the biology, management and conservation of an ancient heritage.* S.L.: Springer.

García López, David; Quintanar Isaías, Alejandra; López Binnqüist, Citlalli (2012). Guía características y usos de la madera de jonote en la carpintería (Trema micrantha). Universidad Autónoma Metropolitana-Iztapalapa y el Centro de Investigaciones Tropicales de la Universidad Veracruzana.

García Martínez A. (2008). *Apicultura* (). Madrid: Ministerio De Medio Ambiente Y Medio Rural Y Marino. Secretaría General Técnica. Centro de Publicaciones, Dl.

Guízar-Nolazco, E., Granados-Sánchez, D., & Castañeda-Mendoza, A. (2010). Flora y vegetación en la porción sur de la Mixteca Poblana. Revista Chapingo Serie Ciencias Forestales y del Ambiente, 16 (2). 95-118 pp.

Hernández White, C. (2014). *MF1004_3, Gestión de proveedores*. Málaga Nuevos Negocios En La Red D.L.

Jiménez, E. M. (2017). *Manejo y mantenimiento de colmenas*. Madrid Mundi-Prensa.

Kasal, B. (2014). *In situ assessment of structural timber.* Germany: Springer.

Manuel Carneiro Caneda. (2004). *La responsabilidad social corporativa interna: la "nueva frontera" de los recursos humanos*. Pozuelo De Alarcón, Madrid: Esic Editorial.

Márquez-Cruz, U., López, C. y Negreros-Castillo, P. 2011. Una especie multiusos del trópico mexicano *Trema micrantha* (L.) Blume. Revista de la Facultad de Ciencias de la Universidad Nacional Autónoma de México. *Ciencias* 101: 16-22. En línea: http://redalyc.uaemex.mx/redalyc/pdf/644/Resumenes/64419046003_Abstract_2.pdf

Mercado libre. (2021). Caja Tecnificada | MercadoLibre.com.mx. Retrieved April 12, 2021, from Mercadolibre.com.mx website: https://listado.mercadolibre.com.mx/caja-tecnificada#D[A: caja%20tecnificada]

Miguel Guzmán, M., Balboa, C., Vandame, R., Luisa Albores, M., & González Acereto, J. (2011). *Manejo de las abejas nativas sin aguijón en México: melipona beecheii y scaptotrigona mexicana: manual técnico*. México: Colegio De La Frontera Sur.

Quezada Euan, J. J. (2018). *Abejas sin aguijón de México* (1st ed.). México: Universidad Autónoma de Yucatán. (Original work published 2018)

Quintanar-Isaías, A., Jacobo Villa M.A., López, C., Flores-Hernández, N., Jaramillo, P. y De la Paz, O.C. 2012 La madera de *Trema micrantha* (L.) Blume de Veracruz. *Madera y Bosques* 18(2):

Wood Products. (2018, June 21). Propiedades térmicas de la madera. Retrieved February 3, 2021, from Wood Products website: https://www.woodproducts.fi/es/content/propiedades-termicas-de-la-madera

Chapter 3 Value chain design to open a recycling plant in the municipalities of Huauchinango-Xicotepec, Puebla

Capítulo 3 Diseño de la cadena de valor para abrir una planta de reciclaje en los municipios de Huauchinango-Xicotepec, Puebla

GONZÁLEZ-MUÑOZ, Lilian†*, SOTO-LEYVA, Yasmin and AHUACATITLA-PÉREZ, José Miguel

Tecnológico Nacional de México/Instituto Tecnológico Superior de Huauchinango, Mexico.

ID 1st Author: *Lilian, González-Muñoz* / **ORC ID**: 0000-0003-2575-0740, **CVU CONACYT ID:** 962092

ID 1st Co-author: *Yasmin, Soto-Leyva*/ **ORC ID**: 0000-0003-2652-7065, **CVU CONACYT ID:** 951464

ID 2nd Co-author: *José Miguel, Ahuacatitla-Pérez*/ **ORC ID:** 0000-0001-5336-8966, **CVU CONACYT ID:** 951466

L. González, Y. Soto and J. Ahuacatitla

* lilian.gm@huauchinango.tecnm.mx

Abstract

At present, the integral conservation of the environment represents one of the concerns with the greatest impact in the social sphere because the preservation and management of the environment are directly interrelated with the different productive activities that contribute to the economic and family well-being of the individuals.With population growth, the generation of urban solid waste (RSU) has increased, causing various problems that affect health, pollution and image aspects of urban sites, for this reason, it seeks to put into practice viable alternatives that lead to designing efficient recycling processes for the transformation of solid waste and the protection of natural resources located in the region and the area of influence. The exposed research develops a value chain prototype for the opening of a recycling plant making use of the Lean Manufacturing technique called VSM proposed for two production lines of MSW obtained from a recycling system of PET, cardboard and paper implementing a work methodology developed from this improvement,later a design of the physical elements (machinery) was elaborated using SolidWorks technological software; Thus, it is also concisely shown the benefits that it will bring to sustainable development and the contribution to ODS 12 through community intervention and the generation of employment sources with the creation of the recycling plant in the proposed municipality.

VSM, Recycling Plant, Prototype, Value Chain

Resumen

En la actualidad, la conservación integral del medio ambiente representa una de las preocupaciones de mayor impacto en el ámbito social debido a que la preservación y el manejo del medio ambiente se interrelacionan directamente con las diferentes actividades productivas que contribuyen al bienestar económico y familiar de los individuos. Con el crecimiento poblacional, la generación de residuos sólidos urbanos (RSU) se ha incrementado, provocando diversos problemas que afectan la salud, la contaminación y los aspectos de imagen de los sitios urbanos, por esta razón, se busca poner en práctica alternativas viables que lleven a diseñar procesos de reciclaje eficientes para la transformación de los residuos sólidos y la protección de los recursos naturales ubicados en la región y el área de influencia. La investigación expuesta desarrolla un prototipo de cadena de valor para la apertura de una planta de reciclaje haciendo uso de la técnica de Lean Manufacturing denominada VSM propuesta para dos líneas de producción de RSU obtenidas de un sistema de reciclaje de PET, cartón y papel implementando una metodología de trabajo desarrollada a partir de esta mejora, posteriormente se elaboró un diseño de los elementos físicos (maquinaria) utilizando el software tecnológico SolidWorks; así mismo se muestra de manera concisa los beneficios que traerá al desarrollo sostenible y la contribución al ODS 12 a través de la intervención comunitaria y la generación de fuentes de empleo con la creación de la planta de reciclaje en el municipio propuesto.

VSM, Planta de reciclaje, Prototipo, Cadena de valor

3.1 Introduction

The indices of impact on the environment in Mexico grow exponentially to alarming levels, in recent years various problems have contributed to the generation of the aforementioned problem one of the factors with the greatest presence focuses on the availability and accumulation of various domestic solid waste in countries in develop which do not have physical infrastructures assigned as warehouses or processing units to promote the improvement of recycling systems,due to the lack of a feasibility analysis that supports a proposal for the construction of validated recycling plants through the application of quantitative and qualitative tools. In response to the above, a correlational study is presented through the analysis of the "VSM" value chain for the opening of a recycling plant in 2 municipalities located in the Sierra Norte of the State of Puebla. In the first instance, a feasibility study was applied analyzing the habits and opinions of the inhabitants of the aforementioned area, then the value chain was created by identifying the main products to be manufactured, the potential suppliers and the target market. In this way, the cost margins are also calculated in comparison with the already established values of similar products. In order to optimize the production process, a mapping of the value stream is designed, determining the optimal operations involved in the processing of the selected waste. Subsequently, a prototype of a potentially recyclable VSM processing line is designed, in the SolidWorks technological software it shows the necessary machinery for each operating station.

Applied research will enrich the sustainable development of the region by directly contributing to Sustainable Development Goal number 12 of the 2030 Agenda (ODS 12), efficiently managing a work system for the elimination of solid waste from the inhabitants, managing efficiently the availability of material resources of the municipalities.

3.2 Problem Statement

The municipality of Huauchinango belonging to the Sierra Norte de Puebla does not have an official sanitary landfill for the treatment of solid waste, causing serious environmental problems for society that are reflected in: a negative urban image, pollution of streets and rivers that causes outbreaks infection, improper incineration practices that release toxic gases into the atmosphere and the environment in which they are located; This growing problem stems from the exponential growth of the population.

According to the percentage of birth (1.70%) and mortality and (1.55%) extracted from INEGI, it was diagnosed that by the year 2022 the municipality of Huauchinango will have approximately 110,022 inhabitants, of which each inhabitant discar an average of 750 grams of RSU daily, generating a total of 82,516.5 kilograms per day. These wastes end their service period in dumps or landfills; Most of the time these materials are recoverable and are suitable to be subjected to recycling processes, in the aforementioned municipalities 9.24% of the total garbage corresponds to the classification of PET and its derivatives, while paper and cardboard make up the 20.64%.

Recycling processes allow the use of the various resources manufactured in sub-processes, positively lengthening the use of the life cycle in subsequent activities to make discarded; The sale of products that result from the combination of elements extracted from recycling with various raw materials generates a source of income for the social sector, thus also ensuring the consumption of goods and resources that will progressively reduce the current ecological footprint. The construction of industries, businesses that are dedicated to recycling contribute directly to ODS 12; With the opening of the recycling plant, a viable solution is evidenced to turn the problem of excess waste into an opportunity for sustainable growth for the municipality.

3.3 Justification

Currently, the amount of MSW (Urban Solid Waste) produced is increasing due to the fact that the population growth rate has constantly increased and there is no methodology in the garbage classification and recycling processes. According to the National Institute of Geography and Statistics (INEGI), more than 2,116 tons of plastic waste are generated annually, and it is essential to create organizations that contemplate the recovery of different components by applying manufacturing methodologies corresponding to recycling.

The State of Puebla is considered one of the states with a reduced culture with respect to implementing recycling systems, on average it reuses only 30% of the total MSW (INECC-SEMARNAT, 2016), a situation that is reflected locally in minimum levels of recycling. The described proposal focuses on two of the main municipalities of the Sierra Norte de Puebla: Huauchinango and Xicotepec, which together have a population of approximately 197,782 in these regions, minor efforts have been concentrated to introduce methods that redirect the correct management of MSW. At the beginning of 2010, seeking to introduce a differentiation collection method, the program known as "My Clean Huauchi" was opened, reaching a reduction rate of 30% of the waste generated being sent to the sanitary landfill that was in use until that date, The planning did not reach the proposed goals and the mixed collection methodology was reintegrated, which is made up of citizen participation and direct delivery to the collection transport units; In subsequent periods, a lack of control was noticed in the final placement of the RSU, depositing them in unauthorized places, significantly reducing the environmental quality indicator in various areas and area of influence, affecting the urban image and the naming of the municipality as a magical town (Ministry of Tourism, 2017).

Considering that in the two aforementioned municipalities considerable amounts of potentially recyclable garbage are discarded daily, of which 9.24% is PET and 20.64% is paper-cardboard and taking into account the economic benefit that will result from the sale of these wastes to superior processing plants, a value chain prototype is proposed for the opening of a dual recycling plant for paper-cardboard and PET

3.4 Objectives

3.4.1 General objective

To develop a value chain prototype for the opening of a recycling plant in the Municipality of Huauchinango providing a positive benefit to the sustainable development of the region, through the application of the VSM analysis tool, the use of software, technological and the evaluation of variables involved in the recycling process.

3.4.2 Specific objectives

- Application of a data collection instrument to know, identify and determine the degree of acceptance and opportunity to open the recycling plant in the Municipality of Huauchinango.

- Diagnose the optimal and sustainable cardboard, paper and PET transformation processes of a recycling plant through a value mapping (VSM) to detect the activities that do not add value to the final product.

- Develop a prototype of a PET and cardboard recycling line through SolidWorks technological design software.

3.5 Scope of the investigation

- The documentary research focuses on the Huauchinango and Xicotepec regions, the data presented correspond to these two areas.

- The VSM model includes two production lines (line A = PET, line B = Paper and Cardboard) according to the amounts of waste produced in the two regions.

- A model of a recycling plant is shown; designed in SolidWorks describing the characteristics of the machinery and optimal working conditions.

3.6 Theoretical Framework

In the first instance, mention will be made of the term environment due to the importance it represents in the development of this application. The environment is defined as a set of physical and biological characteristics that interact between the different components that make up a habitat or ecosystem (Gabriel Quadri, 2006). Next, concepts related to the subject of study are presented.

3.6.1 Recycling

Chang Marcos Alegre, (2005) indicates: "Recycling is the result of a series of activities, through which materials that would become waste are diverted, and separated, collected and processed to make used as raw materials in the manufacture of articles that previously they were made only with virgin raw material. Recycling is to carry out a practical and concise method that originates from one thing to another, it is done in a previous way that is used for its progression, it is an ecological measure to promote reuse that carries with it the reduction of waste and the reduction of the consumption of natural resources (Torres Guarniz, 2016).

3.6.2 Types of recycling

*Selective Collection***:** It is the separation of the components of the garbage, for their direct recovery. For the success of this system, citizen participation is needed, on the one hand, by having to select at source (homes) and deposit the waste to be recovered in separate containers, the selective collection of solid waste implies that the fractions are separated at the source and later collected also separately; This separation greatly reduces the mixing and contamination of materials, which consequently increases their quality (Torres Guarniz, 2016).

Selection Global: It is a not recommended system for our reality, since it is more expensive and complicated. It is a technique based on gross or global waste, used in the mining and metallurgical industry, such as pneumatic crushing, screening and classification, wet, electromagnetic, electrostatic, optical and flotation separations by foams for obtaining and purifying metals and glasses. It is a process that is not recommended because it is expensive and presents great difficulty. It is a process through the garbage discarded in the industry, and they need to be classified to obtain matter such as glass and minerals. (Reyes Curcio, Pellegrini Blanco & Reyes Gil, 2015).

Therefore, it is advisable to carry out selective collection because it not only encourages the recycling and the valuation of municipal solid waste, but also serves to separate hazardous waste thereof.

Recycling of paper

It consists of making paper, using as raw material used or not used papers, such as: paper scraps, cardboard and cardboard, generated during the manufacturing processes of these materials or their transformation into other articles, or also generated in printING. Recycled paper contains secondary fibers that is they have already passed through a paper machine at least once with substances that are impervious to moisture, contaminated with chemicals harmful to health such as: toilet paper, paper towels, napkins and tissues. (Escobar, Quintero and Serradas, 2006)

The recycling of plastics:

It can be classified according to four types of technologies: primary, secondary, tertiary and quaternary.

Primary or pre-consumer recycling: It is the recovery of these wastes carried out in the generating industry itself or by other processing companies. It consists of the transformation of plastic waste through conventional processing technologies, into products with characteristics equivalent to those of products made from virgin resins. These wastes are made up of defective artifacts, discards from molds or from cutting and processing sectors. (Escobar, Quintero, Serradas, 2006).

Secondary or post-consumer recycling: It is the transformation of plastic waste from products thrown away. The materials that enter this group come from garbage dumps, composting plants, selective collection systems, scrap metal, goats. They are made up of the most different types of material and resins, which requires a good separation, so that they can be reused (Escobar, Quintero, Serradas, 2006).

Tertiary recycling: It is the transformation of plastic waste into chemical products and fuels, through thermochemical processes (pyrolysis, catalytic conversion). Through these processes, plastic materials are transformed into raw materials, which can again originate virgin resins or other substances of interest to the industry, such as gases and oils (Escobar, Quintero, & Serradas, 2006).

3.6.3 Value chain

The value chain of an organization includes the main activities that create value for customers and support activities. The chain also makes it possible to identify the different costs incurred by an organization through the different activities that make up its production process, which is why it is an essential element in determining the cost structure of a company. Each activity in the value chain incurs costs and limits assets, in order to achieve their due analysis and consideration, they allow to improve the techno-economic efficiency of a company, a group of companies or a certain industrial sector. From a strategic point of view, the value chain of a company and the way in which it carries out each activity reflects the evolution of its own business and its internal operations; the strategy, the approaches used in its execution and the fundamental economics of the activities themselves. Consequently, it is normal for the heat chains of rival companies to differ, a condition that complicates the task of evaluating the relative cost positions of rivals. (Quintero & Sánchez, 2006)

3.6.4 Value Stream Mapping (VSM)

The mapping of the value stream or VSM (Value Stream Mapping), is a very important Lean tool, it contains all the actions, both those that add and do not add value within the manufacture of a product from the raw material to the finished product in customer's hands. The VSM focuses more on the flow of processes and thus be able to identify improvent areas (Villaseñor, 2007, as cited in Masapanta, 2014).

While for Paredes Rodríguez (2017) Value Stream Mapping or value chain mapping (VSM) is a Lean Manufacturing management tool that uses symbols, metrics and arrows to show and improve the flow of inventory and information required to generate a product or service that is delivered to a consumer, seeking that he only pays for the activities that generate value to the product.

3.6.5 Prototype

According to the RAE (2020) a prototype is the original copy or first mold in which a figure or something else is manufactured. The prototype is, in a general way, a preliminary model of the product that is being designed; As such, this prototype can include the representation of the object, the demonstration of its characteristics or the simulation of the functionality of the product (Maner, 2013).

Inspirational prototypes are developed in the earliest stages of projects and with the simplest and cheapest means possible. Its objective is to explore the main aspects that define a problem or opportunity and facilitate the search for more and better solutions. (CORFO, 2016)

The purpose of evolution prototypes is to mature or improve one or more previously generated prototypes. What is sought with them is to be able to continuously learn and make failure a useful and integral aspect of the innovation process. (CORFO, 2016)

The validation prototypes (type of prototype developed in this application) are intended to validate, through a structured process, the different hypotheses on which the solution is based when it is close to its final version. (CORFO, 2016)

3.7 Methodology

3.7.1 Questions to investigate

- What is the optimal recycling procedure for paper, cardboard and PET?

- What machinery and tools make up a recycling plant?

- What value engineering tool can be useful to analyze the procedure of a recycling plant?

- What range of productive logistics problems can VSM address for the opening a recycling plant?

3.7.2 Tipe of investigation

The research carried out is exploratory-correlational. According to Hernández (2010), exploratory analysis procedures are carried out when the objective is to examine a poorly studied topic or research problem, about which there are many doubts or which has not been addressed before. That is, when the review of the literature revealed that there are only non-researched guides and ideas vaguely related to the study problem, or if we want to inquire about topics and areas from new perspectives. So far there are no studies that allow us to know the degree of acceptance and feasibility for the opening of a recycling plant in Huauchinango. While the same author establishes that correlational studies are intended to know the relationship or degree of association that exists between two or more concepts, categories or variables in a particular context. In this research, in addition to finding what is happening in the municipality, the possible causes that intervene in the problem raised will be analyzed. Therefore, by means of descriptive surveys, we will be able to determine the current situation of the municipality with respect to the treatment carried out to the garbage after its collection.

3.7.3 Research hypothesis

Hypothesis 1: The opening of a recycling plant in the municipalities of Huauchinango and Xicotepec will significantly reduce the existence of products derived from PET, cardboard and paper.

Hypothesis1, analyzes the decrease in damage caused to the environment, as a result of the consumption of products with Polyethylene Terephthalate (PET), cardboard and paper. With the recycling plant it is planned to process 29.87% of the potentially recyclable waste that includes PET, paper and cardboard.

Hypothesis 2: The study and analysis of the value chain, through the VSM, for the opening of a recycling plant will provide us with the necessary tools to build a prototype and adapt it to the proposed regions.

The VSM is an applicable technique in the process of improvement and redesign, based on 4 phases: diagnosis, planning, design, implementation of improvement processes. Through of this tool visualize and identify the problems or waste of the lines of production generating a competitive advantage for the establishment of guidelines that allow the flow of information between the members that make up the value process.

3.7.4 Variables

-   Solid Urban Waste (MSW): They are considered organic and inorganic waste produced by a social community, they are characterized by being sub-classified into various groups; 70% of these are sent to clandestine garbage dumps or deposited in different parts of the region, affecting the urban image and the health of the members of the different communities.

-   Recycling plant: Physical infrastructure that is identified as contributing to the correct transformation process of the MSW, within the processes carried out in the production lines, different materials such as PET, paper and cardboard are transformed and reused, providing them with a second use and obtaining an economic benefit from the sale of the products obtained.

3.7.5 Methodological process

Next, the methodological process applied to achieve the proposed objectives is described (Figure 3.1 Methodology used).

Figure 3.1 Methodology used

Stage 1. Collection of information.	
Documentary research.	Survey application.

Stage 2 Analysis of the value chain.	
Phase 1. Choosing a product family.	Phase 2. Mapping of the initial situation.

Stage 3. Development and design of a recycling plan prototype.
Prototype design in SolidWorks design software.
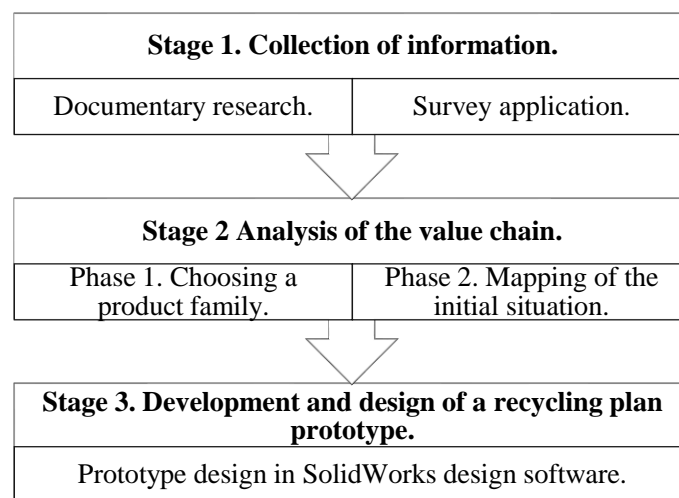
Source: Own elaboration

The different stages are described below:

3.7.6 Stage 1. Collection of information to determine degree of need and acceptance of the opening of a recycling plant

Stage 1 was carried out by conducting a documentary analysis supported by the application of techniques corresponding to field research; Through the documentary, information related to existing cases of recycling plants in the state, as well as the country, was collected. The current advantages of opening a recycling plant were also studied.

In the field research, a survey was designed and implemented as an instrument for collecting information; The survey was structured through 10 multiple-response questions related to: the number of people living in your home, the approximate amount of waste it generates, the knowledge you have about waste treatment as well as the advantages proposed by the waste separation, finally the degree of acceptance of the opening of a recycling plant in the region (Table 3.1 Methodology used**.**).

Table 3.1 Survey questions

N	Question
1	¿How many inhabitants are part of your household?
2	¿How do you rate the garbage problema in your locality, neighborhood, or municipality?
3	How much waste do you normally accumulate per day?
4	¿In your home do you have the habit of separating recyclable garbage (PET, paper and cardboard) and classify?
5	¿If you separate and classify PET, cardboard and paper in your home what do you do with them?
6	¿Do you know of any program, campaigns or movements on the classification of reciclable waste?
7	¿Would it be integrated into programs for the separation and and classification of reciclables?
8	¿If you had the opportunity to generate income with your recyclable solid waste (PET, cardboard, paper) through separation and classification, would you carry out recycling processes?

Source: Own elaboration

For the application of the survey, the following data were taken into consideration. In the first instance, the size of the study population was determined. Taking into account that the municipality of Huachinango has a population of 110022 inhabitants and Xicotepec a population of 87,760, considering that 56.96% of the total community represents the population that generates the greatest amount of recyclable MSW. It is determined that the total population of both municipalities is 112,656. Once the total population has been determined, the sample size calculation is carried out (1) using the formulation of Murray and Larry (2005) for sample size with a finite population and, taking into account the statistical values that are obtained. Indicate (Table 3.2 Statiscal values for the calculation of the study sample), a size (n) of 383 people was obtained.

$$n = \frac{N*z_a^2*p*q}{e^2*(N-1)+z_a^2*p*q} = \frac{(112656*1.96^2*.5*.5)}{((.05^2*112655))+(1.96^2*.5*.5))} = \mathbf{382.857} \tag{1}$$

Table 3.2 Statiscal values for the calculation of the study sample

Value corresponding to the Gauss distribution Zα= 0.05	Z	1.96
Expected prevalence of the parameter to be evaluated, in case of unknown and, considering equal probabilities to make the simple size larger.	p	0.5
1-p, 1-.5	q	0.5
Size of the population to study.	N	112,656
Mistake that is expected to be made with a good requerement of sampling.	e	.05

Source: Own elaboration

The results obtained when carrying out the survey and in conjunction with the statistical analysis, allowed to determine the habits of the members of the community with respect to the treatment. Of waste, as well as its appreciation point in relation to the opening of the recycling plant.

3.7.7 Stage 2 Analysis of the value chain

For the analysis of the value chain, a literary review was developed which allowed develop the ideal sequence to generate the value chain:

Phase 1. Selection of the family of recyclable products that are mainly produced in the Huauchinango region

The value flow system is structured based on recyclable products, which is why a quantitative analysis is carried out to establish the products that are most consumed in the region, later the technique for mapping VSM processes was selected which allowed to show the various recycling operations that constitute the manufacturing process (Rother, 1998).

The generation of RSU on average in the homes of the municipalities analyzed is established at 750 grams per inhabitant, according to the classification proposed by SEMARNAT, the percentages for each group of waste, organic, potentially recyclable and others are shown in the table (Table 3.3 Percentage of waste generated).

Table 3.3 Percentage of waste generated

Type of waste	Percentage
Organic	50%
Potenctially recyclable	30%
Others	20%
TOTAL	100%

Source: SEMARNAT

The information used to choose the family of products for the VSM study is that which corresponds to potentially recyclable waste, of which the most frequent are: PET, paper and cardboard, according to the analyzed population there is a total of 197782. Inhabitants (Huauchinango and Xicotepec), if we consider that on average they generate a total of 750 grams daily, the total RSU is 148336.5 kg, according to the classification proposed by SEMARNAT it follows that the total potentially recyclable waste is 44.501 kg, of which 9.24% is PET and 20.64% of paper and cardboard.

Phase 2. VSM (Current situation of the recycling process)

After the selection of the product family, the process began with the mapping, collecting information from similar processes that have turned out to be effective recycling plants located in other entities, for the information extraction the route of the product family was followed. Contemplating the mapping from the input stage of raw material to the output of the finished product, that is, a system called door-to-door was applied (Rother, 1998).

The analysis to carry out the mapping process originates with the knowledge and description of the optimal activities for carrying out the recycling processes for potentially recyclable Urban Solid Waste, for this the families of products were determined which by their volume and constancy were the PET, paper and cardboard, later the current state of each of the selected products was measured, in terms of its flow of quantity per unit of time, later with the adjustments and implementations of necessary lean manufacturing tools the Future measurement, in which, the flow ratio quantity per unit of product collection time should be greater, finally, a work plan is established which serves as support for the constant maintenance of the value flow of the recycling plant.

3.7.8 Description of the PET process

It is observed that the PET process contains seven operations which are described below continuation:

- **Deposit in the hopper:** The PET (bottles) is deposited in the hopper to move to the next operation.

- **De-labeling:** By means of a conveyor belt they pass to the machine so that the labels are removed from the PET bottles.

- **Grinding:** PET bottles are crushed into flakes the machine has fixed and movable blades that adjust for better performance.

- **Washing:** The flakes are washed to remove impurities and rinse the surface, it has stainless steel reaction tanks, in which the material is driven and aggressively washed. Specially designed machine impellers cause the flakes to collide with each other rather than against walls to prevent wear on the machine.

- **Spin:** It goes through a spinning process that removes the water in an economical way, preventing the temperature from lowering so that the impurities that were previously removed do not re-adhere.

- **Drying:** Consists of drying the leaflets, the greater amount of water is reused, the leaflets come out drier with the unit of the environment.

- **Packaging:** The flakes are bagged in 60 kg sacks and are stored for later commercialization.

3.7.9 Description of the paper and cardboard process

In the paper and cardboard process, it contains five operations which are described below:

- **Fill mill:** The operator is in charge of placing the paper and cardboard in the mill to that can be shredded.

- **Shredding:** An assigned operator is in charge of shredding the 100 kg of paper and cardboard, the essential thing about the shredder are its blades, This kept lubricated for smooth operation find optimal.

- **Fill press:** the paper and cardboard (already shredded) is placed in the press, inside this there is a plate that crushes it, then paper and cardboard continue to be placed until a bullet is formed and it is extracted.

- **Compact:** The operator assigned to this operation has to place the paper and cardboard and the compactor because it is made up of a metal plate that is ordered to push the raw material to an iron box and thus obtain the plates of 2x1x1.

- **Warehouse:** Bales of paper and cardboard are stored in the product warehouse finished.

Once the operational process of the recycling plant has been identified, the VSM process mapping.

3.7.10 Stage 3 Development and design of a recycling plant prototype

Considering what was obtained in the value chain mapping, in which the tools, limitations and procedures necessary for the optimal operation of a recycling plant are detailed, the design of the plant prototype will be carried out, this through the software SolidWorks design technology.

3.8 Results

3.8.1 Results of the surveys

The definition of the means for the extraction of information, as well as the collection of proposed data, and the mapping process proposed in the methodology allowed to obtain the following results for each of the stages described above (Figure 3.1 Methodology used).

The results of Stage 1 made it possible to determine the degree of need and acceptance of the opening of a recycling plant through the observation of the results obtained from the survey: As a first intervention, the number of people living in each household is analyzed (Graph 3.1 Results obtained from question 1) Therefore, we note, according to this, more than 50% of the population lives in the company of 3 to 4 people. This is reflected with the average amount of garbage that a person generates per day (1.2 Kg) representing approximately 4.8 kg of garbage, of which 30% is potentially recyclable. This question is also related to what is obtained in Graph 3.3, since it is indicated that 57% of people claim to generate between 1 and 2 kg of garbage daily.

Graphic 3.1 Results obtained from question 1

Number of people living for each house
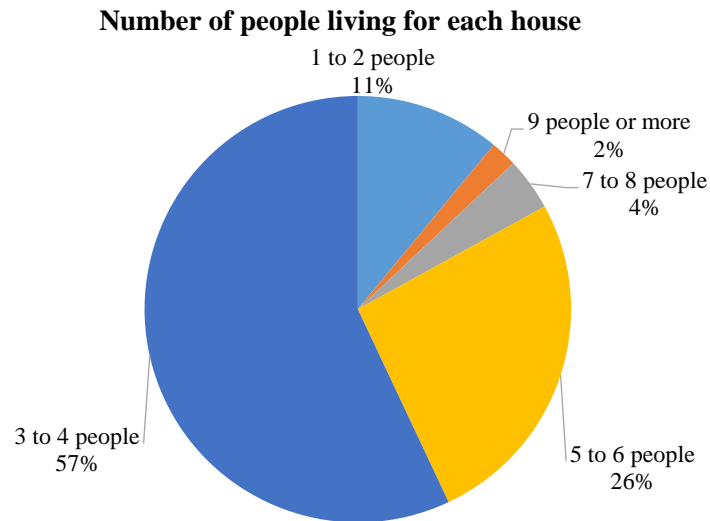
Source: Own elaboration with data obtained from the survey

Subsequently, it is distinguished that 76% of the people consider the garbage problem in Huauchinango and Xicotepec at a critical and bad level (Graph 3.2 Results obtained from question 2), therefore, it is a visible problem and of relevance for their study.

Graphic 3.2 Results obtained from question 2

Consideration of the garbage problem
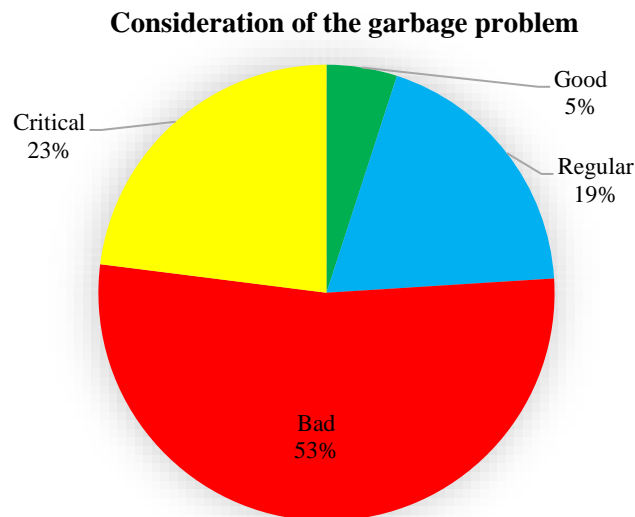
Consultation Source: Own elaboration with data obtained from the survey

As mentioned above, this question is related to the number of people who live in a household, since according to this number it is the amount of garbage that is generated per dwelling unit. 57% of the people surveyed affirm that they generate between 1 and two kg daily, while 24% of them mention generating less than one kg. There are cases where the daily garbage generation is 3 to 4 kg (14% of the study population), while only 5% say they generate the amount of 4 kg or more of garbage daily. Consequently, these data are relevant, since they allow us to determine the approximate amount of garbage that can be collected for later treatment in the recycling plant (Graph 3.3 Results obtained from questions 3).

Graphic 3.3 Results obtained from questions 3

Amount of garbage to collect
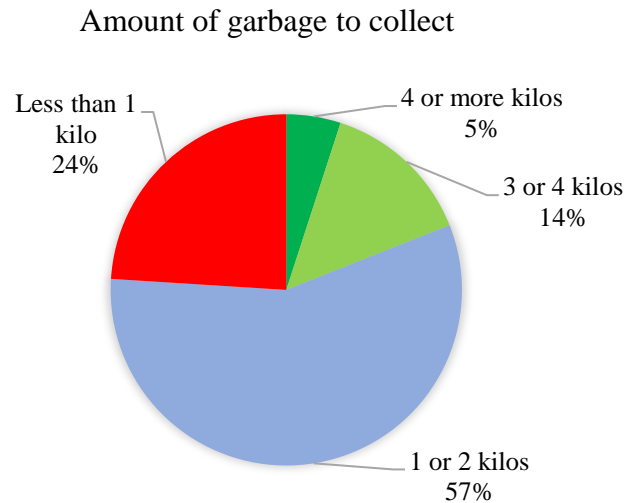
Source: Own elaboration with data obtained from the survey

Now, focusing on the habits that people have regarding waste treatment (Graph 3.4 Results obtained from questions 4), it is observed that 70% of people do not classify waste. To be discarded, a fact that is useful due to its relationship in the process of collecting waste for its subsequent treatment.

Graphic 3.4 Results obtained from questions 4

Garbage selection habits
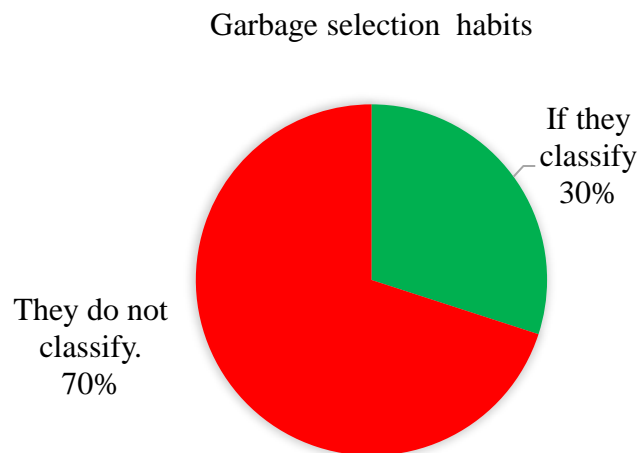
Source: Own elaboration with data obtained from the survey

Regarding the treatment of waste by the community, it is observed that 54% send it to non-established dumpsites, 19% prefer to sell it and 27% give it away to third parties people (Graph 1.5 Results obtained from questions 5).

Graphic 3.5 Results obtained from questions 5

Treatment of waste by the community
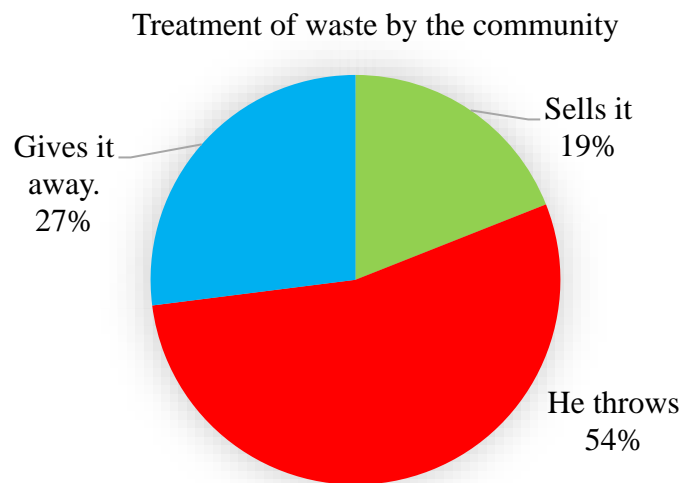
Source: Own elaboration with data obtained from the survey

In order to know the classification habits of the social environment, it was questioned about the knowledge of programs or campaigns for the separation and classification of recyclable waste, and it was found that 90% of the people are unaware of the operation of the collection systems (Graphic 3.6 Results obtained from questions 6).

Graphic 3.6 Results obtained from questions 6

Knowledge of collection systems.
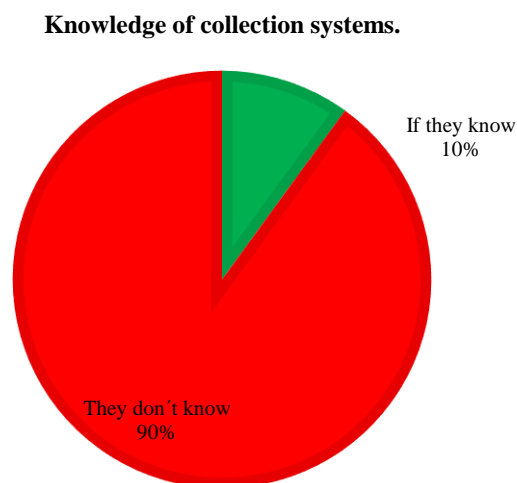
Consultation Source: Own elaboration with data obtained from the survey

The interest in knowing and taking part in recycling processes is visualized in question number 7, where 88% of the surveyed population shows a positive interest in participating in MSW separation campaigns (Graphic 3.7 Results obtained from questions 7), this being a favorable result for the promotion of recycling in the inhabitants, considering them as the main suppliers to supply the production lines of the recycling plant (Graphic 3.7 Results obtained from question 7).

Graphic 3.7 Results obtained from questions 7

Commitment to participate in collection campaigns

There is no
commitment
12%

Is there is
commitment…
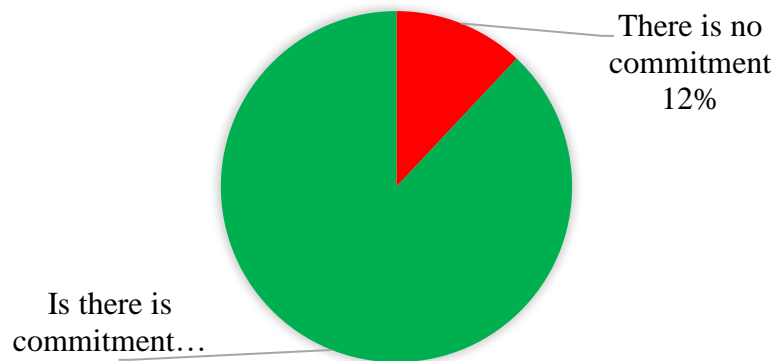
Consultation Source: Own elaboration with data obtained from the survey

Next, the perspective of the respondents was deepened, directing them towards the possibility of generating income with the sale of waste for recycling, the trend shows that 92% of them find the idea attractive (Graph 1.8 Results obtained from questions 8).

Graph 1.8 Results obtained from questions 8

Idea of generating revenue from recycling

No
8%

Yes
92%
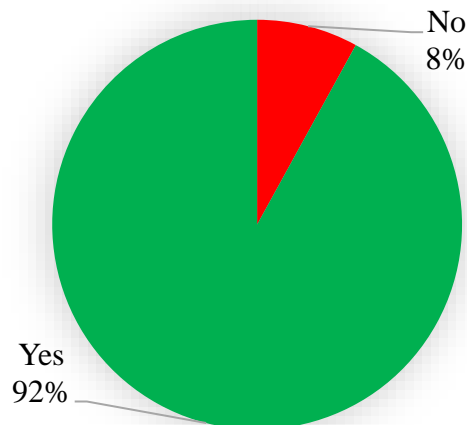
Consultation Source: Own elaboration with data obtained from the survey

While 78% of the population consider the opening of a recycling plant in the municipality beneficial (Graphic 3.9), indicating that it would help to reduce the environmental impact of the waste generated day by day. 15% consider the idea as regular, so it can be taken as positive for the study, and only 7% believe that the idea is bad.

Graphic 3.9 Results obtained from questions 9

How would you rate the idea of a recycling plant in the
Sierra North of Puebla.

Negative
7%

Regular
15%

Good
78%
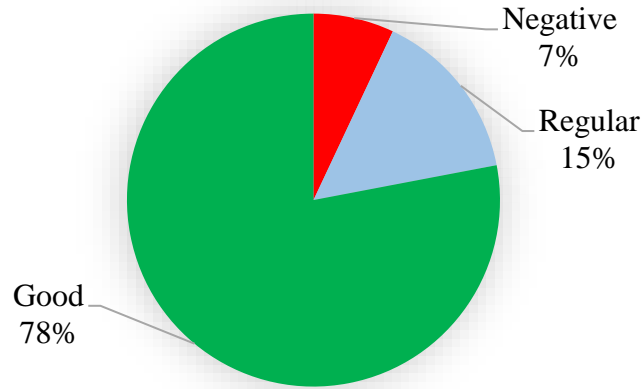
Source: Own elaboration with data obtained from the survey

To conclude the analysis of the results of the study population, it is deduced that 89% believe that the opening of a recycling plant in the Municipality would lead to a reduction in pollution in Huauchinango and Xicotepec (Graphic 3.10 Results obtained from questions 10).

Graphic 3.10 Results obtained from questions 10

¿Do you think that a recycling plant will reduce the
pullution problem in in the Sierra North of Puebla?

Not
interested
11%

If you are
interested
89%
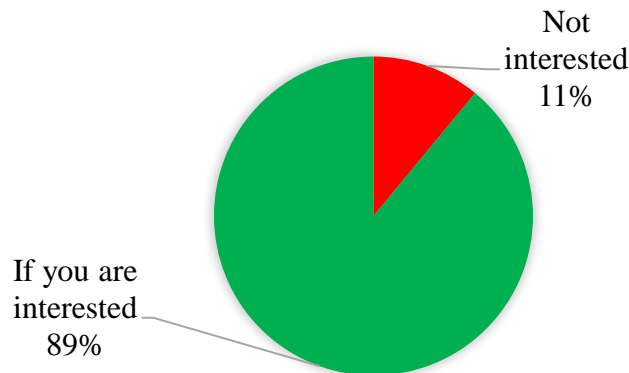
Source: Own elaboration with data obtained from the survey

3.8.2 Results of the value chain analysis

Phase 1: Choice of a product family

The value chain analysis process in Phase 1, conducive to the choice of the product family taking into account potentially recyclable RSU (Figure 3.2 Family of products for Value Mapping).

Figure 3.2 Family of products for Value Mapping

Source: Own elaboration

Through the choice, the final product that the company will offer is determined according to the previously selected products (Figure 3.3 Presentation of final product for sale).

Figure 3.3 Presentation of final product for sale
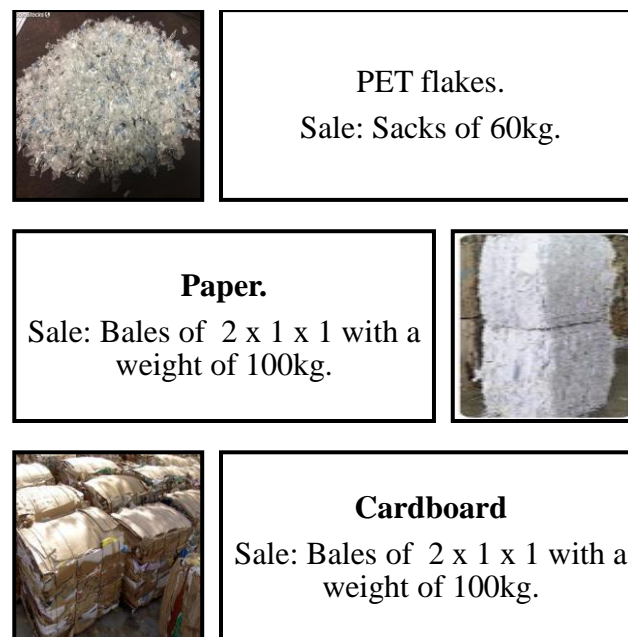
Source: Own elaboration

As mentioned in the methodology, in the market there are several companies and organizations dedicated to the purchase and sale of recycling, however, we undertook the task of looking for some possible clients close to our municipalities, which are dedicated to the purchase of recycled products , which is why the acceptance of the products manufactured by three main clients is proposed (RECYCLING TALISMÁN SA DE CV, COMERCIALIZADORA INDUSTRIAL MILLOP SA DE CV, RECYCLE TOGETHER) (Figure 3.4 Main customers by product sales), located in the area of influence, for the selection of the aforementioned clients, the following two variables were considered: 1) Wholesale purchasing system; the customer makes the purchase in large volumes of product. 2) logistics infrastructure (means of travel and own means of loading), considering that transportation costs are absorbed by customers, it is required that they have logistical means to transport the purchased product.

In this way, it is considered that each time the customers place the order, the recycling company, according to its planning, will execute the necessary activities with the different departments, such as raw material warehouse (collection of separated or non-separated materials), production (garbage separation area) and finishing. product warehouse (materials segmentation area), to meet the needs presented in a timely manner, as well as primary suppliers are identified considering waste collection branches for recycling in order to provide a greater economic benefit to the region (Figure 3.5 Suppliers of waste for processing in recycling plant).

Figure 3.4 Main Clients for product sales

RECICLAJES TALISMÁN S.A. DE C.V.
Address: Ricardo Flores Magón #77. Puebla.

COMERCIALIZADORA INDUSTRIAL MILLOP S.A. DE C.V.
Address: Av. 9 Pte. Puebla

RECICLEMOS JUNTOS
Address: Av. San Antonio #202. CDMX

Source: Own elaboration

Figure 3.5 Suppliers of waste for processing in recycling plant

COMERCIALIZADORA DE ACEROS ISLAS
Address: Rayón #44. Col. El Paraíso

COMPRA Y VENTA DE DESPERDICIOS INDUSTRIALES
Address: Artículo 115 Constitucional, Col. El Potro

CHATARRA
Address: Doctor Río de la Loza, Col. Santa Catarina

RECICLADORA DE MATERIALES
Address: Negrete #14 Col. Centro

BODEGA DE RECICLAJE PAPEL Y PLÁSTICO
Address: Francisco Oropeza, Col. El Ocote

RECYCLING SYSTEM
Address: Hermeregildo Galeana, Col. El Paraíso

CENTRO DE RECICLAJE LA COLMENITA
Address: El Potro

Source: Own elaboration

In the same way, the purchase and sale prices of each of these waste for treatment are established, based on what is estimated by the market value (Table 3.4 Purchase and sale price for product).

Table 3.4 Purchase and sale price for product

	Purchase	Sale
PET (1 kg)	$ 2.50	$ 5
Paper (1 kg)	$0.70	$ 1.50
Cardboard (1 kg)	$0.60	$ 1

Source: Own elaboration

Phase 2. Mapping the initial situation

The result obtained in phase 2 consists of the development of the current VSM, contemplating that the information flow begins when the client requests the order, established in a total of 71 sacks of flakes and 147 bales of paper and cardboard per day. Where the customer is placed at the top of the diagram and begins the flow of information from right to left, which flows to the production control department, this in turn, verifies availability of raw material and schedules the master plan of production, contemplating the requirements of PET bottles, paper and cardboard, for the elaboration of the products. For its part, the information of the material process flows from left to right, and it starts from the moment the supplier delivers the raw material. Once the above requirements had been identified, the VSM of the PET, cardboard and paper recycling process was carried out, considering the required amounts of raw material for daily processing, operating times and machinery capacities (Figure 3.6 Value mapping of the PET, paper and cardboard recycling plant, locating the bottleneck).

Figure 3.6 Value mapping of the PET, paper and cardboard recycling plant, locating the bottleneck
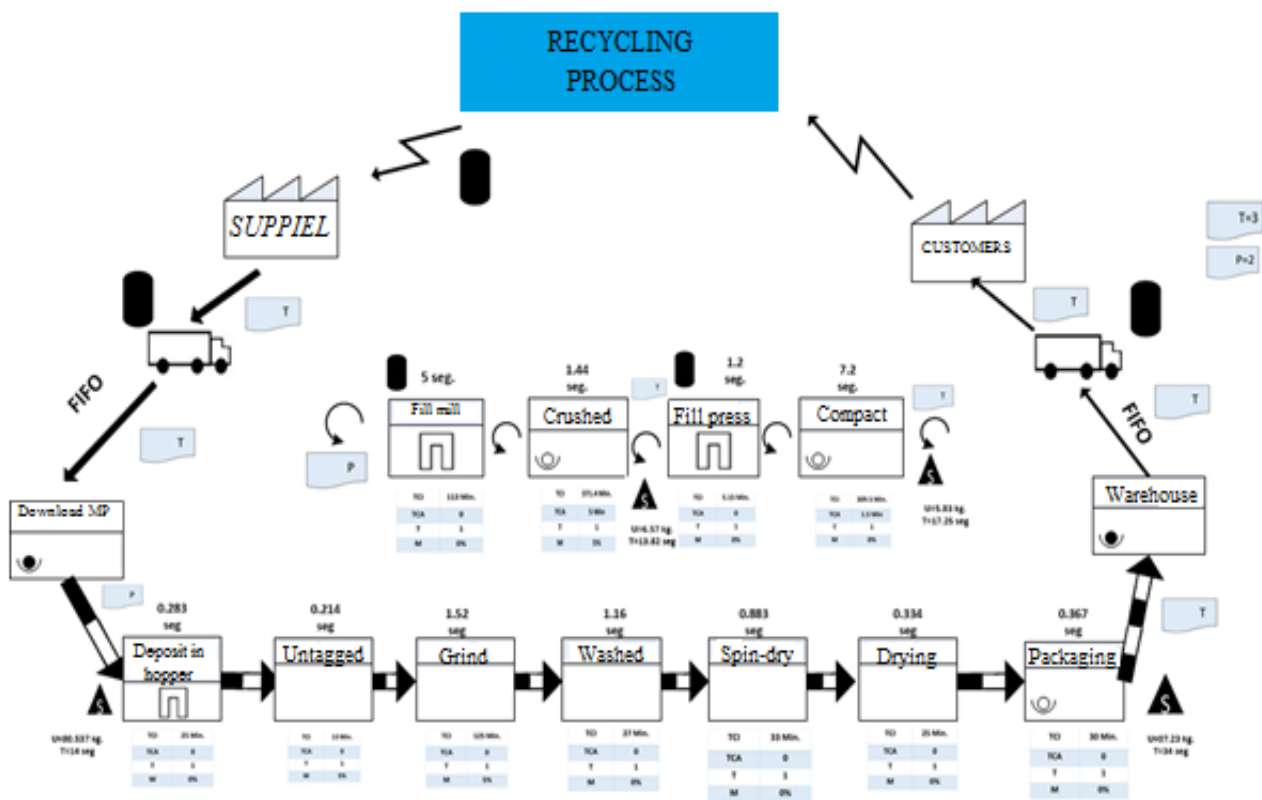
Source: Own elaboration

3.8.4 Development and design of a recycling plant prototype

The design of the recycling plant was based on the sequence of operations that constitute the production process (Figure 3.7 Operations that constitute the production process), designing through SolidWorks technological software the machinery and means of movement required for the process of transformation of PET into flakes and of the paper-cardboard in packages.

Figure 3.7 Operations that constitute the production process

| 1) Conveyor belt | 2) Mill | 3) Washed | 4) Centrifute | 5) Drying | 6) Pressing |
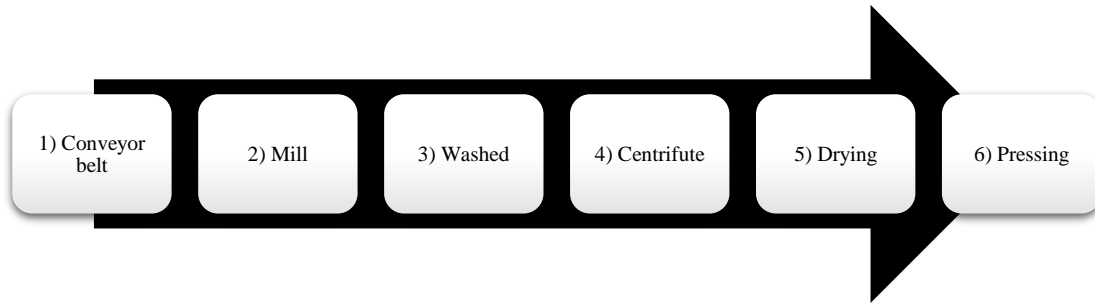
Source: Own elaboration

The means of movement selected and designed are chain conveyors, which due to their construction and low flexibility (Table 3.5 Conveyor Belt Characteristics) stabilize the passage of material; they are welded modular frame structures (Figure 3.8 Conveyor belt), with tall vertical sides, fully equipped with high quality bearings and gearboxes. All chain conveyors can be equipped with stepless speed control ("Modular conveyor belt from ANIS TREND d.o.o. Directindustry", 2020).

Table 3.5 Conveyor Belt Characteristics

Characteristics	
Types	Modular, spike-shaped.
Material	Metal, galvanized, elastomer.
Applications	For the paper industry, for waste treatment, for the recycling industry, for printing.
Resistence	High-strength, wear-resistant, high-strength, with anti-fatigue resistance.
Other Features	Heavy Duty, Heavy Duty, Easy Clean, Continuous, Custom, All Purpose, Chain, Sidewall, Rubber Lined
Width	Mín.: 80 cm (31,5 in)
	Máx.: 200 cm (78,7 in)
Length	Mín.: 4 m (13'01")
	Máx.: 40 m (131'02")

Source: Own elaboration with data obtained from the network

Figure 3.8 Conveyor belt
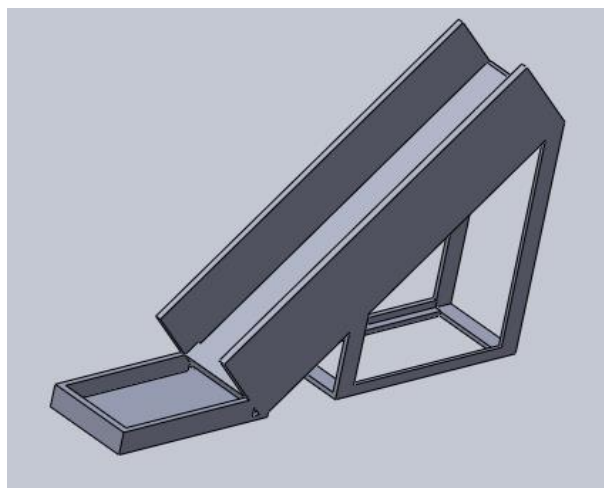
Source: Own elaboration, SolidWorks 2012

The grinding process is carried out using a grinding mill (Figure 3.9 PET mill), this consists of an inlet mouth, which allows access to the plastic pieces prepared to avoid projecting raw material to the outside, through the use of blades (Table 1.6 Features of PET Crusher Mill), the plastic pieces are cut and crushed, later they are passed to a sieve to shape the grains / flakes, to finish the finished product is sent by means of conveyor belts to the assigned warehouse.

Figure 3.9 PET mill
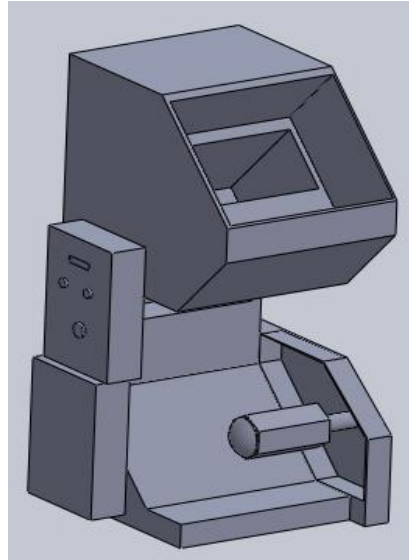
Source: Own elaboration, SolidWorks 2012

Table 3.6 Features of PET Crusher Mill

Technical characteristics	
Model	M20-Motor Eléctrico
Motor	20 HP
KW	15
V/KVA	220 V Trifásico/ 18.75 KVA
Production	Por jornada laboral
Kg/h	180-350
Blades	Varias
Type of cut	Tijera
Rotating	6
Fijas	4
Screen / Flake Size	3/4"
Blades material	Acero D2 56
Sharp frequency	Cada 8 ton
Maximum number of affiliates	45
Approximate weight	400 Kg

Source: Own elaboration with data obtained from the network

The activities that comprise the washing process are carried out in the machine called a paddle washer (Figure 3.10 Paddle Washer) which, through a complementary module (Table 1.7 Add-on module features), washes the material to remove contaminants or unwanted material spilled on the ground plastic flakes (PET, PP, PE, PS, ABS). Thus, it is also used as a means of transport between modules to move the product during the recovery cycle.

Figure 3.10 Paddle Washer
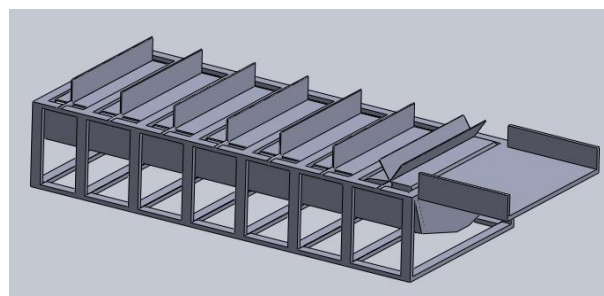
Source: Own elaboration, SolidWorks 2012

Table 3.7 Add-on module features

Characteristics	
Motor	7.5kw/11kw/22kw
Screw diameter	300mm/500mm
Speed	700-900rpm
Length	2500-3500mm

Source: Own elaboration with data obtained from the network

The operating process of centrifugation is carried out in centrifuge machines (Figure 3.11 Centrifuge), by means of these operating actions the moisture is eliminated from the flakes of plastic bottles by high-speed rotating blades. Moisture extraction is done on PP / HDPE / PET materials.

Figure 3.11 Centrifuge
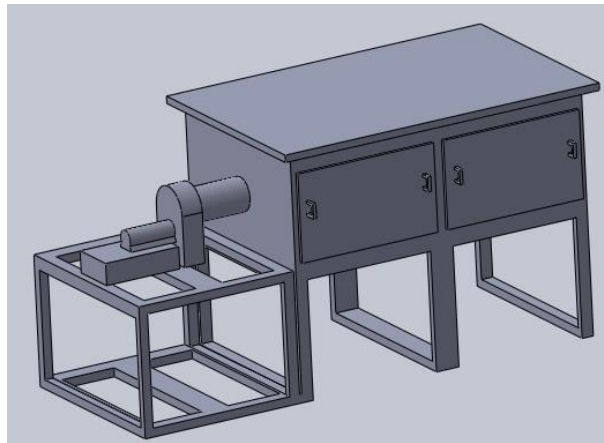
Source: Own elaboration, SolidWorks 2012

The fifth stage of the recycling production process is drying, the operational actions are carried out in the dryer hopper (Figure 3.12 Dryer); This machine guarantees 100% drying of the materials that are introduced through precise temperature adjustments and controls.

Figure 3.12 Dryer
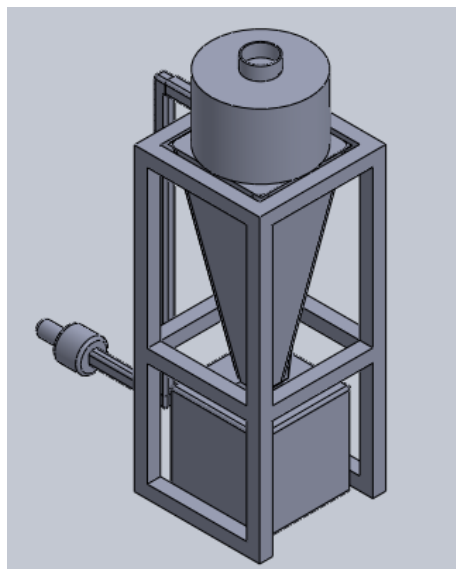
Source: Own elaboration, SolidWorks 2012

The pressing process is carried out in a hydraulic compactor press which compresses or compacts waste materials, reducing the volume of materials providing more space for additional waste material by compacting it until the moment of collection (Figure 3.13 Compactor).

Figure 3.13 Compactor
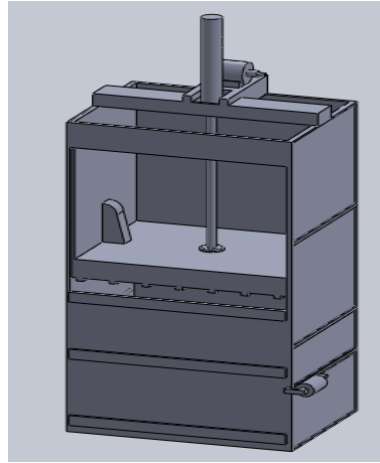
Source: Own elaboration, SolidWorks 2012

The recycling plant model (Figure 3.14 Abstract of recycling production line) for the processing of potential MSW allows the continuous production of waste originated by the inhabitants of the municipalities of Xicotepec and Huauchinango.

Figure 3.14 Abstract of recycling production line
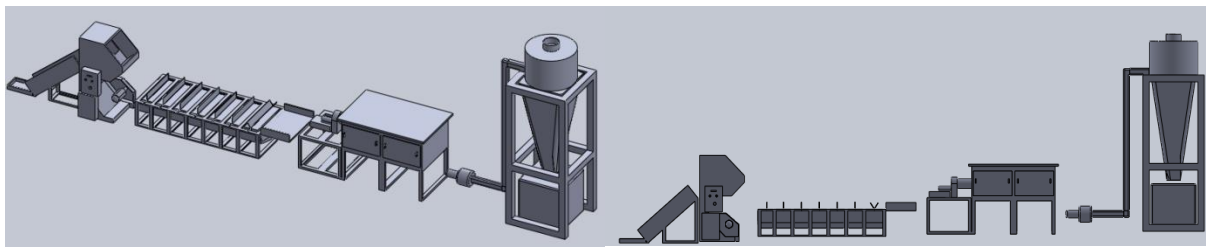
Source: Own elaboration, SolidWorks 2012

The results obtained and described above allow us to compare the hypotheses raised; In reference to Hypothesis 1, it is concluded that the opening of a recycling plant will significantly reduce the existence of products derived from PET, cardboard and paper in the environment, since the population will be able to count on a way to contribute to the environment and receive in return an economic remuneration. Regarding Hypothesis 2, the study and analysis of the value chain through the VSM, for the opening of a recycling plant effectively provided us with the necessary tools to build a prototype, because all the operations involved in each line of processing, and the appropriate machinery for these was identified.

3.9 Conclusions

Fulfilling the objectives set at the beginning of this research and following the suggested methodology, a study of the value chain of the PET, cardboard and paper recycling process was carried out, in which the operations, machinery, and client suppliers that comprise it were identified. The potential RSU for the recycling process was determined, a projection was made to visualize the number of kilograms that are generated and are daily, in the same way the inhabitants of the two municipalities were involved through the application of a survey which was a guideline for determine the acceptance or rejection of the project; Subsequently, the optimal prototype was designed in SolidWorks technological software. What was described above allowed us to assess the proposal to open a recycling plant in the Sierra Norte of the State of Puebla. The analysis presented is relevant, because it will guarantee a sustainable consumption and production modality through recycling; supporting the fulfillment of Sustainable Development Goal number 12 of the 2030 Agenda, the establishment of the recycling plant to serve the municipalities of Huauchinango and Xicotepec will promote the efficient use of MSW; The correct application of the designed production lines will contribute to the achievement of the municipal development plans that derive from the reduction of polluting sources for the environment, reducing the main problem of the effects produced by the consumption of products with PET, cardboard and paper, having economic, social but mainly environmental impacts.

3.10 Acknowledgments

To the Instituto Tecnológico Superior de Huauchinango, to the Division of Industrial Engineering and Electrical Engineering, the facilities provided for the preparation of the presented chapter.

3.11 References

Arboleda Germán, Proyectos, Formulación, Evaluación y Control, Editorial San Fernando Cali – Colombia, año 2007.

Buchenau, M., & Suri, J. F. (2000, August). Experience prototyping. In Proceedings of the 3rd conference on Designing interactive systems: processes, practices, methods, and techniques (pp. 424-433). ACM

Cinta transportadora modular de ANIS TREND d.o.o. DirectIndustry. (2020). Consultado el 24 de diciembre de 2020, de https://www.directindustry.es/prod/anis-trend-doo/product-200888-2143467.html

CORFO. (2016). Prototipos. In *Corfo.cl* (p. 6). Retrieved from Creative Commons website: https://innovacioncomunitaria.files.wordpress.com/2018/10/prototipos_corfo0.pdf

Escobar, A., Quintero, D., & Serradas, D. (2006). *El reciclaje como instrumento para la concientización de la conservación del ambiente, en el Preescolar "Mi Casita de Colores"* (Thesis; p. 32). Retrieved from http://biblioteca2.ucab.edu.ve/anexos/biblioteca/marc/texto/AAQ6004.pdf

Espinoza Oscar, Folleto Segregación, Reciclaje y Comercialización de los Residuos Sólidos, Primera Edición, Lima año 2005.

Frances, A. (2001). Estrategias para la Empresa en la América Latina. Ediciones IESA Caracas.

Gabriel Quadri (2006). *Políticas Públicas. Sustentabilidad y medio ambiente*, en prensa, Miguel Ángel Porrúa, México, p.22

Gerstein, Marc S. (1988). Encuentro con la tecnología. Estrategias y cambios en la era de la información. Addison Wesley Iberoamericana, México.

HILL, CH. JONES, G (2001). "Administración Estratégica". Un Enfoque Integrado. Editorial McGraw-Hill. Tercera Edición. Bogotá.

http://femsa.com/es/assets/003/15669.pdf

IMER (2010) Industria Mexicana de Reciclaje, S.A. de C.V. Recuperado en:

INEGI (2010) Instituto Nacional de Geografía e Informática. Recuperado en: http://www.inegi.gob.mx Kotter, P. (2004). Fundamentos de Mercadotecnia. Prentice-Hall.

Los molinos trituradores en el proceso de reciclaje de plásticos. (2020). Consultado el 24 de diciembre de 2020, de https://www.interempresas.net/Plastico/Articulos/197049-Los-molinos-trituradores-en-el-proceso-de-reciclaje-de-plasticos.html

Maner, W. (2013). Prototipado. Obtenido de SIDAR: https://www.sidar.org/recur/desdi/traduc/es/visitable/maner/Prototipado.htm

Masapanta Serpa, M. R. (2014). *Análisis de despilfarros mediante la técnica value stream mapping (VSM) en la fábrica de calzado lenical* (Thesis; p. 31). Retrieved from http://dspace.ucuenca.edu.ec/bitstream/123456789/20654/1/TESIS.pdf

NAPCOR The National Association for PET Container Resourses. Recuperado en: http://www.napcor.com/index.html

PAREDES-RODRÍGUEZ, Andrés Mauricio. Aplicación de la herramienta Value Stream Mapping a una empresa embaladora de productos de vidrio. En: Entramado. Enero - Junio, 2017. Vol. 13, no. 1, p. 262-277 http://dx.doi.org/10.18041/entramado.2017v13n1.25103

Porter, M. (1986). Ventaja Competitiva. Editorial C.E.C.S.A. México.

Prensa eléctrica para cartón y plástico E319. (2020). Consultado el 24 de diciembre de 2020, de https://www.miltek.com.mx/product/prensa-electrica-para-carton-y-plastico-e319

Prensas y Compactadoras de Residuos. (2020). Consultado el 24 de diciembre de 2020, de https://www.miltek.com.mx/prensas-y-compactadoras

Quintero, Johana, & Sánchez, José (2006). La cadena de valor: Una herramienta del pensamiento estratégico. Telos, 8(3) ,377-389. [Fecha de Consulta 13 de Mayo de 2021]. ISSN: 1317-0570. Disponible en: https://www.redalyc.org/articulo.oa?id=99318788001

Quiñones S. (2015) Larga vida al PET. Revista Expansión, Ed. 874. Recuperado en: http:/www.expansión.com.mx/default.asp

RAE. (2020). Diccionario de la lengua española RAE - ASALE. Retrieved May 13, 2021, from "Diccionario de la lengua española" - Edición del Tricentenario website: https://dle.rae.es/prototipo

Reyes Curcio, A., Pellegrini Blanco, N., & Reyes Gil, R. E. (2015). El reciclaje como alternativa de manejo de los residuos sólidos en el sector minas de Baruta, Estado Miranda, Venezuela. *Revista de Investigación*, *39*(86), 157–170. Retrieved from https://www.redalyc.org/jatsRepo/3761/376144131008/html/index.html

Sandoval Alvarado Leonardo, Folleto Disposición Final y Tratamiento de los Residuos Sólidos, Primera Edición, Lima 2005.

SEMARNAT. (2012). Compendio de Estadísticas Ambientales. Retrieved May 13, 2021, from Semarnat.gob.mx website: https://apps1.semarnat.gob.mx:8443/dgeia/Compendio_2012/dgeiawf.semarnat.gob.mx_8080/ibi_apps/WFServlet5c54.html#:~:text=Recolecci%C3%B3n%20selectiva%20(separada%20o%20segregada,separaci%C3%B3n%20de%20los%20materiales%20valorizables.

Thompson, A. Strickland III, A. (2000). Administración Estratégica. Conceptos Tipo Horizontal De Plástico Para Mascotas De Bomba Centrífuga De Secador - Comprar Centrífugo Secador de Copos De Pet, Secador De Copos De Pet Máquina de Secado de Plástico Producto en Alibaba.com. (2020). Consultado el 24 de diciembre de 2020, de https://spanish.alibaba.com/product-detail/horizontal-type-plastic-pet-flakes-centrifugal-dryer-1968680854.html

Torres Guarniz, G. (2016). *El uso de facturas falsas en la compra de productos reciclables de la empresa* (Thesis; p. 16). Retrieved from http://repositorio.usanpedro.edu.pe/bitstream/handle/USANPEDRO/10599/Tesis_60899.pdf?isAllowed=y&sequence=1

Chapter 4 Ion exchange of heavy metals using a modified zeolite filter integrated into a prototype autonomous water purifier (AWP) on a community scale

Capítulo 4 Intercambio iónico de metales pesados mediante un filtro de zeolita modificado integrado en un prototipo de purificador de agua autónomo (PAA) a escala comunitaria

BECERRA-PANIAGUA, Dulce K.†*, HERNÁNDEZ-GRANADOS, Araceli, RUIZ-SUAREZ, Alison and CEDANO-VILLAVICENCIO, Karla

Universidad Nacional Autónoma de México. Renewable Energy Institute. Priv. Xochicalco S/N, 62580 Temixco, Morelos, Mexico.

ID 1st Author: *Dulce K., Becerra-Paniagua* / **ORC ID:** 0000-0003-0471-7044, **CVU CONACYT ID:** 457428

ID 1st Co-author: *Araceli, Hernández-Granados* / **ORC ID:** 0000-0001-9439-5362, **CVU CONACYT ID:** 442077

ID 2nd Co-author: *Alison, Ruiz-Suarez* / **ORC ID:** 0000-0003-4694-8465, **CVU CONACYT ID:** 796976

ID 3rd Co-author: *Karla, Cedano-Villavicencio* / **ORC ID:** 0000-0002-8102-7226, **CVU CONACYT ID:** 84872

D. Becerra, A. Hernández, A. Ruiz and K. Cedano

* dkbp@ier.unam.mx

Abstract

In Latin America and the Caribbean, the second leading cause of death is from diarrheal diseases. The main causes come from the consumption of water contaminated mainly by *Escherichia coli (E. coli)* and heavy metals, both associated with toxicity and bioaccumulation in living beings. In this chapter we study the exchange of ions of mercury (Hg^{2+}), lead (Pb^{2+}), cadmium (Cd^{2+}) and copper (Cu^{2+}) from aqueous solutions on an unmodified and modified clinoptilolite-K zeolite. To validate a prototype of the Autonomous Water Purifier (AWP) with the integrated zeolite filter, which helps solve problems in marginalized communities where they do not have access to drinking water, electricity and suffer from water-borne diseases. For this, adsorption and removal tests were carried out at different concentrations from 20 to 100 mg/l of heavy metals in aqueous solution with a certain amount of unmodified and modified zeolite. The recorded data represented by the Langmuir isotherm show that the metal ions Hg^{2+} and Cu^{2+} were exchanged very slightly, on the other hand, the metal ions of Pb^{2+} and Cd^{2+} were exchanged on the zeolites in greater quantity than the previous ions.

Heavy metals removal, Water purification, Water treatment, Zeolite

Resumen

En América Latina y el Caribe, la segunda causa de muerte es por enfermedades diarreicas. Las principales causas provienen del consumo de agua contaminada principalmente por Escherichia coli (E. coli) y metales pesados, ambos asociados a la toxicidad y bioacumulación en los seres vivos. En este capítulo se estudia el intercambio de iones de mercurio (Hg^{2+}), plomo (Pb^{2+}), cadmio (Cd^{2+}) y cobre ($Cu2+$) de soluciones acuosas sobre una zeolita clinoptilolita-K sin modificar y modificada. Validar un prototipo de purificador de agua autónomo (AWP) con el filtro de zeolita integrado, que ayuda a resolver los problemas de las comunidades marginadas que no tienen acceso al agua potable ni a la electricidad y sufren enfermedades transmitidas por el agua. Para ello, se realizaron pruebas de adsorción y eliminación a diferentes concentraciones de 20 a 100 mg/l de metales pesados en solución acuosa con una determinada cantidad de zeolita no modificada y modificada. Los datos registrados representados por la isoterma de Langmuir muestran que los iones metálicos Hg^{2+} y Cu^{2+} se intercambiaron muy ligeramente, en cambio, los iones metálicos de Pb^{2+} y Cd^{2+} se intercambiaron en las zeolitas en mayor cantidad que los anteriores.

Eliminación de metales pesados, Purificación del agua, Tratamiento del agua, Zeolita

4.1 Introduction

Today the shortage of safe water in the world has become a serious problem, since it affects thousands of people, mainly the vulnerable population in rural and remote areas. This problem does not arise from the "lack of water" in the area and even areas with high water resources are facing it. For example, Latin America and the Caribbean (LAC) are regions with high water resources, they have almost 34% of the world's fresh water (Mekonnen, Pahlow, Aldaya, Zarate, & Hoekstra, 2015). However, access to potable and purified water is insufficient and its quality is inadequate (Flachsbarth et al., 2015). According to the World Health Organization (WHO) and the United Nations International Children's Emergency Fund (UNICEF), around 2.2 billion people around the world do not have safe water services, which are managed safely, 4.2 billion people do not have safely managed sanitation services and 3 billion people lack basic facilities to wash their hands (UNICEF and World Health Organization, 2015, 2019). In addition, the COVID-19 pandemic has triggered serious alerts about these mentioned problems.

Lack of water is known to bring many social problems. For example, in 2017 almost 1.6 million people died from diarrheal diseases worldwide (WHO & UNICEF, 2017) and in Latin America and the Caribbean, it is the second leading cause of death (PAHO/WHO, 2019). Diarrheal disease is completely predictable and treatable and the main causes come from the consumption of water contaminated mainly by Escherichia coli (E. coli) and heavy metals (Jaishankar, Tseten, Anbalagan, Mathew, & Beeregowda, 2014), both associated with toxicity and bioaccumulation in living beings (Marazzato et al., 2020; Shaharoona et al., 2019).

In the case of Latin America and the Caribbean, 74.3% and 31.3% of the population respectively have access to safely managed water and sanitation services (Pan American Health Organization (PAHO), 2017). Mexico is one of the Latin American countries with the largest supply of fresh water in the world, each year Mexico receives around 1,449,471 million cubic meters of water in the form of precipitation. The North, Center and Northwest regions have 1/3 of the renewable water equivalent to 4/5 of the population (1,581.28 m³/inhab/year) which is less than the Southeast region, which has 2/3 of the renewable water equivalent to 1 / 5 of the population (10, 718.25 m³ / inhab / year) (National Water Comission (NWC), 2017). Although the southeast region has more water, this region is the least developed in Mexico. The most affected states are Oaxaca, Guerrero, Campeche, and Chiapas. Among all these states, in 2016, the state of Chiapas had the highest renewable water resources per year and per capita in the country, 113,903 hm³/year and 21,419 m³/inhab/year, respectively (National Water Comission (NWC), 2017). Even with these water resources, most of the rural communities in this state do not have access to clean water, electricity and suffer from water-borne diseases.

Based on this situation and with the social problems mentioned above, it is convenient to work on the development of new concepts of water treatment systems that allow treating natural surface and underground waters with various pollutants, among the most alarming heavy metals. In addition, it is also important to use renewable energy as an energy supply for its operation. This, in order to be implemented in rural areas, helping to provide solutions to improve the quality of life and health of society.

For those reasons, this chapter is organized into the following sections: Introduction, describes a general panorama in Latin America and the Caribbean of the problems caused by contaminated water and its social impact; background, state of the art of the most used water treatment methods and zeolite as an adsorbent for pollutants, as well as the justification for the work; methodology, materials and methods used to evaluate zeolite with heavy metals and validate it in the Autonomous Water Purifier prototype (AWP); results and discussion, the results of the cation exchange modification of the zeolite are discussed, the study of the structural, morphological and chemical properties of the zeolites, the evaluation of the zeolites with heavy metals and the validation of this in a treatment system of water on a community scale. Finally, the conclusions, acknowledgments, and references are presented.

4.1.1 Overview of contaminated water treatments

In order to provide solutions to these types of problems, many lines of research have shown that household water treatment can be the most profitable option (Holtman, Haldenwang, & Welz, 2018; Murray et al., 2020). However, this method has a disadvantage, such as taste and poor disinfection efficiency. Other options are the use of solar radiation for the treatment of drinking water using SODIS (solar water disinfection) (Kohn, Mattle, Minella, & Vione, 2016; Parsa et al., 2020; Vivar, Pichel, & Fuentes, 2017); this method confirmed its effectiveness in eliminating bacteria, fungi and viruses. However, the time required for sun exposure is at least 6 hours; if it is cloudy, this is up to 2-3 days (Wang et al., 2016). In addition, in another article it was reported that to improve the efficiency of solar disinfection it was done by adding a photocatalyst, such as titanium dioxide (TiO_2) (Fernández-Ibáñez et al., 2015; Wu et al., 2014). Although TiO_2 increased the effectiveness of SODIS, the TiO2 nanoparticle suspension had to be separated before human consumption (otherwise it could be a risk to human health), and the process is expensive and difficult. Even with this great potential, SODIS is limited to disinfection efficiency and scale, because large-scale systems such as continuous flow or pump circulation need electricity and are no longer useful for rural and remote areas that lack of sanitation, water, and electricity. For these reasons, other works have developed photocatalytic-photovoltaic hybrid prototypes for the treatment of polluted water (Qin et al., 2015; Vivar et al., 2012). Other works reported the use of hybrid systems that use solar radiation, these systems were pilot-scale solar photoreactors, which included flat plate reactors (FPR) and compound parabolic collector (CPC) reactors (Ochoa-Gutiérrez, Tabares-Aguilar, Mueses, Machuca-Martínez, & Li Puma, 2018; Wang et al., 2016). Many hybrid systems have been developed for remote locations to desalinate water using reverse osmosis (Alghoul et al., 2016; Peng, Maleki, Rosen, & Azarikhah, 2018) and ultra-filtration membranes (Clayton, Thorn, & Reynolds, 2019).

The main advantage of hybrid systems is that they do not require conventional energy for their operation; therefore, it favors its implementation in remote areas that lack potable water and electricity. However, despite its great functionality, each method has its disadvantages, such as high cost, inappropriate taste, low scalability, and most importantly, low removal efficiency of toxic contaminants such as heavy metals (mercury, lead, arsenic, cadmium, and copper). Those studies only showed a low range of removal of contaminants such as dyes, salts, microorganisms.

On the other hand, in recent years zeolites have received a lot of attention in the scientific field for the removal of contaminants in water on a large scale. Zeolites are micro-porous aluminosilicate minerals that stand out for their ability to hydrate and dehydrate reversibly (Lin et al., 2013). The structure consists of a three-dimensional network of $[SiO_4]^{-4}$ and $[AlO_4]^{-5}$ tetrahedra, with the silicon or aluminum atoms in the center, and the oxygens at the vertices. The substitution of aluminum atoms for silicon in the crystal structure leads to the additional negative charge being balanced by adjacent counter ions (such as Na^+, K^+, Ca^{2+} and Mg^{2+} and these counterions are easily exchanged for other adjacent cations in an exchangeable solution (Dyer, 2007). In addition, zeolites have certain qualities and characteristics such as a high ion exchange and adsorption capacity (Kithome, Paul, Lavkulich, & Bomke, 1998). In Mexico, there are large deposits of rock rich in zeolites in the states of Sonora, San Luis Potosí, Guerrero, Tamaulipas, Puebla, Guanajuato, Oaxaca, Zacatecas and Baja California Sur (Cucchiella, D'Adamo, Lenny Koh, & Rosa, 2015) the current shortage of competitive minerals and the relatively low market price, make it optimal candidates, as ion exchangers in domestic and commercial water purification, and other applications (Y. Li, Li, & Yu, 2017) improve the ammonium adsorption capacity of zeolite, different methods of modifying it have been reported, among them, treatment with an exchangeable solution of sodium hydroxide (NaOH), hydrochloric acid (HCl) or sodium chloride (NaCl) (Kotoulas et al., 2019; Shi et al., 2017), microwave pretreatment (Lei, Li, & Zhang, 2008) and calcination (Liang & Ni, 2009). Being the method with interchangeable solutions where the highest adsorption capacity has been obtained (Ates, 2014).

Because of this situation, it is intended to improve the performance of these devices with the study and coupling of the zeolite material in one of the ion exchanges stages of the autonomous water purifier prototype (AWP). This material, by possessing certain qualities and characteristics of porosity, adsorption and ion exchange capacity make it an ideal material for the removal of heavy metals in water; and thus, obtain a wide range of pollutant removal compared to those of conventional solar and wind purifiers, helping to improve their quality and use. Therefore, in this chapter we show the results on: (1) the modification of zeolite by cationic exchange with NaCl, (2) the study of the structure, morphology and chemical composition of a natural and modified zeolite; (3) adsorption and removal tests at different concentrations from 20 to 100 mg/l of mercury (Hg^{2+}), lead (Pb^{2+}), cadmium (Cd^{2+}) and copper (Cu^{2+}) in aqueous solution with a certain amount of natural and modified zeolite; (4) the validation of the modified zeolite in the Autonomous Water Purifier (AWP) prototype. The recorded data represented by the Langmuir isotherm of ion exchange on zeolitic minerals revealed that the metal ions Hg^{2+} and Cu^{2+} were exchanged very slightly, on the other hand, the metal ions of Pb^{2+} and Cd^{2+} were exchanged on the zeolites in greater quantity than previous ions. And that the exchange capacity of the modified zeolite increases with respect to the unmodified one, thus increasing the number of exchangeable ions. In addition, those in the validation showed that the AWP prototype has a wide range of pollutant removal compared to equivalent water treatment systems in the same locations, and the electricity generated by the solar cells can be used to power the entire system. The prototype was evaluated with river and spring water from different rural communities in Chiapas, Mexico. The results indicate that the prototype it can eliminate pollutants in natural waters and obtaining water that complies with the guidelines established by the official Mexican standards.

4.2 Materials y methods

Next, the methodology used for the adsorption and ion exchange of mercury (Hg^{2+}), lead (Pb^{2+}), cadmium (Cd^{2+}) and cooper (Cu^{2+}) ions on natural and modified zeolite is described. Throughout this section, the procedure, tools, and parameters used to achieve the planned objective are shown. Likewise, it describes the characteristics and conditioning of the type of zeolite that was used, the type of isotherm, the factors that were considered in the ionic exchange, the time in which they were stirred, at which temperature and pH were maintained. On the other hand, the techniques used for the characterization of materials and the technique used for the quantification of the equilibrium concentration of heavy metals in aqueous solution are described.

4.2.1 Experimental methodology

Stage 1. Conditioning of natural zeolite

A clinoptilolite-K type natural zeolite was used with a chemical composition of $K_3 (Si_30Al_6) O_{72} \cdot 20H_2O$, endemic to the Etla deposit (17° 12′ 24″ Norte, 96° 47′ 53″ West) of the state of Oaxaca. For this, a significant amount of the zeolite mineral was washed several times using deionized water, separated by decantation, dried for 24 hours in a Riossa H-33 oven at 110 °C (Figure 1.1a) and stored in closed containers and dry.

Stage 2. Preparation of exchangeable metal ion solutions

The precursors that were used to prepare the exchangeable solutions of the metal ions were the following inorganic salts: $CdCl_2$; $HgCl_2$; Pb $(C_2H_3O_2)_2$ $3H_2O$; Zn $(NO_3)_2$; $CuSO_4$ $5H_2O$ due to its high degree of solubility in aqueous media. From the following hydrolysis chemical reactions, the amount in grams was determined despite the precursors to obtain concentrations of A=20, B=40, C=60, D=80 y F=100 mg/l of the metal ions.

$$CdCl_2\, H_2O \rightarrow Cd^{2+} + 2Cl^-$$

$$HgCl_2\, H_2O \rightarrow Hg^{2+} + 2Cl^-$$

$$Pb\, (C_2H_3O_2)_2 3H_2O\, H_2O \rightarrow Pb^{2+} + 2(C_2H_3O_2)^- + 3H_2O$$

$$CuSO_4 5H_2O\, H_2O \rightarrow Cu^{2+} + (SO_4)^{2-} + 5H_2O$$
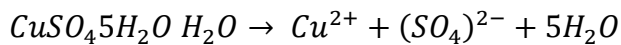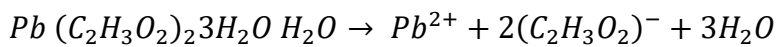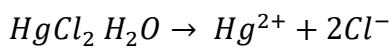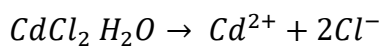
Stage 3. Ion exchange isotherms

Since ion exchange is a form of adsorption, the experimental data of equilibrium of metal ions were interpreted by means of the Langmuir isotherm model, which are represented mathematically as (Mihaly-Cozmuta et al., 2014):

$$N = \frac{N_{max}KC}{1+KC} \tag{1}$$

Where: C is the concentration of metal ions at equilibrium, K is the Langmuir isotherm constant related to the enthalpy of adsorption, N is the amount of metal ion exchanged per unit mass of the adsorbent and N_{max} represents the maximum amount of Hg^{2+}, Pb^{2+}, Cd^{2+} y Cu^{2+} that is exchanged.

The data were adjusted to this model because it is the most used in adsorption phenomena at the solid-liquid interface on microporous materials such as zeolites. The isotherm constant was estimated using the least squares method by plotting the C/N ratio as a function of the equilibrium concentration C adjusting to a straight line of slope $1/N_{max}$ and ordered to the origin $1/KN_{max}$ for the Langmuir isotherm, using the following equation (Mihaly-Cozmuta et al., 2014):

$$\frac{C}{N} = \frac{C}{N_{max}} + \frac{1}{KN_{max}} \tag{2}$$

For the experiments with natural and modified zeolite, the experimental data of the exchange isotherm were obtained in a batch exchanger that consisted of a 500 ml Erlenmeyer flask, to which 500 ml of a solution containing an initial concentration of the ion were added. metallic from 20 to 100 mg/l. In a fabric made of nylon mesh, 26 g of zeolite were added in the form of a filter, as expressed in Figure 4.1 (b), then it was placed into the exchanger solution, as shown in Figure 4.1 (c).

Stage 4. Ion exchange kinetics

The solution was mixed by means of a Teflon coated magnetic stir bar and driven by a stir plate, as shown in Figure 1.1 (d). The solution and the zeolite were left in contact until they reached equilibrium at room temperature (25 °C) and 500 rpm.

It was found that in a period of 24 hours it is enough to reach equilibrium. This procedure was carried out for each exchangeable solution of the metal ion at five different concentrations, in total 25 samples were obtained. Which were stored in amber containers and kept at low temperatures, as shown in Figure 4.1 (d). To subsequently measure the concentration of the analyte in the solution by means of the Inductively Coupled Plasma Optical Emission (ICP-OES) technique, using a Thermo Scientific iCAP 6000 SERIES spectrometers.

Stage 5. Modification of the zeolite by cation exchange (effect of pH)

The process of modification by cationic exchange of zeolite has the purpose of replacing the cations that the natural mineral contains in its structure by sodium ions, coming from the sodium salt. The modification of the zeolite was carried out by a cation exchange procedure. 110 g of the natural zeolite and 200 ml of the exchangeable solution of NaCl at 2M were added to four 250 ml Erlenmeyer flasks. The solution and the zeolite were placed on a heating plate and heated to a temperature of 50 °C, the assembly can be seen in Figure 4.1 (e), for 12 h and then allowed to cool for the next 12 h; the exchangeable solution was separated from the zeolite by decantation. Next, 200 ml of a new exchangeable solution were added, and it was heated again to 50°C. This procedure was repeated for five days. At the end of this period the zeolite was separated from the solution, washed repeatedly with distilled water until the rinse solution was no longer cloudy, and dried in an oven at 110 ° C for 24 h. Hydrochloric acid (HCl) was used to adjust the initial pH from 7 to 5, because the maximum and optimal pH values for metal adsorption are reported to be between 5 and 6.5 (Elboughdiri, 2020). The modified zeolite was stored in a dry and closed container. The experimental data of the isotherm were obtained following the same procedure of the natural zeolite with the same conditions.

Stage 6. Validation of zeolite as a filter in the Autonomous Water Purifier (AWP) prototype

The ion exchange of heavy metals in aqueous solution in the zeolite column (10) was studied as shown in Figure 4.1 (f), of the Autonomous Water Purifier (AWP) prototype with patent registration number MX/a/2016/006341 (377936B, 2021). The absorbance of the final ion concentration was measured after being filtered by the AWP prototype using an ICP-OES spectrometer. The concentration was calculated by the calibration curve method, this process was carried out by establishing the calibration curve on standard metallic solutions at concentrations of 10 to 100 mg/ml.

The percentage of removal of metal cations (% R) was calculated from the difference in the concentration of initial metal cations (C_i) and final (C_f) in each sample, using the following equation (Erdem, Karapinar, & Donat, 2004).

$$\%R = \frac{C_i - C_f}{C_f} x100 \tag{3}$$

Figure 4.1 Scheme of the natural and modified zeolite adsorption and ion exchange methodology: a) conditioning of natural zeolite, b) preparation of exchangeable metal ion solutions, c) ion exchange isotherms, d) ion exchange kinetics, e) modification of the zeolite by cation exchange (effect of pH) and, f) validation of zeolite as a filter in the Autonomous Water Purifier (AWP) prototype

Source: Prepared by the authors with the help of https://www.klipartz.com/ and https://www.flaticon.com/
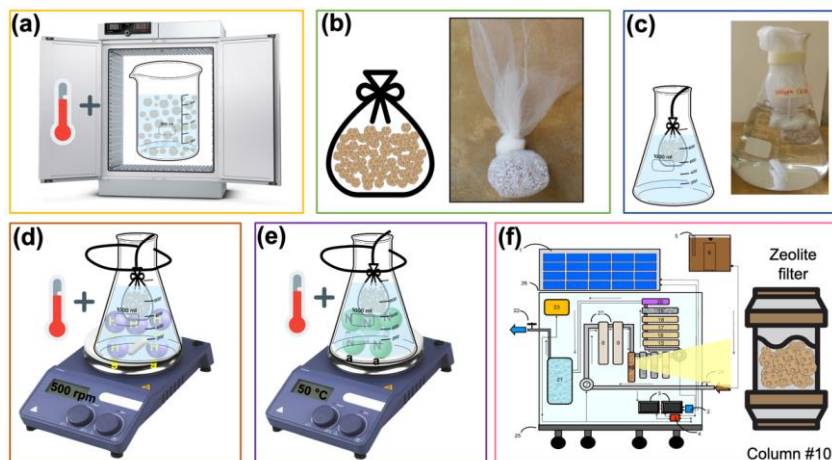
4.2.2 Characterization

To study the effect of the cation exchange of the modified zeolite on the natural zeolite in the structural, morphological, and chemical properties, the following techniques and analyzes were used. The identification of the crystalline phases and the determination of the crystalline structure of the natural and modified zeolite samples were carried out by X-ray Diffraction (XRD). The equipment used was a Rigaku powder diffractometer, Ultima IV model, using radiation CuKα (λ=1.54Å), operating at 40 kV and 44 mA. The samples were analyzed in a diffraction angle interval 2θ= 4-60° with a step size of 0.02° and a span of 2 s. The data treatment was carried out with *Integrated X-Ray Powder Diffraction Software* (PDXL). The zeolite samples were ground in an agate mortar until obtaining a homogeneous fine powder. The morphological analysis of the natural and modified zeolite was carried out through the Scanning Electron Microscopy (SEM) technique, obtaining as a result, photomicrographs of the surfaces of the respective zeolites. A Jeol JSM-5300 scanning electron microscope (SEM) with tungsten filament, operating at 10 kV at a temperature of 298 K, was used to obtain the microphotographs of the surface morphology of the zeolites. To determine the chemical composition and the amount of metal cations adsorbed in the natural and modified zeolite samples, the X-Ray Fluorescence (XRF) technique was used. For this, a Rigaku brand spectrometer, model supermini 200, was used.

4.3 Results and discussion

In this section, the results obtained from the characterization of the zeolite material with different techniques are presented. For that purpose, we analyze the effect of cation exchange on its structure, morphology, and chemical composition in zeolite; These techniques allowed us to know and deduce its porosity, ion exchange capacity, Si / Al ratio and the amount of metal ions exchanged and adsorbed on its surface. And thus, be able to conclude if said zeolite is efficient to remove heavy metals in water and decide on its validation as a material to be integrated into the Autonomous Water Purifier prototype (AWP). In addition, the evaluation of the zeolites on heavy metals, the graphs of ion exchange isotherms, the mass balance of exchanged ions, the removal percentages and the theoretical and experimental exchange capacity of the zeolites are presented; and the validation of the Autonomous Water Purifier prototype (AWP) with the integrated zeolite.

4.3.1 Structural analysis

The XRD technique allowed us to determine the crystalline phases of the material, which provides us with information about the type of zeolite and to verify if it is one of the 8 types of zeolites suitable for the removal of heavy metals; The crystal size allowed us to deduce its Silicon/Aluminum (Si/Al) ratio, which is a function of the ion exchange capacity of the zeolite.

Graphic 4.1 shows the X-ray diffraction spectra for natural and modified zeolite powders. Crystalline networks are observed in the monoclinic structure with a predominance of intensity and width of the peak in the plane of (131) of the reflection of natural zeolite and a predominance of intensity in the plane (220), and width of the peak (131) from the reflection of the modified zeolite. The diffractogram in Figure 4.1 (a) corresponds to the diffraction pattern ID: 01-089-7539, K_3 $(Si_{30}Al_6)$ $O_{72}\cdot 20H_2O$. The type of zeolite identified is a K-clinoptilolite phase. The most characteristic peaks are recognized at 2θ equal to 9.87°, 22.35°, 29.94° and 42.42°. The X-ray diffractogram from graphic 4.1, corresponds to the diffraction patters of ID 01-079-1460, Na_4 $(Si_{30}Al_6)$ $O_{72}\cdot 20H_2O$. The zeolite type identified is a clinoptilolite-Na phase. The most characteristic peaks observed are located at 2θ, with values of 9.84°, 22.30°, 27.31° and 41.52˚. Also, it is observed that in the modified zeolite, as the silicon/aluminum molar ratio decreases, the intensity of the diffractogram peaks increases, increasing their crystallinity due to the presence of the increase in sodium concentration, while the presence of potassium in the natural zeolite attenuates it.

Graphic 4.1 X-ray diffractograms of (a) natural zeolite with the clinoptilolite-K pattern and (b) for modified zeolite with the clinoptilolite-Na pattern
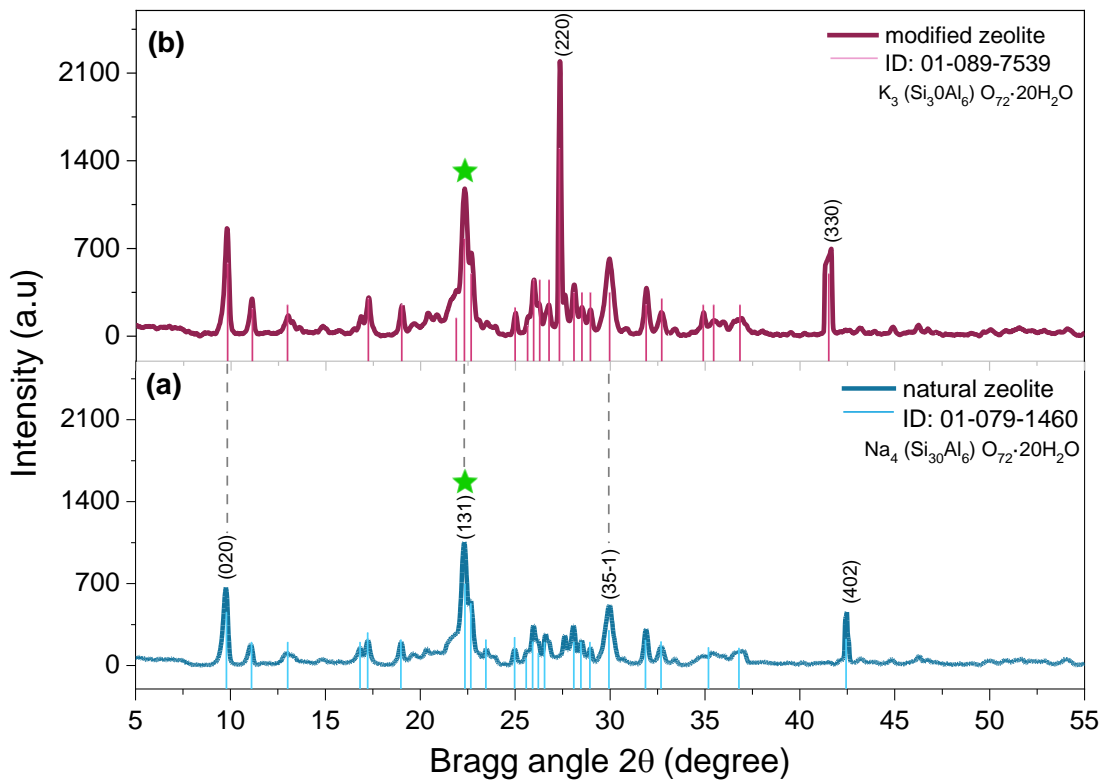
Source: Elaborated by authors with Software Origin

By means of the patterns of natural and modified zeolite XRD, it was possible to obtain the crystallite size (D), which shows the polycrystalline nature of zeolites. The realization of these calculations was conceived using the Debye-Scherrer equation, which establishes that the crystallite size is inversely proportional to the width of the peak at half the maximum diffraction height and the cosine of the maximum peak angle, according to the following formula:

$$D = \frac{K\lambda}{\beta cos\theta} \qquad (4)$$

Where θ is the Bragg angle and $\beta^2 = (FWHM)^2 - b^2$; *FWHM* is the full width at half the maximum peak of the sample, *b* instrumental error 0.101°, λ= 1.54056 Å corresponds to the Cu K_α radiation, *D* is the size of the crystallite, *K* is the shape factor that is approximately the unit of samples. Plane (131) was chosen as the representative of the samples and sizes obtained from Graphic 4.1. The crystallite size was 327 Å with a 20% error for the natural zeolite and 391 Å with a 22% error for the modified zeolite. By decreasing the Si / Al molar ratio in the zeolites, a tendency to form larger crystals is obtained, due to the presence of the increase in Na$^+$ in their structure, favoring crystallinity in it.

4.3.2 Morphology analysis

The SEM technique allowed obtaining information about the morphology, the particle size distribution, and the types of particle shapes that the natural and cation exchange modified zeolite samples presented, through visualization and microstructural analysis at a resolution of 100 μm.

The zeolite samples presented four different types of particle shapes: angular-subangular-wavy, angular-smooth-wavy, subangular-rough and sub-round-wavy according to the literature (Li et al., 2019), whose variability is related to particle size and in turn to pore diameter. Larger particles, as in the case of natural zeolite, presented a greater variety in the types of shapes and greater distribution of the particles; while in the modified zeolite samples, because they had smaller particles, they presented a lower distribution of the particles and uniformity in the shapes of the particles. Figure 4.2 (a) shows the SEM image of the natural zeolite while Figure 4.2 (b) shows the SEM image of the cation exchange modified zeolite.

Particles were measured using ImageJ software from a section of the image; The area (μm^2) of more than 40 particles was measured and for regular and two-dimensional particles we calculated their diameter (μm), which we will call particle size, assuming a circular geometry ($A=r^2\pi$). The natural and modified zeolite distributions are presented in Graphic 4.2 (c) and (d) respectively. A broader size distribution is observed for the natural zeolite sample, with diameters from 3.0 μm to 9.1 μm and an average of 5.1 $\pm$1.5 μm. In contrast, the modified zeolite sample has a shorter distribution, with diameters from 3.2 μm to 8.8 μm and an average of 4.8 $\pm$1.32 μm. The particles of a zeolite form three types of pores: packing, simple and cavities according to the literature (Anicua Sánchez et al., 2009); and have been determinate by Brunauer–Emmett–Teller (BET) and SEM techniques (Ramesh, Reddy, Rashmi, & Biswas, 2014). It can be established that the highest pore percentages are presented by the smaller sized particles, consequently the larger sized particles have a lower porosity percentage. Due to this, the zeolite conditioned with NaCl, by presenting smaller particle sizes compared to the natural zeolite, presented greater ion exchange and removal capacity, as will be seen later, by increasing its channels and cavities that vary according to size. particle. Therefore, metal cations in aqueous solution will more easily penetrate the crystal structure through their series of intersecting channels.

Graphic 4.2 SEM images of samples of (a) natural zeolite and (b) modified zeolite; (c and d) particle size distribution of natural zeolite and modified zeolite respectively
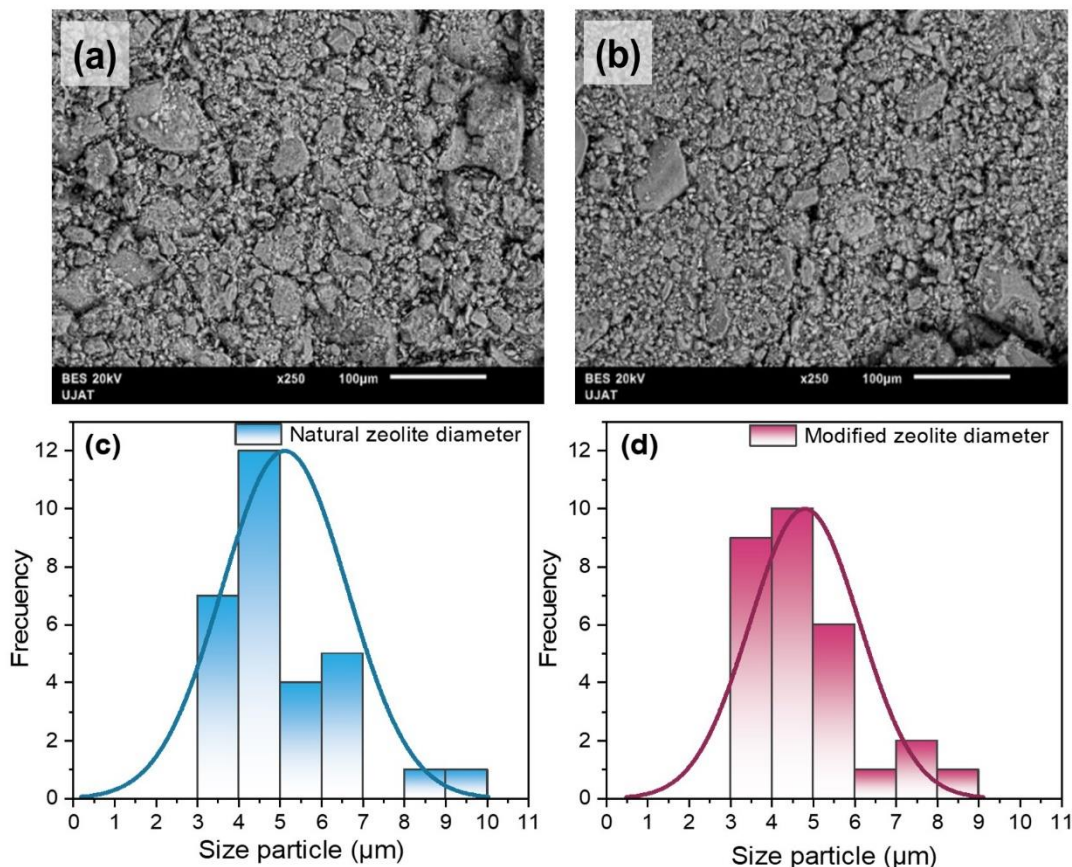
Source: Elaboration by authors with Software Origin; SEM images acquired from Jeol JSM-5300

4.3.3 Chemical composition analysis

The XRF technique allowed to determine the elemental chemical composition and the ion exchange capacity as a function of the Si/Al ratio of the natural and modified zeolite; the results obtained are shown in Table 4.1.

Table 4.1 Elemental composition of natural and modified zeolite, in percent by weight (wt%)

Zeolite samples	Molar ratio Si/Al	SiO_2 (wt%)	Al_2O_3 (wt%)	Na_2O (wt%)	MgO (wt%)	K_2O (wt%)	CaO (wt%)	Fe_2O_3 (wt%)
Natural	4.63	68.877	14.862	1.840	0.990	7.806	3.384	2.237
Modified	4.30	64.668	15.026	10.970	0.798	5.402	0.365	2.767

The unmodified zeolite is the one with the lowest ion exchange capacity, Si/Al= 4.63, this capacity is directly related to the aluminum present in the zeolite crystal lattice and depends directly on its chemical composition. The exchange capacity was modified by varying the silicon-aluminum ratio of the zeolite, increasing as this ratio decreased. For this, once the mineral was conditioned with NaCl, an increase of approximately 10 times the amount of sodium was obtained compared to the content of said element in the unconditioned mineral.

A high ion exchange capacity corresponds to zeolites with a low ratio SiO_2/Al_2O_3, or ratio Si/Al as is the case of modified zeolite, which was equal to 4.30. This ratio determined the number of cations that can be interchangeable in the zeolite, since by changing the Si / Al ratio of a zeolite, its cation content also changed.

4.3.4 Evaluation of heavy metals on zeolites

Considering the analytical technique of composition of analytes in aqueous solution mentioned in the methodology section, in Graphic 4.3 (a) and (b) the results of the adsorption and ion exchange of the experiment with natural zeolite and modification are summarized. The equilibrium concentrations (C) registered in the ICP-OES equipment of the metal ions in aqueous solution are represented against the amount of metal ion adsorbed per gram of experimental zeolite (N_{exp}) calculated by the following equation:

$$N_{exp} = V_s * \frac{C_0 - C}{m_z} \tag{5}$$

The experimental data of the exchange isotherms of Hg^{2+}, Pb^{2+}, Cd^{2+} y Cu^{2+} on the natural and modified zeolite at T=25°C and with adjustment of pH=5, were interpreted by means of the model of the Langmuir isotherm represented in the Graphic 4.3. The results of the ion exchange isotherms reveal that the metal ions Pb^{2+} y Hg^{2+} were the ones that were exchanged in greater quantity on the natural zeolite, obtaining the highest concentrations of 1.69 mg/gr and 1.56 mg/gr respectively at 100 mg/l. This is caused by the concentration of the related exchangeable cations K^+ and Ca^{2+} present in greater quantity in the natural zeolite, 7.80 wt% and 3.38 wt% respectively.

On the other hand, the Cd^{2+} and Cu^{2+} metal ions exchanged very slightly on the natural zeolite, this caused by the low concentration of exchangeable related cations Na^+ present in the natural zeolite samples of approximately 1.840 wt%. Other important results were on the modified zeolite samples, the metal ions Cd^{2+} and Cu^{2+} were the ones that were exchanged in greater quantity on this zeolite, obtaining the highest concentrations of 2.10 mg/ gr and 2.030 mg/gr respectively at 100 mg/l. This is due to the concentration of the affinity exchangeable cation Na^+ present in greater quantity in the modified zeolite of 10.97 wt%. On the other hand, the metal ions Pb^{2+} and Hg^{2+} exchanged very slightly on the modified zeolite, this caused by the low concentration of exchangeable related cations K^+ and Ca^{2+} present in the modified zeolite samples of5.40 wt% and 0.36 wt% respectively.

Graphic 4.3 Ion exchange isotherm of Pb^{2+}, Hg^{2+}, Cd^{2+} and Cu^{2+} on (a) natural zeolite and (b) modified zeolite
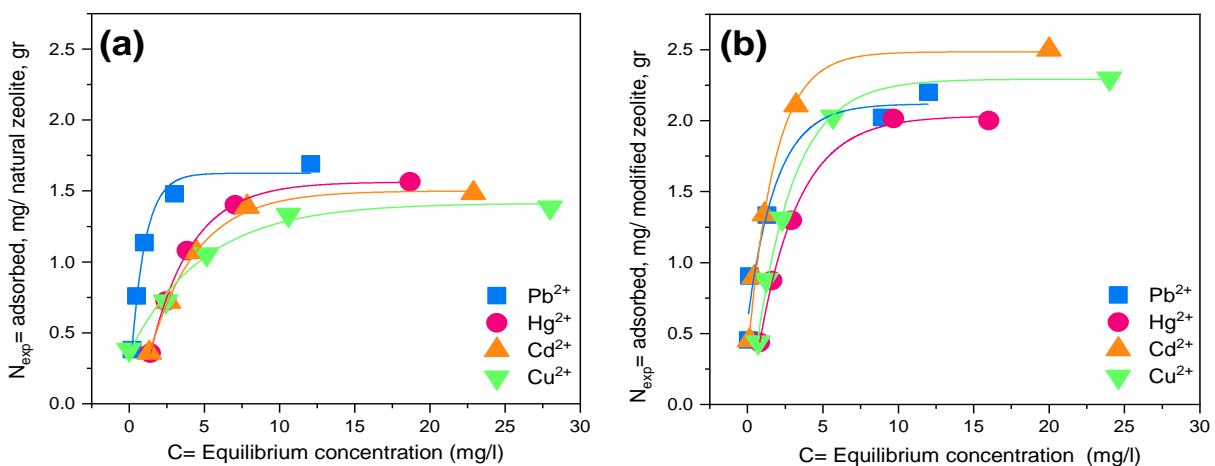
Source: Elaboration by authors with Software Origin; data obtained from the ICP-OES equipment

The isotherm constants were estimated using the least squares method of equation (2), plotting the C/N ratio as a function of the equilibrium concentration C for each metal ion. To obtain the constant of each isotherm, N_{max}, the value of the slope was cleared for each line of natural and modified zeolite of each metal ion: $m = \dfrac{1}{N_{max}}$. The values of the constant of each isotherm are shown in Table 4.2.

In addition, the average deviation percentage (% D) for each isotherm was evaluated using the following equation:

$$\%D = \left(\frac{1}{n}\sum_{i=1}^{n} \quad \left|\frac{N_{exp}-N_{cal}}{N_{exp}}\right|\right) x100\% \tag{6}$$

It was considered that the natural zeolite isotherms were the ones that best fit the data, since in all cases they presented a lower percentage of deviation compared to the results of the percentage of deviation of modified zeolite. The explanation for this behavior is based on the variation of basicity and pH of the natural zeolite in the experiments. Caused that the ion exchange is slightly different. The exchange equilibrium is affected by the modification of NaCl on the natural zeolite causing variations that cause deviations in the data of the exchange isotherm. On the other hand, the results indicate that the metal ion Pb^{2+} and Cu^{2+} has the highest maximum amount of mg of metal ion that can be adsorbed on one gram of natural and modified zeolite, respectively. While Cu^{2+} and Hg^{2+} have the lowest maximum amount of mg of metal ion that can be adsorbed in a gram of natural and modified zeolite respectively.

Table 4.2 Values of the Langmuir isotherm constant

Ion	Zeolite	N_{max} (mg/gr)	%D
Pb^{2+}	Natural	1.785	3.33
Hg^{2+}		1.769	8.96
Cd^{2+}		1.753	10.73
Cu^{2+}		1.446	9.11
Cd^{2+}	Modified	2.610	11.20
Cu^{2+}		2.559	9.80
Pb^{2+}		2.349	27.81
Hg^{2+}		2.227	8.54

Source: Prepared by authors

In addition, the adsorbed and exchanged metal ions were quantified in each of the zeolite samples. To obtain the balance of the maximum metal ions exchanged on the surface of the zeolite mass, the N_{max} values already calculated and recorded in Table 4.2 were taken, and each value was multiplied by the mass of zeolite used (26 gr for natural zeolite and 22 gr for modified zeolite) to have the total mg exchanged of each metal ion on the surface of natural and modified zeolite. Regarding the balance of the metal ions adsorbed on the surface of the zeolite mass, they were obtained from the compositional characterization by the XRF technique, the team gave the results in percentage by mass and through calculations it was converted to mass units of mg.

The results of the mass balance of the metal ions that were exchanged, and the mass of the metal ions adsorbed in the natural and modified zeolite samples are shown in Table 4.3.

Table 4.3 Mass balance of adsorbed and exchanged ions during ion exchange

Initial concentration (mg/l)	Zeolite	Ions adsorbed on the zeolite (mg)				Ions exchanged in zeolite (mg)			
		Pb^{+2}	Hg^{+2}	Cd^{+2}	Cu^{+2}	Pb^{+2}	Hg^{+2}	Cd^{+2}	Cu^{+2}
100	Natural	31.5	25.3	24.4	21.5	46.4	45.9	45.5	37.5
100	Modified	35.3	31.8	39.3	37.8	51.6	48.4	57.4	56.2

Source: Prepared by authors

The total ions that are transferred from the solution to the zeolite (Pb^{+2}, Hg^{+2}, Cd^{+2} and Cu^{+2}) do not correspond to the total ions that are adsorbed from the solution to the zeolite. Since the zeolite operates as an exchanger and adsorber at the same time. The sum of the adsorbed ions and the exchanged ions gives us the total amount of the ion that was removed through the zeolite. It can be observed that the ion most exchanged and adsorbed was Pb^{2+} and Cd^{2+} on natural and modified zeolite, respectively. This means that clinoptilolite is much more selective for Pb^{2+} and Cd^{2+} ions than for Hg^{2+} and Cu^{2+} ions.

4.3.4 Application of zeolite filter in the Autonomous Water Purifier prototype (AWP)

In Graphic 4.4 (a), the removal percentage (% R) is shown against the initial concentration (C_i), while in Graphic 4.4 (b) the final concentration (C_f) is shown against C_i of heavy metals in the zeolite ion exchange column (Figure 4.1f, column 10) in the AWP prototype, obtained by equation (3) and the ICP-OES equipment respectively. The curves were fitted with the following mathematical equation by exponential model:

$$y = y_0 + Ae^{bx} \tag{7}$$

The removal rate of a cation in aqueous solution depends on the amount exchanged in the zeolite ion exchange column (column 10), as well as on the function of ion exchange. Thus, it was considered that, under the same experimental conditions, the sample that has a greater ionic exchange capacity is the one that exhibits the highest removal percentage for that ionic capacity (Erdem et al., 2004; Mihaly-Cozmuta et al., 2014).

In Graphic 4.4 (a) and (b), it can be observed that the %R and C_f decrease as the initial concentration of the metal increases in aqueous solutions, since the zeolite has a maximum adsorption capacity and tends to become saturated at high concentrations. The % R ranged from 87 to 99% for Pb^{2+}, 81 to 99% for Hg^{2+}, 77 to 98% for Cd^{2+} and 72 to 97% for Cu^{2+}. Comparing the %R obtained from the zeolite ion exchange column (10) for each metal, it is observed that the exchange selectivity in the zeolite is $Pb^{2+} > Hg^{2+} > Cd^{2+} > Cu^{2+}$, that is, that for the natural zeolite the Pb^{2+} is exchanges in greater quantity than the metal Hg^{2+} and thus for the metals Cd^{2+} and Cu^{2+}.

This cationic exchange can be attributed to the substitution of the exchangeable ions Na^+, Ca^{2+} and K^+ that constitute the zeolite with the divalent cations of Pb^{2+}, Hg^{2+}, Cd^{2+} and Cu^{2+}. This isomorphic substitution is due to the similarity in their ionic radius that metal cations have with exchangeable ions, the affinity of the dimensions in their cavities of the zeolite makes one cation take the place of the other, by simple interaction between their chemical bonds. Due to the similarity between their ionic radius, the replacement is concluded as follows (Shannon, 1976).

	Ion exchange	
K^+ (138 pm)	⟷	Pb^{2+} (119 pm)
Ca^{2+} (100 pm)	⟷	Hg^{2+} (102 pm); Cd^{2+} (95 pm)
Na^+ (102 pm)	⟷	Hg^{2+} (102 pm)

Graphic 4.4 (a) Percentage of removal (circles) and (b) final concentration (squares) of Pb^{2+}, Hg^{2+}, Cd^{2+} and Cu^{2+} in the zeolite ion exchange column as a function of the initial concentration.
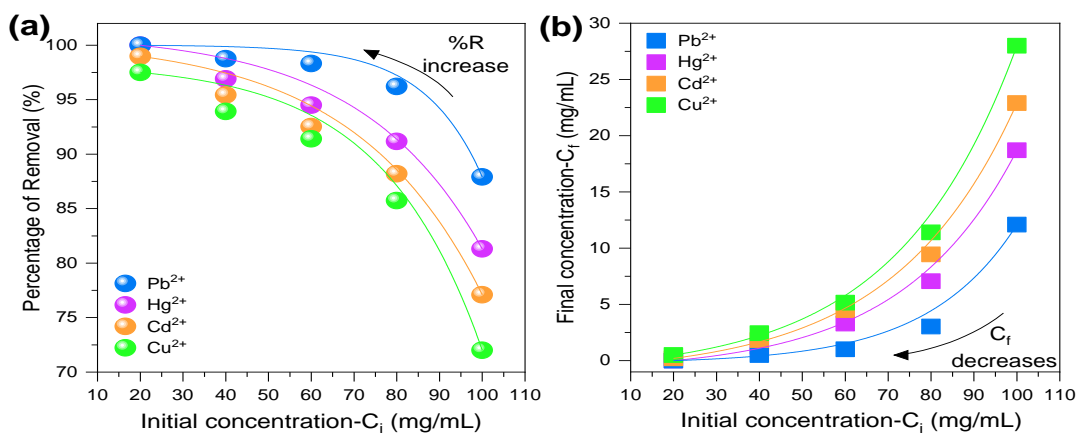
Source: Elaboration by authors in Software Origin; data obtained from the ICP-OES equipment

The literature indicates that, in the case of metal cations and natural zeolites, the predominant mechanism is ion exchange. It can be assumed that the zeolite had a higher amount of exchangeable K^+ ions, therefore, the highest exchange occurred with the Pb^{2+} cation. Final concentrations were 12.09 to 0.002 mg/ml for Pb^{2+}, 18.7 to 0.002 mg/ml for Hg^{2+}, 22.9 to 0.204 mg/ml for Cd^{2+} and 28 to 0.5 mg/ml for Cu^{2+} at an initial concentration of 100 to 20 mg/ml. The latest values at 20 mg/ml starting concentration are within the permissible limits for purified water according to OMS guidelines which are 0.01 mg/ml, 0.006 mg/ml, 0.003 mg/ml, and 2.00 mg/ml for Pb^{2+}, Hg^{2+}, Cd^{2+} and Cu^{2+} respectively.

These results indicate that the AWP prototype was designed to remove the major heavy metals to the permissible limits of the zeolite ion exchange column. The absorption of heavy metals is attributed to different mechanisms of the ion exchange processes, as well as the adsorption process. During the ion exchange process, the metal cations had to move through the pores of the zeolite and the channels of the network, which in turn replaced the exchangeable cations (mainly Na^+, Ca^{2+} and K^+). In this case, the uptake of metal ions could be attributed mainly to ion exchange reactions in the microporous minerals of the zeolite ion exchange column.

4.4 Conclusions

As a result of the structural, morphological, and chemical composition characterizations carried out on natural zeolite and zeolite modified by cationic exchange, we can conclude that:

The type of natural and NaCl-conditioned zeolite was successfully identified, as well as the crystal size of each type of sample using the XRD technique. Clinoptilolite-K crystalline phase predominates for natural zeolite and clinoptilolite-Na for modified zeolite with a crystal size range of 327 a 391 Å. The SEM technique allowed obtaining morphological information of the samples, which revealed the distribution and shapes of the particles presenting four types: angular-subangular-wavy, angular-smooth-wavy, subangular-rough, and sub-round-wavy. With diameters from 3.0 μm to 9.1 and an average of 5.1 ±1.5 μm for the natural zeolite and for the modified zeolite sample, it presented a shorter distribution, with diameters from 3.2 μm to 8.8 μm and an average of 4.8 ±1.32 μm. From the XRF technique it was possible to know the chemical composition and the ion exchange capacity as a function of the Si/Al ratio of each type of zeolite. This relationship indicates that natural zeolite has an ion exchange capacity, Si/Al= 4.63. By conditioning the natural zeolite with NaCl by cation exchange, it was possible to increase the ion exchange capacity, Si/Al= 4.30, increasing the amount of the exchangeable sodium ion approximately 10 times that of the original sample. A high ion exchange capacity corresponds to zeolites with a low Si/Al ratio.

As a result of the evaluation of the natural and modified zeolite by cationic exchange in aqueous solution with heavy metals, we can conclude that:

The recorded data represented by the Langmuir isotherm of ion exchange on the minerals revealed that the metal ions Hg^{2+} and Cu^{2+} were exchanged very slightly. On the other hand, the metal ions of Pb^{2+} and Cd^{2+} were exchanged on the zeolites in greater quantity than the other ions. In addition, the increasing order of the selectivity of the zeolites for the metal ions was reported, which was: $Pb^{2+} > Hg^{2+} > Cd^{2+} > Cu^{2+}$ for the natural resin and $Cd^{2+} > Cu^{2+} > Pb^{2+} > Hg^{2+}$ for the modified resin. This means that for the natural resin, Pb^{2+} is exchanged in greater quantity than Hg^{2+} and for modified resin, Cd^{2+} is exchanged in greater quantity than Cu^{2+} and so on. The theoretical exchange capacity ranged from 2.789 to 3.202 mg Al/gr and the decreasing order of the theoretical exchange capacity of the zeolite samples is as follows: conditioned zeolite> natural zeolite. This is because the amount of aluminum in these zeolites decreases in the same order. The experimental exchange capacity ranged from 1.785 to 2.349 mg/gr for Pb^{2+} ions, from 1.769 to 2.227 mg/gr for Hg^{2+} ions, from 1.753 to 2.610 mg/gr for Cd^{2+} ions and from 1.446 to 2.559 mg/gr for Cu^{2+} ions. The natural zeolite presented a higher exchange capacity for the Pb^{2+} ion and the modified zeolite for the Cd^{2+} ion. The experimental exchange capacity is less than the theoretical exchange capacity because not all active sites are accessible to cations and not all exchangeable cations present in zeolites can be exchanged.

The zeolite filter as a prototype Autonomous Water Purifier (AWP) reveals that the autonomous purifier is suitable and ideal for treating water from different sources, with high concentrations of heavy metals. Obtaining because of the purification process a clean, healthy, and suitable water for human consumption, with a good taste, smell, and color. Reducing gastrointestinal diseases and mortality rates in children transmitted by the consumption of this contaminated resource. Ensuring the health of society in rural areas where they lack quality of life and potable, purified water, and electricity services.

4.5 Acknowledgments

4.6 References

Alghoul, M. A., Poovanaesvaran, P., Mohammed, M. H., Fadhil, A. M., Muftah, A. F., Alkilani, M. M., & Sopian, K. (2016). Design and experimental performance of brackish water reverse osmosis desalination unit powered by 2 kW photovoltaic system. *Renewable Energy*, *93*, 101–114. https://doi.org/10.1016/j.renene.2016.02.015

Anicua Sánchez, R., Del Carmen Gutiérrez Castorena, M., Sánchez García, P., Ortiz Solorio, C., Volke Halle, V. H., Enrique, J., & Panta, R. (2009). Particle size and micromorphological relation on physical properties of perlite and zeolite, *35*, 147–156.

Ates, A. (2014). Role of modification of natural zeolite in removal of manganese from aqueous solutions. *Powder Technology*, *264*, 86–95. https://doi.org/10.1016/j.powtec.2014.05.023

Clayton, G. E., Thorn, R. M. S., & Reynolds, D. M. (2019). Development of a novel off-grid drinking water production system integrating electrochemically activated solutions and ultrafiltration membranes. *Journal of Water Process Engineering*, *30*(August 2017), 100480. https://doi.org/10.1016/j.jwpe.2017.08.018

Cucchiella, F., D'Adamo, I., Lenny Koh, S. C., & Rosa, P. (2015). Recycling of WEEEs: An economic assessment of present and future e-waste streams. *Renewable and Sustainable Energy Reviews*, *51*, 263–272. https://doi.org/10.1016/j.rser.2015.06.010

Dyer, A. (2007). Natural Zeolites by G. V. Tsitsishvili, T. G. Andronikashvili, G. R. Kirov and L. D. Filizova. Ellis Horwood, Chichester 1991. No. of pages: 297. Price: £69.00 (hardback). ISBN 0 13 612037 7. *Geological Journal*, *29*(2), 192–192. https://doi.org/10.1002/gj.3350290217

Elboughdiri, N. (2020). The use of natural zeolite to remove heavy metals Cu (II), Pb (II) and Cd (II), from industrial wastewater. *Cogent Engineering*, *7*(1). https://doi.org/10.1080/23311916.2020.1782623

Erdem, E., Karapinar, N., & Donat, R. (2004). The removal of heavy metal cations by natural zeolites. *Journal of Colloid and Interface Science*, *280*(2), 309–314. https://doi.org/10.1016/j.jcis.2004.08.028

Fernández-Ibáñez, P., Polo-López, M. I., Malato, S., Wadhwa, S., Hamilton, J. W. J., Dunlop, P. S. M., … Byrne, J. A. (2015). Solar photocatalytic disinfection of water using titanium dioxide graphene composites. *Chemical Engineering Journal*, *261*, 36–44. https://doi.org/10.1016/j.cej.2014.06.089

Flachsbarth, I., Willaarts, B., Xie, H., Pitois, G., Mueller, N. D., Ringler, C., & Garrido, A. (2015). The role of Latin America's land and water resources for global food security: Environmental trade-offs of future food production pathways. *PLoS ONE*, *10*(1), 1–24. https://doi.org/10.1371/journal.pone.0116733

Holtman, G. A., Haldenwang, R., & Welz, P. J. (2018). Biological sand filter system treating winery effluent for effective reduction in organic load and pH neutralisation. *Journal of Water Process Engineering*, *25*(July), 118–127. https://doi.org/10.1016/j.jwpe.2018.07.008

Jaishankar, M., Tseten, T., Anbalagan, N., Mathew, B. B., & Beeregowda, K. N. (2014). Toxicity, mechanism and health effects of some heavy metals. *Interdisciplinary Toxicology*, *7*(2), 60–72. https://doi.org/10.2478/intox-2014-0009

Kithome, M., Paul, J. W., Lavkulich, L. M., & Bomke, A. A. (1998). Kinetics of Ammonium Adsorption and Desorption by the Natural Zeolite Clinoptilolite. *Soil Science Society of America Journal*, *62*(3), 622–629. https://doi.org/10.2136/sssaj1998.03615995006200030011x

Kohn, T., Mattle, M. J., Minella, M., & Vione, D. (2016). A modeling approach to estimate the solar disinfection of viral indicator organisms in waste stabilization ponds and surface waters. *Water Research*, *88*, 912–922. https://doi.org/10.1016/j.watres.2015.11.022

Kotoulas, A., Agathou, D., Triantaphyllidou, I. E., Tatoulis, T. I., Akratos, C. S., Tekerlekopoulou, A. G., & Vayenas, D. V. (2019). Zeolite as a potential medium for ammonium recovery and second cheese whey treatment. *Water (Switzerland)*, *11*(1). https://doi.org/10.3390/w11010136

Lei, L., Li, X., & Zhang, X. (2008). Ammonium removal from aqueous solutions using microwave-treated natural Chinese zeolite. *Separation and Purification Technology*, *58*(3), 359–366. https://doi.org/10.1016/j.seppur.2007.05.008

Li, S., Li, J., Dong, M., Fan, S., Zhao, T., Wang, J., & Fan, W. (2019). Strategies to control zeolite particle morphology. *Chemical Society Reviews*, *48*(3), 885–907. https://doi.org/10.1039/C8CS00774H

Li, Y., Li, L., & Yu, J. (2017, December 14). Applications of Zeolites in Sustainable Chemistry. *Chem.* Elsevier Inc. https://doi.org/10.1016/j.chempr.2017.10.009

Liang, Z., & Ni, J. (2009). Improving the ammonium ion uptake onto natural zeolite by using an integrated modification process. *Journal of Hazardous Materials*, *166*(1), 52–60. https://doi.org/10.1016/j.jhazmat.2008.11.002

Lin, L., Lei, Z., Wang, L., Liu, X., Zhang, Y., Wan, C., … Tay, J. H. (2013). Adsorption mechanisms of high-levels of ammonium onto natural and NaCl-modified zeolites. *Separation and Purification Technology*, *103*, 15–20. https://doi.org/10.1016/j.seppur.2012.10.005

Marazzato, M., Aleandri, M., Massaro, M. R., Vitanza, L., Conte, A. L., Conte, M. P., … Longhi, C. (2020). Escherichia coli strains of chicken and human origin: Characterization of antibiotic and heavy-metal resistance profiles, phylogenetic grouping, and presence of virulence genetic markers. *Research in Veterinary Science*, *132*(June), 150–155. https://doi.org/10.1016/j.rvsc.2020.06.012

Mekonnen, M. M., Pahlow, M., Aldaya, M. M., Zarate, E., & Hoekstra, A. Y. (2015). Sustainability, efficiency and equitability of water consumption and pollution in latin America and the Caribbean. *Sustainability (Switzerland)*, *7*(2), 2086–2112. https://doi.org/10.3390/su7022086

Mihaly-Cozmuta, L., Mihaly-Cozmuta, A., Peter, A., Nicula, C., Tutu, H., Silipas, D., & Indrea, E. (2014). Adsorption of heavy metal cations by Na-clinoptilolite: Equilibrium and selectivity studies. *Journal of Environmental Management*, *137*, 69–80. https://doi.org/10.1016/j.jenvman.2014.02.007

Murray, A. L., Napotnik, J. A., Rayner, J. S., Mendoza, A., Mitro, B., Norville, J., … Lantagne, D. S. (2020). Evaluation of consistent use, barriers to use, and microbiological effectiveness of three prototype household water treatment technologies in Haiti, Kenya, and Nicaragua. *Science of the Total Environment*, *718*, 134685. https://doi.org/10.1016/j.scitotenv.2019.134685

National Water Comission (NWC). (2017). Statistics on Water in Mexico, (November), 292.

Ochoa-Gutiérrez, K. S., Tabares-Aguilar, E., Mueses, M. Á., Machuca-Martínez, F., & Li Puma, G. (2018). A Novel Prototype Offset Multi Tubular Photoreactor (OMTP) for solar photocatalytic degradation of water contaminants. *Chemical Engineering Journal*, *341*(July 2017), 628–638. https://doi.org/10.1016/j.cej.2018.02.068

PAHO/WHO. (2019). Nearly 16 million people still practice open defecation in Latin America and the Caribbean. Retrieved from https://www3.paho.org/hq/index.php?option=com_content&view=article&id=15601:nearly-16-million-people-still-practice-open-defecation-in-latin-america-and-the-caribbean&Itemid=1926&lang=en

Pan American Health Organization (PAHO). (2017). *Health in the Americas+, 2017 Edition. Summary: Regional Outlook and Country Profiles.*

Parsa, S. M., Rahbar, A., Koleini, M. H., Davoud Javadi, Y., Afrand, M., Rostami, S., & Amidpour, M. (2020). First approach on nanofluid-based solar still in high altitude for water desalination and solar water disinfection (SODIS). *Desalination*, *491*(June), 114592. https://doi.org/10.1016/j.desal.2020.114592

Peng, W., Maleki, A., Rosen, M. A., & Azarikhah, P. (2018). Optimization of a hybrid system for solar-wind-based water desalination by reverse osmosis: Comparison of approaches. *Desalination*, *442*(November 2017), 16–31. https://doi.org/10.1016/j.desal.2018.03.021

Qin, L., Wang, Y., Vivar, M., Huang, Q., Zhu, L., Fuentes, M., & Wang, Z. (2015). Comparison of photovoltaic and photocatalytic performance ofnon-concentrating and V-trough SOLWAT (solar water purification and renewable electricity generation) systems for water purification. *Energy*, *85*, 251–260. https://doi.org/10.1016/j.energy.2015.03.106

Ramesh, K., Reddy, K. S., Rashmi, I., & Biswas, A. K. (2014). Porosity Distribution, Surface Area, and Morphology of Synthetic Potassium Zeolites: A SEM and N2 Adsorption Study. *Https://Doi.Org/10.1080/00103624.2014.929699*, *45*(16), 2171–2181. https://doi.org/10.1080/00103624.2014.929699

Shaharoona, B., Al-Ismaily, S., Al-Mayahi, A., Al-Harrasi, N., Al-Kindi, R., Al-Sulaimi, A., … Al-Abri, M. (2019). The role of urbanization in soil and groundwater contamination by heavy metals and pathogenic bacteria: A case study from Oman. *Heliyon*, *5*(5), e01771. https://doi.org/10.1016/j.heliyon.2019.e01771

Shannon, R. D. (1976). Revised effective ionic radii and systematic studies of interatomic distances in halides and chalcogenides. *Acta Crystallographica Section A*, *32*(5), 751–767. https://doi.org/10.1107/S0567739476001551

Shi, J., Yang, Z., Dai, H., Lu, X., Peng, L., Tan, X., … Fahim, R. (2017). Preparation and application of modified zeolites as adsorbents in wastewater treatment. *Water Science and Technology*, *2017*(3), 621–635. https://doi.org/10.2166/wst.2018.249

UNICEF and World Health Organization. (2015). *Progress on Sanitation and Drinking Water – 2015 update and MDG assessment.*

UNICEF and World Health Organization. (2019). *Progress on household drinking water, sanitation and hygiene 2000-2017. Special focus on inequalities. Launch version July 12 Main report Progress on Drinking Water , Sanitation and Hygiene.*

Vivar, M., Fuentes, M., Dodd, N., Scott, J., Skryabin, I., & Srithar, K. (2012). First lab-scale experimental results from a hybrid solar water purification and photovoltaic system. *Solar Energy Materials and Solar Cells*, *98*, 260–266. https://doi.org/10.1016/j.solmat.2011.11.012

Vivar, M., Pichel, N., & Fuentes, M. (2017). Solar disinfection of natural river water with low microbiological content (10–103CFU/100 ml) and evaluation of the thermal contribution to water purification. *Solar Energy*, *141*, 1–10. https://doi.org/10.1016/j.solener.2016.11.019

Wang, Y., Jin, Y., Huang, Q., Zhu, L., Vivar, M., Qin, L., … Cui, L. (2016). Photovoltaic and disinfection performance study of a hybrid photovoltaic-solar water disinfection system. *Energy*, *106*, 757–764. https://doi.org/10.1016/j.energy.2016.03.112

WHO, & UNICEF. (2017). *Progress on drinking water, sanitation and hygiene*.

Wu, M. J., Bak, T., Moffitt, M. C., Nowotny, J., Bailey, T. D., & Kersaitis, C. (2014). Photocatalysis of Titanium Dioxide for Water Disinfection: Challenges and Future Perspectives. *International Journal of Photochemistry*, *2014*, 1–9. https://doi.org/10.1155/2014/973484

Chapter 5 Approach to the optimization of parameters of a truncated cone solar concentrator using the Excel Solver tool

Capítulo 5 Acercamiento a la optimización de parámetros de un concentrador solar troncocónico, utilizando la herramienta Solver de Excel

DE ANDA-LÓPEZ, Rosa María†*, BETANZOS-CASTILLO, Francisco, SÁNCHEZ-SALINAS, Agripín and AGUIRRE-ARANDA, Rodolfo

Universidad Tecnológica del Sur del Estado de México, Directorate of Mechatronics. Mexico.

Tecnológico Nacional de México/TES Valle de Bravo, Mexico.

ID 1st Author: *Rosa María, De Anda-López* / **ORC ID:** 0000-0003-3326-2528, **Researcher ID Thomson:** C-7103-2019, **CVU CONACYT ID:** 596793

ID 1st Co-author: *Francisco, Betanzos-Castillo* / **Researcher ID Thomson:** 0000-0002-7245-703X, **CVU CONACYT ID:** 206209

ID 2nd Co-author: *Agripín, Sánchez-Salinas* / **Researcher ID Thomson:** 0000-0002-6199-733X

ID 3rd Co-author: *Rodolfo, Aguirre-Aranda* / **ORC ID:** 0000-0002-2968-9732, **Researcher ID Thomson:** 2939956, **CVU CONACYT ID:** 990003

R. De Anda, F. Betanzos, A. Sánchez and R. Aguirre

* rossyanda.utsem@gmail.com

Abstract

This chapter deals with the optimization of the design parameters of a truncated cone type concentrator to capture, transfer and diffuse sunlight, so that the light reflections are concentrated and multiplied on the walls of the cone and then inside the tube to project them to the interior of any building. As an initial parameter, the length of the zenithal opening of an active Ciralight dome with a square section through which the sun's rays enter vertically was considered. Considering the aperture length as the largest diameter (b) and a concentration factor (CF) of 2.46, an Excel Solver tool was used to calculate the optimal fundamental dimensions: angle of the generatrix (α), cone height (h) and smallest diameter (a), for which a desired concentration is achieved. In addition, a truncated cone concentrator was calculated and designed graphically in Mechanical Desktop 6 Power Pack, starting from a unit cone according to the active dome previously mentioned. Finally, a 1:100 scale model was built to measure the illuminance under open sky and controlled conditions, using temperature sensor and photo detectors with ranges of $0 - 130 \, Klx$, finding a FC of 1,78 under open sky and 1,89 with a halogen lamp under controlled conditions.

Sunlight, Concentrator, Dome, Illuminance, Optimization

Resumen

El presente capítulo se trata sobre la optimización de los parámetros de diseño de un concentrador tipo troncocónico para captar, transferir y difundir luz solar, de tal forma que los reflejos de la luz se concentren y multipliquen en las paredes del cono y posteriormente dentro del tubo para proyectarlos al interior de cualquier construcción. Como parámetro inicial se consideró la longitud de la apertura cenital de un domo activo de la marca Ciralight de sección cuadrada por el cual entran los rayos solares de forma vertical. Considerando la longitud de apertura como diámetro mayor (b) y un factor de concentración (FC) de 2,46, se empleó herramienta Solver de Excel para calcular las dimensiones fundamentales óptimas: ángulo de la generatriz (α), altura del cono (h) y diámetro menor (a), para los cuales se logra una concentración deseada. Además, se calculó y diseñó concentrador troncocónico gráficamente en Mechanical Desktop 6 Power Pack, a partir de un cono unitario acorde a domo activo anteriormente señalado. Finalmente, se construyó modelo a escala 1:100 para medir la iluminancia bajo condiciones de cielo abierto y controladas, empleando sensor de temperatura y foto detectores con rangos de $0 - 130 \, Klx$, encontrándose un FC de 1,78 a cielo abierto y de 1,89 con una lámpara de halógeno en condiciones controladas.

Luz solar, Concentrador, Domo, Iluminancia, Optimización

5.1 Introduction

Most human and biological activities on earth are governed and powered by the sun, as the sun has been a source of illumination throughout human history. The development and use of efficient artificial lights has led humans to separate themselves from the healthiest and best source of illumination: natural light. Studies have shown the benefits in health, safety and labor productivity when buildings are naturally illuminated (Roche, 2000). In addition to the quality of natural light, another reason to use it is its compatibility with lighting control systems to achieve a reduction in the use and cost of conventional energy, thus achieving a sustainable system.

Undoubtedly, sunlight is beneficial inside facilities that house living beings (air quality, non-toxic materials and occupant health) (Gissen, 2002), but the use of artificial light during daylight hours is paradoxical, since there is an abundance of natural light for illumination (Muhs, 2000). Consequently, although artificial light provides sufficient levels of illumination, it cannot provide physiological and psychological comfort (Brainard & Glickman, 2003) (Jenkins & Munner, 2003:2004), benefits of natural light. However, transporting natural light into the facility is sometimes not possible with simple windows and/or domes. Solar concentrators coupled with light pipes are passive systems and represent a simple solution to the problem of natural light deficiency.

In order to transport natural light from the exterior to the interior of a physical space, lumiducts, which are simple structures that allow the transmission of natural light, are being used; there is currently a considerable increase in the use of this technology, with an estimated three million ducts installed worldwide (CIBSE, 2003). Generally, they consist of a collector (usually a hemispherical polycarbonate dome), the duct itself and an emitter. The design of lumiducts has different geometries and improvements and updates are constantly being made, Carter (2002) and Jenkins (2003:2004), used aluminum coated ducts (96% reflection), to such a degree, the light is transmitted in a specular (transparent) way. There are reflective films developed by 3M with a reflection index between 98 and 99%, so that the light is totally transmitted towards the interior. Each innovation made to lumiducts increases their efficiency, but it is important to verify the reliability of this efficiency and its pertinent technological application, hence the importance of corroborating and generating methodologies to quantify the illumination levels achieved (Mohammed & Carter, 2006). Callow (2003), pointed out the benefits of the use of natural light, both for the health of human beings and the world, as well as the reduction in the use of fossil fuels and greenhouse gases. Goulding, Lewis and Steemers (1994), focus their attention on the costs associated with the use of natural lighting inside buildings, as well as the fact of increasing its use.

There is work on the coupling of concentrators with optical fibers (Jutta Schade, 2002) (Hansen, Sato, Ruedy, Lo, Lea, & Medina-Elizalde, 2006), but they have disadvantages due to their high cost and low performance in light transport. On the other hand, commercially and physically, lumiducts are of considerable dimensions, which can hardly be adapted to small spaces and section changes (Jenkins & Munner, 2003:2004).

5.2 Benefits of daylight in buildings

It is a fact that, when it comes to illuminating a visual task, human beings prefer natural light to artificial light or electric light. Light coming from the sun has a perfect color rendering and brings very proactive elements in people's behavior. In addition lower electricity bills and healthier working conditions could be achieved by making better use of daylight. "Numerous studies show that living and working for long periods in areas that receive low levels of daylight disrupts a number of biological cycles" (NewScientist, 2008). Daylight falls broadly into the category of energy efficiency, as it does not generate energy, but reduces the demand for it. The amount of energy demand generated by the use of electric lights is considerable and gives the possibility of significant daylight savings. Peak demand for electric lighting occurs at the same time as low daylight availability.

An additional savings associated with daylighting is a reduction in the cooling load for air-conditioned buildings. Because the luminous efficacy (number of lumens per watt) of natural daylight is higher than most artificial light sources, few radiant watts of energy are required for a given level of illumination. In an office building with artificial lights on, it generates a considerable percentage of the heat that needs to be removed and the overall savings with daylighting are significant (Bodart & De Herde, 2002). Although it has been proven many times that the use of daylight reduces electricity consumption, and automated controls are available for the transition from artificial to daylight, it still generates distrust among users. This is because a gradual changeover between the two sources by means of dimmers is necessary.

A form of artificial energy saving, which is taking a lot of strength to optimize the use of energy in artificial sources is intelligent lighting, which provides quality lighting in a very efficient way, helps reduce the price in bills and maintenance costs, in addition to helping to care for the environment and provides a more comfortable life and generates a quiet environment, but even so natural lighting could never be replaced.

An efficient lighting system is one that satisfies visual needs, generates healthy, comfortable and safe environments, makes adequate use of technological resources such as luminaires, optical systems, to mention a few, and makes rational use of energy, which helps to minimize the ecological and environmental impact. Facing the challenge of sustainable development, where non-renewable resources are diminishing rapidly, a fundamental change is needed in the way we use them. It is necessary to act and promote the use of alternative energies in our modern life to reduce the consumption of fossil fuels and therefore to slow down or stop global warming.

Finding a sustainable balance of world life is a challenge today, with a great decrease of resources, this is a primordial call for a change of idea and the conservation of these resources.

5.3 Natural light in agricultural engineering

In agricultural constructions such as greenhouses, Figure 5.1, light is a determining factor for production. However, there is great confusion about the terminology of the radiation factor, since in practice, the application of this knowledge has not been explored, so it is an area of knowledge that presents many opportunities.

It is therefore necessary to consider the implementation of technological strategies to maintain the amount of light at levels not lower than 200 Wm^{-2}, since the average amount of light required by crops ranges between 120-180 Wm^{-2}.

Figure 5.1 Natural light inside a greenhouse

Source: (Melgarejo Moreno, Navarro Quercop, Legua Murcia, & Lidón Noguera, 2002)

Each type of plant requires a different light intensity. The intensity (or quality) of light is difficult to measure without a lux meter, which measures in units of lux. A value of 100 lux or less is usually considered "low intensity" or "indirect" light. A bright office has an illumination of approximately 400 lux. On the other hand, a value of 1,000 lux or more is considered "high density" lighting. Direct sunlight outdoors is on the order of 32,000 to 100,000 lux.

5.4 Quality of light

A balance of light in the entire PAR (photosynthetically active radiation) range shows us the range visible to the human eye, which is the one we are interested in studying in this work, as shown in Figure 5.2.

Numerous researches in the area of light modify the spectrum to improve plant growth. Diffuse light is better than direct light, as it is able to reach the lower parts of the canopy (less shading), and will not cause sunburn. Regardless of whether the light is direct or diffused, it should be of sufficient intensity (lux). The selected coating material can also be used to increase the amount of diffused light. A texture to the glass surface, for example, can increase the proportion of diffuse light, without much reduction in the level of transmitted light. On a cloudy day, most of the light is diffused.

In plant growth control or photomorphogenesis, there are 5 concepts related to ambient radiation:

1) Quantity of radiation.

2) Quality of radiation.

3) Direction of radiation.

4) Duration (time and transition of light and dark).

5) Polarization (arrays of different photoreceptors).

Of these only 1 and 4 are used for design and management decisions.

Figure 5.2 Light spectrum in the PAR (photosynthetically active) range
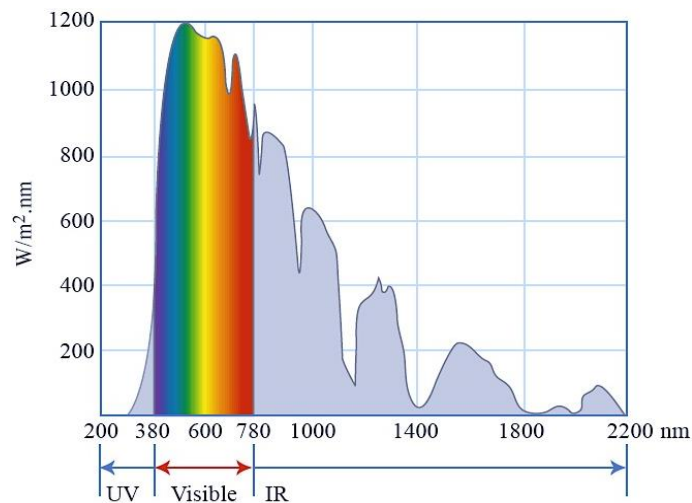
Source: (Comisión internacional de la iluminación , 1993)

5.5 Intensity of the light

Plants have an optimum light intensity. This is the point at which the process of photosynthesis is at its maximum and plant growth is at its highest. If the light level is lower, growth is reduced. In chrysanthemums, a light level of 4 000 lux is sufficient to equalize the rate of photosynthesis and the rate of respiration. This is known as one-point compensation light. At this point, there is no growth, but the plant can survive.

The point at which an increase in light intensity does not increase photosynthesis any further is called saturation light. In many crops, a top leaf saturates around 32 000 lux. However, due to shading on lower leaves, light levels of around 100 000 lux may be needed throughout the plant to become saturated light. In a greenhouse, light intensity can range from 130 000 lux on a clear summer day to less than 3 000 lux on cloudy days.

5.6 Light level in livestock activity

Among the biological activities that living beings perform throughout their lives, those that occupy most of it, not only in time but also in space, are work, production, rest, among others. In this sense, these activities, in order to be developed in an effective way, require that light (environmental characteristic) and vision (personal characteristic) complement each other, since it is considered that 50% of the sensory information received by animals is visual, that is, it has light as its primary origin, and in the case of plants it is required to carry out the photosynthesis process. The integration of these aspects will result in greater productivity, comfort and safety in an efficient and effective manner.

The light intensity experienced by animals housed close to the source can differ markedly from that experienced by others farther away, because intensity is inversely proportional to the square of the distance from the light source.

There are few studies on the effect of light quality or light spectrum on animals. It has been found that the lighting in rooms where animals are housed should have as much as possible the characteristics of sunlight.

Photoperiod is a set of processes that allows plants to regulate their biological functions by using the number of hours of light throughout the year. Photoperiod influences seasonal changes, the breeding season of various species, bird migration, plumage coloration of some birds and the fur of some mammals. It is probably the characteristic of light that most influences animals, in humans, being exposed to very abrupt changes of light, in terms of intensity and wavelengths, this photoperiod has been losing strength, even when working in natural light, generates more visual comfort and improves their quality of life.

It has an influence on circadian rhythms found in biochemical, physiological, and behavioral aspects in animal models stimulated and synchronized through the neuroendocrine pathway. The circadian cycle may affect the animal's response to drugs or its resistance to inoculated infectious organisms (Mcsheehy, 1983). The light/dark relationship may affect reproductive performance and sexual maturity. It is believed that if a change occurs in an animal's photoperiod, experiments should not be performed on it for at least one week (Davis, 1978). If the light period is interrupted by darkness, there are few important effects; conversely, if the reverse occurs, endogenous rhythms may be significantly affected.

Table 5.1 Specific environmental lighting considerations *

Species	Illuminance [Lx]
Cattle	215 - 538
Rams	538
Pigs	500-1000
Horses	200-800
Poultry	10-35

Source: Canadian Council for Animal Welfare (CCPA)

5.7 Light transport systems

Basically, there are two main groups of innovative devices for transporting natural light: Light Conductor Systems and Light Transporter Systems. The former, although very efficient in redirecting sunlight over considerable distances into the interior of spaces, hardly reach more than 10 m, so for longer distances it is necessary to use systems that transport the light to the heart of the buildings.

Providing natural lighting to all interior spaces is not always possible with traditional strategies (side windows) and therefore new natural lighting strategies have been incorporated, such as lumiducts.

Lumiducts are reflective internal wall ducts that, through successive reflections, transmit light to the interior of homes and buildings that normally require artificial lighting during the daytime period. Although the reflective materials convert part of the visible radiation into heat, the high luminous efficacy of the solar radiation allows high luminous fluxes to be obtained at the exit of the ducts.

These systems for transporting natural light through ducts with a reflective internal surface are used when a room has no possibility of receiving natural light because it has no wall exposed to the outside or because the natural light that enters is considered insufficient.

The main function of light transport systems is to transfer the external light resource to an internal emitter. The transport system can be divided into different types, the most basic form being a simple empty cylinder along which a collimated light beam can travel. Mirrored ducts, for example, are a system where the light is guided using the reflectance of the mirror surface to reflect and diffract the light to a required distance, likewise the surface can be another reflective material. As mentioned above, this system consists of three main components, as shown in Figure 5.3:

1. Collector, which can be a concentrator, heliostat, mirror or transparent dome.

2. Duct, the light transport system,

3. Emitter, an element for diffusion or distribution of light into the interior spaces.

Figure 5.3 Design of lumiduct (with indication of its components)
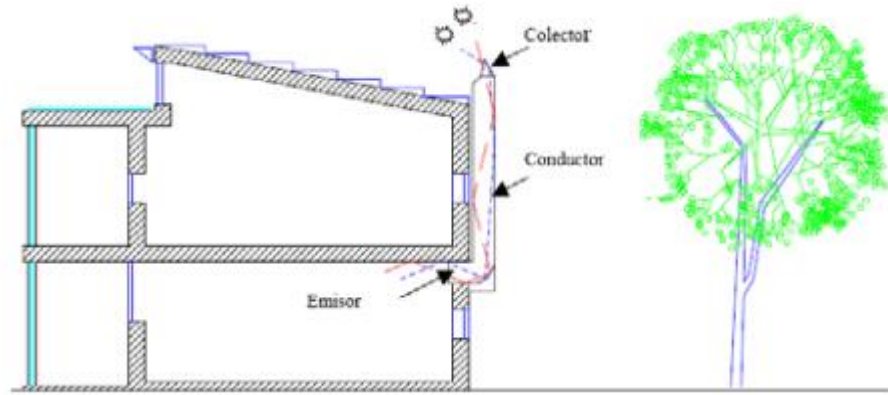
Source: (Melgarejo Moreno, Navarro Quercop, Legua Murcia, & Lidón Noguera, 2002)

5.8 Optical geometry

Considering a typical optical system with input aperture A_1 and output aperture A_2, light enters the system within a cone defined by $\pm\theta_1$ and output within $\pm\theta_2$ measured with respect to the optical axis (Figure 8.1). The radiance of light, L, is the flux per unit solid angle Ω, per unit projected (Welford and Winston, 1989; Sizmann and et. a 1990; Siegel and Howell, 1981). The incident flux over the top of a Lambertian surface is given by the area integral of the radiance and the projection of the solid angle.

$$\Phi_1 = \int L_1 A_1 \cos\theta d\Omega = \int_0^{\theta_1} 2\pi L_1 A_1 \sin\theta \cos\theta d\theta = \pi L_1 A_1 \sin^2\theta_1 \tag{1}$$

A similar expression is obtained for the output aperture with subscript 2, the concentration C is given by the ratio of illumination over the output and input apertures.

$$C \equiv \frac{\frac{\Phi_2}{A_2}}{\frac{\Phi_1}{A_1}} \tag{2}$$

In a geometric system, the concentration is obtained by the conservation of the flow through the system, under the condition of $2 = L1$. This means that the area decreases, the divergence or angle increases for compensation (Welford and Winston, 1989; Sizmann and et. al. 1990; Siegel and Howell, 1981).

Figure 5.4 (Typical concentrator). Typical configuration of solar concentrators. Light incident on input area A_1 with $\pm\theta_1$ and output area A_2 with $\pm\theta_2$
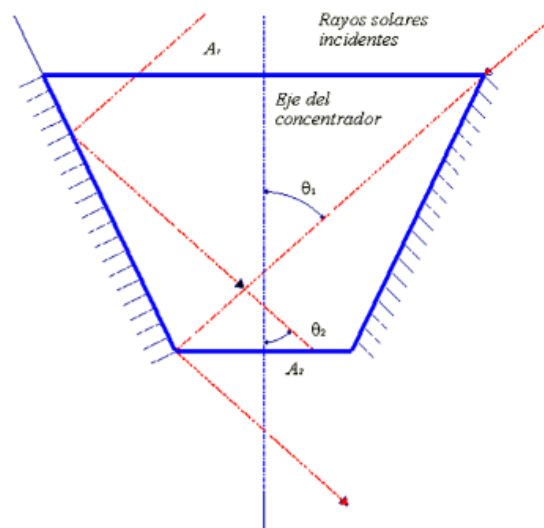
Source: Author's own

This can be viewed as if the area were exchanged so that the angle determines the concentration. The maximum geometric concentration rate is given by:

$$C \leq \frac{sin^2\theta_2}{sin^2\theta_1} = \frac{1}{sin^2\theta_1} \tag{3}$$

Where the exit angle is normally taken to be 90°. If the concentrator is constructed in a medium with refractive index n, and the output plane is immersed in this medium it is necessary to modify the concentrator equation. The extreme ray θ_1 is refracted to θ'_1 in the concentrator, where $sin\,\theta_1 = n\,sin\,\theta'_1$, where from Snell's Law. For when the concentrator whose output is immersed in the environment with θ_2, changes or is not refracted, the concentration is characterized by:

$$C \leq \frac{sin^2\theta_2}{sin^2\theta_1} = \frac{n^2 sin^2\theta_2}{sin^2\theta_1} \tag{4}$$

For convenience, the concentration is defined by a maximum external angle of incidence θ_1 and a final angle of departure θ_2 . It follows that for a passive system. This means that the traversal within a medium with high refractive index, the radiation is confined to a small solid angle, and thus we would have the maximum radiance (Seigel and Howel, 1989; Born and Wolf, 1975). For a 2D system, where light is reduced to one direction, the concentration is the square root of the 3D value.

There are many image-forming concentration systems, such as fresnel lenses and parabolic reflectors, whose concentration obeys equation (4.4) for a factor C=4 (Welford and Winston, 1989; Gleckman, et al., 1989). Both are particular cases, since they partially transfer the image of the sun at its exit and the exit angle is less than 90°, thus obtaining the maximum luminous fluxes.

5.9 Method

Among the biological activities that living beings carry out throughout their lives, one of the activities that occupies most of it, not only in time but also in space, is work, production, rest, etc. In this sense, these activities, in order to be carried out efficiently, require that light (environmental characteristic) and vision (personal characteristic) complement each other, since it is considered that 50% of the sensory information received by animals is visual, that is, it has light as its primary origin, and in the case of plants it is required to carry out the photosynthesis process. The integration of these aspects will result in greater productivity, comfort and safety in an efficient and effective manner.

An optimization problem consists of finding those values of certain variables that optimize (i.e., make maximum or minimum, as the case may be) a function of these variables. The best known method to find the optimum of a function is through the analysis of its derivatives. This method has two limitations: the function is not always derivable, and, in addition, the optimum does not always give us a solution that makes sense in practice. The complexity of this method converged in the so-called numerical methods, added to this the programming in different languages made the process simpler, so the tool we will use to achieve this optimization will be Solver, popular because it is in Excel and easy to use.

First the objective function subject to be optimized (angle of the truncated cone generatrix α, see figure 9.1; which contains the parameters or variables to be determined (height of the cone (h)) and minor diameter of the cone (a) and the constant parameter (major diameter of the cone $(b = 1181,1mm)$, then it is expressed by:

$$\alpha = tan - 1\,[2h/b - a]$$

Once the objective function is established, it is subject to the following restrictions:

$$a > 0\,mm;$$

$$h > 0\,mm;$$

$$\alpha min = 1,107062344\,rad;$$

$$\alpha max = 1{,}570796327 \; rad \; y$$

$$FC = 2{,}46$$

Figure 5.5 Definition of initial design parameters for optimization

The constraint values of FC, αmax y αmin were determined graphically using the geometry of a cone in Mechanical Desktop (Figure 9.1). Once these values have been defined and set, the Solver tool is accessed from the Data menu bar and then Solver, see Figure 5.6.

Figure 5.6 Access to the Solver tool

The following window will appear containing the following characteristics, as shown in Figure 5.7:

Figure 5.7 Definition of a and minimum h according to restrictions

In the target cell parameter the cell containing the target function $\alpha = tan-1\,[2h/b - a]$, will be entered, valued with proposed constant starting values: $b = 1181{,}1$, the constraint of $FC = 2{,}46$ and for the variables a and h possible starting values are assigned. The required function is selected, whether it is the calculation of a maximum or a minimum.

The cells containing the values of the variables to be optimized (a and h) subject to the above-mentioned constraints (Figure 9.3) are entered in the estimation point. In the Add section, the constraints to which they are subject are defined (Figure 5.8).

Figure 5.8 Parameters and Solver options
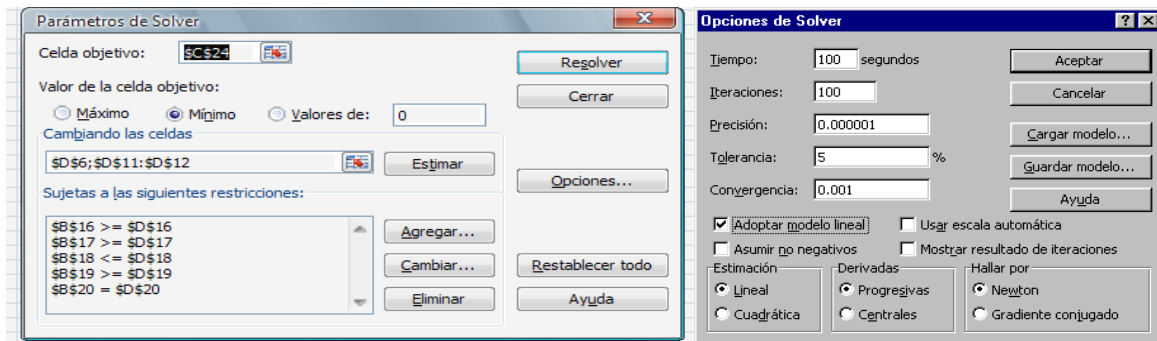
Once these data are entered, select Solve, and Solver, if everything is OK, will display, the data of the optimal a and h variables and 3 reports, one of Answers, one of Sensitivity and Limits of the solution found that satisfies all the given constraints and conditions (Figure 5.9).

Figure 5.9 Solver results
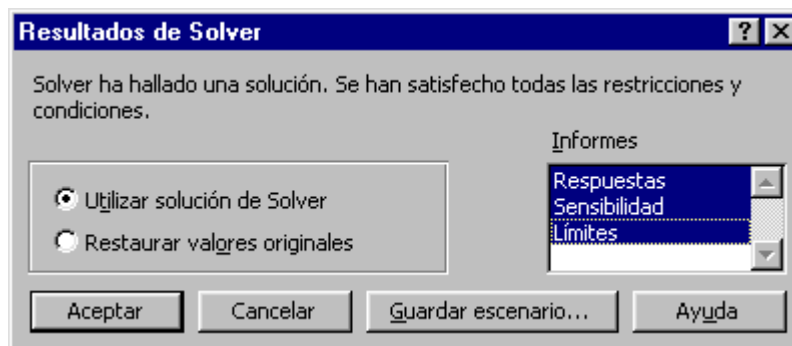
To determine the permissible angles for all the rays that fall vertically on the truncated cone concentrator to enter it and then the duct that will transfer them to the interior of the physical space to be illuminated, the graphic design method was used, starting from the geometric characteristics of a cone such as: angle of the generatrix, diameter of the base and height, and once this is truncated, the optimal smaller diameter (equal to the diameter of the duct) is obtained, all this supported by the CAD Mechanical Desktop 6 Power Pack software.

Then we proceeded to build a scale model to concentrate and transport light through luminous pipelines with energy concentrator, so the necessary materials are:

- Physical space.

- Portable computer equipment.

- Physical components to generate prototypes: passive and active dome, tube, extractor, aluminum foil light concentrator and accessories.

- DB-526 Multilog datalogger.

- Light sensors range 0-130 klx.

- Temperature sensors range -25 - 110 ºC.

- Software: Solver , Mechanical Desktop.

5.10 Results

The results obtained in the design of the solar concentrator are shown; we take as a starting point the largest diameter (b = 1181.1 mm) of the dome to calculate the fundamental dimensions: optimum angle of the generatrix (α), cone height (h), largest diameter (b) and smallest (a), for which an optimum concentration is achieved (Figure 5.10).

Using the Solver we have:

Figure 5.10 Report of responses

Celda objetivo (Mínimo)

Celda	Nombre	Valor original	Valor final
$C$24	α (rad) = <=	1,107062813	1,107062813

Celdas cambiantes

Celda	Nombre	Valor original	Valor final
$D$11 =		753,0418558	753,0418558
$D$12 =		427,9662298	427,9662298

Restricciones

Celda	Nombre	Valor de la celda	Fórmula	Estado	Divergencia
$B$16	a Restricciones	753,0418558	$B$16>=$D$16	Opcional	753,0418558
$B$17	ángulo mínimo αmin Restricciones	1,107062813	$B$17>=$D$17	Obligatorio	0
$B$18	ángulo máximo αmax Restricciones	1,107062813	$B$18<=$D$18	Opcional	0,463733513
$B$19	h Restricciones	427,9662298	$B$19>=$D$19	Opcional	427,9662298
$B$20	FC Restricciones	2,46	$B$20=$D$20	Opcional	0

In Figure 5.10, the response report is shown, we have that in Objective Cell appears the cell of the objective function (Figure 5.1) which is in cell C24, the Name, the initial value before optimizing and the optimal value (final value). In Changing Cells appear the cells of the controllable variables, the name, the initial solution or initial values of the variables and the optimal solution (final value), i.e. a in cell D11 with final value of 753.04 mm and h=427.96 mm in cell D12.

In Constraints we have: Cell value: it is the value taken by the left side of each constraint in the optimal solution (figure 1). Formula: reminds us of the constraints we have entered, including whether it is ≤, or ≥ . State: tells us whether the constraint is exactly met, with an equality, and there is no margin. In other words, it tells us if the constraint is active. Divergence: is the margin that each constraint has. If the inequality is ≤, then it is the right-hand side of the constraint (the constant) minus the left-hand side. If the inequality is ≥, then it is the left side minus the right side (the constant). If the constraint is active, then of course the margin will be zero.

In the sensitivity report (Figure 5.11) it shows: in the Changing Cells part the Value cell: reminds us of the optimal values of the controllable variables a and h cells D11and D12 respectively. Reduced Gradient: indicates how much the coefficient of the objective function should change for the variable to take a positive controllable value, in this case it is 0.

Constraints.

Equal value: is the final value taken by the left-hand side of each constraint in the optimal solution of a (cells B16), h (cell B19), FC (cell B20), α_{min} and α_{max} (cells B17 and B18 respectively). The constraints (cells D16-D20), indicate the right-hand sides of the inequalities to which the objective function was conditioned and which are satisfied.

Figure 5.11 Boundaries report

	Celda objetivo						
Celda	Nombre	Igual					
$C$24	α (rad) = <=	1,107062813					

Celdas cambiantes			Límite	Celda	Límite	Celda
Celda	Nombre	Igual	inferior	objetivo	superior	objetivo
$D$11 =		753,0418558	753,0418558	1,107062813	753,0418558	1,107062813
$D$12 =		427,9662298	427,9662298	1,107062813	#N/A	#N/A

Changing cells

Value: reminds us of the optimal values of the controllable variables. Lower bound: is the smallest value that the variable can take (assuming that the others maintain the optimal value found), and satisfy all constraints. Objective cell (cell C24): value of the objective function if the variable takes the value of the lower limit and the others maintain the optimal value found. Upper bound: the largest value that the variables *a* and *h* (cells D11 and D12) can take (assuming that the others maintain the optimal value found) without violating the constraints. Objective cell: value of the objective function if the variable takes the value of the upper limit for variables *a* and *h* and the others maintain the optimal value found. Finally, the drawing of the final plane of the truncated cone concentrator with optimal parameters was made in Mechanical Desktop (Figure 10.3). All sun rays entering at b are concentrated and finally enter at a. The parameters of the truncated cone concentrator are shown in Table 5.2.

Table 5.2 Dimensions of the solar energy concentrator

Optimum parameters of the truncated cone concentrator			
b [mm]	a [mm]	h [mm]	α [rad]
1181,1	753,0418558	427,9662298	1,107

With the dimensions obtained, a concentration *FC*= 2.46 is achieved; if a different concentration is required, the values of *a* and *h* can be varied while maintaining the value of α. A 1:100 scale prototype of the concentrator covered with a reflective aluminum foil film (Figure 10.3) was built and placed on a closed cardboard box 300 mm long, 120 mm high and 150 mm wide. The external illuminance (*Ie*) [Klx] unconcentrated light, the internal illuminance (*Ii*) [KLx] concentrated light and the temperature (*T*) [ºC] were measured to determine the gradient inside the prototype.

Figure 5.12 Final design of the truncated cone solar concentrator
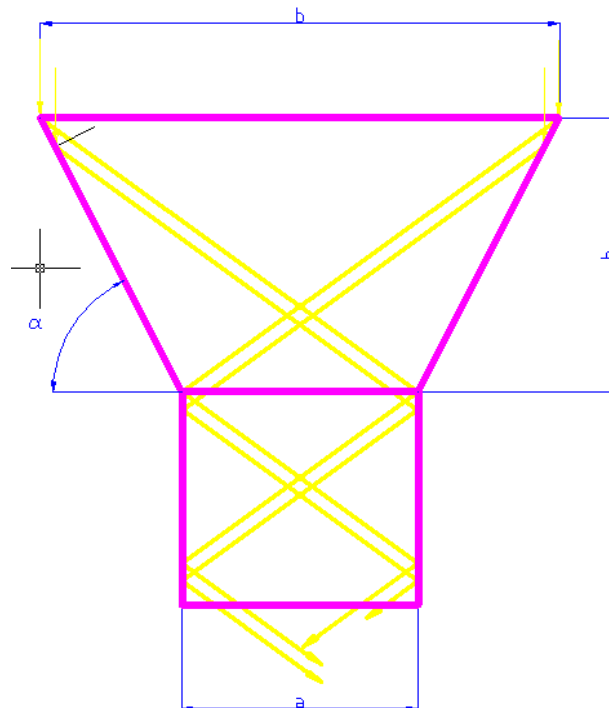
Figure 5.13 Scale model, concentrator and sensors
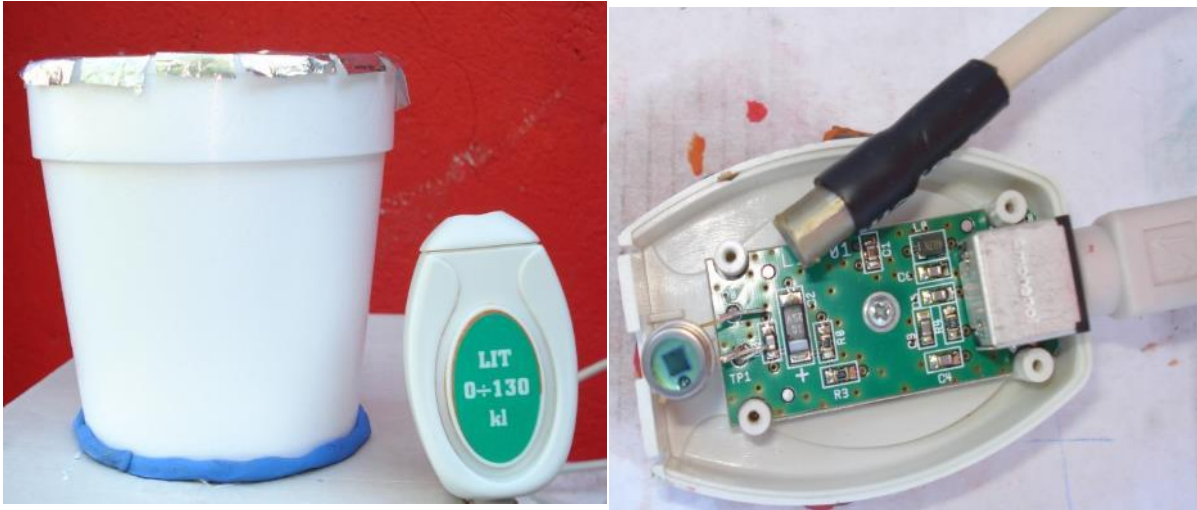
Figure 5.14 *Ie, Ii and T,* under controlled conditions
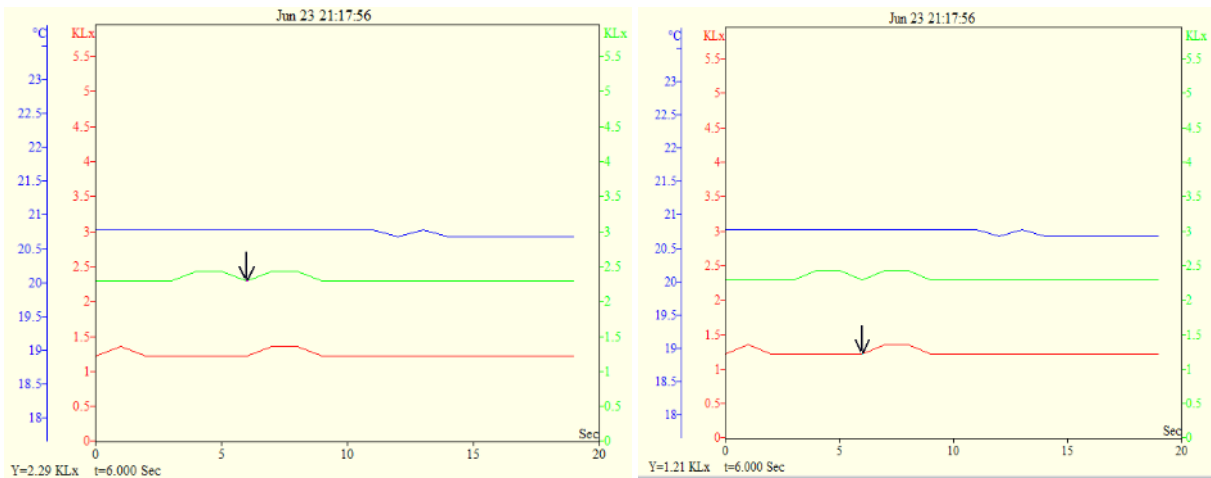
Figure 5.15 *Ie, Ii* and *T*, under open sky conditions
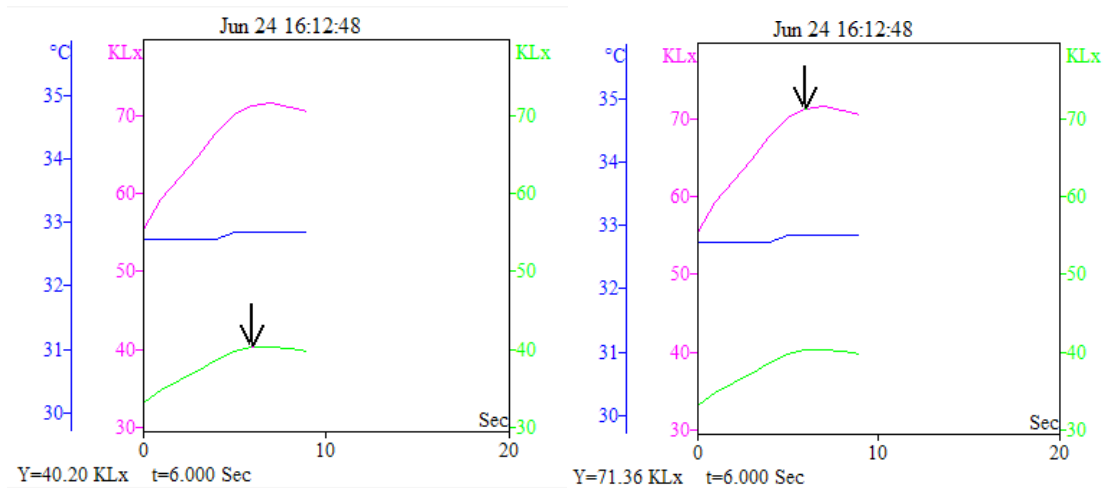
Figure 5.15 shows the behavior of the light under controlled conditions, using a 35 W halogen lamp, 120 V, 29 A and 60 Hz, with which an *FC*= 1.89 was obtained, considering the digital values at the base of the graph and indicated by the arrows inside the graph. The green line shows the value of Ii (concentrated light), Ie (unconcentrated light) in red and T in blue.

Figure 5.16 shows the values of *Ii* (concentrated light) magenta line, in green *Ie* (unconcentrated light), with which *FC* = 1.78 was obtained, as additional data in blue is observed the behavior of the temperature inside the prototype.

Figure 5.16 shows the behavior of the light over time, as well as the temperature gradient affected by the solar concentration inside the prototype. 15,000 samples were taken every second in total. A sampling time of 12 minutes is shown under combined sunny and cloudy sky conditions, i.e. direct light and diffuse light, so that for certain values of Ii (green line) is lower than Ie (magenta line), T (blue line), such situations should be studied in more detail, increasing the sampling time and determine the concentration ratio of the concentrator when there are open sunny-cloudy sky conditions where the values of internal and external illuminance change continuously. Additionally, a direct relationship is observed in the change of temperature (increase of 1 °C on average) with respect to the increase and decrease of the illuminance values in the presented ranges of Ie = 94 - 102 klx and Ii = 105 - 130 klx.

Figure 5.16 *Ie, Ii* and *T*, under sunny - cloudy open sky conditions
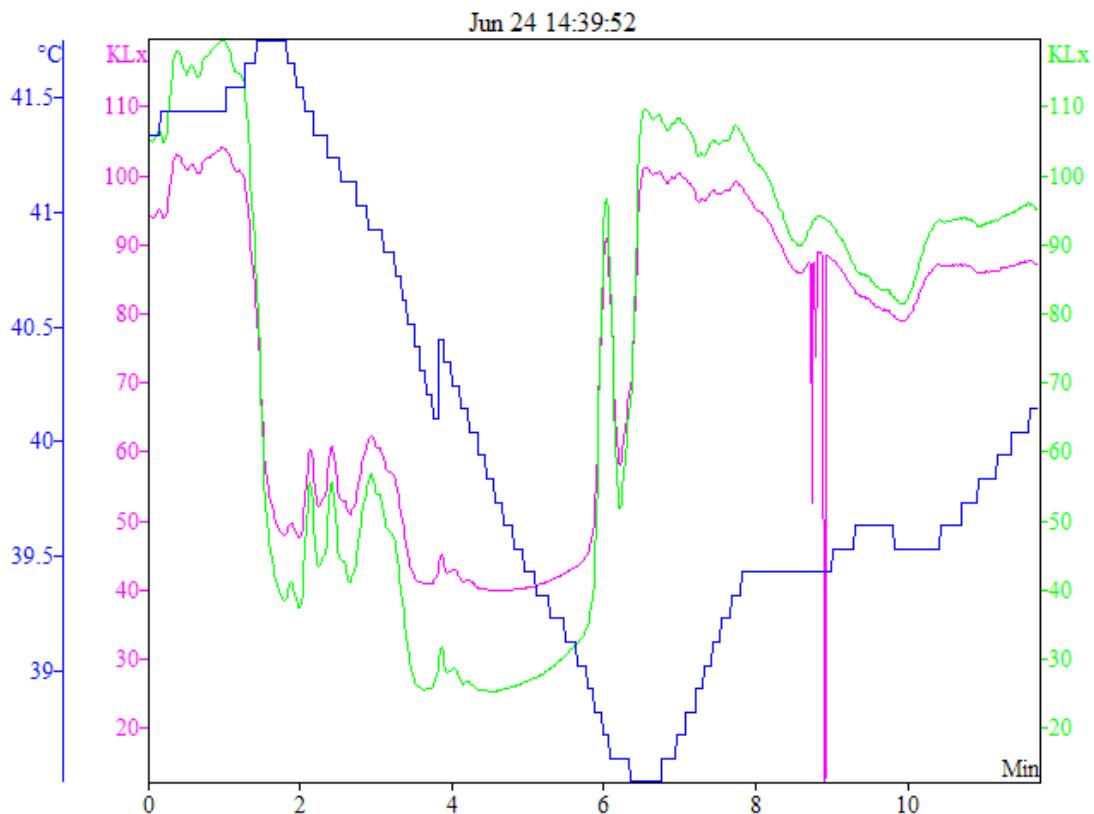
5.11 Conclusions

A truncated cone solar concentrator was designed using computer tools to optimize the sizing, leaving: $b = 1181,1\ mm, a = 573,04\ mm, h = 427,96, FC = 2,46\ y\ \alpha = 63,43°$.

A scale model was built to measure the illuminance at the entrance and exit of the truncated cone concentrator covered with aluminum reflective film, with which it was possible to capture, transfer and diffuse concentrated sunlight at average ratios of 1.78 for open sky, 1.89 with halogen lamp, which are below the FC = 2.46, which would be the ideal according to the sizing of the concentrator, This shows that it is possible to achieve higher concentrations depending on the angle of the generator, the height and diameter of the exit section of the cone according to the desired illumination levels inside a building with deficient or no natural lighting.

5.12 References

Bodart, M., & De Herde, A. (2002). Global Energy Savings in Offices Buildings by the Use of Daylighting. *34*, págs. 421-431. Canada: Research Council Canada. Energy and Buildings.

Boyce, P., Hunter, C., & Howlett, O. (2003). The benefits of daylight trhough windows. *Ligthing Research Center- Renssealer Polytechnic Institute*.

Brainard, G., & Glickman, G. (2003). The biological potency of light in humans: Significance to health and behaviour. *Proceedings of 25th Session of the CIE, 1*, págs. I.22-I.23. San Diego, USA.

Callow, J., & Shao, L. (2003). Air-clad optical rod daylighting system. *Lighting Research and Technology, 35*, 31-38.

Carter, D. J. (2002). The mesured and predicted performance of passive solar light pipe systems. *Lighting research technology*(34), 39-52.

CIBSE. (septiembre de 2003). *Building Journal*.

Comisión internacional de la iluminación . (1993). *cie.com*.

Comisión Internacional de la Iluminación. (1970). *cie.co.at*. Obtenido de http://www.cie.co.at/

Comisión internacional de la iluminación. (1994). *cie.com.* Obtenido de Principles of light measurement.

Davis, D. E. (1978). Social behavoir in a laboratory environment. *National Academy of Sciences*, 44-64.

García Hansen, V. (2006). Innovative daylighting systems for deep-plan commercial buildings. Queensland: Queensland University of Technology.

Gissen, D. (2002). Big & green: toward sustainable architecture in the 21 st century. *Princeton Architectural Press*.

Hansen, J., Sato, M., Ruedy, R., Lo, K., Lea, D., & Medina-Elizalde, M. (26 de septiembre de 2006). Global temperature change. *The National Academyof Sciens of the USA, 103*(29).

Jenkins, D., & Muneer, T. (2004). Light-pipe prediction methods. *Applied energy*(79), 77-86.

Jenkins, D., & Munner, T. (2003:2004). Modelling light-pipe performances a natural daylighting solutions. *Building and Environment, 38*, 965-972.

Jutta Schade, E. A. (2002). Daylighting by optical fiber. *Master Thesis*. Lulea.

Mcsheehy, T. (1983). The overview of the state-of-the-art in environmental monitoring. *Academic Press*, 161-182.

Mohammed, A., & Carter, D. (2006). Tubular Guidance Systems for Daylighting: Achieved and Predicted Installation Performances. *Elsevier Science, 83*(7), 774-788.

Muhs, J. (2000). Design and Analysis of Hybrid Solar Lighting and Full-Spectrum Solar Energy Systems. *Solar 2000 Conference.* Madison: Proceedings os America Solar Energy.

Muneer, T. (1997). *Solar radiation & daylight models for the energy efficient design of buildings.* Oxford: Architectural Press.

NewScientist. (noviembre de 2008). *newscientist.com*. Recuperado el 23 de enero de 2014, de http://www.newscientist.com/article/mg20026833.600-add-daylight-save-energy.html#

Siegel, R., & Howell, J. R. (1981). *Thermal radiation heat transfer* (2nd. ed.). New York: Mc Graw-Hill.

Welford, W. T., & Winston, R. (1989). High collection nonimaging optics. *Academic press, Inc.*

Chapter 6 Evaluation of the heavy metal's levels in PM10 particles in air of an urban site of Leon City, in the cold dry climatic season 2018

Capítulo 6 Evaluación de los niveles de metales pesados en partículas PM10 en aire de un sitio urbano de la Ciudad de León, en la temporada climática seca fría 2018

CERON-BRETON, Julia Griselda†*´, CERON-BRETON, Rosa María´, LARA-SEVERINO, Reyna del Carmen´´ and MARTÍNEZ-MORALES, Stephanie´´´

´Universidad Autónoma del Carmen, Faculty of Chemistry, Mexico.
´´Universidad Autónoma del Carmen, Faculty of Health Sciences, Mexico.
´´´Instituto Potosino de Investigación Científica y Tecnológica, Post-Graduate Studies in Geo-Sciences, Mexico.

ID 1st Author: *Julia Griselda, Ceron-Breton* / **ORC ID:** 0000-0003-1551-7988, **CVU CONACYT ID:** 122903

ID 1st Co-author: *Rosa María, Ceron-Breton* / **ORC ID:** 0000-0001-8647-022X, **CVU CONACYT ID:** 30106

ID 2nd Co-author: *Reyna del Carmen, Lara-Severino* / **ORC ID:** 0000-0001-6173-0187, **CVU CONACYT ID:** 357254

ID 3rd Co-author: *Stephanie, Martínez-Morales* / **ORC ID:** 0000-0003-3465-7644, **CVU CONACYT ID:** 849451

J. Ceron, R. Ceron, R. Lara and S. Martínez

* jceronbreton@gmail.com

Abstract

This work reports the levels of atmospheric particles concentrations PM10 and their content of trace metals (Cd, Co, Cu, Fe and Zn) collected in an urban site of Leon City, Guanajuato during the cold dry climatic season 2018. The analysis for heavy metals determination in the collected particulates were carried out by Atomic Absorption Spectrophotometry (AA). The elemental and morphological analysis of the particulates were carried out by scanning electronic microscopy with energy dispersive spectroscopy (SEM-EDS). Fe was the more abundant metal (1.50 µg m^{-3}), followed in order of importance by Zn (0.65 µg m^{-3}), due to these metals are abundant in the crustal. In minor proportions were found Cu (0.09 µg m^{-3}), Cd (0.28 µg m^{-3}) and Co (0.11 µg m^{-3}). Enrichment Factors analysis showed that all the analyzed metals were highly influenced by anthropogenic activity. Bi-variate and multivariate analysis confirm the anthropogenic origin of Cd, Cu and Zn. SEM-EDS analysis demonstrated Fe was the dominant metal and it was possible to relate the morphology of particulates with their elemental content and their emission sources.

PM10, Heavy metals, Leon

Resumen

El presente trabajo reporta los niveles de concentración de partículas atmosféricas PM10 y su contenido de metales traza (Cd, Co, Cu, Fe y Zn) colectadas en un sitio urbano de la ciudad de León, Guanajuato durante la temporada de seca fría 2018. Los análisis para la determinación de los metales pesados en las partículas colectadas se realizaron mediante Absorción Atómica (AA). El análisis elemental y morfológico de las partículas se llevó a cabo mediante microscopía electrónica de barrido con espectroscopia de energía dispersiva (SEM-EDS). Fe fue el metal más abundante (1.50 µg m^{-3}), seguido en orden de importancia por Zn (0.65 µg m^{-3}), debido a que estos metales abundan en la corteza terrestre. En menores proporciones se encontraron Cu (0.09 µg m^{-3}), Cd (0.28 µg m^{-3}) y Co (0.11 µg m^{-3}). Los Factores de enriquecimiento mostraron que todos los metales analizados fueron altamente influenciados por la actividad antropogénica. Los análisis bi-variado y multivariado confirmaron el origen antropogénico de Cd, Cu y Zn. El análisis SEM/EDS confirmó que Fe fue el metal dominante y fue posible relacionar la morfología de las partículas con su contenido elemental y sus fuentes de emisión.

PM10, Metales pesados, León

6.1 Introduction

Currently, air quality degradation represents a serious threat to human health and ecosystems (Molina L. & Molina N., 2004). Clean air is a basic right for human well-being (SEMARNAT, 2012). According to the World Health Organization (WHO), air pollution cause 2 millions of premature deaths a year in the whole world (WHO, 2006). This mortality index is due to exposure to fine particulates of aerodynamic diameter les or equal than 10 microns (PM10), which may cause cardiovascular and respiratory diseases and cancer (WHO, Air Quality and Health).

Air pollutants may exist in gas phase or in particulate form. Particulate matter is a mixture of liquid and solid particles, organic and inorganic substances, which are suspended in the air. Atmospheric particles can be emitted by a wide variety of sources of natural or anthropogenic origin. Regarding the formation mechanisms, the particles can be emitted as such to the atmosphere (primary) or be generated by chemical reactions (secondary particles). These chemical reactions can consist of the interaction between precursor gases in the atmosphere to form a new particle by condensation, or between a gas and an atmospheric particle to give rise to a new aerosol by adsorption or coagulation (Warneck, 1999). The composition of the particulate material is very varied and we can find, among its main components, sulfates, nitrates, ammonia, sodium chloride, coal, mineral dust, metallic ash and water, as well as certain metals such as As, Cd, Fe, Zn, Cr, Cu, Al, V, Ni and P (Wichman & Peters, 2000).

Atmospheric particles are also classified according to their size and, in the field of air quality, we speak of PM10 particles, which would be the largest, whose theoretical aerodynamic diameter would be less than or equal to 10 µm (microns of meter = millionth of a meter) and fine particles known as PM2.5 whose diameter is less than or equal to 2.5 µm.

This type of pollutant can cause serious effects in human health not only due to its mass concentration but also due to its chemical constitution, and may also contain viruses, bacteria, spores, etc. While PM10 particles are retained in the respiratory tract, producing effects at the respiratory system level, minor particles, such as PM 2.5, have the ability to pass into the bloodstream and can potentially damage any organ or system (INSAG, 2019).

Heavy metals are one of the most harmful constituents of atmospheric particles, due to the toxicity that they represent. Heavy metals have a high density (greater than $4 \text{ g} / cm^3$), mass and atomic weight above 20, and are toxic in low concentrations. Some of these elements are: cobalt (Co), copper (Cu), iron (Fe), manganese (Mn), cadmium (Cd), lead (Pb), zinc (Zn) (Concon, 2009). The risks caused by heavy metals in the atmosphere are manifested when their absorption and accumulation in animal tissues exceeds certain limits; however there are metals that are toxic even at low concentrations, such as: Pb, Cd, As and Hg (OSHA). In the PM10 fraction, there are 75 to 90% metals such as: Cu, Cd, Ni, Zn and Pb, which implies that there is a high percentage of risk and probability of generating serious damage to the exposed organism (Báez et al., 2001). On the other hand, there are also some pollutants that have been designated as main pollutants or criteria, which include PM10 and PM2.5 particles, sulfur dioxide (SO_2), carbon monoxide (CO), nitrogen oxide (NO_2), volatile organic compounds (VOC), and ozone (O_3). They are called "criteria air pollutants" because they are regulated by national and international regulations or standards that establish the maximum permissible limits in ambient air. These pollutants are the most common and ubiquitous in urban centers, where the population is concentrated. The knowledge of the concentration levels of the criteria air pollutants makes it possible to assess air quality in large urban centers and to develop public policies and strategies to protect the health of the population (Henry & Heinke, 1999). In Mexico, maximum permissible levels for PM10 particles in ambient air are regulated in the Mexican Official Standard NOM-025-SAA1-2014, published in the DOF on August 20, 2014. This standard establishes limits of 75 µg m^{-3} average 24 hours and 40 µg m^{-3} annual average.

Mexico has long faced air quality problems in its main metropolitan areas, registering an increase in hospital admissions and mortality related to air pollution in the Valley of Mexico. In addition to the local effects associated with poor air quality on people's health, there are also effects at the regional level, such as the impact on forests and aquatic ecosystems due to acid rain or even globally, such as climate change and the reduction of the thickness of the stratospheric ozone layer, being more obvious these effects in Antarctica. The Bajío area in Guanajuato is one of the commercial and industrial areas more developed in the country, so urban and population growth has increased in recent years, resulting in a deterioration in air quality, especially in the City of Leon, which constitutes the commercial operations center of the Bajío. In the emissions inventory of the State of Guanajuato 2016, it was estimated that the area sources are those that have the main contribution to the emissions of PM10, PM2.5 and NH_3, contributing 84.69%, 78.85% and 98.60% respectively of the total emitted. On the other hand, mobile sources contribute significantly to CO and NO_X emissions, generating 80.74% and 40.05% of the total of these pollutants, respectively; while, in the case of stationary sources, these contribute to almost all SO_2 emissions, with a contribution of 91.68%. In the particular case of VOCs, area sources and natural sources generate 48.45% and 39.95% of the total emissions, respectively.

Therefore, atmospheric monitoring is one of the main indicators of air quality, and in the State of Guanajuato, this monitoring process has been carried out for several years through the State Air Quality Information System, allowing citizens, companies, organizations and institutions, to obtain information on the environment and air quality regarding criteria pollutants and greenhouse gases. This information is generated by the Ministry of the Environment and Territorial Planning through programs and regulations, as well as strategic management instruments, seeking to improve the dissemination of knowledge for the improvement of air quality in the State of Guanajuato and well-being of its citizens. (SEICA, 2019). However, the continuous monitoring of particulate matter (PM10 and PM2.5) is only carried out considering the mass composition of the particles without chemical speciation of its content, hence, the levels of toxic agents such as heavy metals associated with the particles is unknown. Therefore, the effects on health that these pollutants could have on the exposed population is unknown too. For this reason, the present research work evaluated the atmospheric concentrations of the criteria pollutants, the gravimetric concentrations of PM10 particles and their content of trace metals (Zn, Cd, Fe, Cu, Co) in the ambient air of an urban site of the city of Leon, Guanajuato, evaluating the elemental composition, morphology and compliance with current applicable regulations.

This work also provides objective and reliable information about the behavior of the monitored pollutants that may be of help to government institutions to generate and / or update plans that mitigate the health risk to which the population in the study site could be exposed.

The general objective of this study was to evaluate the atmospheric levels of trace heavy metals in PM10 particles, their origin and their relationship with criteria pollutants, as well as their impact on health at a site in the city of Leon, Guanajuato during the cold dry climatic season 2018. The gravimetric concentration of suspended PM10 particles and the concentration of trace metals in trace ambient air (Zn, Cd, Fe, Cu, Co) were determined by atomic absorption spectrophotometry. In addition, the morphology of the particles and its elemental composition was studied by scanning electron microscopy-energy dispersive spectroscopy (SEM-EDS). The influence of the winds at the local level on the concentrations of the pollutants measured was analyzed by means of an analysis of wind roses and the influence of the winds at the regional level on the concentrations of the atmospheric pollutants measured was studied by calculating the air mass trajectories using the NOAA HYSPLIT model. The probable sources of the measured pollutants were inferred from the results of the meteorological and statistical analysis (Pearson's correlation matrix and Principal Component Analysis). Finally, the health risk of PM10 particles and their heavy metal content were evaluated considering carcinogenic and non-carcinogenic risk.

This chapter is structured as follows: The first section provides the Introduction to the research work, Background Section (Section 1) gives information on the study of atmospheric particle levels and their trace metal content registered by other researchers around the world. Section 2 provides the study methodology, considering both the collection methods of PM10 particles, the analysis for the determination of heavy metals by atomic absorption spectrophotometry and SEM-EDS technique used to study the elemental characterization and morphology of the particles. A description of the method used for the meteorological analysis is also provided, which made it possible to determine the influence of local and regional winds on the levels of the measured atmospheric particles, as well as the identification of possible sources contributing to the levels of this pollutant. This section also provides descriptive information on the statistical tools and analysis applied to the data to determine the relationships between the measured air pollutants and the meteorological variables recorded (bi-varied and multivariate analysis: principal component analysis). This section also describes the method used for the evaluation of health risk considering both the cancer risk coefficient in the life time and the non-cancer risk coefficient (risk of contracting diseases other than cancer: cardiovascular and respiratory diseases) due to inhalation of trace metals contained in PM10 particles. Section 3 shows the results of the study, considering the concentration levels of both the PM10 particles and their trace metal content, the exceedances of current national and international regulations, the possible sources contributing to the levels of the pollutants measured and its location, based on statistical analysis and meteorological analysis. An analysis of enrichment factors is also carried out in order to determine which metals had a greater enrichment from anthropogenic sources and which metals were more influenced by the earth's crust. This section also shows the results of the health risk assessment for inhalation of these pollutants. Finally, section 4 provides the conclusions of the study, as well as the recommendations for future work.

6.2 Background

Heavy metal contamination is a current issue in both the environmental and public health areas, mainly due to the negative impact on public perception.

In several cities around the world the chemical characterization of the particulate material has been studied and one of the biggest concerns is always the content of metals in particles due to their toxicity (Molina et al. 2021; López Ayala, 2021). In Ecuador, cities such as Quito (Zalakeviciute et al., 2019) and Cuenca (Zegarra et al., 2020) reported content of metals in PM10, such as Cd ($2.9 \, \mu g \, m^{-3}$), Cu ($1.06 \, \mu g \, m^{-3}$), Fe ($0.229 \, \mu g \, m^{-3}$) and Zn ($1.99 \, \mu g \, m^{-3}$. One of the countries known for its high concentration of atmospheric pollutants is Thailand, where metal content in particles has also been reported, as it was shown by a study carried out in the city of Phitsanulok (Srithawirat et al., 2016) where the health risk assessment revealed that the carcinogenic effects of heavy metals are just below the maximum allowable values, which could pose a cancer risk for the site's population.

In southwestern Italy (Contini et al., 2014) low PM10 values of 34.4 µg m^{-3} were reported with metal content such as Cu (0.012 µg m^{-3}), Fe (0.229 µg m$^{-3)}$ and Zn (0.023 µg m^{-3}). In Havana, Cuba, Cruz and Valdivia (2017) found PM10 values of 39.5 (µg m^{-3}) with high concentrations of Cd (7.74 µg m^{-3}), Cu (100.31 µg m^{-3}) and low values for Zn (0.655 µg m^{-3}).

In Mexico, some studies have also been carried out on particulate matter and their heavy metals content in several cities such as Cananea, Sonora where it was found that the air quality during the study period was always from bad to regular with very few days with a good condition of air quality. In Puebla (Morales et al., 2014) reported PM10 concentrations of 55.9 µg m^{-3} with a trace metal content such as Cd (0.005 µg m^{-3}), Co (0.002 µg m^{-3}), Cu (0.09 µg m^{-3}) and Fe (1.203 µg m^{-3}). Morton and collaborators reported in 2021 for Mexico City, a PM10 concentration of 40.7 µg m^{-3}, with mean concentrations for Cd, Co and Cu of 1.5 µg m^{-3}, 0.5 µg m^{-3} and 123.6 µg m^{-3} respectively. In Tampico, Tamaulipas the concentrations for PM10 were 23.44 µg m^{-3} with concentrations of 0.033 µg m^{-3}, 0.236 µg m^{-3}, 0.04 µg m^{-3} for metals such as Cu, Fe and Zn respectively (Flores et al., 2015).

6.3 Methodology

6.3.1 Study Area

The city of Leon is located in the north of the state of Guanajuato, at an altitude of 1,798 meters above sea level, limiting to the north with San Felipe; to the east with Guanajuato and Silao; to the south with Silao, Romita, and San Francisco del Rincón; and to the west with Purísima del Rincón and the State of Jalisco. The urban sampling site was located within the Medicine Faculty facilities at 20. 13° North Latitude and 101.68° West Latitude, in the downtown. Leon is a Mexican city, head of the homonymous municipality, located in the State of Guanajuato. According to the interest survey carried out by the National Institute of Statistics and Geography (INEGI, 2015), it has a population of 1,578,626 inhabitants, which makes it the most populated town in the state of Guanajuato. The Leon Metropolitan Area is classified within the group 2 of CONAPO Metropolitan Zones Ranking that corresponds to "Metropolitan Zones and cities with more than 1 million and less than 4 million inhabitants" together with the Metropolitan Area of the Toluca Valley, Tijuana and Ciudad Juarez. Therefore, the urban and industrial development in the area has resulted in population growth and the need for services, as well as an increase in transportation vehicles resulting in a degraded air quality. The Institute of Ecology of Guanajuato State has an atmospheric monitoring network, measuring the criteria air pollutants and reporting emissions inventories since 2006. The study site is located within one of the stations of this network, (Station of the Faculty of Medicine), at 21.133 ° N and 101.68 ° W.

6.3.2 PM10 Sampling

The air sampler used was the Airmetrics miniVol TAS which is a portable sampler for suspended particles and non-reactive gases (Figure 6.1). This device was developed by the Environmental Protection Agency (EPA) and the Lane Regional Air Protection Agency in an effort to address the need for portable air pollution sampling technology. The sampling technique used by the miniVol is a modification of the PM10 reference method described in the United States Code of Federal Regulations (40 CFR part 50, appendix J). The sampling was carried out during the cold dry climatic season 2018 (January 05 to 12, 2018). The sampler was placed at the measurement site, where it was assembled, adjusted, and its correct operation verified, leaving the equipment ready to collect air samples. The sampling device sucked ambient air at a controlled flow of 7.2 L min^{-1} that passed through a particle size separator and then through a Whatman brand 47 mm quartz fiber filter during a 24 h sampling period. The particle size separation is achieved by impaction.

Figure 6.1 PM10 Sampling using the Minivol sampling device

Source: Own elaboration from photographs taken at the study site.

6.3.3 Mass concentration of PM10: gravimetric analysis

Before sampling, all the filters were conditioned at constant temperature and humidity values, to be gravimetrically calibrated. After the samples were collected, they were conditioned again in the laboratory at constant temperature and humidity. Filters with any visual irregularities were completely discarded. The procedure for weighing the filters is based on the document "Reference Method for the Determination of Suspended Matter in the Atmosphere" 40 CFR 50, appendix B, which indicates that the filters must be conditioned at least 24 hours at a controlled temperature between 15 ° C and 30 ° C with less than ± 3 ° C variation during the conditioning period (25 ° C for this study), while for humidity it must be less than 50% of constant relative humidity with a variation of the ± 5%. Filters were handled with vinyl gloves (no powder) and the use of metal tweezers was avoided so as not to interfere with the metal determination analysis. Filters were carefully stored in plastic Petri dishes, labeled for 24 hours of conditioning. Each filter was weighed in triplicate with a previously calibrated Sartorious LA 130 SF Analytical Microbalance (with 1 mg resolution) and the results were recorded.

The calculation of the gravimetric concentration is given by the following equation:

$$CPM_{10} = \frac{W_f - W_i}{Vol.} \times 10^6 \tag{1}$$

Where:

CPM_{10} = Gravimetric concentration

W_f = final weight

W_i = starting weight

Vol = standard sample volume

6.3.4 Determination of heavy metals in PM10 by Atomic Absorption Spectrometry

Acid digestion of metals: Filters were placed in 150 ml glass beakers, and 10 mL of aqua regia (25 mL of HNO_3 + 75 mL of HCl) and 1.065 mL of $HClO_4$ were added, leaving them in contact for 18 hours. The contents of each glass were heated at 60 ° C for approximately 70 minutes, until almost dry. Then 20 mL of hot water were added to facilitate the filtration that was carried out when the content of each glass was cooled. Finally, the content of each glass was placed in flasks that were graduated to 50 mL using deionized water, after which the samples were stored in polypropylene containers for later analysis (Machado et al., 2007).

Calibration curves preparation: The standard solutions of Cd, Co, Fe, Zn and Cu were prepared by successive dilution from standard solutions of 1000 ppm HYCEL brand for atomic absorption. The stock solutions of each metal were prepared with a concentration of 10 mg / L of the standard solutions, graduated in 100 mL flasks, with a 2% HNO_3 solution. For each metal, 5 dilutions were prepared from each stock solution, which were measured at 100 mL each and used for the calibration curve of each metal.

Samples Analysis: For the analysis of the samples, an atomic absorption spectrophotometer was used. Thermo Scientific iCE 3000 Series AAS (Figure 2). Measurements were carried out according to the standard conditions recommended by the spectrophotometer manual, that is, specific wavelengths for each metal (Table 6.1). In all measurements, a deuterium lamp was used as a background corrector (Mahecha et al., 2015). Table 6.1 shows the wavelengths used to determine each of the metals considered in the study.

Table 6.1 Wavelength used for the analysis of each metal

Wavelenght (nm)				
Cd	Co	Cu	Fe	Zn
2288	**240.7**	**324.8**	**248.3**	**213.9**

Source: Own elaboration

Figure 6.2 Atomic Absorption Spectrophotometer, Thermo Scientific Brand, model iCE 3000 Series AAS used in this work

Source: Own elaboration from pictures taken in the laboratory

The basic instrumentation for atomic absorption equipment is constituted by a monochromatic radiation source (specific for each element), or polychromatic, an atomizer to produce the excited atoms of the substance to be analyzed: a mono-chromator to select the desired wavelength; a detector sensitive to the emitted radiation and a processor of the signal and the output reading. In general terms, it goes through the atomization system that contains the sample in atomic gas state, it reaches the mono-chromator that eliminates the radiation that is not of interest for the study, passing to the developer or absorbed radiation detector, which is then processed and amplified, giving as result in a read-out. The type of flame used to determine the metals analyzed in PM10 samples was a mixture of air (oxidant) - acetylene (fuel) – at a temperature between 2.100 to 2.400 ° C, being optimal for bring atoms to their fundamental state (Gallegos et al., 2012).

6.3.5 Scanning electronic microscopy- energy dispersive spectroscopy analysis (sem/eds) of selected particles

The analysis was made according to the guide for the monitoring of particles published in 1998 by the EPA (method of analysis of individual particles by SEM). This analysis uses electrons instead of light to form an image, the equipment has a device (filament) that generates an electron beam to illuminate the sample and with different detectors, the electrons generated from the interaction with the surface are then collected to create an image that reflects the surface characteristics of the same, being able to provide information on the shapes, textures and chemical composition of its constituents.

The morphology of the particles and their elemental composition with respect to metal content was evaluated using a Hitachi FLEXSEM-SU1000 (Scanning Electron Microscope) scanning electron microscope equipped with an Energy Dispersive (EDS) X-ray detection system TM 40000 Quantax 75/80 of Bunker that works at 20kV. The low vacuum scanning electron microscope was calibrated with a copper (Cu) grating, a filament current of 300 mA, and a working distance of 5 cm. A 1 mm x 0.5 mm rectangle was cut for analysis and the filters were analyzed as received after sampling, that is, no pre-treatment was necessary for this analysis. Figure 6.3 shows an image of the SEM /EDS equipment used, as well as the way in which the filter sections were mounted for analysis.

Figure 6.3 Electronic Microscope used for the elemental and morphological analysis of PM10 particles and view of the filters mounted on the equipment
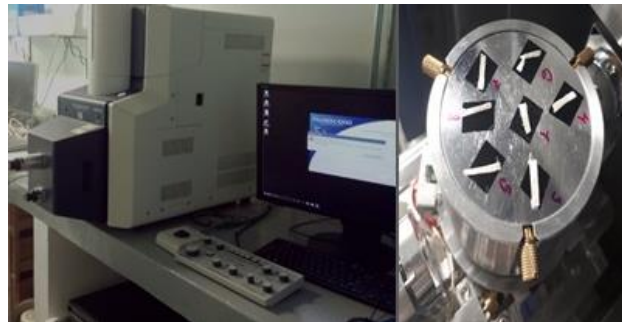
Source: Own elaboration from pictures taken in the laboratory

6.3.6 Measurement of Air criteria pollutants and meteorological parameters

The criteria air pollutants and meteorological parameters data were monthly provided by the SEICA of the state of Guanajuato. Pollutants and meteorological parameters measurements were averaged to determine the average concentrations for each period. The measured meteorological parameters were the following: Temperature ($^\circ$C), relative humidity (%), wind speed (m/s), wind direction (degrees azimuth), atmospheric pressure (mm Hg) and solar radiation (W/m^2). The criteria air pollutants were measured by automatic analyzers: CO (Teledyne Model 3000E Equipment, Filter Correlation Method), NO$_2$ (Teledyne Model 200E Equipment, Chemiluminescence Method), O$_3$ (Teledyne Model 400E Equipment, UV Absorption Method), and PM10 (Met One Instruments Equipment model BAM 1020, Beta-ray attenuation method).

6.3.7 Statistical Analysis

Pearson's correlation were calculated in order to identify bivariate relationships between heavy metals in PM10, criteria air pollutants, and meteorological variables. Similarly, a principal component analysis (PCA) was performed to explain the variation and discover the structure of the data set. The results of the ACP analysis generally is represented in bi-plots or factor loading tables, which reveal correlations between the observations. The information disclosed by ACP is useful to identify whether a pollutant is primary or secondary, or to identify the specific source of the pollutants.

6.3.8 Meteorological analysis

The wind direction data was ordered and reviewed, with which it was possible to perform a wind analysis to determine the origin of the pollutants with respect to the wind direction on each of the sampling days.

Wind Rose Analysis: Wind rose diagrams show the distribution of wind direction and speed at a specific location. This analysis was made with the WRPLOT software (Wind Rose Plots for Meteorological data) that simulates the direction and speed of the prevailing winds in the study site, available at: www.weblakes.com/products/wrplot/index.html

Air mass 24-h backward trajectories calculation: Air mass 24-h backward trajectories were calculated for the sampling period. This type of model is useful to determine the origin and to infer probable sources of the measured air pollutants. This analysis was made using the HYSPLIT tool (Hybrid Lagrangian Integrated Trajectory Model) available in: https//ready.arl.noaa.gov/HYSPLIT_traj.php.

6.3.9 Health Risk Assessment

Carcinogenic and Non-carcinogenic Health Risk Assessment of metals in PM10: The exposure to heavy metals in PM10 was expressed in terms of the daily dose per lifetime or LADD, which allows calculating the corresponding level of risk of each metal, considering two groups of population: adults and children. The LADD helps determine the amount in which a pollutant has negative effects on health when it is absorbed by the human body in a given period of time and is calculated with the following equations (Di Vaio et al., 2018).

$$LADD = E \times C \tag{2}$$

$$E = \frac{IR}{BW} \times \frac{ET \times EF \times ED}{AT \times 365} \tag{3}$$

Where for equation (2), C is the concentration of the metal of interest in PM10, which is assumed to be the same at the point of exposure, while E in equation (2) is obtained from equation (3), where IR ($m^3\ h^{-1}$) is the rate of air inhalation, ET (24 h day^{-1}) is the exposure time, EF (350 day $year^{-1}$) is the exposure frequency, ED (years) is the duration of the exposure, BW (Kg) is the body weight and finally AT (days) is the average time, using ATc for carcinogenic risk and ATn for non-carcinogenic risk (U.S. EPA, 2009). Table 6.2 provides the parameters used to calculate the exposure.

Table 6.2 Parameters used to calculate exposure. *25550 days corresponding to the age according to the typical life expectancy (70 years x 365 days/year); **ED (24 years) multiplied by 365 days/year x 24 days; *** ED (6 years) multiplied by 365 days/year x 24 h/day

Parameter	Symbol	Units	Adults	Children
			Numeric Value	
Inhalation rate	IR	m^3/h	0.9	0.7
Body weight	BW	Kg	40	15
Exposure time	ET	h/day	24	24
Exposure frequency	EF	Days/year	350	350
Exposure duration	ED	Year	24	6
Average time	ATc	Days	25550*	25550*
Average time	ATn	Days	210240**	52560***

Source: DiVaio, 2018

CR represents the increased likelihood of disease caused by tumors above average due to the impact of compounds that produce carcinogenic effects. Values below 10^{-6} are considered negligible. For carcinogenic substances the CR is determined with the following equation:

$$CR = LADD \times CSF \tag{4}$$

Where, CR = probability of cancer occurrence during a life time of 70 years, LADD = daily dose per lifetime expressed in mg $Kg^{-1}day^{-1}$. Carcinogenic risk is defined as the increased likelihood of a person experiencing cancer during a lifetime as a result of exposure to a specific carcinogenic potential (U.S. EPA 2009). The SF is calculated with the following equation:

$$SF = IUR \times \frac{BW}{(IR \times ET)} \times 1000 \tag{5}$$

Where, IUR=Reference value reported in data base by EPA. The following table (Table 6.3) presents the values for IUR and RfC. With regard to inhalation risk units (IUR) and reference concentrations (RfC), only values for Cd, Co and Mn are reported, of which we are interested in the first two.

Table 6.3 Inhalation Unit Risk (IUR) Reference Concentration (RfC) from EPA expressed in mg m^{-3}

Metal	CAS	IUR	RfC
Cd	7440-43-9	1.8 x 10^{-3}	1.00 x 10^{-5}
Co	7440-48-4	9.00 x 10^{-3}	6.00 x 10^{-6}

Source: Environmental Protection Agency (EPA 2009)

The information on the human health assessment on metals is based on EPA guidelines that take into account the IRIS toxicity database (https://www.epa.gov/iris), Sections I (Assessments of health hazards due to non-carcinogenic effects) and II (Lifetime Exposure Carcinogenicity Assessment). The methods used to derive the values given in IRIS were taken from the guidance documents located on the IRIS website. The carcinogenic assessment of metals considers the judgment of the weight of evidence of the probability that the substance is a carcinogen to humans and quantitative estimates of the risk of exposure by inhalation. Quantitative estimates of inhalation risk are presented in three ways. The slope factor is the result of applying a low-dose extrapolation procedure and is presented as the risk per (mg / kg) / day. The unit risk is the quantitative estimate in terms of risk per μg m^{-3} of air breathed. The third way in which the risk is presented is to inhale a certain concentration of air containing the substance in question (heavy metal) that can cause cancer risks of 1 in 10,000, 1 in 100,000 or 1 in 1,000,000. The methods used to develop carcinogenicity information in IRIS are described in The Risk Assessment Guidelines 1986 (EPA / 600 / 8-87 / 045) and in the IRIS background document. Of the metals studied in this work, only Cadmium and Cobalt are considered by the EPA: Cadmium is assessed by the IRIS Program and Cobalt is assessed by the Superfund Health Risk Technical Support Center. According to IRIS-EPA, Cadmium is classified as B1 (probable human carcinogen) (https://iris.epa.gov/ChemicalLanding/&substance_nmbr=141), although, the human carcinogenity data is limited. Cadmium has been associated to lung, trachea, bronchus cancer deaths (in test animals and humans (Thun et al, 1985). The Supperfund Health Risk Technical Support Center has published provisional peer reviewed toxicity values for cobalt. IARC (IARC, 1991) has classified Cobalt sulfate and other soluble cobalt II salts as possibly carcinogenic to humans. ACGIH (2004) has classified Cobalt in category A3 (confirmed animal carcinogenic with unknown relevance to humans). The Integrated Risk Information System (IRIS) does not report a Reference Dose (RfD) for cobalt (U.S. EPA, 2007). We used the values of IUR (Inhalation unit risk) reported by HEA (Health Effects Assessment) (US EPA, 1987) derived form a sub chronic inhalation (9x10^{-3} mg/m^3) and a chronic inhalation (RfC of 9x10^{-6} mg/m^3). Adverse health effects of Cobalt inhalation has been reported in humans, resulting in an increase in cancer mortality (Moulin et al. 1998). There is substantial evidence from some studies that Cobalt is associated to respiratory tumors (Morgan et al 1983; Tuchsen et al. 1996). Carcinogenic risk for zinc, iron and cupper was not determined in this study, since these metals are classified as D (Not classifiable as to human carcinogenicity) and the Quantitative Estimate of Carcinogenic Risk from Inhalation Exposure is not assessed under the IRIS Program.

With respect to the non carcinogenic risk, the THQ (risk coefficient) is calculated as follows:

$$THQ = \frac{ADI}{RfDi} \tag{6}$$

Considering that for THQ there is an exposure level (RfDi) below which it is unlikely for any type of population to experience adverse health effects. When the exposure level (ADI) exceeds the stated value of 1, there may be concern about possible non-carcinogenic health risks; THQ values greater than 1 could suggest further concern. The RfDi represents the inhaled dose at which there are considered no negative effects (EPA, 2009) and is defined as:

$$RfDi = RfC \times \frac{20m^3}{day} \times \frac{1}{70kg} \quad (for\ adults) \tag{7}$$

$$RfDi = RfC \times \frac{7.6m^3}{day} \times \frac{1}{15kg} \quad (for\ children) \tag{8}$$

Where ADI, is the estimated dose that the recipient receives from exposure to polluted air (Di Vaio et al,, 2018), and is calculated with the same variables for cancer risk.

$$ADI = E \times C \tag{9}$$

6.3.10 Enrichment Factor Analysis

The enrichment factor (EF) was used to calculate the contribution of anthropogenic emissions to the levels of metals in the atmosphere, it evaluates the degree of enrichment of an element compared to its relative abundance in the earth's crust. One of the metals with the greatest presence in the earth's crust is iron, for this reason, it was used as a tracer of natural origins. Wedepohl, 1995 indicates the chemical composition of the earth (Table 4). EF then, was calculated using the following equation:

$$EF = \frac{\left(\frac{X}{Ref}\right)air}{\left(\frac{X}{Ref}\right)crustal} \tag{10}$$

Where: X= Concentration of metal to be analyzed and Ref= concentration of the reference metal. Fe was used as the reference metal in this study. The following table (Table 6.4) shows the composition of the metals of interest that has their origin in the earth's crust. Elements with an EF close to 1 have a natural source, while those with high values mostly come from anthropogenic sources (Marcazzan, 2001). The following table (Table 6.5) determines the enrichment indication according to Lawson and Winchester in 1979.

Table 6.4 Metals concentration in the earth's crust

Cd	Co	Cu	Fe	Zn
ppm	ppm	ppm	ppm	ppm
0.102	11.6	14.3	30,890	52

Source: Wedepohl, 1995

Table 6.5 Levels of the enrichment factor

EF Value	Origin Interpretation
<10	Suggests that the metal has its origin in the crustal
100-1000	The element concentration is affected by one or several anthropogenic sources (moderate enrichment)
>1000	It is considered that the element is highly enriched by anthropogenic sources

Source: Lawson D.R, 1979.

6.4 Results and discussion

6.4.1 Mass concentration of PM10

Concentrations of PM10 are shown in Graphic 6.1, where the daily average values observed in this study were within the range of 76.8 (μg m^{-3}) to 130.1 (μgm^{-3}), with an average of 104.2 (μg m^{-3}) for the winter season. NOM-025-SSAI-2014 indicates that the maximum permissible exposure limit in 24 h is 75 (μg m^{-3}), however, the 2005 WHO guide indicates that the health of the exposed population is at risk when the limit of 50 (μg m^{-3}) is exceeded. All days of the sampling period showed exceedances to these limits. The high reported concentrations in this period may be due to the fact that in winter it is common to develop thermal inversions that limit the dispersion of pollutants, causing that their concentrations to remain high during the early hours of the morning and until noon-afternoon, when the inversion is broken. This fraction of particulate material is related to primary particles that are mechanically generated in the atmosphere, such as the re-suspension of dust and particles that can come from unpaved highways and roads. The high incidence of vehicular traffic during the early mornings coincides with the peak hours due to the beginning of the school and work activities. Table 6.6 shows the data of the meteorological parameters recorded during the sampling period.

6.4.2 Trace metals concentrations in *PM10*

Five metals were detected: Cd, Cu, Co, Fe and Zn. The results can be seen in Graphic 6.2, where the average per metal is shown. Fe and Zn were the metals with the highest concentrations during the study period; 1.5 (µg m^{-3}) and 0.6 (µg m^{-3}) respectively, which is not surprising because Fe is one of the most abundant elements in the earth's crust (Acevedo et al., 2004), this agree with that found in other similar studies (Table 6.7), where these metals also had a high value of concentration.

Graphic 6.1 PM10 Mass concentrations in the study site

	1	2	3	4	5	6	7	8
Dry Season (This Study)	102.65	104.75	76.87	101.82	96.14	131.98	89.78	130.14
NOM-025-SSA1-2014, Mexican standard (75 ug/m3)	75	75	75	75	75	75	75	75
WHO Guidelines (50 ug/m3)	50	50	50	50	50	50	50	50
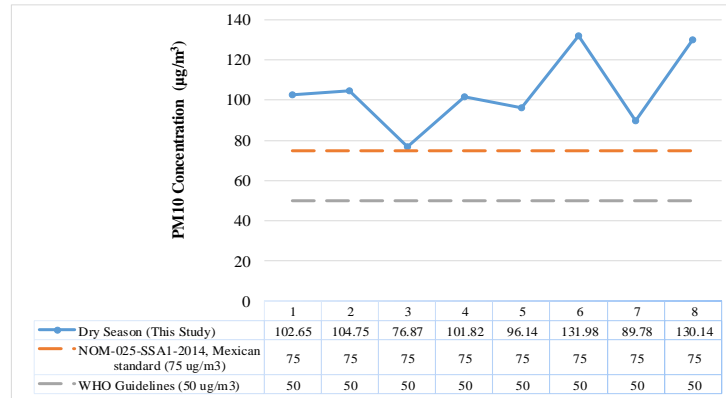
Source: Own elaboration from gravimetric concentrations data

Table 6.6 Meteorological parameters

Wind Speed Km/h	Wind Direction °Azimut	Temperature °C	Relative Humidity %	Barometric Pressure mmHg
1.062	258.085	17.368	43.261	617.959
0.896	218.647	16.644	39.053	618.268
0.930	193.053	16.333	37.545	617.221
1.236	181.070	17.081	35.789	616.723
1.079	211.865	15.851	30.795	617.071
1.224	210.306	16.395	26.584	615.689
1.296	249.074	17.895	35.293	615.581
1.110	184.750	16.335	22.165	617.010

Source: Own elaboration from meteorological parameters measurements.

Followed in abundance were Cd with 0.281 (µg m^{-3}), Co with 0.119 (µg m^{-3}) and Cu with 0.094 (µg m^{-3}). Cadmium is observed to exceed the limit established by the WHO (0.015 µg m^{-3}) although it is significantly lower than in previous and subsequent studies as shown in Table 6.7. The anthropogenic contribution of Cd is due to the iron and steel foundry industry (Oldiges & Glaser, 1986) and since this region is an important production area for the foundry industry, the high concentrations found at the site are not surprising.

Graphic 6.2 Heavy metals concentrations in PM10 in the study site

	Cd	Co	Cu	Fe	Zn
Dry Season 2018	0.281	0.119	0.094	1.506	0.655
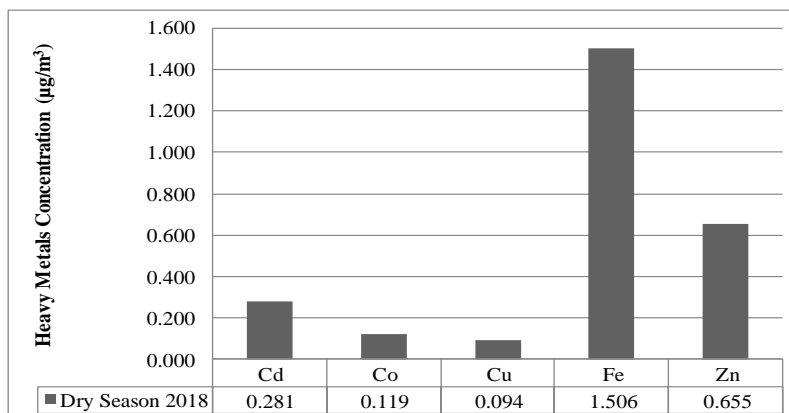
Source: Own elaboration from heavy metals concentrations data.

The average gravimetric concentration of PM10 found in the city of Leon is lower than the studies carried out in Havana (Cruz & Valdivia, 2018), southwestern Italy (Contini et al., 2014), Ecuador (Zalakeviciute et al., 2019) (Zegarra et al., 2020) and lower than in Phitsanulok, Thailand (Srithawirat et al., 2016). In addition, the maximum permissible limits of NOM-025-SSA1-2014 and WHO are exceeded. Co compared to that reported in other studies resulted in intermediate concentrations (Table 6.7). Although the concentration of Cu in this study is higher than that reported for the cities of Tampico and Puebla, as well as in Southwest Italy, it was exceptionally less than that reported for Mexico City (Morton et al., 2021) with a value of 123.6 (μg m^{-3}). Higher concentrations of this metal were found in Havana (Cruz & Valdivia, 2018) and in Quito, Ecuador (Zalakeviciute et al., 2019) where concentrations of 100.31 (μg m$^{-3)}$ and 97.7 (μg m^{-3}) respectively were reported.

Table 6.7 Comparison of results of studies carried out in other sites

	PM$_{10}$ (μg/m^3)	Cd	Co	Cu	Fe	Zn
This study	104.2	0.28	0.094	0.119	1.506	0.655
Cruz et a.l. 2018, Cuba	39.85	7.74	N/M	100.3	N/A	54.82
Contini et al. 2014, Italy	34.4	<0.6	N/M	0.012	0.229	0.023
Zalakeviciute et al. 2019, Quito	24.9	2.9	N/M	97.7	0.44	121.2
Zegarra et al. 2020, Cuenca	50.0	3.14	N/M	1.06	N/A	1.99
Srithawirat et al. 2016, Phitsanulok	123.5	0.5	N/M	0.6	5.8	0.9
Martínez. 2019, Sonora	32	N/M	N/M	0.208	0.627	N/M
Morton-Bermea et al. 2021, CDMX	40.7	1.5	0.5	123.6	N/M	N/M
Flores-Rangel et al. 2015, Tampico	23.44	N/M	N/M	0.033	0.236	0.04
Morales-Garcia et al. 2014, Pueblala	55.9	0.005	0.002	0.09	1.203	N/A
N/M: Not measured						

Source: Own elaboration from cited references showed in the Table

6.4.3 Morphology and elemental content of particles

SEM-EDS Analysis: The particulate material has a wide range of morphological, chemical, physical and thermodynamic properties (EPA, 2004). These pollutants are emitted into the atmosphere as a result of different activities, both natural and anthropogenic (Artiñano, 2003). The particles analyzed in this work showed differences in morphology, which include amorphous and spherical irregularities and groups of small particles that form larger particles. For this study, several particles were analyzed, for practical purposes only the 5 most representative ones are shown for the analysis of their elemental content (Table 6.8) and 3 micrographs of the three most representative types of particles (Figures 6.4-6.6). As it can be observed in Table 6.8, particle marked as 991 is rich in C, Ca, P and Zn. Particle identified as 999 showed a high content of Cl, P, Zn, Pb and Ca, whereas, particle labelled as 1005 showed high mass percentages of Ca, Mg, P and Zn. Particles marked as 1013 and 1034 showed high content of Ca, Cr, P, S and Zn; and Ca, O, P, Si and Zn, respectively. The presence of zinc, phosphorus, calcium and magnesium in the analyzed particles shows the influence of agricultural activities in the area on PM10 particles, since these metals could come from the application of fertilizers on crops. The Bajío area is characterized not only by being an important industrial zone but also by the rise of agriculture at the national level. The particle marked 999 shown in Figure 4 denotes a typical formation of Calcium Carbonates (Calcite). Various studies attribute this mineral to the brick, ceramic and cement industries. The presence of these particles is closely related to processes that involve the firing of bricks and ceramics, where Silica is also present to obtain the products, although little is known about the transformations undergone by the silicate and carbonate phases at the interfaces of reaction (Cultrone et al., 2001). The EDS analysis presents higher mass content for Ca, Si and O, which confirms the presence of Calcite and Silicate, while the elements C, F, Na, Mg, Al, P, S, Cl and Fe are in percentages very small.

Table 6.8 Elemental Content (% mass) of analyzed selected particles

Elemental Content	Identification Code of selected particles				
Al	**991**	**999**	**1005**	**1013**	**1034**
Ba	0.35	0.51	0.39	0.21	0.35
C	12.33		0.39		
Ca	4.59	4.5	7.78	4.47	2.37
Cl	0.49	12.85	0.62		0.23
Cr		0.16		2.08	
Cu					
Fe					
Mg	0.23	0.36	25.29		
Mn	0.31	0.24	0.27		0.40
Na			0.32		
O	0.96	0.34	0.71	0.45	16.36
P	45.88	53.74	42.92	27.09	51.38
Pb		5.5			
S				54.07	
Si	2.48		0.53		9.28
Zn	32.39	21.31	20.78	10.76	18.52
Summation (%)	**100**	**100**	**100**	**100**	**100**

Source: Own elaboration from the SEM-EDS results

The spherical shape of particle 1005 shown in the lower center of Figure 6.5 is a typical indicator of iron oxides (ferrites). The formation of these spherical particles is an indicator of material melting under oxidizing conditions. The origin of these particles is closely related to processes that involve the condensation of vapors in the atmosphere once they have been emitted by industries such as iron foundry, in this way, an important contribution in the generation of spherical ferrite particles, are steel companies or steel mills (Aragón, 2011). The EDS analysis shows a higher content of O, Fe and Si, which confirms the presence of ferrites, while the elements C, Na, Mg, Al, S, Ca, Mn and Ba have very low percentages. An analysis of particle 1043 is shown in Figure 6.6 and concentrations of Pb, O and Si were found. Although Pb was not analyzed in atomic absorption (because this analysis requires that the atomic absorption spectrometer be equipped with a graphite furnace) several lead particles were still found contained in the filters. In the Metropolitan Area of the Valley of Mexico, the presence of lead in PM10 has been related to vehicular emissions (Labrada, 2007), since in areas such as the central and south of Mexico City, there are no industrial establishments; However, they are considered by the Ministry of Transportation and Roads as areas in which the largest number of trips are made by means of transportation in the Valley of Mexico (PITV, 2002). Generally, these lead oxide particles are presented as spheres that form conglomerates, although the size of the conglomerates can range between 1 and 5 µm, each of the constituent particles is of the order of 400 nm on average. Human exposure to lead for prolonged periods, greater than or equal to one year, has an impact on people's health, and can cause chronic effects, therefore in Mexico the air quality standard NOM-026-SAA1-1993 indicates that it does not the exposure limit of 1.5 μgm^{-3} must be exceeded within an arithmetic period of 3 months.

Figure 6.4 SEM-EDS analysis of the selected 999 particle showing Ca and Si content
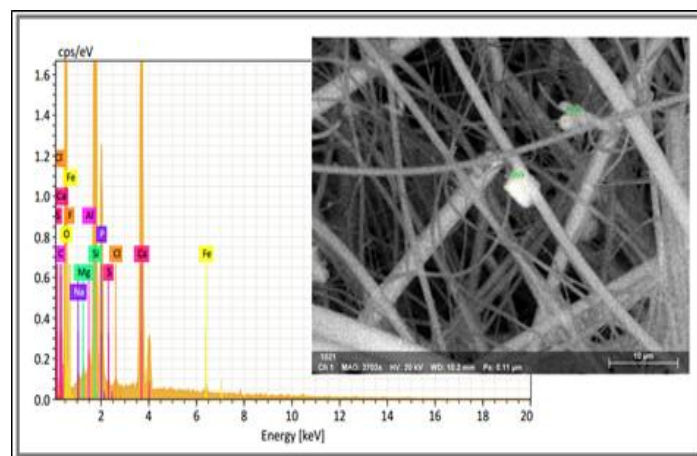
Source: Own elaboration from SEM / EDS analysis

According to the results shown, an evident relationship is observed among the presence of certain anthropogenic particles, their morphology and elemental content, and the activities carried out around the study area. The above due Leon city is an important industrial zone with at least 9 industrial parks distributed in this area, with a constant growth and development, therefore, it is not surprising the found composition of the particles suspended in the air. It should be noted that geography, meteorological conditions such as temperature, rainfall and weather season are also an important part of the development and composition of the particles.

Figure 6.5 SEM-EDS analysis to the selected 1005 particle showing Fe content
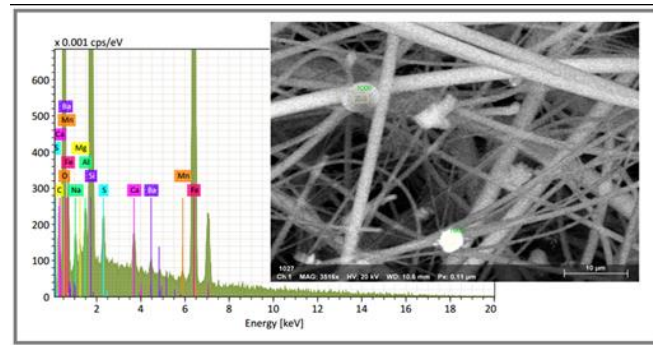
Source: Own elaboration from SEM / EDS analysis

Figure 6.6 SEM-EDS analysis of selected 1043 particle showing high Pb content
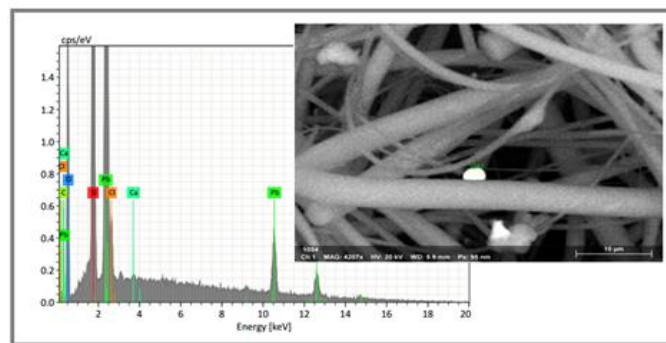
Source: Own elaboration from SEM / EDS analysis

6.4.4 Wind analysis

To determine the possible origin of the pollutants of interest, daily wind analysis were carried out, taking into account the speed and direction parameters of the sampling period. In Figure 7 it can be observed a representative wind rose for the sampling period (cold dry). The rose petals indicate the different wind directions, being the largest petal the predominant wind, the percentage values indicate the frequencies of occurrence and the colors indicate the wind speed in m/s. For this season the winds came from different directions, being more representative the vectors resulting from NE and SW. Based on the results, possible emission sources were identified in the study area with the help of the Google Earth software. At least 7 industrial parks were found, distributed in the in the study area, being San Cristin, Bicentennial Industrial Cluster, and Colinas de Leon, the closest industrial parks (at 5.2 km, 9 km, and 10 km, respectively), located at SW, NE, and SW, respectively. The main economic activity in this area is related to the automotive industry (assembly, manufacture or assembly of auto parts). Other important economic which can be an important source of metallic particles is mining. The municipality of Leon is part of the mining region No. 1 also made up of Guanajuato, Sierra, San Antonio de las minas and La Sauceda where Ag, Au, Pb, Zn and Hg are extracted (SGM, 2018). Fine particles are suspended in the air and these interact depending on their size and morphology, making it possible to transport them over long distances (Balán, 2013). In Figure 6.7 you can see one of the trajectories of air masses during sampling, generally used to determine the impact of meteorology on the measured pollutants, seem to reinforce the idea of mining, being one of the main anthropological activities that contribute to the increase of the concentrations of these metals, having a greater influence on the SW direction where the mines are located.

It is evident that not only these activities, but also the meteorological conditions of the region influence the level of pollution in the air, by allowing pollutants to travel long distances, generating a negative impact.

Figure 6.7 Representative wind rose and trajectory of air masses for the studied period
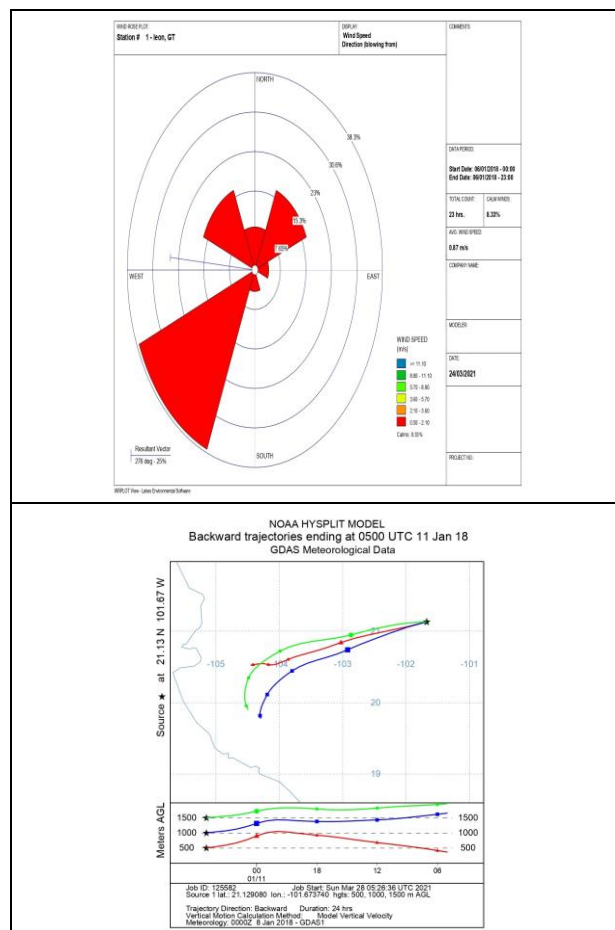
Source: Own elaboration from the result of WRPLOT tool and HYSPLIT software.

6.4.5 Statistical analysis

More detailed information about the behavior of the pollutants studied was revealed through bi-varied (Pearson) and multi-varied (ACP) analysis. Table 6.9 shows Pearson's correlation analysis, where a strong correlation was observed between Zn with Cd and Zn with Cu (0.84 and 0.66 respectively). These metals are associated with industrial emissions. Cd had a moderate correlation with Cu (0.57), these elements are mainly produced by incineration waste, electricity generation plants and industrial sources (Barratt, 1988).

In multivariate analysis or principal component analysis (PCA) the relationship between multiple variables is detailed. In Figure 6.8 the results for PCA are shown, as it can be seen in the bi-plot, two factors (F1 and F2) were needed to explain 60.61% of the variability of the data. 3 groups and variables could be identified where F1 represents the metals (Cd, Cu and Zn) associated with industrial sources, especially Zn that is generated by mobile sources, in road sediments and soil in an area of high vehicular density (Machado et al., 2008). The second group of variables F2, included the meteorological parameters, while the third group F3 included only cobalt, indicating that this metal could have its origin in a different source.

Table 6.9 Elemental Content (% mass) of analyzed selected particles

	Zn	Cd	Fe	Cu	Co	WS	WD	T	RH
Zn	1								
Cd	**0.84**	1							
Fe	0.50	0.19	1						
Cu	0.66	**0.57**	0.08	1					
Co	-0.39	-0.01	-0.50	0.008	1				
WS	0.31	0.26	0.15	0.23	0.32	1			
WD	-0.003	-0.04	0.007	0.27	0.37	0.60	1		
T	0.130	-0.21	0.13	0.05	-0.45	0.48	0.34	1	
RH	-0.66	**-0.90**	0.04	-0.44	-0.12	-0.02	0.26	0.50	1
Values in bold are different at a significant level of alfa=0.05; WS: Wind speed; WD: Wind direction; T: Temperature; RH: Relative humidity									

Source: Own elaboration from data using XLSTAT software

6.4.6 Enrichment factor analysis

The enrichment factor (EF) is used to evaluate the degree of enrichment of a single element compared to the relative abundance of that element in a cortical material. Iron (Fe) was used as the reference metal in this study due to its abundance in the terrestrial crust. Table 6.10 shows the results of the EF calculation for each of the metals analyzed. A separation of two groups can be made, the first, made up of Co (166.212), Cu (170.688) and Zn (258.36) presenting values between 100-1,000. These metals are considered highly enriched by anthropogenic sources (see Table 6.10), agreeing with the previous discussion where it is pointed out that these metals can have industrial origins and come from burning of fossil fuels. The second group is made up of Cd with the highest EF value of 56,566.915, indicating that this metal had its origin in anthropogenic processes without any influence from the earth's crust.

Figure 6.8 Analysis of principal components for winter (factor table and biplot)

Square cosines of the variables			
Variables	F1	F2	F3
Zn	**0.908**	0.018	0.062
Cd	**0.893**	0.029	0.014
Fe	0.125	0.087	0.351
Cu	**0.533**	0.030	0.032
Co	0.020	0.010	**0.905**
WS	0.104	**0.543**	0.159
WD	0.001	**0.538**	0.261
T	0.006	**0.700**	0.103
RH	**0.658**	0.252	0.046
Values in bold correspond to those who were significant at a level of significance of alfa=0.05			
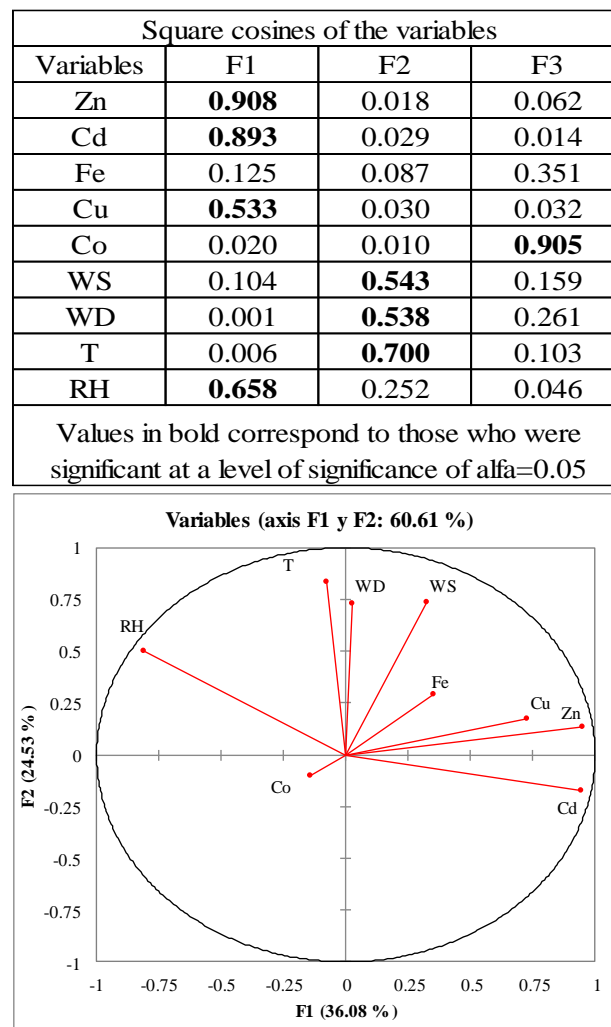
Source: Own elaboration from data using XLSTAT software

Table 6.10 Enrichment factor results for metals

Enrichment Factor (EF)		
Cold dry climatic season	Cd	56566.915
	Co	166.212
	Cu	170.688
	Fe	1
	Zn	258.363

Source: Own elaboration from metals concentrations.

6.4.7 Health risk assessment

The risk coefficients (CR) of suffering cancer in the life time for Cadmium and Cobalt were estimated, presenting values lower than those established by the WHO (1×10^{-6}) (See Table 6.11), however, they are only one order of magnitude below the acceptable limit, so if emissions of particles containing these metals are not reduced, in the future carcinogenic effects related to the inhalation of these metals in PM10. Cancer risk coefficient values were higher for the adult population compared to the child population. These differences may be due to the greater mobility of the adult population due to their work and occupations, spending more time than the child population exposed to the open air. Breathing air even at low cadmium concentrations for a long time (for years) causes cadmium accumulation in the kidneys; if it reaches high enough levels it can cause kidney disease. In the case of chronic inhalation cobalt can lead to chronic lung problems. Inhalation for long periods can lead to breathing problems that are similar to asthma or pulmonary fibrosis, such as shortness of breath and a reduction in resistance to exercise. Table 6.12 shows the results for the non-carcinogenic risk (THQ) for cadmium and cobalt. These values must be <1 in order not to present a health risk, as is evident, although the Cd value in infants is higher than in adults, neither of the two metals exceeded this parameter. The above suggests that the child population is at greater risk of suffering some negative effect related to the respiratory tract, however, the risk is low, taking into account that it does not exceed the value established by the WHO of 1.0.

Table 6.11 Average values of carcinogenic risk coefficients of metals

Risk Cancer Coefficient (CR)	Metal	Adult population	Child Population
	Cadmium	4.56×10^{-7}	1.14×10^{-7}
	Cobalt	9.65×10^{-7}	2.41×10^{-7}

Source: Own elaboration from calculated data.

Table 6.12 Average values of non-carcinogenic risk coefficients of metals

Non-cancer Risk Coefficient (Hazard Quotient: HQ)	Metal	Adult population	Child Population
	Cadmium	0.0439	0.205
	Cobalt	0.0310	0.144

Source: Own elaboration from calculated data

6.5 Conclusions

The gravimetric concentrations of PM10 in the study site exceeded the maximum permissible limits established by the Mexican Regulations (NOM-025-SAA1-2014: 75 µg m^{-3}) and by the World Health Organization (50 µg m^{-3}), indicating that exposure to PM10 at the study site may represent a potential risk to the health of the population established in the center of the city of Leon. The results of the analysis of the content of heavy metals (Cd, Co, Cu, Fe and Zn) in the collected PM10 particles showed that the dominant metal was Fe, followed in order of importance by Zn during the study period. This finding was to be expected since because these metals are abundant in the earth's crust, which is consistent with what has been reported around the world by other authors. Cu and Co were found in lower proportions, the latter being the one that presented the lowest concentrations of all the metals measured. Cd presented lower values than those reported in most international studies but exceeded the values reported in Mexican studies.

The meteorological analysis showed that sources located to the southwest and northwest of the study site (industrial complexes and metal and mineral extraction activities) could contribute to the levels of PM10 and its content of heavy metals. The enrichment factor (EF) analysis showed that all the analyzed metals were highly influenced by anthropological activity (industrial sources, biomass burning and vehicular traffic). Cd was the metal that showed the highest EF values, probably due to a poor efficiency of the internal combustion engines of the vehicles in the area, without any contribution from the earth's crust. This is in agreement with what has been reported in other studies. The bi-variate analysis (Pearson's correlation matrix) and the multivariate analysis (Principal Component Analysis) confirmed the anthropogenic origin of Cd, Cu and Zn and their common source (burning of fossil fuels). Co was probably originated from production of batteries, industrial processes of metal refining and the expulsion of smoke and gases from these processes. The results of the health risk assessment showed that the cancer risk coefficients values (CR) did not exceed the threshold value established by the EPA of 10^{-6} for Cd and Co during the sampling season. Despite this, CR values in adults are higher than in infants, which is to be expected due to mobility related to their work activities and occupations. The non-cancer risk coefficients (HQ) were higher for the child population in both Cadmium and Cobalt, although neither of the two metals exceeded the maximum allowable limit established by the WHO and the EPA. The SEM-EDS analysis of selected particles allowed to study the morphology and content of the main metals in the PM10 samples. From the morphological analysis of the studied particles it was possible to deduce their possible origin. It was confirmed that Fe was the dominant metal in the collected particles with spherical and irregular shapes, so this metal could have its origin beyond natural sources (the earth's crust) and it could be influenced by re-suspension processes, mining, smelting and welding activities. It is recommended for future work to carry out more intensive sampling campaigns that cover more climatic seasons throughout the year at the study site (cold dry, warm dry and rainy), as well as include the determination of a greater number of trace metals contained in PM10 particles.

6.6 References

Acevedo, O., Ortiz, E., Cruz, M., & Cruz, E. (2004). El papel de óxidos de hierro en suelos. Terra Latinoamericana, 22(4), 485-497. https://www.redalyc.org/articulo.oa?id=57311096013

ACGIH (American Conference of Governmental Industrial Hygienists). 2004. TLVs® and BEIs®: Threshold Limit Values for Chemical Substances and Physical Agents, Biological Exposure Indices. Cincinnati, OH.

Aragón, A. (2011). ¿Cómo son las particulas atmosfericas antropogenicas y cuál es su relación con los diversos tipos de fuentes contaminantes? San Luis Potosi, S.L.P, México: Editorial Groppe Libros (1ra edición).

Artiñano, B. S. (2003). Anthropogenic and natural influence on the PM10 and PM2.5 aerosol in Madrid (Spain). Analysis of high concentration episodes. Environmental Pollution, 125, , 453-465.

Báez, A., García, R., & Belmont, R. (2001). Trace heavy elements in rain water collected in México city. Universidad Nacional Autónoma de México, México.

Balán, R. A. (2013). Estudio del contenido de hidrocarburos policíclicos aromáticos y metales en partículas atmosféricas de diferentes diámetros aerodinámicos de La Comarca Lagunera, México [Tesis de doctorado, CIMAV] http://cimav.repositorioinstitucional.mx/jspui/handle/1004/898 .

Barratt, R. S. (1988). Cadmium in urban atmospheres. Science of the total environment, 72, 211-215.

Concon, J. (2009). Heavy metals in food. Food Toxicology. New York Dekker (pp. 1043-1045).

Cruz , L., & Valdivia, J. A. (2017). Cuantificación de la concentración de Zn, Cu, Pb y Cd en partículas menores de 10µm procedentes del aerosol atmosférico. Clasificación de las fuentes contaminantes en la zona de estudio. Killkana Técnica, 1(3), 17-24. https://doi.org/10.26871/killkana_tecnica.v1i3.82

Contini, D., Cesari, D., Donateo, A., Chirizzi, D., & Belosi, F. (2014). Characterization of PM10 and PM2. 5 and their metals content in different typologies of sites in South-Eastern Italy. Atmosphere, 5(2), 435-453.

Cultrone, G., Rodriguez, C., Sebastian, E., Cazalla, O., & De La Torre, M. J. (2001). Carbonate and silicate phase reactions during ceramic firing. European Journal of Mineralogy, 13(3), 621-634.

Di Vaio, P., Magli, E., Caliendo, G., Corvino, A., Fiorino, F., Frecentese, F., ... & Perissutti, E. (2018). Heavy metals size distribution in PM10 and environmental-sanitary risk analysis in Acerra (Italy). Atmosphere, 9(2), 58.

Gallegos, W., Vega, M., & Noriega, P. (2012). Espectroscopía de absorción atómica con llama y su aplicación para la determinación de plomo y control de productos cosméticos. Revista de ciencias de la vida, 15, 19-26.

Guanajuato. (2016). Inventario de Emisiones del Estado de Guanajuato. Leon de los Aldama: Instituto de Ecologia del Estado de Guanajuato.

Henry, J. G., & Heinke, G. W. (1999). Ingeniería ambiental. Pearson Educación.

IARC (International Agency for Research on Cancer). 1991. IARC Monographs on the Evaluation of Carcinogenic Risks to Humans. Volume 52: Chlorinated Drinking-Water; Chlorination By-Products; Some Other Halogenated Compounds; Cobalt and Cobalt Compounds. p. 363-472.

INSAG. (2019). Instituto para la Salud Geoambiental. Consultado el 9 de marzo de 2019, de https://www.saludgeoambiental.org/

IPCS. (2002). Environmental Health Criteria: Copper. Geneva: World health Organization, 234-252.

Lawson, D. R., & Winchester, J. W. (1979). A standard crustal aerosol as a reference for elemental enrichment factors. Atmospheric Environment (1967), 13(7), 925-930.

López Ayala, O. (2021). Evaluación de la distribución de hidrocarburos aromáticos policíclicos en material particulado suspendido en sitios críticos del área metropolitana de Monterrey y su relación con la exposición de población infantil Tesis para obtener el grado de Doctor con orientación en química analítica ambiental, Universidad Autónoma de Nuevo León, Marzo 2021. http://eprints.uanl.mx/id/eprint/21003

Machado, A., García, N., García, C., Acosta, L., Córdova, A., Linares, M., Giraldoth, D., & Velásquez, H. (2008). Contaminación por metales (Pb, Zn, Ni y Cr) en aire, sedimentos viales y suelo en una zona de alto tráfico vehicular. Revista internacional de contaminación ambiental, 24(4), 171-182.

Machado, A., Velázquez, H., García, N., García, C., Acosta, L., Córdova, A., & Linares, M. (2007). Metales en PM10 y su dispersión en una zona de alto tráfico vehicular. Interciencia, 32(5), 312-317.

Mahecha, J. D., Trujullo, J. M., & Torres, M. A. (2015). Contenido de metales pesados en suelos agrícolas de la región del Ariari, Departamento del Meta. Orinoquia, 19(1), 118-122.

Mar, V. (2003). Niveles, composición y origen del material particulado atmosférico en los sectores Norte y Este de la Península Ibérica y Canarias. Universidad de Barcelona.

Marcazzan, G. M., Vaccaro, S., Valli, G., & Vecchi, R. (2001). Characterisation of PM10 and PM2. 5 particulate matter in the ambient air of Milan (Italy). Atmospheric Environment, 35(27), 4639-4650.

Martínez, T. (2019). Estudio de PM10 y metales (Cu, Fe, Mn, Pb) en aire ambiente, en la región de Cananea, Sonora, México. Sonora, México: universidad de Sonora.

Molina L. T. and Molina M. J. (2004). Diseño, evaluación y preparación de mecanismos de ejecución para las estrategias de mejoramiento de la calidad de aira en la ZMVM 2001-2010. Informe Final. Elaborated for CAM. MIT.

Molina, Y.H., Monrroy, V., and Rosa, X. (2021). Biomonitoreo de elementos traza en área urbana e industrial de Lurigancho-Chosica utilizando especies Tillandsia latifolia y T. purpurea como biomonitores. Tesis para obtener el Título Profesional de Ingeniero Ambiental. Universidad Peruana Unión. Lima, Perú, Mayo de 2021. http://hdl.handle.net/20.500.12840/4477.

Morales, S. S., Rodriguez, P. F., Jonathan, M. P., Navarrete, M., Herrera, M. A., & Munoz-Sevilla, N. P. (2014). Characterization of As and trace metals embedded in PM 10 particles in Puebla City, Mexico. Environmental monitoring and assessment, 186(1), 55-67.

Morgan, L. G. (1983). A study into the health and mortality of men exposed to cobalt and oxides. Occupational Medicine, 33(4), 181-186. https://doi.org/10.1093/occmed/33.4.181

Morton, O., Hernández, E., Almorín, M. A., Ordoñez, S., Bermendi, L., & Retama, A. (2021). Historical trends of metals concentration in PM 10 collected in the Mexico City metropolitan area between 2004 and 2014. Environmental Geochemistry and Health, 1-18. https://doi.org/10.1007/s10653-021-00838-w.

Moulin, J. J., Wild, P., Romazini, S., Lasfargues, G., Peltier, A., Bozec, C., ... & Perdrix, A. (1998). Lung cancer risk in hard-metal workers. American journal of epidemiology, 148(3), 241-248. https://doi.org/10.1093/oxfordjournals.aje.a009631

NOM-025-SAA1-2014. (2014). Salud Ambiental. Valores límite permisibles para la concentración de particulas suspendidas PM10 y PM2.5 en el aire ambiente y criterios para su evaluación.

Oldiges, H., & Glaser, U. (1986). The inhalative toxicity of different cadmium compounds in rats. Trace elements in medicine, 3(2), 72-75.

OMS. (s.f.). Recuperado el 6 de septiembre de 2018, de Calidad del Aire y Salud: https://www.who.int/es/news-room/fact-sheets/detail/ambient-(outdoor)-air-quality-and-health

OMS. (2006). Guias de calidad dela ire de la OMS relativas al materal particulado, el ozono, el dioxido de nitrogeno y el dioxido de azufre. Actualizacion mundial 2005.

OSHA. (n.d.). United State Department of Labor. Consultado el 15 de marzo de 2019, de Occupational Safety and Health Administration: www.osha.gov

PITV. (2002). Programa Integral de Transporte y Vialidad 2001-2006. Consultado en: http://www.setravi.df.gob.mx/programas/pitv.pd

Pritchard, J. (2019). No mandatory Cadmium Limits. Consultado el 15 de noviembre de 2019. Associated press: http://tinyurl.com/27ywhzc.

Flores, R. M., Rodríguez, P. F., de Oca, J. M., Mugica, V., Ortiz, M. E., Navarrete, M., ... & Morales, S. S. (2015). Temporal variation of PM 10 and metal concentrations in Tampico, Mexico. Air Quality, Atmosphere & Health, 8(4), 367-378. https://doi.org/10.1007/s11869-014-0291-6.

SEICA. (2019). Sistema Estatal de Información de Calidad del Aire (SEICA) del Estado de Guanajuato. Consultado el 9 de marzo de 2019, de https://smaot.guanajuato.gob.mx/sitio/seica/

SEMARNAT. (2012). Informe de la Situacion del Medio Ambiente. Compendio de Estadisticas Ambientales. Indicadores Clave, de Desemeño Ambiental y de Crecimineto Verde. México: Semarnat.

SGM. (2018). Panorama minero del Estado de Guanajuato. Secretaria de minería .

Srithawirat, T., Latif, M. T., & Sulaiman, F. R. (2016). Indoor PM10 and its heavy metal composition at a roadside residential environment, Phitsanulok, Thailand. Atmósfera, 29(4), 311-322.

Tüchsen, F., Jensen, M. V., Villadsen, E., & Lynge, E. (1996). Incidence of lung cancer among cobalt-exposed women. Scandinavian journal of work, environment & health, 444-450.

Thun, M.J., T.M. Schnorr, A.B. Smith and W.E. Halperin. (1985). Mortality among a cohort of U.S. cadmium production workers: An update. J. Natl. Cancer Inst. 74(2): 325-333.

U.S. EPA. (1996). Air Quality Criteria for Particulate Matter. U.S. Environmental Protection Agency, EPA 600/P-95/001.

U.S. EPA. (2007). ATSDR. Recuperado el 15 de Marzo de 2021, de Resúmenes de Salud Pública - Bario (Barium): https://www.atsdr.cdc.gov/es/phs/es_phs24.pdf.

U.S. EPA. Risk Assessment Guidance for Superfund—Vol. I: Human Health Evaluation Manual (Part F, Supplemental Guidance for Inhalation Risk Assessment); US EPA: Washington, DC, USA, 2009.

U.S. EPA. 1987. Health Effects Assessment for Cobalt. Prepared by the Office of Health and Environmental Assessment, Environmental Criteria and Assessment Office, Cincinnati, OH for the Office of Solid Waste and Emergency Response, Washington, DC. ECAO-CIN-H120.

Warneck, P. (1999). chemistry of the natural atmosphere. Academic Press, Ink London.

Wedepohl, K. H. (1995). The composition of the continental crust. Geochimica et cosmochimica Acta, 59(7), 1217-1232. https://doi.org/10.1016/0016-7037(95)00038-2.

Wichman, E. and Peters A. (2000). Epidemmiological Evidence on the Effects of Ultrafine Particle Exposure. in L. M. Brown, N. Collins, R. M. Harrison, A. D. Maynard and R. L. Maynard. (Ed.), Ultrafine Particles in the atmosphere. (pp. 243-267). Imperial College Press.

Zalakeviciute, R., Rybarczyk, Y., Granda-Albuja, M. G., Suarez, M. V. D., & Alexandrino, K. (2020). Chemical characterization of urban PM10 in the Tropical Andes. Atmospheric Pollution Research, 11(2), 343-356.

Zegarra, R., Andrade, S., Parra, M., Mejía, D., & Roda, C. (2020). Análisis espacial de PM10 en el aire y su composición de metales con relación a factores ambientales alrededor de centros de educación preescolar en Cuenca. Maskana, 11(1), 57-68.

Chapter 7 Methodology for processing meteorological and hydrometric data at basin level

Capítulo 7 Metodología para el tratamiento de datos meteorológicos e hidrométricos a escala de cuenca

SÁNCHEZ-QUISPE, Sonia Tatiana†*, NAVARRO-FARFÁN, María del Mar and GARCÍA-ROMERO, Liliana

Universidad Michoacana de San Nicolás de Hidalgo, Postgraduate course of the School of Civil Engineering, Mexico

Universidad Michoacana de San Nicolás de Hidalgo; Postgraduate studies at the School of Chemical Engineering, Mexico

ID 1st Author: *Sonia Tatiana, Sánchez-Quispe* / **ORC ID:** 0000-0002-8394-495X, **CVU CONACYT ID:** 202363

ID 1st Co-author: *María del Mar, Navarro-Farfán* / **ORC ID:** 0000-0002-8423-3092, **CVU CONACYT ID:** 859151

ID 2nd Co-author: *Liliana, García-Romero* / **ORC ID:** 0000-0002-6537-7736, **CVU CONACYT ID:** 557195

S. Sánchez, M. Navarro and L. García

* pvieyrar@uaemex.mx

Abstract

Meteorological and hydrometric data recorded by stations require analysis and processing before being used in any study as recommended by the World Meteorological Organization to ensure the reliability of the results obtained from these series. Currently, there is a vast number of tests that can be used for this purpose, generally applied in isolation. However, there is no clear methodology that specifies the conditions of application of the tests, the order, and the conditions of application for meteorological and hydrometric series. This research proposes a methodology for the selection and validation of meteorological and hydrometric data according to the characteristics of the available information and the study area. This methodology is the result of the work carried out for several years, where through the analysis of different series it has been concluded that the methodology presented here allows the efficient treatment and discretization of meteorological and hydrometric information, where it has been verified that the results obtained from the different studies where this information has been used have given reliable results. An application case has been selected for the description of the methodology and the analysis of the results. This chapter will be developed through 6 sections. Section 7.1 gives a brief introduction to the treatment of meteorological and hydrometric stations. Section 7.2 shows the development of the methodology proposed in this work. Section 7.3 describes the application case and the characteristics of the implemented data. Sections 7.4 and 7.5 describe the development of the tests used for meteorological and hydrometric data processing, respectively. Finally, section 7.6 concentrates on the conclusions obtained from the application of this work.

Data processing, Meteorological, Hydrometric, Selection criteria

Resumen

Los datos meteorológicos e hidrométricos registrados por las estaciones, requieren de un análisis y tratamiento antes de ser utilizados en cualquier estudio según recomienda la Organización Meteorológica Mundial para garantizar la fiabilidad de los resultados obtenidos a partir de estas series. Actualmente, existe un vasto número de pruebas que pueden ser utilizadas para tal fin, aplicadas generalmente de forma aislada. Sin embargo, no hay una metodología clara que especifique las condiciones de aplicación de las pruebas, el orden y las condiciones de aplicación para series meteorológicas e hidrométricas. Este trabajo propone una metodología para la selección y validación de los datos meteorológicos e hidrométricos de acuerdo a las características de la información disponible y la zona de estudio. Esta metodología es el resultado del trabajo realizado por varios años, donde a través del análisis de distintas series se ha llegado a la conclusión que la metodología que aquí se presenta permite el tratamiento y discretización eficiente de la información meteorológica e hidrométrica, dónde se ha podido constatar que los resultados obtenidos de los distintos estudios donde esta información se ha utilizado, han dado resultados fiables. Se ha seleccionado un caso de aplicación para la descripción de la metodología y el análisis de resultados. Este Capítulo se desarrollará a través de 6 secciones. En la sección 7.1 se da una breve introducción sobre el tratamiento de estaciones meteorológicas e hidrométricas. La sección 7.2 muestra todo el desarrollo de la metodología propuesta en este trabajo. En la sección 7.3 se describe el caso de aplicación y las características de los datos implementados. En las secciones 7.4 y 7.5 se describe el desarrollo de las pruebas utilizadas para el tratamiento de datos meteorológicos e hidrométricos, respectivamente. Finalmente, en la sección 7.6 se concentran las conclusiones obtenidas de la aplicación de este trabajo.

Tratamiento de datos, Meteorológicos, Hidrométricos, Criterios de selección

7.1 Introduction

The reliability of meteorological information is substantial in any research related to hydrology and water resources systems at the basin scale; therefore, it is important to implement tools and methodologies that allow the identification of data containing errors, whether due to data collection, instrument failures, sensor and/or communication failures, transcription of information, or relocation of the stations where these variables are measured. Precipitation is the component of the hydrological cycle that represents the main input of hydrological models, since it represents the amount of water that falls on the earth's surface, and, therefore, the starting point for the evaluation of available water resources, the analysis of extreme events, or the evaluation of climate change. In Mexico, there are precipitation records through 3266 meteorological stations distributed throughout the country (Salvador-González et al., 2018).

However, the spatial and temporal coverage of the available information is often deficient due to instrument failures or errors in data collection. These errors cause the meteorological series available to be incomplete and unreliable records.

Precipitation information recorded at meteorological stations must be representative and accurate of the place where it is measured, to be used reliably in hydrological analysis and water resource management, the series used must comply with two properties: they must be homogeneous and independent (Cao & Yan, 2012). This will provide greater reliability in the results obtained from the investigations where it is intended to use such series (flood events, frosts, droughts or climate change), reducing the uncertainty associated with hydrological modelling.

Similarly, the time series of flow measurements recorded at hydrometric stations is another basic information for studies related to hydrology or water resource systems. It is common that, like precipitation records, these series contain errors and missing data, generated by technical failures in the instruments, errors in the handling of the equipment or recording of the information. In Mexico, the measurement of these data is performed through 861 points for the measurement of flows that give rise to the network of piezometric stations in our country (CONAGUA, 2016). To ensure the reliability of data from hydrometric stations, as well as precipitation series, they must comply with at least two properties: they must be homogeneous and persistent (Merlos et al., 2014).

Both meteorological and hydrometric data may not represent the actual weather variation due to failures in the measuring instruments, errors caused accidentally by the person responsible for data collection, the location of the station, among others, resulting in variations in real data, and causing the user of this climatic information to obtain erroneous results or to make erroneous inferences. Having meteorological and hydrometric data series under homogeneous conditions is currently of interest to the scientific community (Costa & Soares, 2006), so it must go through a validation process before being used in other applications. To achieve this objective, it is necessary to apply verification and processing methodologies to identify the stations that provide users with reliable data.

Currently, there are several methods that allow evaluating the properties of precipitation or flow time series, i.e., evaluating the consistency of the series (Salas, 1980). Authors such as Campos Aranda (1998) have implemented some tests to evaluate the properties of the series, but the procedure is oriented to the isolated application of the tests. Currently, there is no joint methodology that frames the process to be followed for the evaluation and validation of precipitation and flow time series in water-related studies. The current literature, shows the consistency tests par excellence: to test the independence of meteorological series, the Anderson Limits test is used; for homogeneity, Helmert statistical test, sequence test, double mass curve, or some more specific ones such as Student's t or Cramer; for flow series, tests such as the Runoff Coefficient or Relative Modulus are used (Sanchez, 2017; Campos, 2007). These methods can be a powerful tool in the data management stage, if they are applied correctly and timely under a methodology that allows the orderly and comprehensive analysis of precipitation and flow series, which also shows the guidelines to consider a time series as valid.

In this sense, this article proposes an integral methodology for the treatment and validation of time series, both of precipitation and flow rates. The methodology is based on existing statistical methods that have proven to be valid and reliable, classifying them in different stages of application according to the characteristics of the series and the case under study; so that, from the data provided by official institutions, users can evaluate the series provided, to ensure that they are reliable, or otherwise allow them to be discarded if they do not meet the minimum characteristics for the results obtained to be valid.

The methodology proposes a set of ordered tests to evaluate the consistency in the precipitation and flow series, in such a way that it complies with the conditions of randomness, homogeneity, independence (persistence for the hydrometric series) and seasonality (Merlos et al., 2014), providing users of this information with less uncertainty associated with these series, which are often the basis for the study of other variables such as floods, droughts or climate change.

7.2 Methodology

The methodology proposed in this work can be divided into two main aspects. On the one hand, the proposal for the treatment of meteorological data is presented, and on the other hand, the analysis of data from hydrometric series is shown. In most studies related to hydrology and in research related to water resources and the environment, both types of data are always involved: precipitation and hydrometry (Guajardo-Panes et al., 2017; Walker, 2000). However, their implementation and reliability depend entirely on the quantity, quality and characteristics of their data, which generally present errors and failures due to various factors.

Figure 7.1 shows the general scheme of the methodology proposed in this work, two branches can be clearly distinguished. The one on the left side represents the treatment of the meteorological series or stations (EM), and the branch on the right side shows the stages for the treatment of the flow series (mean flows) or hydrometric stations (EH). Three stages can be distinguished on both sides: selection of the stations suitable for analysis, obtaining or generating the series, and analysis of the consistency of the series to determine their reliability as a time series of precipitation or flow rates.

Figure 7.1 General methodological scheme
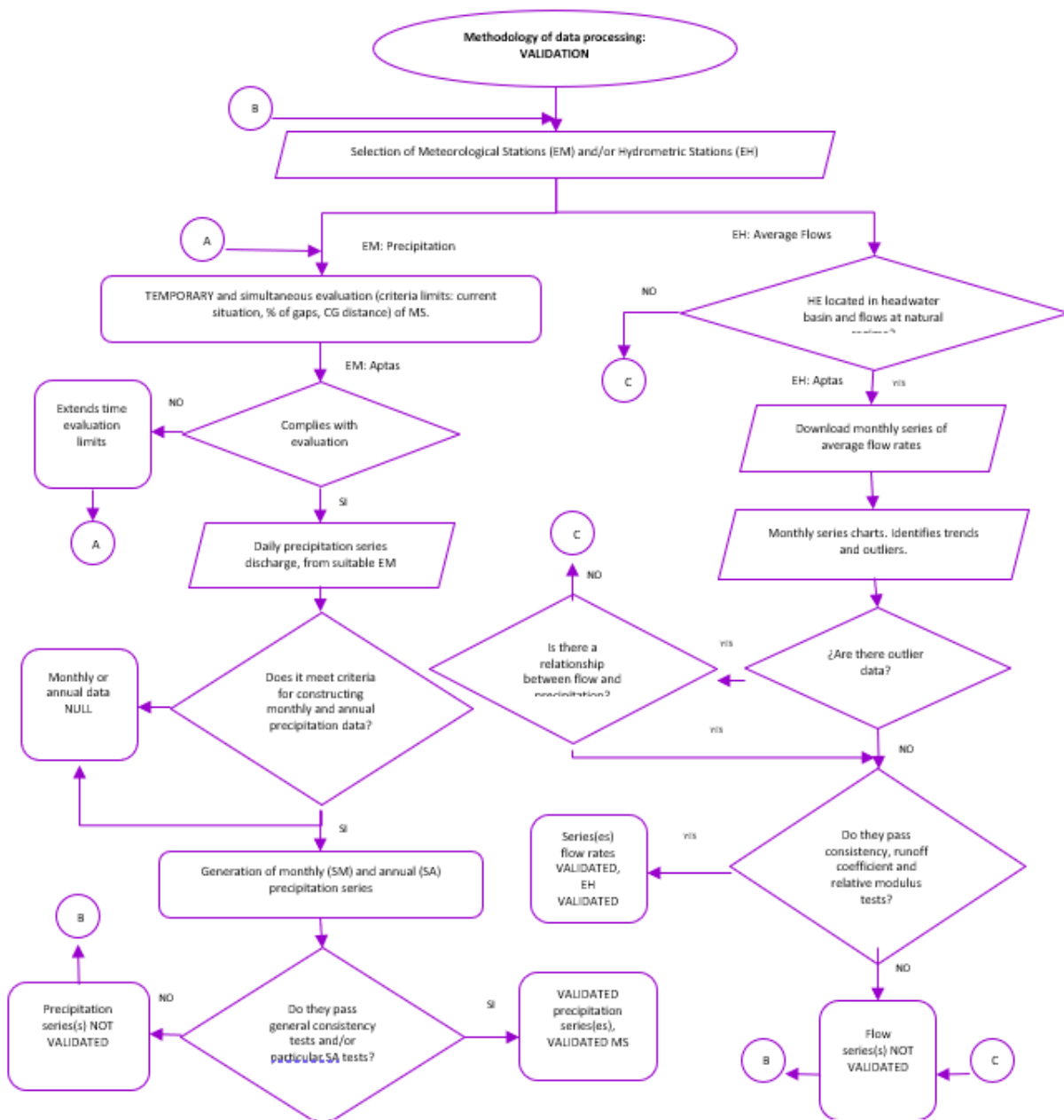
Source: Own elaboration

The left branch (Figure 7.1) allows the meteorological data to be analyzed. The first stage of the methodology shows the process to be followed for the *selection of weather stations*, and subsequently obtain the precipitation time series. The first step for the selection of the meteorological stations consists of carrying out an exploration of all the existing stations in the study area (spatial distribution). Subsequently, a classification of the available stations should be made in order to select the best ones based on five criteria: i) number of years of service, ii) percentage of missing data, iii) distance of the stations from the center of gravity of the area under study (or hydrological basin), iv) degree of data updating and v) geographical location of the station with respect to the rest of the available stations (generally a uniform distribution of the stations is sought, so that they cover the area). From the above classification, only the stations considered as suitable should be selected, those with the highest number of years of service, the lowest percentage of missing data, the shortest distance to the center of gravity of the area under study, those with the most updated information and those with a useful geographic location. Generally, this information is concentrated in a table, where the stations should be classified based on the selection criteria described above. Subsequently, weights are assigned by intervals of each criterion and weights for each criterion of the station, allowing the first group of weights, assigning a weight to each criterion interval of the station and to determine the overall weight of each station the second group of weights is applied (this second group of weights can be one or more scenarios of combination of weights for the criteria), it can be decided by a single scenario, or by the average of weights of the scenarios. The stations with a high overall weight are the best rated and will in turn be the selected stations.

Once the best stations have been selected, we will then proceed with the *obtaining and generating series for analysis*. The first step is to access the precipitation time series (only from the selected stations) through the official databases. Generally, the data available to the user are on a daily scale (CICESE, 2018). Starting from the data obtained, generally incomplete and discontinuous series, it is necessary to *the generation of the series* which will be used in the last stage of the meteorological series analysis (series consistency stage).

The generation of the series makes it possible to obtain the data on the indicated time scale (daily, monthly or annual) for the application of each of the tests necessary to evaluate the two indispensable properties of the precipitation series: homogeneity and independence. To generate these series, it is necessary to perform a previous analysis of the available data in each one, since they are series, usually incomplete, it is necessary to establish criteria to select the data that will be part of the series to be analyzed in the data consistency stage. Due to the variability that characterizes precipitation, the annual precipitation obtained from a year in which the missing data were wet months is not considered with the same degree of uncertainty as that in which the missing data correspond to dry months. The diagram in Figure 7.2 establishes the criteria proposed in this methodology for deciding which data are suitable for consideration in the data consistency stage and which should be left out due to the degree of uncertainty associated with the availability of the information.

Figure 7.2 Criteria for the generation of monthly and yearly series from daily data
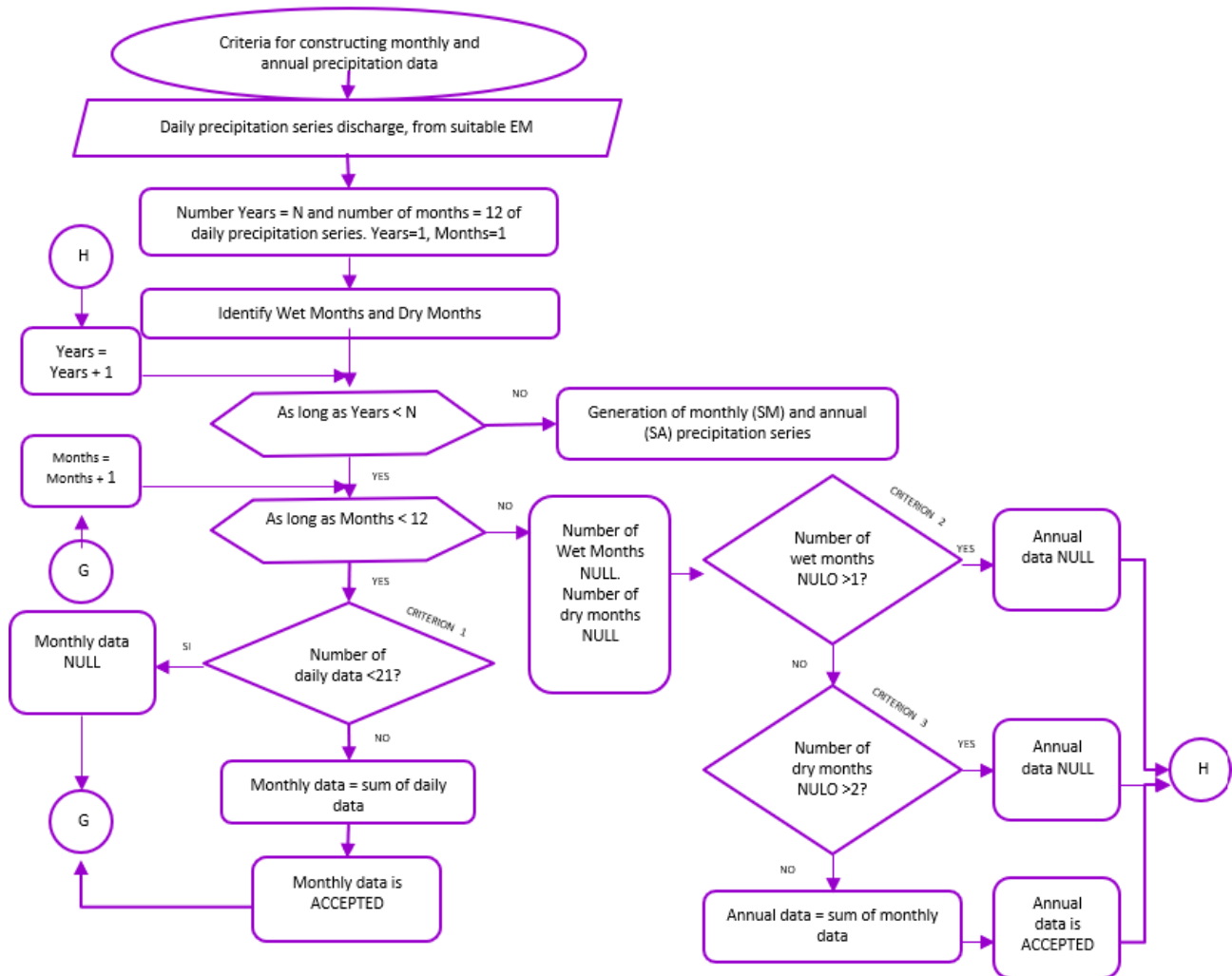
Source: Own elaboration

The criteria establish that monthly series are generated from daily data, and annual series from monthly data. Basically, three criteria are established: i) if a month has less than 21 days of information, then the month cannot be considered in the data consistency stage and is considered null. ii) If a year lacks two or more wet months, the year is considered null. iii) Finally, if a year lacks 3 or more dry months, then the year must be considered null. These criteria established in the methodology may vary and in some cases more risky or more conservative criteria may be selected, especially according to the study to be carried out. The important thing at this stage is to establish and apply criteria with knowledge of the risk assumed in the generation of the monthly and annual series.

The time series (annual scale) obtained at this point will be evaluated through the data consistency stage, where the objective is to evaluate the reliability of the precipitation data through the application of general and specific tests to prove the homogeneity and independence of the series, characteristics of a precipitation series. Here begins the third stage, series consistency analysis.

Homogeneity and independence are two properties that precipitation series must have to be considered valid (Guajardo-Panes et al., 2017). If any of these characteristics is not met in a series, it is advisable that it not be used for other studies. For homogeneity, two types of tests have been proposed: general and specific. The former should be applied in all cases, and when there is a discrepancy between the results of these, then at least one specific test should be applied. To the first group belong: the Sequence test, Helmert statistical test and Double Mass Curve. As specific tests, the proposed methodology suggests:

Cramer's statistical test, Student's t-test and the Wald-Wolfowitz statistical test; there is the possibility of performing more than one specific test and if there is discrepancy between the results, homogeneity is accepted or rejected by establishing the criterion of the number of tests that pass homogeneity. Regarding the independence of the series, the Anderson Limits test has been selected with 95% reliability. If the application of the tests selected and proposed in this phase shows that the analyzed precipitation series comply with the properties of homogeneity and independence, then the reliability of the series can be guaranteed for use in other studies.

Note the right branch of the diagram in Figure 7.1. This phase shows the process for the analysis of the series of mean flows recorded at the hydrometric stations. Again, three stages can be distinguished: selection of the stations suitable for analysis, obtaining or generating the series, and analyzing the consistency of the series.

The selection of a suitable hydrometric station depends mainly on the nature of the data recorded by the station, since the station should be in a natural regime. As a result of water management and watershed regulation, some of the data measured by the stations are altered. In this case, prior to analyzing the reliability of the hydrometric data, they must undergo a process called restitution of flows to the natural regime (Solera, 2003). According to the methodology proposed in this work, the flow series (in natural regime) must comply with two characteristics or properties: homogeneity and persistence.

If it is a station in natural regime, generally located in the headwaters of the basins (areas where regulation is practically null), the suitable hydrometric station has been selected, and the corresponding information will be downloaded, accessing the time series of average flows through the official databases (CONAGUA, 2016). These are generally available to the user on a monthly scale.

At this stage it is established that the generation of annual series is made from monthly scale data. Basically, a criterion is established: if a year lacks three or more months, the year is considered null. This criterion established in the methodology may vary, selecting in some cases riskier or more conservative criteria, especially according to the study to be carried out. It can also be considered to establish two criteria instead of one criterion: one for dry months and another for wet months, as indicated in the precipitation. The important thing at this stage is to establish and apply criteria with knowledge of the risk assumed in the generation of the annual series.

In the consistency analysis stage, general and specific procedures are identified. Within the general procedures, it is recommended to perform a graphic analysis of the data obtained in order to identify the trend and outliers that may represent Sánes in the records or the measuring instruments. To determine if it is an erroneous value, the first step should be to compare the flow recorded at a given time with the precipitation values recorded for the same date, then determine if the data comes from an extreme event or if it is an error in the data obtained. In this case, it is suggested not to consider the hydrometric station in the data consistency analysis and therefore reject the station for the study.

Once the hydrometric stations have been visually purified, three specific procedures are performed on the annual series of mean flows; first, two procedures are applied: the Runoff Coefficient (Ce) and Relative Modulus (Mr). Finally, consistency tests are applied to the data: the Sequences test, the Helmert statistical test (both evaluate homogeneity); and the Anderson limits test (evaluates persistence). If the series meet the conditions established in these tests, then it can be said that the hydrometric data analyzed are validated, and therefore can be used with certain reliability in other studies or research. It should be noted that in the case of the consistency tests, if only one test meets the homogeneity, it is at the modeler's discretion to reject; and with respect to the persistence test, the test is not necessarily met in all the average flow series.

The mathematical description and the theoretical basis of the statistical tests selected in this methodology can be found in the following sections. The methodology was applied in a zone of the metropolitan area of the city of Guadalajara in Mexico. The theoretical development of the tests is accompanied by the result obtained for the application case, in order to achieve a better understanding of the methodology proposed in this work.

The meteorological and hydrometric stations thus validated in this methodology contain the precipitation and mean flow series, respectively, with gaps at the monthly and annual scales. There are several methods for the deduction, estimation or filling of missing data in order to make the series robust, in quantity and quality of information. Once the missing data have been estimated, it is recommended to go to the data generation and consistency stage of the proposed methodology, either in the left or right branch of the methodology in Figure 7.1, in order to validate the deduced data.

A methodological proposal for the deduction of missing data for precipitation series is presented in Figure 7.3. This is done on a monthly scale, for Normal and Maximum Daily precipitation data. This deduction of missing data is limited to Normal precipitation when the hydrological study is of average flows; and is extended to Maximum Daily precipitation if the hydrological study is of maximum flows. The deduction of Normal precipitation requires surrounding meteorological stations, and the deduction of Maximum Daily precipitation requires the Normal precipitation deduced from the same station.

The deduction of missing data from the Monthly Normal Series (NMSS) of precipitation considers 2 methods of selection of surrounding stations: spatial correlation and +/- 10% mean annual precipitation. It also considers the following missing data deduction methods: IDW, simple or double linear regression, averages and natural neighbor method (Mejía et al., 2019). The deduction of missing data, differentiating or not, wet months from dry months, is at the discretion of the user. The generation of missing data of the Normal Annual Series (SAN) follows Criterion 2 and Criterion 3 established in Figure 7.2. The deduction of data from the Monthly Maximum Daily Series (MMDS) of precipitation considers the simple linear regression method, and is only performed for the wet months because these are the ones that have an impact on the annual maximum daily precipitation. The generation of the missing data of the Annual Maximum Daily Series follows Criterion 2 established in Figure 7.2.

Figure 7.3 Deduction, estimation or filling of missing precipitation data in the data measured at weather stations
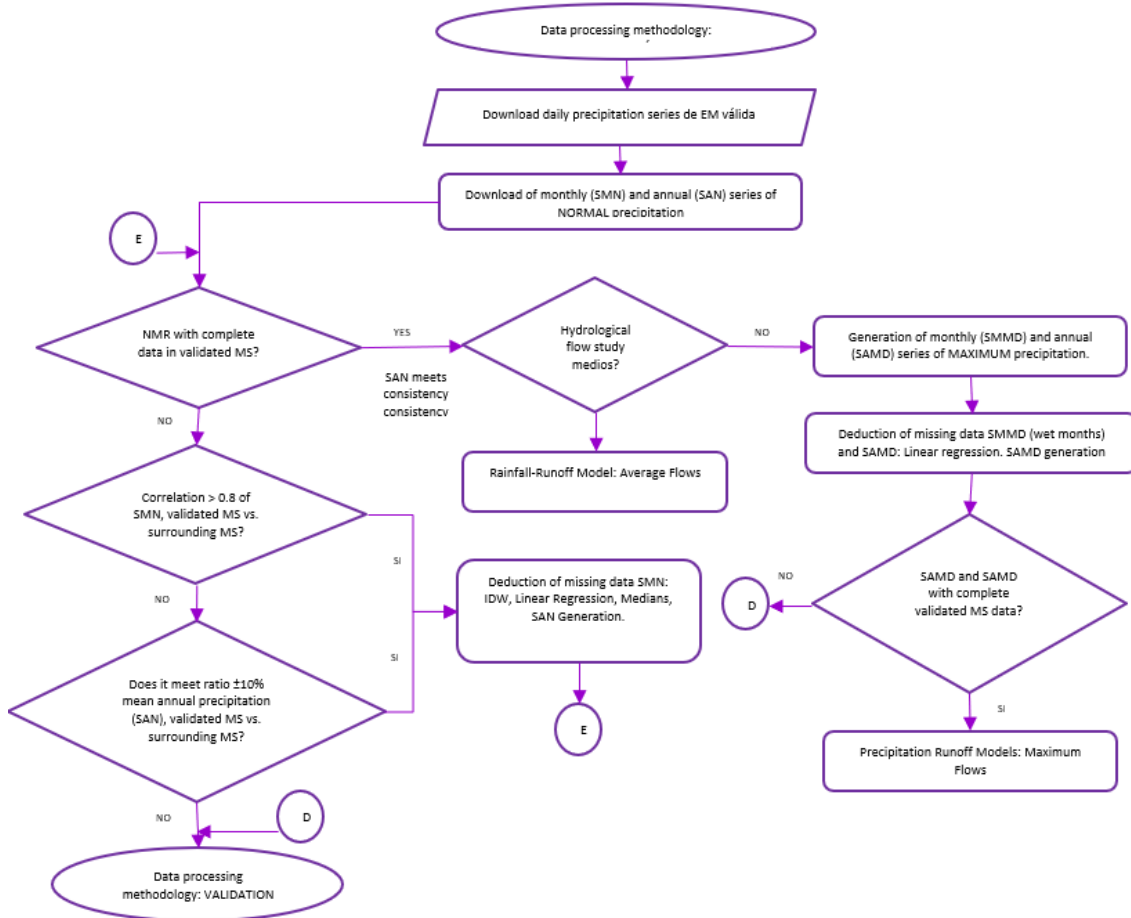
Source: Own elaboration

7.3 Application case

The Guadalajara Metropolitan Area (ZMG) in the state of Jalisco is the second largest urban center in the country. (Some of the cities that make up the region were formerly agricultural towns (i.e. Zapopan), but accelerated population growth in urban areas, inadequate planning of water infrastructure and inefficient regulation of pollutants have become some of the causes that affect the supply, distribution and quality of the water resources available in the area. The search for alternative water supply systems and the reuse of water are nowadays imperative functions for cities and municipalities. Taking care of water and giving it an efficient use with a focus on sustainability is fundamental for the development of the state of Jalisco (Lugo, 2014). The inputs for any study focused on the conservation of water resources are mainly time series of precipitation and flow rates.

 7.4). Some of the cities that make up the region were formerly agricultural towns (i.e. Zapopan), but accelerated population growth in urban areas, inadequate planning of water infrastructure and inefficient regulation of pollutants have become some of the causes that affect the supply, distribution and quality of the water resources available in the area. The search for alternative water supply systems and the reuse of water are nowadays imperative functions for cities and municipalities. Taking care of water and giving it an efficient use with a focus on sustainability is fundamental for the development of the state of Jalisco (Lugo, 2014). The inputs for any study focused on the conservation of water resources are mainly time series of precipitation and flow rates.

Figure 7.4 Macro-localization of the application case (hydrological basin)
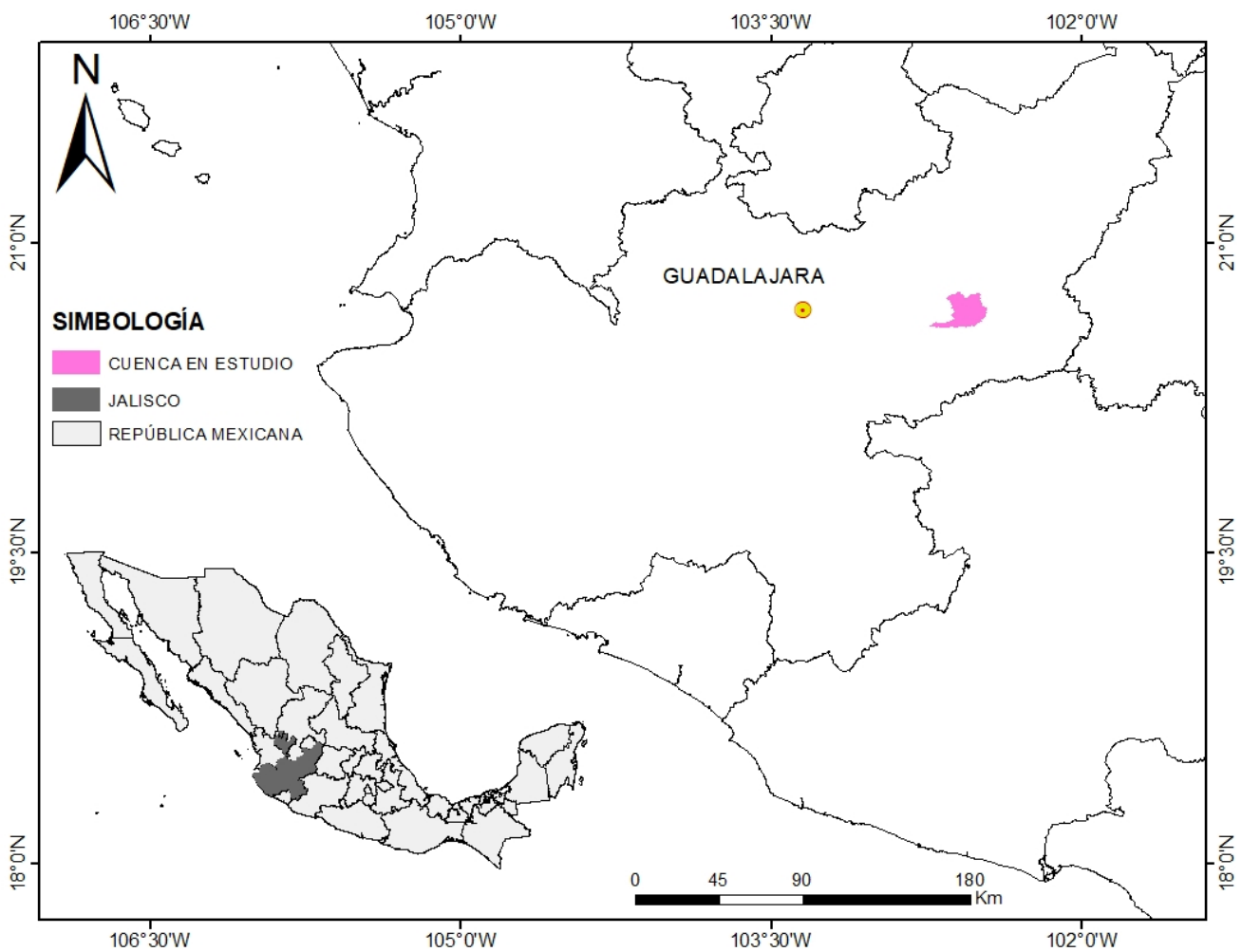
Source: Own elaboration

Figure 7.5 shows the location of the application case or study basin, it is located at the intersection of the municipalities: Atotonilco el Alto, San Ignacio Cerro Gordo, Tepatitlán de Morelos and Tototlán; with a population of approximately 226,536 inhabitants. The economy of this zone depends mainly on cattle raising, agriculture, fishing and commerce. The main watercourse in the area is the Los Morales stream (IIEG, 2020).

An initial exploration of all meteorological and hydrometric stations available in the study area was carried out. In order to perform a first discretization of the stations, the closest surrounding stations with a low percentage of missing data were selected. This ensures that the sample is representative for the analysis and, therefore, the application of the consistency tests is simpler and more reliable.

Selection of weather stations (temporal and spatial analysis)

In this sense, Table 7.1 shows information on the 5 stations closest to the basin under study. Criteria have been applied to qualify the stations taking as a reference the temporal selection criteria established in Section 2 (years of service, percentage of missing data, distance to the center of gravity of the area under study), where it is observed that one of the most influential parameters is the Euclidean distance between the station and the center of gravity of the watershed, since this ensures that the information is representative of the area under study.

Table 7.1 General information on weather stations

Code	Name	Period of Service	Years Cash	% Voids	D.E.* (m)
14076	Jesús María, Jal	70.9	67.2	5.3%	38,932
14080	La Cuña, Jal	65.6	63.2	3.7%	44,161
14086	La Manzanilla de la Paz, Jal.	64.3	54.3	15.6%	99,177
14087	La Red, Jal.	53.6	52.2	2.6%	24,609
14121	Guadalajara (SMN), Jal	42.0	38.0	9.5%	86,934
near the basin under study.					
* Euclidean distance to the center of gravity of the basin.					

Source: Own elaboration

The calculation of the Euclidean distance corresponds to the distance from the meteorological station to the center of gravity of the basin and is obtained with the expression of Equation 1. To apply it, it is necessary to know the geographic location of each station in UTM coordinates and the coordinates of the center of gravity of the basin. This information is summarized in Table 7.2.

$$D.E. = \sqrt{(x_2 - x_1)^2 + (y_2 - y_1)^2 + (z_2 - z_1)^2} \tag{1}$$

Where:

- x_i is the x-coordinate of station i; x_j represents the x-coordinate of station j (in this case the center of gravity of the basin).

- y_i is the y-coordinate of station i; y_j represents the y-coordinate of station j (in this case the center of gravity of the basin).

- z_i is the z-coordinate of station i; z_j represents the z-coordinate of station j (in this case the center of gravity of the basin).

Table 7.2 UTM coordinates of the meteorological stations and center of gravity of the basin

Code	Coordinates UTM		
	X (m)	Y (m)	Z (m)
14076	791857	2280390	2129
14080	728685	2323722	1490
14086	688313	2212493	2050
14087	729140	2290502	1746
14121	666632	2289769	1567
C.G.*	753528	2287213	1893
* Center of gravity of the basin.			

Source: Own elaboration

Since the problem is to identify the most suitable meteorological station or stations, the decision is based on a discrete multi-criteria structure, very useful when more than 3 stations are to be evaluated. The criteria analyzed in the case study are: effective years of precipitation, percentage of gaps and Euclidean distance to the center of gravity of the basin.

For each criterion, criterion intervals are established, for which the maximum and minimum value of each criterion is identified, and the number of intervals is defined, assigning 5 criterion intervals in our case, this value is higher or lower, according to the number of stations under analysis. Table 7.3 presents the weights per criterion interval, where the highest weight is assigned to the highest number of effective years, the lowest percentage of voids, and the smallest Euclidean distance to the center of gravity.

In the table 7.3, for each station, weights are assigned to each criterion, following Table 3.4, establishing different scenarios, which can be two or three; for the example, two scenarios were established; the first scenario considers equal weight to the three criteria, assigning 0.33 to each one. The second scenario considers 0.5 for the percentage of voids criterion, 0.3 for the Euclidean distance criterion and 0.2 for the effective years of precipitation criterion.

The result per scenario is an overall weight per station, which allows assigning a priority to the station, with 1 corresponding to the highest priority and therefore the most suitable. For the two scenarios, the priority results do not coincide with the same stations as the best. In this situation, the most representative scenario of the weight of the criteria is selected, selecting scenario 2. The best stations are those that correspond to the lowest priority order, thus selecting stations 14076 (priority 2) and 14087 (priority 1).

It is important to point out that the number of stations to be selected depends on whether there are stations within the basin and the area of the basin under study (if there are no stations within the basin), in the case of the study corresponds to 2 stations (Aparicio, 1989).

Table 7.3 Assignment of weights to criterion and criterion intervals for case studies

Stations	Criteria						Scenarios			
	Effective years Precipitation		Percentage of voids Precipitation		Euclidean Distance Station with Basin (m)		E1		E2	
	C1		C2		C3		0.33C1+0.33C2+ 0.33C3		0.20C1+0.50C2+ 0.30C3	
	Value	Weight	Value	Weight	Value	Weight	Overall weight	Priority	Overall weight	Priority
14076	67.2	5	5.3	4	38,932	5	4.7	1	4.5	2
14080	63.2	5	3.7	4	44,161	4	4.3	2	4.2	3
14086	54.3	3	15.6	1	99,177	1	1.3	4	1.4	5
14087	52.2	3	2.6	5	24,609	5	4.3	2	4.6	1
14121	38.0	1	9.5	3	86,934	1	1.7	3	2	4

Source: Own elaboration

Table 7.4 Assigning weights to criterion and criterion intervals

	Effective Years of Precipitation. C1		Percentage of voids. C2		Euclidean distance. C3	
Maximum Value	68		1		100,000	
Minimum Value	38		16		25,000	
Interval	Intervalo	Weight	Intervalo	Weight	Intervalo	Weight
1	38-44	1	1-4	5	25,000-40,000	5
2	44-50	2	4-7	4	40,000-55,000	4
3	50-56	3	7-10	3	55,000-70,000	3
4	56-62	4	10-13	2	70,000-85,000	2
5	62-68	5	13-16	1	85,000-100,000	1

Source: Own elaboration

From the analysis of Table 7.3, it is concluded that giving equal weight to the criteria may not be correct (scenario 1), and it is advisable to give different weights (scenario 2) when the interaction of the criteria is understood, for the case study, more weight is given to the percentage of voids, and the second in importance is the distance of the station to the center of gravity, leaving in third place the effective years. In both scenarios, stations 14076 and 14087 have a high priority to be selected.

It can be seen that the stations with the shortest distance and the lowest percentage of voids out of the 5 have been selected. Station 14080 (priority 3) would be the next useful station, if spatially evaluating the selected stations does not meet the spatial coverage of the basin, this third station would be used. According to the Thiessen polygon plot, it was determined that stations 14076 and 14087 are the ones that cover the entire basin, and therefore it is not necessary to select more support stations.

Precipitation generation and series generation

Table 7.5 and Table 7.6 present the annual precipitation series for stations 14076 and 14087, respectively. The generation of these series was performed based on the criteria for series generation shown in the Methodology section of this work. These data are basic for the application of the tests selected in this methodology. Each test has specific considerations that will be specified in each case, but without exception they must be continuous series (except for the Double Mass Curve test) with at least 12 years of data.

Table 7.5 Annual precipitation series for station 14076

# Data	Year	PMA	# Data	Year	PMA	# Data	Year	PMA
1	1944	659.1	25	1968	995.9	49	1992	NULL
2	1945	665.5	26	1969	675.9	50	1993	NULL
3	1946	999.1	27	1970	613.8	51	1994	583.5
4	1947	964.5	28	1971	1079.6	52	1995	1019
5	1948	862	29	1972	764.2	53	1996	630.5
6	1949	851	30	1973	980.7	54	1997	798
7	1950	774.5	31	1974	884.2	55	1998	941.5
8	1951	640.5	32	1975	997.1	56	1999	515.5
9	1952	1109	33	1976	1078.3	57	2000	703
10	1953	998.5	34	1977	935.9	58	2001	842.5
11	1954	838.5	35	1978	640.3	59	2002	814
12	1955	1213	36	1979	608.6	60	2003	1126
13	1956	818.5	37	1980	856.4	61	2004	1033.4
14	1957	645	38	1981	881.5	62	2005	817.3
15	1958	1261	39	1982	676.5	63	2006	923.5
16	1959	1211.5	40	1983	454.7	64	2007	921.5
17	1960	716.5	41	1984	762.9	65	2008	808.5
18	1961	1022.5	42	1985	1015.8	66	2009	948.3
19	1962	854	43	1986	984.3	67	2010	985.7
20	1963	1202.3	44	1987	533.7	68	2011	651
21	1964	846.3	45	1988	757.5	69	2012	738.6
22	1965	943.4	46	1989	802.7	70	2013	1150.5
23	1966	767.8	47	1990	835.8	71	2014	1145.5
24	1967	997.6	48	1991	NULL			

Source: Own elaboration

Table 7.6 Annual precipitation series for station 14087

# Data	Year	PMA	# Data	Year	PMA	# Data	Year	PMA
1	1961	802	19	1979	625.5	37	1997	869.6
2	1962	823.9	20	1980	896.1	38	1998	910.8
3	1963	871.	21	1981	898.4	39	1999	700
4	1964	865.4	22	1982	696.6	40	2000	668
5	1965	1121.9	23	1983	913.5	41	2001	514.9
6	1966	1070.7	24	1984	867.8	42	2002	931.2
7	1967	1360.7	25	1985	833.5	43	2003	904.3
8	1968	915.2	26	1986	943	44	2004	991.5
9	1969	37.3	27	1987	873.4	45	2005	829.3
10	1970	849	28	1988	822.5	46	2006	847
11	1971	884	29	1989	605.9	47	2007	893.1
12	1972	1011.4	30	1990	990.2	48	2008	1103.4
13	1973	1060.8	31	1991	960.8	49	2009	893.3
14	1974	864.4	32	1992	1128.7	50	2010	971.4
15	1975	948.8	33	1993	638.6	51	2011	471
16	1976	1081.4	34	1994	745.5	52	2012	775.7
17	1977	739.9	35	1995	928	53	2013	1114.8
18	1978	878.5	36	1996	829.2	54	2014	731.2

Source: Own elaboration

Selection of hydrometric stations

For the selection of hydrometric stations, it is suggested to generate a buffer of influence over the study area, in order to determine the stations that can be modeled, and in this case, to perform the modeling, it is necessary to consider that the basins must be in a natural regime.

For the case of application, the hydrometric station that generates the basin under study has the code 12607 "La Yerbabuena", located in the state of Jalisco, which has information from August 1965 to November 1992. The annual data series used for the review of the station in question consists then of 27 years and is presented in Table 7.7. The hydrometric station in question generates a basin of 299.20 km^2 of surface area.

Obtaining and generating series of average flow rates

To obtain the information for each year, the hydrometric station was checked to ensure that it had at least 75% of the monthly information (9 months minimum).

Table 7.7 Annual series of hydrometric station 12607 "La Yerbabuena"

Year	Annual Volume (hm^3)	Year	Annual Volume (hm^3)
1966	67.40	1980	50.48
1967	177.48	1981	72.42
1968	167.50	1982	15.02
1969	21.59	1983	92.17
1970	94.29	1984	133.05
1971	103.60	1985	91.37
1972	34.39	1986	48.36
1973	170.79	1987	29.55
1974	41.07	1988	87.55
1975	127.08	1989	12.73
1976	189.41	1990	54.02
1977	92.64	1991	146.46
1978	38.57	1992	120.55
1979	18.15		

Source: Own elaboration

Also shown is the monthly mean flow information (Table 7.8) from hydrometric station 12607, which will be useful for the calculation of the relative modulus.

Table 7.8 Monthly average flows from hydrometric station 12607

Month	Average monthly flow rate (hm³)
October	9.57
November	2.11
December	0.76
January	0.94
February	0.54
March	0.38
April	0.32
May	0.36
June	2.10
July	20.97
August	26.00
September	22.85

Source: Own elaboration

Validation of precipitation and average flow stations

For the case under study, two meteorological stations and one hydrometric station are available (Figure 7.5). According to the established methodology, all the consistency tests proposed in the methodology will be applied to the corresponding stations, and the results and analysis obtained in each case will be shown in the following sections.

Figure 7.5 Location of the basin under study, hydrometric station and meteorological stations
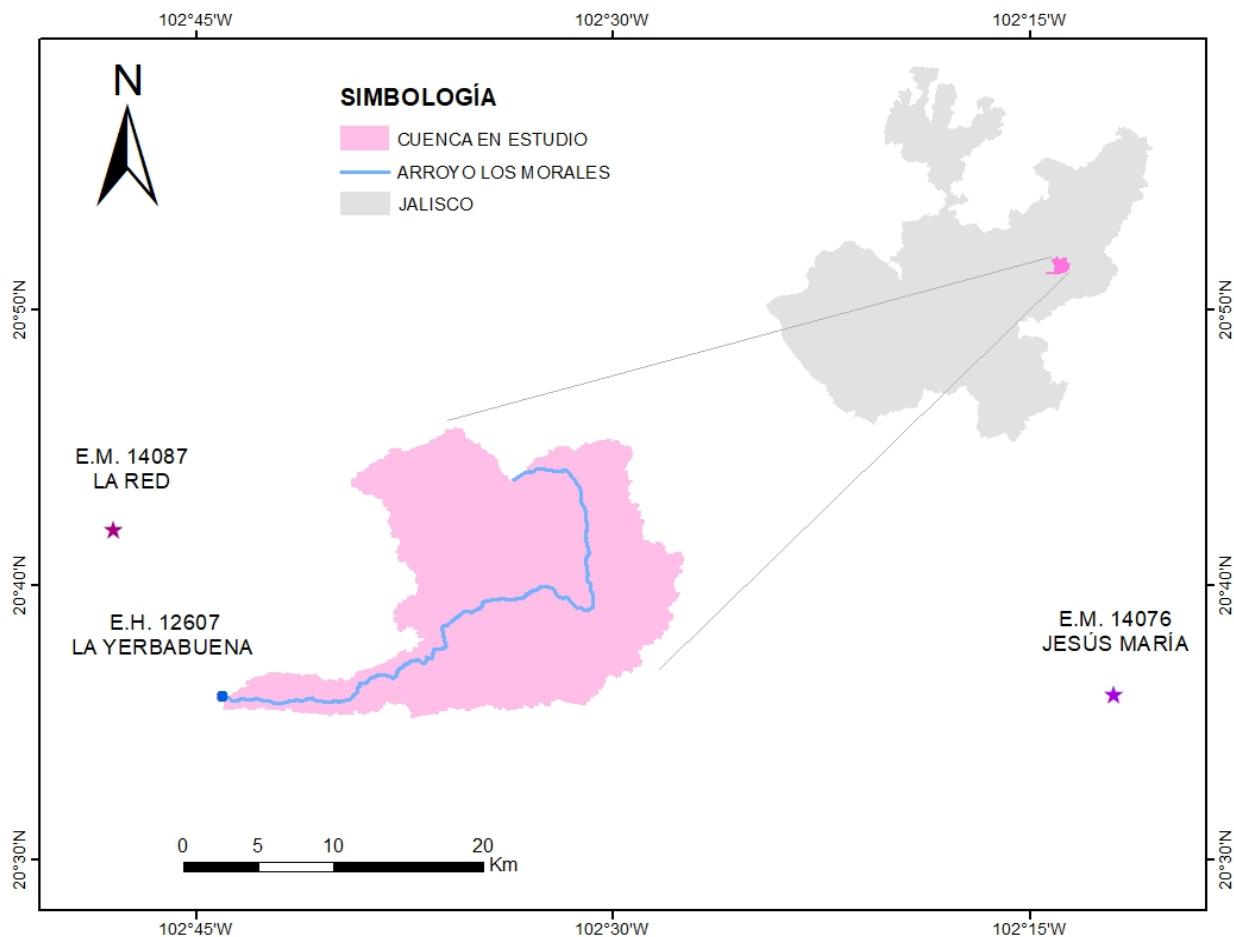
Source: Own elaboration

7.4 Validation of Meteorological Stations

This section describes in detail each of the tests applied to the series from the meteorological stations. In order to facilitate the understanding of each test, the theoretical basis of each one will be developed, and at the same time the results of its application will be presented.

The importance of meteorological stations in a region should be emphasized, since precipitation as an element that defines the climatic conditions of any area is unquestionable. Precipitation data obtained by instruments require, however, specific treatments in order to make them more reliable. Several techniques have been developed over time to process this climatic variable. This section proposes tests that can be applied to precipitation data to ensure their reliability for use in other studies.

For Salas et al. (1980), non-homogeneity in data is common in hydrological time series; it is either human-induced or produced by significant, evolutionary or sudden natural disturbance factors (such as natural disasters or system regulation). In addition, hydrologic data can have significant systematic errors that produce inconsistent series, meaning that they do not meet any of the properties of homogeneity or independence.

Precipitation time series should demonstrate homogeneity in their data. This is achieved through the implementation of the Sequences test (Mather, 1975), the Helmert test (Doorembos, 1976), or Double Mass Curve (Martinez et al., 2006), or Wald-Wolfowitz (Siegel, 2015); in addition to specific tests such as Student's t-test (WMO, 1966), or Cramer's t-test (WMO, 1966). A series is said to be homogeneous when the tests show that the elements present in the sample come statistically from the same population. Similarly, the rainfall series must demonstrate independence. This property is evaluated through the Anderson Bounds test (Salas, 1980). It is said that a series is independent when it is demonstrated that the probability that the occurrence of any precipitation data present in the sample does not depend on the occurrence of the subsequent or preceding precipitation value in time or space.

Several characteristics of the time series, such as the mean, standard deviation and serial correlations, can be affected when a trend and/or a positive or negative jump (slip) occur in hydrological series due to lack of homogeneity and independence, generating greater uncertainty associated with the data. In addition, it should be added that the longer a precipitation series is, the greater the probability that the homogeneity of the series, produced by human activities or by an accidental interruption of nature, or the non-independence of the series, is incurred, attributing this problem to systematic errors (inconsistency).

Table 7.9 shows the meteorological stations selected for this analysis, in addition to the information and characterization of each one (station code, name, period of years of service, percentage of gaps, mean annual precipitation (MAP) and coordinates).

Table 7.9 General data of the weather stations to be used

Code	Name	Period of years		% gaps	PMA (mm)	Coordinates UTM		
		Service	Cash			X (m)	Y (m)	Z (m)
14076	Jesús María, Jal	70.9	67.2	5.3%	864.34	791857	2280390	2129
14087	La Red, Jal	53.6	52.2	2.6%	861.20	729140	2290502	1746

Source: Own elaboration

7.4.1 Homogeneity

Homogeneity tests can be classified into two groups, parametric and nonparametric. The latter are less rigorous than the former, but much simpler to perform. Based on the above, one can speak of general tests and specific tests. Among the general (or non-parametric) tests are: Sequences test, Helmert test and Double Mass Curve; and specific (or parametric) tests are: Student's t, Cramer and Wald-Wolfowitz (Campos, 1998).

It is advisable to apply, as a first approximation, the general tests. If there are discrepancies in the results obtained (one indicates homogeneity and the other does not), then we proceed with the application of the specific tests in order to clarify whether the station is homogeneous or does not comply with this characteristic. The particular tests are generally probability-based tests, where the homogeneity of the series is determined from a null hypothesis (H0) and a rule to accept or reject H0 based on an associated probability.

Additionally, homogeneity tests can be classified into two groups:

- Tests that do not require an additional station to determine the homogeneity of their data, where the analysis is performed with the station's own data: Helmert, Sequences, Student's t-test and Cramer's test, which are explained in the following sections.

- Tests that require at least one auxiliary station nearby to perform the analysis: Double Mass Curve and Wald-Wolfowitz test.

In the following sections, the theoretical basis of each test and an example of application are developed.

Sequence testing

This test consists of analyzing the sign of the deviations of each data with respect to the sample median, and comparing the number of allowed changes (*u*) based on the sample size *(n)*. There is a number of allowed changes depending on the sample size. If the number of changes recorded is between the values established in the ranges presented in Table 7.10, then the series is said to be homogeneous (Mather, 1975), otherwise the series is non-homogeneous.

Table 7.10 Ranges of changes allowed for the Sequence test, according to the number of data

n	u	n	u	n	u	n	u
12	5 – 8	22	9 – 14	32	13 – 20	50	22 – 30
14	5 – 10	24	9 – 16	34	14 – 21	60	26 – 36
16	6 – 11	26	10 – 17	36	15 – 22	70	31 – 41
18	7 – 12	28	11 – 18	38	16 – 23	80	35 – 47
20	8 – 13	30	12 – 19	40	16 – 25	100	45 – 57

Source: Own elaboration

For the Sequence test, we will then need to obtain the median of the continuous series according to the number of data we have. In this sense, we continue comparing the chronologically ordered series with the value of the mean or median, so if the value in the series is less than the median we place an L (lower, lower) or M (major, higher); then, we continue marking the sequences that are formed with the L/M column, taking into account that when we have a change from L to M or vice versa, the number of sequences that are formed is increased by one.

For the test of sequences in station 14076 (Table 7.10); having a series of 21 years of continuous data (odd number) it is required to obtain the median of the series, which is 842.5 and, we have that the number of sequences that are formed according to the series is 12; This value is within the range established as adequate in Table 7.10, where for a series of 21 data, a number of changes from 8 to 14 are allowed (values rounded to the lower and upper limits for 20 and 22 data), which means that the station is homogeneous.

Helmert test

This test consists of a simple procedure where the series must be ordered chronologically and the sign of the deviations of each data with respect to the arithmetic mean of the series is analyzed. If a deviation with a certain sign is followed by another of the same sign, then it is said that there is an "S" sequence, otherwise it is considered a "C" change. Once the entire series has been analyzed, the number of changes and the number of sequences are counted, and the inequality of Equation 2 is applied. If the inequality is satisfied, the station can be considered as homogeneous (Doorembos, 1976).

$$-\sqrt{n-1} \le (S - C) \le \sqrt{n-1} \qquad (2)$$

For the Helmert test, a procedure quite similar to the Sequence test is used, however, the value with which the precipitation series will be compared is the mean (in the same way, marking with M and L; however, now the number of changes between L and M will be considered; in this sense, as long as the series remains at L (M) an S (sequence) is written and, if this value changes from L to M (or vice versa), a C (change) will be written. At the end, we count the S and C and apply the formula proposed in Equation 2.

It is recommended that the Sequence and Helmert homogeneity tests be performed simultaneously. Table 7.11 shows the results obtained from the application of both tests for station 14076 and Table 4.4 for station 14087.

For the Helmert test, it is compared with the mean value of 871.8 mm, which gives a total of 11 changes and 9 sequences, so the range of application is as shown below:

$$-\sqrt{21-1} \le 9-11 \le \sqrt{21-1}$$
$$-4.47 \le -2 \le 4.47$$

Therefore, according to Helmert's test, the station is homogeneous.

Table 7.11 Sequence and Helmert test for station 14076

Year	PMA	Sequence Testing		Helmert test	
		Comparison	Sequence	Comparison	Changes
1994	583.5	L	1	L	
1995	1019	M	2	M	C
1996	630.5	L	3	L	C
1997	798	L	3	L	S
1998	941.5	M	4	M	C
1999	515.5	L	5	L	C
2000	703	L	5	L	S
2001	842.5	L	5	L	S
2002	814	L	5	L	S
2003	1126	M	6	M	C
2004	1033.4	M	6	M	S
2005	817.3	L	7	L	C
2006	923.5	M	8	M	C
2007	921.5	M	8	M	S
2008	808.5	L	9	L	C
2009	948.3	M	10	M	C
2010	985.7	M	10	M	S
2011	651	L	11	L	C
2012	738.6	L	11	L	S
2013	1150.5	M	12	M	C
2014	1145.5	M	12	M	S

Source: Own elaboration

The results obtained for station 14087 are shown in Table 7.12 The series has 33 years of consecutive data. The median value for this series is 873.4 mm. Analyzing the deviations of each data with respect to the median value, 20 sequences were counted. According to the information in Table 7.10, for a 33-year series, between 13 and 20 sequences are allowed (taking the value for 32 data), so the series can be considered as homogeneous.

For the Helmert test, the mean value for the series is 851.8 mm. The analysis of the deviations from the mean value accounted for a total of 17 changes and 15 sequences. Applying Equation 2, it is observed that the inequality is fulfilled, so the station can be considered as homogeneous.

$$-\sqrt{33-1} \le 15-17 \le \sqrt{33-1}$$

$$-5.66 \le -2 \le 5.66$$

Table 7.12 Sequence and Helmert test for station 14087

Year	PMA	Sequence Testing		Helmert test	
		Comparison	Sequence	Comparison	Changes
1970	849	L	1	L	
1971	884	M	2	M	C
1972	1011.4	M	2	M	S
1973	1060.8	M	2	M	S
1974	864.4	L	3	M	S
1975	948.8	M	4	M	S
1976	1081.4	M	4	M	S
1977	739.9	L	5	L	C
1978	878.5	M	6	M	C
1979	625.5	L	7	L	C
1980	896.1	M	8	M	C
1981	898.4	M	8	M	S
1982	696.6	L	9	L	C
1983	913.5	M	10	M	C
1984	867.8	L	11	M	S
1985	833.5	L	11	L	C
1986	943	M	12	M	C
1987	873.4	L	13	M	S
1988	822.5	L	13	L	C
1989	605.9	L	13	L	S
1990	990.2	M	14	M	C
1991	960.8	M	14	M	S
1992	1128.7	M	14	M	S
1993	638.6	L	15	L	C
1994	745.5	L	15	L	S
1995	928	M	16	M	C
1996	829.2	L	17	L	C
1997	869.6	L	17	M	C
1998	910.8	M	18	M	S
1999	700	L	19	L	C
2000	668	L	19	L	S
2001	514.9	L	19	L	S
2002	931.2	M	20	M	C

Source: Own elaboration

Double mass curve test

The Double Mass Curve method (Martinez et al., 2006) consists of checking whether the records of a rainfall station have suffered variations that lead to erroneous values. These variations may be due to a change in the instrumental location, a variation in the peripheral conditions of the measurement site or a change in the operator of the equipment of the observer taking the readings.

The mass curve method considers that, in a homogeneous meteorological area, the precipitation values occurring at different points of that area in annual or seasonal periods, have a relationship of proportionality that can be represented graphically. This representation consists of identifying the station to be monitored (main station) and obtaining the annual precipitation value. For the contrast, it will be necessary to have at least one base station whose annual data series must coincide with that of the station to be monitored.

For each station (main and base station), in each year, starting from the first year with a record, the accumulated value of the base station is obtained (if there is more than one, then the values of the base stations are averaged and accumulated for successive years), and the accumulated value of the station to be monitored.

Then, on a system of orthogonal axes, the cumulative annual precipitation values of the station to be monitored are plotted in ordinates and the cumulative mean annual precipitation values of the base station in abscissae. If the records have not undergone variations, the points are aligned in a line with a single and uniform slope, therefore, it will not be necessary to make corrections. If, on the other hand, there are variations in the slope of the line, it means that part of the series contains erroneous values and the data record must be corrected from the year in which the slope of the line changes before it can be used. For this case, it is necessary to obtain a Correction Factor that is proportional to the variation of the slope of the line (Graphic 7.1).

Figure 7.1 Representation of the double mass curve test

Accumulated precipitation from base station
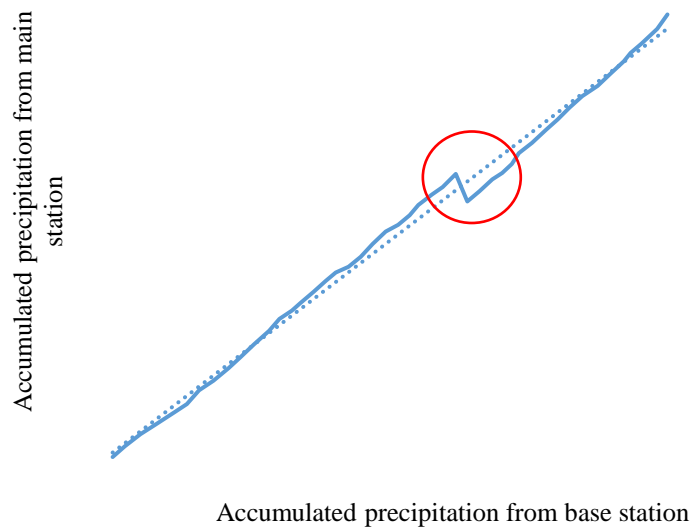
Source: Own elaboration

For the application case, station 14087 has been considered as the main station (E1) and station 14076 as the base station (E2). The coincident period for both stations is from 1962 to 2014. Once the accumulated precipitation has been obtained for the main station and the base station, the station homogeneity was determined from the graph in Graphic 7.2.

Graphic 7.2 Results of the double mass curve test, performed with data from stations 14076 and 14087
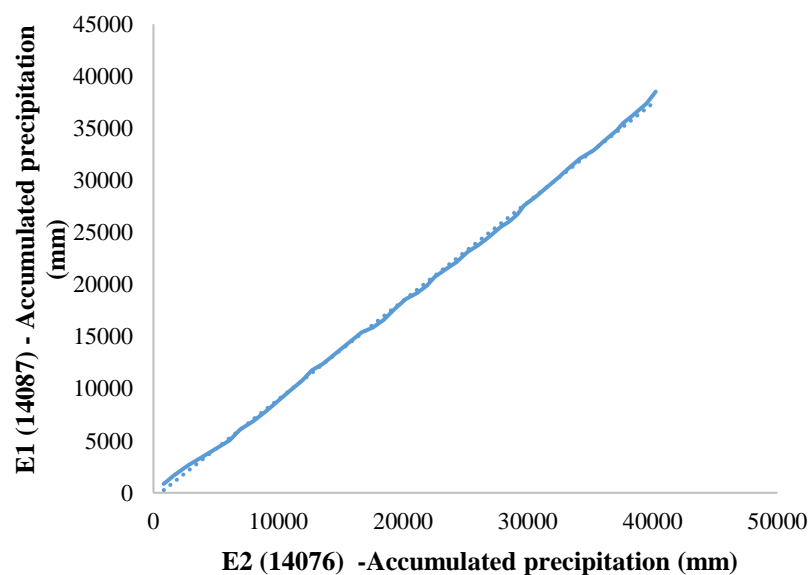
Source: Own elaboration

In order to make the graphic, the information on mean annual precipitation (MAP) presented in Table 7.13 is used.

Table 7.13 Annual rainfall series for the double mass curve test

Year	PMA (mm) 14087	PMA (mm) 14076	Accumulated (mm) 14087	Accumulated (mm) 14076	Year	PMA (mm) 14087	PMA (mm) 14076	Accumulated (mm) 14087	Accumulated (mm) 14076
1962	823.9	854	823.9	854	1988	822.5	757.5	21931.1	19915.1
1964	865.4	846.3	1689.3	1700.3	1989	605.9	802.7	22537	20717.8
1965	1121.9	943.4	2811.2	2643.7	1990	990.2	835.8	23527.2	21553.6
1966	1070.7	767.8	3881.9	3411.5	1994	745.5	583.5	24272.7	22137.1
1967	1360.7	997.6	5242.6	4409.1	1995	928	1019	25200.7	23156.1
1970	849	613.8	6091.6	5022.9	1996	829.2	630.5	26029.9	23786.6
1971	884	1079.6	6975.6	6102.5	1997	869.6	798	26899.5	24584.6
1972	1011.4	764.2	7987	6866.7	1998	910.8	941.5	27810.3	25526.1
1973	1060.8	980.7	9047.8	7847.4	1999	700	515.5	28510.3	26041.6
1974	864.4	884.2	9912.2	8731.6	2000	668	703	29178.3	26744.6
1975	948.8	997.1	10861	9728.7	2001	514.9	842.5	29693.2	27587.1
1976	1081.4	1078.3	11942.4	10807	2002	931.2	814	30624.4	28401.1
1977	739.9	935.9	12682.3	11742.9	2004	991.5	1033.4	31615.9	29434.5
1978	878.5	640.3	13560.8	12383.2	2005	829.3	817.3	32445.2	30251.8
1979	625.5	608.6	14186.3	12991.8	2006	847	923.5	33292.2	31175.3
1980	896.1	856.4	15082.4	13848.2	2007	893.1	921.5	34185.3	32096.8
1981	898.4	881.5	15980.8	14729.7	2008	1103.4	808.5	35288.7	32905.3
1982	696.6	676.5	16677.4	15406.2	2009	893.3	948.3	36182	33853.6
1983	913.5	454.7	17590.9	15860.9	2010	971.4	985.7	37153.4	34839.3
1984	867.8	762.9	18458.7	16623.8	2011	471	651	37624.4	35490.3
1985	833.5	1015.8	19292.2	17639.6	2012	775.7	738.6	38400.1	36228.9
1986	943	984.3	20235.2	18623.9	2013	1114.8	1150.5	39514.9	37379.4
1987	873.4	533.7	21108.6	19157.6	2014	731.2	1145.5	40246.1	38524.9

Source: Own elaboration

Statistical test t of Student

When the cause of the loss of homogeneity of the series is due to an abrupt change in the mean, the parametric Student's t-test is especially useful. So, first of all, what is recommended is to make a graph of the annual rainfall, in which the behavior of the series with respect to time can be observed, in this way, we can delimit the periods of time in which there is a jump (change in the trend of the mean of the series) and that, makes the mean of the rainfall increase or decrease; so, we will have two periods n_1 and n_2, each one with the calculation of the value of the mean X_1 and X_2 respectively.

This test is powerful for detecting inconsistency in the means, and it is a robust test (except when the length of the two periods selected for comparison of their means is unequal, because then the distribution of the data may not be skewed).

It is understood that a test is robust when it is insensitive to the shape of the probability distribution of the series. Due to the above, it is recommended to apply the test of the *t* that the values of n1 and n2 of each mean to be compared $\bar{x}_1$ y $\bar{x}_2$, no sean similares (Campos, 1998).

Student's t statistic is defined by Equation 3 (WMO, 1966):

$$t_d = \frac{\bar{x}_1 - \bar{x}_2}{\left[\frac{n_1 S_1^2 + n_2 S_2^2}{n_1 + n_2 - 2}\left(\frac{1}{n_1} + \frac{1}{n_2}\right)\right]^{1/2}} \tag{3}$$

Being S_1^2 y S_2^2 the variances of x_i in the two periods of record, respectively. Then, $n_1 S_1^2$ can be calculated with Equation 4.

$$n_1 S_1^2 = \sum_1^{n_1} x_i^2 - \frac{1}{n_1}\left(\sum_1^{n_1} x_i^2\right)^2 \tag{4}$$

And similarly it can be calculated $n_2 S_2^2$.

The absolute value of t_d is generally compared to the value of *t* of the distribution *t* two-tailed Student's method with $v = (n_1 + n_2 - 2)$ degrees of freedom and a 5% significance level. The values of *t* are concentrated in Table 7.14.

Table 7.14 Significance values for the values of the distribution of the t de Student and Cramer

Degrees of Freedom	Level of Significance		Degrees of Freedom	Level of Significance	
	5% *	5% **		5% *	5% **
1	6.314	12.706	18	1.734	2.101
2	2.920	4.303	19	1.729	2.093
3	2.353	3.182	20	1.725	2.086
4	2.132	2.776	21	1.721	2.080
5	2.015	2.571	22	1.717	2.074
6	1.943	2.447	23	1.714	2.069
7	1.895	2.365	24	1.711	2.064
8	1.860	2.306	25	1.708	2.060
9	1.833	2.262	26	1.706	2.056
10	1.812	2.228	27	1.703	2.052
11	1.796	2.201	28	1.701	2.048
12	1.782	2.179	29	1.699	2.045
13	1.771	2.160	30	1.697	2.042
14	1.761	2.145	40	1.684	2.021
15	1.753	2.131	60	1.671	2.000
16	1.746	2.120	120	1.658	1.980
17	1.740	2.110	∞	1.645	1.960
* One-tailed test					
** Two-tailed test					

Source: Own elaboration

Cramer's statistical test

Sometimes, it may be more convenient to compare the mean of the whole series and the mean of a certain part of the record, to investigate the homogeneity; for such purpose Cramer's test is quite useful, when the periods of the series are different. n_1 y n_2 are so similar that the *t* de Student loses validity (Campos, 1998).

The Cramer's test requires the arithmetic mean values $\bar{x}$ (Equation 4) and standard deviation S (Equation 5) of the total log of *n* values:

$$\bar{x} = \frac{\sum x_i}{n} \tag{4}$$

$$S = \frac{\sum(x_i - \bar{x})^2}{n-1} \tag{5}$$

On the other hand, $\bar{x}_k$ is the average of the period of n' values (subperiod of n), that has the greatest difference with respect to the average ($\bar{x}$) of the complete series (n); so that the value t_k is calculated according to the formulation shown in Equation 6 to Equation 8 (WMO, 1966):

$$\bar{x}_k = \frac{\sum_{i=k-1}^{i=k+n} x_i}{n'} \tag{6}$$

$$\tau_k = \frac{(\bar{x}_k - \bar{x})}{S} \tag{7}$$

$$t_k = \left[\frac{n'(n-2)}{n-n'[1+(\tau_k)^2]}\right]^{1/2} \cdot (\tau_k) \tag{8}$$

As with the Sequences and Helmert tests, it is recommended that the Studen and Cramer's t-tests be performed at the same time, since: i) they are complementary, ii) they are based on the understanding of the graph of the annual total rainfall series and, iii) the significance value with which they are compared is the same (Table 7.15).

Graphic 7.3 represents the annual precipitation values for station 14076, such that two well-marked time periods can be distinguished, with N_1 being the period from 1994 to 2000 and N_2 from 2001 to 2014.

Graphic 7.3 Behaviour of total annual rainfall through time at station 14076
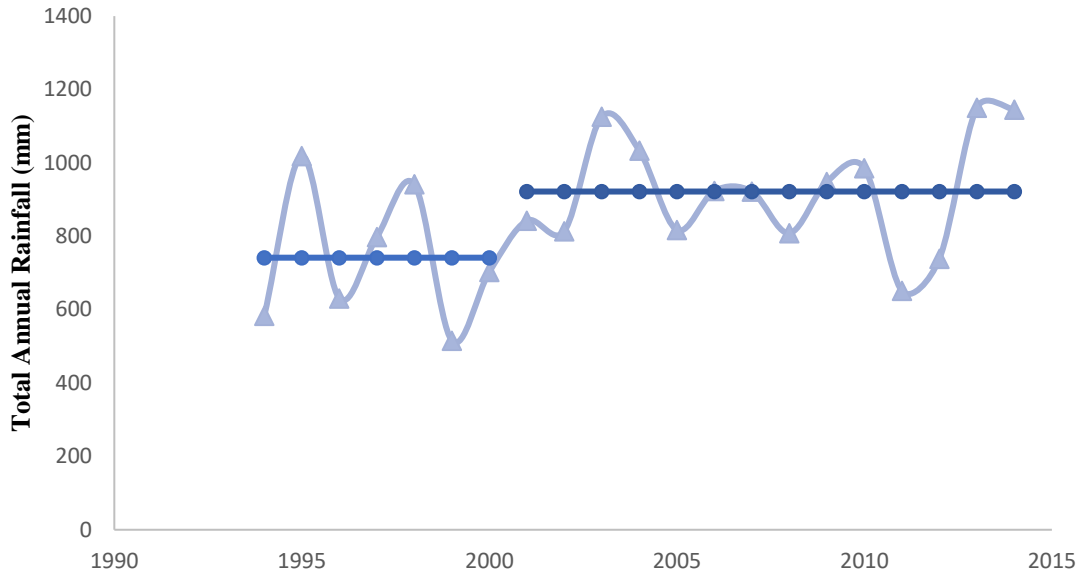
Source: Own elaboration

Once the periods have been delimited, the basic statistics for each period should be obtained, such as mean, variance and number of data (Table 7.15).

Table 7.15 Values for the test of *t* de Student for station 14076

$\overline{x_1}$	741.57	N_1	7	S_1^2	30005.96
$\overline{x_2}$	921.88	N_2	14	S_2^2	22131.95

Source: Own elaboration

These values are substituted into Equation 2, so that the following value of t_d.

$$t_d = \frac{741.57 - 921.88}{\left[\frac{(7*30005.96)+(14*22131.95)}{7+14-2} \cdot \left(\frac{1}{7}+\frac{1}{14}\right)\right]^{1/2}}$$

$$t_d = -1.43$$

In this case, the absolute value obtained from t_d is 1.43 and, according to the values in Table 4.6, a value of 1.729 is allowed for the 19 degrees of freedom. In this case the series can be considered as homogeneous, since the allowed value is less than the value calculated by the test statistic *t* de Student. Likewise, the Cramer's test is applied, which makes use of the second period of data from the original series (Graphic 7.3) of the Cramer's test (Graphic 7.2). *t* de Student, Therefore, as shown in Table 7.16, we have the information required to apply the formula described in Equation 8.

Table 7.16 Station 14076 values for Cramer's test

Values of the complete series		Secondary series values with jump	
$\overline{x}$	861.78	$\overline{x_k}$	921.88
S	178.83	n'	14
n	21		

Source: Own elaboration

By applying the values shown in Table 7.16 for Equation 7 and Equation 8, it is obtained:

$$\tau_k = \frac{(921.88 - 861.78)}{178.83} = 0.34$$

$$t_k = \left[\frac{14 * (21 - 2)}{21 - 14 * [1 + (0.34)^2]}\right]^{1/2} \cdot (0.34) = 2.35$$

The calculated value of Cramer's statistic (t_k) is 2.35. According to the data shown in Table 4.6, the allowed value for 19 degrees of freedom is 1.729 for a significance value of 5% (one-tailed test). Since the value calculated with Cramer's formula is greater than the allowed value, the series cannot be considered homogeneous. If the analysis is performed for a two-tailed test, the allowed value is 2.093, but likewise the value of $t_k = 2.35$ is still higher, so the series cannot be considered as homogeneous.De forma similar, tal como se realizó para la estación 14076, se tiene la gráfica de las precipitaciones totales anuales de la estación 14087 (Figura 4.4). En la cual se muestran los tramos de estudio de N_1 (1970 - 1977) y N_2 (1978 - 2002), con los cuales se puede obtener la información mostrada en la Tabla 7.17.

Graphic 7.4 Behaviour of total annual rainfall through time at station 14087
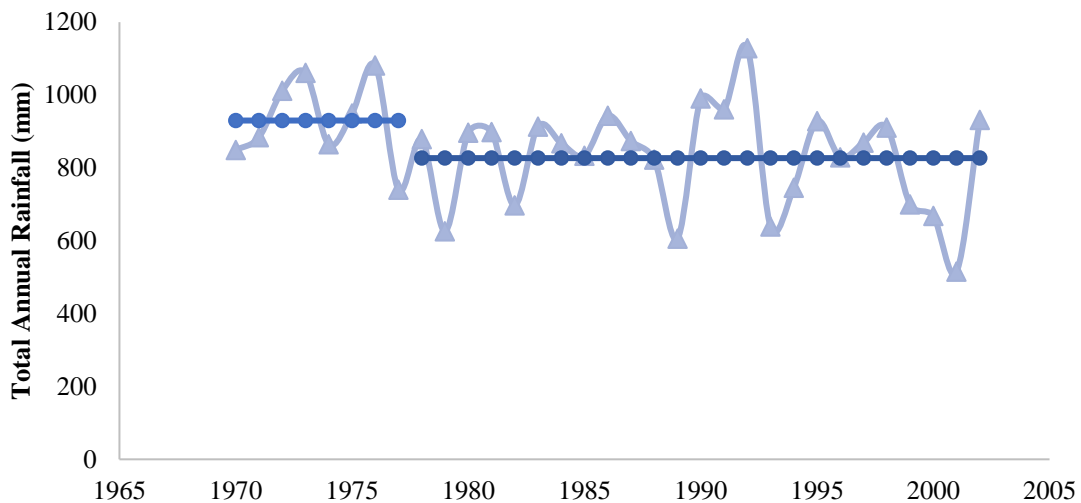
Source: Own elaboration

Table 7.17 Values for the test of *t* de Student for station 14087

$\overline{x_1}$	929.96	N_1	8	S_1^2	12016.04
$\overline{x_2}$	826.81	N_2	25	S_2^2	19609.90

Source: Own elaboration

With the above values, we obtain the value of t_d, such that:

$$t_d = \frac{929.96 - 826.81}{\left[\frac{(8 * 12016.04) + (25 * 19609.90)}{8 + 25 - 2} \cdot \left(\frac{1}{8} + \frac{1}{25}\right)\right]^{1/2}}$$

$$t_d = 094$$

The value obtained from t_d is 0.94 and, for the 31 degrees of freedom that the series has, it is necessary to have a maximum value of 1.697, which is fulfilled; therefore, it is said that the series is homogeneous by means of the test of *t* de Student.

Now, the same is done for Cramer's test, so the results of the test in question are presented, considering the information shown in Table 7.18.

$$\tau_k = \frac{(826.81 - 851.82)}{140.44} = -0.18$$

$$t_k = \left[\frac{25*(33-2)}{33-25*[1+(-0.18)^2]}\right]^{1/2} \cdot (-0.18) = -1.85$$

Table 7.18 Station 14087 values for Cramer's test

Values of the complete series		Secondary series values with jump	
$\bar{x}$	851.82	$\overline{x_k}$	826.81
S	140.44	n'	25
n	33		

Source: Own elaboration

Now, we have that, for Cramer's test, the absolute value of t_k is 1.85 and, according to Table 4.6, the maximum allowable value for the 31 degrees of freedom and with a 5% significance level for a one-tailed test is 1.692, so the series is considered to be inhomogeneous; however, when using the 5% significance level for a two-tailed test, the maximum allowable value is 2.042, which is not exceeded and therefore, station 14087 is considered to be homogeneous by the Cramer's test with a 5% significance level for a two-tailed test. 042, which is not exceeded and therefore, station 14087 is homogeneous by means of Cramer's test with a 5% significance level and for a two-tailed test.

Thus, we can determine that, by performing the exercise for the two stations presented in the case study, both are homogeneous by means of the test station. t de Student but, not homogeneous according to Cramer's test; in this sense, we also know that Cramer's test was not necessary to apply because the length of the series proposed for the Cramer's test is not homogeneous according to the Cramer's test. *t* de Student (N_1 y N_2) are different, which indicates, in principle, that it is only necessary to apply this test.

Wald - Wolfowitz Statistical Test

This test makes it possible to determine whether there is any difference between two annual rainfall series of size N_1 y N_2 (from two different weather stations). To apply the test, a single series should be generated by mixing the data coming from the two stations and sorting them in an increasing order. Subsequently, the number of sequences or spells of the ordered series is determined. A sequence is defined as any succession of values of the same series, which are indicated with *X* for the season in which homogeneity is being investigated and with *Y* for the auxiliary station (Campos, 1998).

When samples are small ($N_1, N_2 \leq 20$) Table 7.19 presents the critical values of the number of sequences, so that if a number of spurts were found to be (r) equal to or less than the tabulated value, the series will be different due to a certain cause, at a significance level of 5%.

This test is complementary to any other statistical test for homogeneity of a meteorological station, such as Cramer or t de Student. Then, if the probability obtained for this test exceeds the significance percentage (5% or 10%), one series is homogeneous and the other is non-homogeneous; on the contrary, if the probability value is within the range of the significance level, the two series will be homogeneous or non-homogeneous. This is determined by knowing the homogeneity or non-homogeneity of the series through the results of the test of *t* de Student o Cramer.

Table 7.19 Critical values of the number of sequences in the Wald-Wolfowitz test, for small samples

N₁/N₂	2	3	4	5	6	7	8	9	10	11	12	13	14	15	16	17	18	19	20
2											2	2	2	2	2	2	2	2	2
3					2	2	2	2	2	2	2	2	2	3	3	3	3	3	3
4				2	2	2	3	3	3	3	3	3	3	3	4	4	4	4	4
5			2	2	3	3	3	3	3	4	4	4	4	4	4	4	5	5	5
6		2	2	3	3	3	3	4	4	4	4	5	5	5	5	5	5	6	6
7		2	2	3	3	3	4	4	5	5	5	5	5	6	6	6	6	6	6
8		2	3	3	3	4	4	5	5	5	6	6	6	6	6	7	7	7	7
9		2	3	3	4	4	5	5	5	6	6	6	7	7	7	7	8	8	8
10		2	3	3	4	5	5	5	6	6	7	7	7	7	8	8	8	8	9
11		2	3	4	4	5	5	6	6	7	7	7	8	8	8	9	9	9	9
12	2	2	3	4	4	5	6	6	7	7	7	8	8	8	9	9	9	10	10
13	2	2	3	4	5	5	6	6	7	7	8	8	9	9	9	10	10	10	10
14	2	2	3	4	5	5	6	7	7	8	8	9	9	9	10	10	10	11	11
15	2	3	3	4	5	6	6	7	7	8	8	9	9	10	10	11	11	11	12
16	2	3	4	4	5	6	6	7	8	8	9	9	10	10	11	11	11	12	12
17	2	3	4	4	5	6	7	7	8	9	9	10	10	11	11	11	12	12	13
18	2	3	4	5	5	6	7	8	8	9	9	10	10	11	11	12	12	13	13
19	2	3	4	5	6	6	7	8	8	9	10	10	11	11	12	12	13	13	13
20	2	3	4	5	6	6	7	8	9	9	10	10	11	12	12	13	13	13	14

Source: Own elaboration

When N_1 o $N_2 > 20$, Table 4.11 cannot be used, then the statistic is evaluated. z, according to Equation 9 (Siegel, 2015).

$$z = \frac{\left|r - \left(\frac{2N_1N_2}{N_1+N_2}+1\right)\right| - 0.50}{\sqrt{\frac{2N_1N_2(2N_1N_2-N_1-N_2)}{(N_1+N_2)^2(N_1+N_2-1)}}} \tag{9}$$

If the calculated value of z in Equation 4.9 has an associated probability 'p', read directly in Table 7.20, equal to or less than the adopted significance level (5% and 10%) the series will be different and, therefore, if one of them is known to be homogeneous, the other will be non-homogeneous. Therefore, according to the values in Table 4.12, it is recommended that the absolute value of z be greater than or equal to 1.65 for a significance value of 5% and greater than or equal to 1.29 for a significance value of 10%.

Table 7.20 Associated probabilities 'p' auxiliary in the Wald-Wolfowitz test

Z	0	0.01	0.02	0.03	0.04	0.05	0.06	0.07	0.08	0.09
0	0.5000	0.4960	0.4920	0.4880	0.4840	0.4801	0.4761	0.4721	0.4681	0.4641
0.1	0.4602	0.4562	0.4522	0.4483	0.4443	0.4404	0.4364	0.4325	0.4286	0.4247
0.2	0.4207	0.4168	0.4129	0.4090	0.4052	0.4013	0.3974	0.3936	0.3897	0.3859
0.3	0.3821	0.3783	0.3745	0.3707	0.3669	0.3632	0.3594	0.3557	0.3520	0.3483
0.4	0.3446	0.3409	0.3372	0.3336	0.3300	0.3264	0.3228	0.3192	0.3156	0.3121
0.5	0.3085	0.3050	0.3015	0.2981	0.2946	0.2912	0.2877	0.2843	0.2810	0.2776
0.6	0.2743	0.2709	0.2676	0.2643	0.2611	0.2578	0.2546	0.2514	0.2483	0.2451
0.7	0.2420	0.2389	0.2358	0.2327	0.2296	0.2266	0.2236	0.2206	0.2177	0.2148
0.8	0.2119	0.2090	0.2061	0.2033	0.2005	0.1977	0.1949	0.1922	0.1894	0.1867
0.9	0.1841	0.1814	0.1788	0.1762	0.1736	0.1711	0.1685	0.1660	0.1635	0.1611
1	0.1587	0.1562	0.1539	0.1515	0.1492	0.1469	0.1446	0.1423	0.1401	0.1379
1.1	0.1357	0.1335	0.1314	0.1292	0.1271	0.1251	0.1230	0.1210	0.1190	0.1170
1.2	0.1151	0.1131	0.1112	0.1093	0.1075	0.1056	0.1038	0.1020	0.1003	0.0985
1.3	0.0968	0.0951	0.0934	0.0918	0.0901	0.0885	0.0869	0.0853	0.0838	0.0823
1.4	0.0808	0.0793	0.0778	0.0764	0.0749	0.0735	0.0721	0.0708	0.0694	0.0681
1.5	0.0668	0.0655	0.0643	0.0630	0.0618	0.0606	0.0594	0.0582	0.0571	0.0559
1.6	0.0548	0.0537	0.0526	0.0516	0.0505	0.0495	0.0485	0.0475	0.0465	0.0455
1.7	0.0446	0.0436	0.0427	0.0418	0.0409	0.0401	0.0392	0.0384	0.0375	0.0367
1.8	0.0359	0.0351	0.0344	0.0336	0.0329	0.0322	0.0314	0.0307	0.0301	0.0294
1.9	0.0287	0.0281	0.0274	0.0268	0.0262	0.0256	0.0250	0.0244	0.0239	0.0233
2	0.0228	0.0222	0.0217	0.0212	0.0207	0.0202	0.0197	0.0192	0.0188	0.0183
2.1	0.0179	0.0174	0.0170	0.0166	0.0162	0.0158	0.0154	0.0150	0.0146	0.0143
2.2	0.0139	0.0136	0.0132	0.0129	0.0125	0.0122	0.0119	0.0116	0.0113	0.0110
2.3	0.0107	0.0104	0.0102	0.0099	0.0096	0.0094	0.0091	0.0089	0.0087	0.0084
2.4	0.0082	0.0080	0.0078	0.0075	0.0073	0.0071	0.0069	0.0068	0.0066	0.0064
2.5	0.0062	0.0060	0.0059	0.0057	0.0055	0.0054	0.0052	0.0051	0.0049	0.0048
2.6	0.0047	0.0045	0.0044	0.0043	0.0041	0.0040	0.0039	0.0038	0.0037	0.0036
2.7	0.0035	0.0034	0.0033	0.0032	0.0031	0.0030	0.0029	0.0028	0.0027	0.0026
2.8	0.0026	0.0025	0.0024	0.0023	0.0023	0.0022	0.0021	0.0021	0.0020	0.0019
2.9	0.0019	0.0018	0.0018	0.0017	0.0016	0.0016	0.0015	0.0015	0.0014	0.0014
3	0.0013	0.0013	0.0013	0.0012	0.0012	0.0011	0.0011	0.0011	0.0010	0.0010
3.1	0.0010	0.0009	0.0009	0.0009	0.0008	0.0008	0.0008	0.0008	0.0007	0.0007

Source: Own elaboration

For the application of the Wald-Wolfowitz test, the precipitation series of the two selected weather stations 14076 and 14087 shown in Table 7.5 and Table 7.6, respectively, are required.

For this test, it is not necessary that the periods be equal or consecutive; it is sufficient that they be representative series (it is recommended to have at least 25 years of data) for each of the stations under study. The data from both stations are combined in the same series and are ordered from lowest to highest, always taking into account which value belongs to each station; henceforth, the values of station 14076 will be referred to as the series *X* and for those of station 14087 such as the series *Y*.

Table 7.21 Number of sequences obtained for the Wald-Wolfowitz test

P (mm)	Serie	# sec.	P (mm)	Serie	# sec.	P (mm)	Serie	# sec.	P (mm)	Serie	# sec.	P (mm)	Serie	# sec.
454.7	X	1	716.5	X	13	842.5	X	21	921.5	X	29	1015.8	X	41
471	Y	2	731.2	Y	14	846.3	X	21	923.5	X	29	1019	X	41
514.9	Y	2	738.6	X	15	847	Y	22	928	Y	30	1022.5	X	41
515.5	X	3	739.9	Y	16	849	Y	22	931.2	Y	30	1033.4	X	41
533.7	X	3	745.5	Y	16	851	X	23	935.9	X	31	1060.8	Y	42
583.5	X	3	757.5	X	17	854	X	23	941.5	X	31	1070.7	Y	42
605.9	Y	4	762.9	X	17	856.4	X	23	943	Y	32	1078.3	X	43
608.6	X	5	764.2	X	17	862	X	23	943.4	X	33	1079.6	X	43
613.8	X	5	767.8	X	17	864.4	Y	24	948.3	X	33	1081.4	Y	44
625.5	Y	6	774.5	X	17	865.4	Y	24	948.8	Y	34	1103.4	Y	44
630.5	X	7	775.7	Y	18	867.8	Y	24	960.8	Y	34	1109	X	45
638.6	Y	8	798	X	19	869.6	Y	24	964.5	X	35	1114.8	Y	46
640.3	X	9	802.7	X	19	871.7	Y	24	971.4	Y	36	1121.9	Y	46
640.5	X	9	808.5	X	19	873.4	Y	24	980.7	X	37	1126	X	47
645	X	9	814	X	19	878.5	Y	24	984.3	X	37	1128.7	Y	48
651	X	9	817.3	X	19	881.5	X	25	985.7	X	37	1145.5	X	49
659.1	X	9	818.5	X	19	884	Y	26	990.2	Y	38	1150.5	X	49
665.5	X	9	822.5	Y	20	884.2	X	27	991.5	Y	38	1211.5	X	49
668	Y	10	823.9	Y	20	893.1	Y	28	995.9	X	39	1213	X	49
675.9	X	11	829.2	Y	20	893.3	Y	28	997.1	X	39	1261	X	49
676.5	X	11	829.3	Y	20	896.1	Y	28	997.6	X	39	1360.7	Y	50
696.6	Y	12	833.5	Y	20	898.4	Y	28	998.5	X	39			
700	Y	12	835.8	X	21	910.8	Y	28	999.1	X	39			
703	X	13	838.5	X	21	913.5	Y	28	1011.4	Y	40			

Source: Own elaboration

As shown in Table 4.13, we have a total of 50 sequences (r), which are obtained considering the change of the series (from *X* to *Y* or vice versa). In addition to the number of sequences, it is necessary to know the number of data of each series, being 67 and 50 data for stations 14076 and 14087 respectively; given that the number of data per series exceeds 20 values, it is not possible to use the **¡Error! No se encuentra el origen de la referencia.**4.11, so that the value of z is obtained according to the formulation described in Equation 9, such that:

$$z = \frac{\left|50 - \left(\frac{2*67*50}{67+50} + 1\right)\right| - 0.50}{\sqrt{\frac{(2*67*50)\left((2*67*50) - 67 - 50\right)}{(67+50)^2(67+50-1)}}}$$

$$z = 1.473$$

Calculating the z value, the probability is obtained according to the information shown in Table 4.12, which results in 0.0708, which exceeds the 5% significance value, it is known that one of the two series is not homogeneous. In this sense, and when reviewing the information obtained with the other consistency tests, it is known that station 14076 did not pass the homogeneity test by Cramer (with 5% significance for one tail), so it is then considered that station 14076 would also be inhomogeneous by means of the Wald-Wolfowitz test and, thus, station 14087 would be homogeneous.

However, when using a significance level of 10%, it is required that the value of the probability obtained by means of the value of *z* is less than 0.10, which is true and, thus, both stations 14076 and 14087 are homogeneous by means of the Wald-Wolfowitz test for a significance level of 10%.

Independence

Anderson limits

It is said that the data in a sample are independent when the value of one of them does not affect the value of the next data in the same series. To determine the probability limits of independent series, the Anderson Limits test with 95% confidence is used (Anderson, 1941).

The independence of the series is determined by means of a graph named *correlogram*. This is constructed through the estimation of the confidence limits, called Anderson limits, hence the name of the test, and the determination of the autocorrelation coefficients. (r) which are plotted on the ordinates, while on the abscissa axis are plotted the time delays of the series or lags. (k). The number of lags depends on the number of data in the series, i.e., the greater the number of data, the greater the number of lags needed to evaluate the independence of the series, and can be calculated with Equation 4.10. Both elements, Anderson bounds and the autocorrelation coefficients (r_k), dependen de los tiempos de retraso de la serie (Salas et al., 1980).

$$k = \frac{n}{3} \tag{10}$$

To calculate the correlogram, it should be considered that from the original data series (*X*) a modified series is generated (*Y*) which depends on the time lag (*k*) that applies to the series. Thus, for the same k, you have a series of X and a series Y.

Then, according to the number of lags (*k*), will be the number of values you have in the correlogram (ρ), represented in Equation 11 and Equation 12; where σ_x y σ_y are the standard deviations of the series *X* y *Y*, respectively and *n* represents the number of data in the series.

$$r_k = \beta \frac{\sigma_x}{\sigma_y} \tag{11}$$

Where:

$$\beta = \frac{n\sum XY - \sum X \sum Y}{n\sum X^2 - (\sum X)^2} \tag{12}$$

To determine the probability limits of independent (or persistent for flow series), i.e. the upper and lower Anderson limits (Anderson, 1941) with a 95% confidence level, they are calculated using Equation 13.

$$l_{r(95\%)} = \frac{-1 \pm 1.96\sqrt{n-k-1}}{n-k} \tag{13}$$

If, when applying the test with a significance level of 5%, it is found that the series is dependent (not independent), it is recommended to use a significance level of 1% (Equation 14).

$$l_{r(99\%)} = \frac{-1 \pm 2.326\sqrt{n-k-1}}{n-k} \tag{14}$$

As for the meteorological stations, if and only if less than 10% of the values of the calculated correlogram exceed the confidence limits, the data series is said to be independent.

When this test is applied to the hydrometric stations, it does not seek independence of the series, but rather evaluates its dependence due to the nature of the information.

In the series of runoff volumes or flow rates there must be a dependence of the data (due to the regulation of the systems) that translates into a relationship of the data evaluated with that which precedes it. Such dependence increases as the sampling interval of a series is reduced, so that there is more dependence between successive monthly values than between annual magnitudes (Campos, 2007).

Therefore, the interpretation of the dependence of a flow series requires that at least 90% of the values of the correlogram are outside the Anderson Limits, then the series is said to be persistent (dependent).

For the application case, we will refer to the data in Table 3.5 and Table 3.6 for the annual precipitation series for stations 14076 and 14087 respectively, whose number of data in each series are 21 and 30. Using Equation 4.13 the Anderson Limits were calculated with 7 lags for station 14076 and 10 lags for station 14087.

Table 7.22 shows the value of the calculated autocorrelation coefficients, and the value of the Anderson Limits for station 14076.
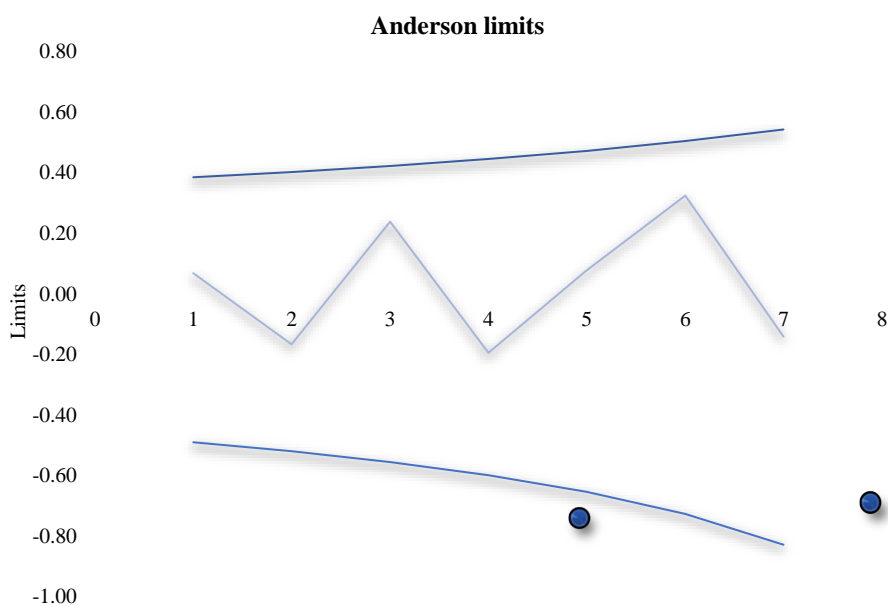
Table 7.22 Autocorrelation coefficients for station 14076

k	X	X²	Y	XY	n
1	16951.8	14955257.4	17513.8	14884535.2	20
2	15801.3	13631607.2	16499.8	13633640.8	19
3	15062.7	13086077.2	15869.3	13398143.7	18
4	14411.7	12662276.2	15071.3	12684408.7	17
5	13426	11690671.7	14129.8	11892451.5	16
6	12477.7	10791398.9	13614.3	11449383.1	15
7	11669.2	10137726.6	12911.3	10711077	14

β	σx	σy	r_k	l_r inf	l_r sup
0.07	175.78	176.26	0.07	-0.49	0.39
-0.18	165.08	178.18	-0.17	-0.52	0.40
0.25	168.27	173.50	0.24	-0.56	0.42
-0.21	166.73	177.54	-0.19	-0.60	0.45
0.08	168.24	182.78	0.08	-0.65	0.47
0.30	171.52	159.68	0.32	-0.73	0.50
-0.12	177.87	154.95	-0.14	-0.83	0.54

Source: Own elaboration

Graphic 7.5 shows the correlogram for station 14076. In this plot it is observed that there are no values of the autocorrelation coefficients that are outside the Anderson Limits, so the series can be considered as independent.

Graphic 7.5 Correlogram and Anderson Limits for station 14076

Source: Own elaboration

Table 7.23 concentrates the results obtained for the autocorrelation coefficients and values of the Anderosn Limits for station 14087. Thirty years of data corresponding to the period (1973 - 2002) were analyzed.

Figure 7.6 shows the resulting correlogram for station 14087. It is observed that all the autocorrelation coefficients are within the Anderson Limits, which means that the series can be considered as independent.

Table 7.23 Autocorrelation coefficients for station 14087

K	X	X²	Y	XY	n
1	24434.3	21202984.2	24304.7	20468555.3	29
2	23919.4	20937862.2	23637.8	20286289.8	28
3	23251.4	20491638.2	23302.8	20057288.1	27
4	22551.4	20001638.2	22682.1	19550941.4	26
5	21640.6	19172081.6	22370.9	19337523.4	25
6	20771	18415877.4	21710.3	18663447.5	24
7	19941.8	17728304.8	21343.9	18485558.5	23
8	19013.8	16867120.8	20747.3	17874067.2	22
9	18268.3	16311350.5	20049.6	17347303.9	21
10	17629.7	15903540.6	19736.2	17350902.9	20
β	σx	σy	r_k	l_r inf	l_r sup
-0.02	148.27	143.33	-0.02	-0.40	0.33
0.19	136.68	155.07	0.16	-0.42	0.34
-0.02	134.22	152.06	-0.02	-0.43	0.35
-0.28	132.88	152.81	-0.24	-0.45	0.36
-0.06	135.32	156.74	-0.05	-0.48	0.38
-0.29	138.23	167.01	-0.24	-0.50	0.39
-0.05	141.11	165.15	-0.04	-0.54	0.41
-0.13	143.79	172.45	-0.11	-0.58	0.43
-0.22	144.81	180.82	-0.18	-0.63	0.46
-0.13	138.26	170.63	-0.10	-0.69	0.49

Source: Own elaboration

Graphic 7.6 Correlogram and Anderson Limits for station 14087
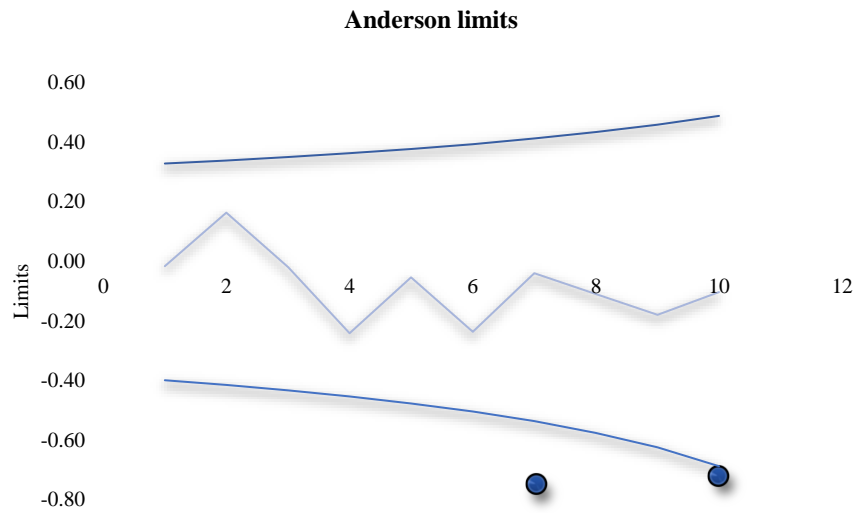
Source: Own elaboration

Summary of results. Validation of weather stations

Table 7.24 shows the summary results of the consistency tests applied to meteorological stations 14076 and 14087. With the exception of the Cramer's test, all the others allowed homogeneity to be demonstrated for all cases. The non-homogeneity of Cramer's test, considered as specific, was verified again through the Wald-Wolfowitz test, since this is a complementary test for any of the statistical homogeneity tests shown in this work, it was determined that the series can be considered as homogeneous. In addition, the rest of the tests applied showed that the data can be considered homogeneous, which is an indication that gives robustness to the results presented.

Table 7.24 Consistency test results for weather stations 14076 and 14087

Test	Station	
	14076	14087
Sequences	Homogeneous	Homogeneous
Helmert	Homogeneous	Homogeneous
Double Mass Curve	Homogeneous	Homogeneous
t de Student	Homogeneous *	Homogeneous *
Cramer	Non-homogeneous **	Homogeneous **
Wald - Wolfowitz	Homogeneous ***	Homogeneous ***
Anderson limits	Independent *****	Independent
* 5% significance level for one-tailed.		
** Two-tailed significance level of 5%.		
*** 10% significance level		
**** Significance level of 5%.		

Source: Own elaboration

The application of at least two homogeneity tests is recommended in all cases. Generally, it is recommended to start with the general tests, and if there is a discrepancy of results, then the application of at least a third specific test that can help in the validation of the homogeneity of the series is recommended.

The test used to verify the independence of the series, Anderson Limits, is a very robust test, in this case the series analyzed were found to be independent.

7.5 Validation of hydrometric stations

7.5.1 Natural regime stations

The natural regime hydrometric series is given by the historical series of flows that would have flowed through that place if there were no human intervention in the basin. Anthropogenic actions are all works of regulation or use of surface or groundwater that alter the amount of flow that would have flowed through the river (Solera, 2003).

Therefore, if a mathematical model is configured to simulate its operation and is fed with the natural regime series, the result will be the series also simulated in natural regime.

In Mexico, the necessary information is not available to carry out a restitution to a natural regime; for this reason, it is proposed to work with undisturbed hydrometric stations, with which high or headwater basins are created. These basins are areas adjacent to the water divide or watershed in the highest altimetric portion of the basin and, in this zone, the first runoff is formed after the soil has retained or absorbed the water according to its capacity (Cotler et al., 2013).

When starting from hydrometric series in which there are no anthropogenic actions, it is necessary to check that there are no important works in the basin; in addition to the behavior of the hydrometric series itself. Therefore, in addition to homogeneity and persistence tests, a visual review of the flow series over time is performed; thus, for the basins generated from the hydrometric stations, the runoff coefficient is obtained, and the relative modulus is calculated.

Visual Review of Runoff Series

As mentioned by Campos Aranda in his book: Estimación y Aprovechamiento del Escurrimiento (2007), hydrology defines a chronological series or time series as a succession of observations that measure the variation over time of some aspect of a phenomenon, such as the flow or volume of a watercourse, the water level in a lake or reservoir, etc. In hydrology only two components are accepted: deterministic and random or stochastic.

The deterministic component is that which can be evaluated for prediction purposes and consists mainly of trend-like behavior and cyclic or periodic form, as well as sudden changes, called jumps, which are inhomogeneities of a particular type. On the other hand, the stochastic component consists of irregular oscillations and random effects that cannot be strictly explained physically and require probabilistic concepts for their description. Graphic 7.6 schematizes time series with various types of deterministic components.

Graphic 7.6 Time series with various types of deterministic components
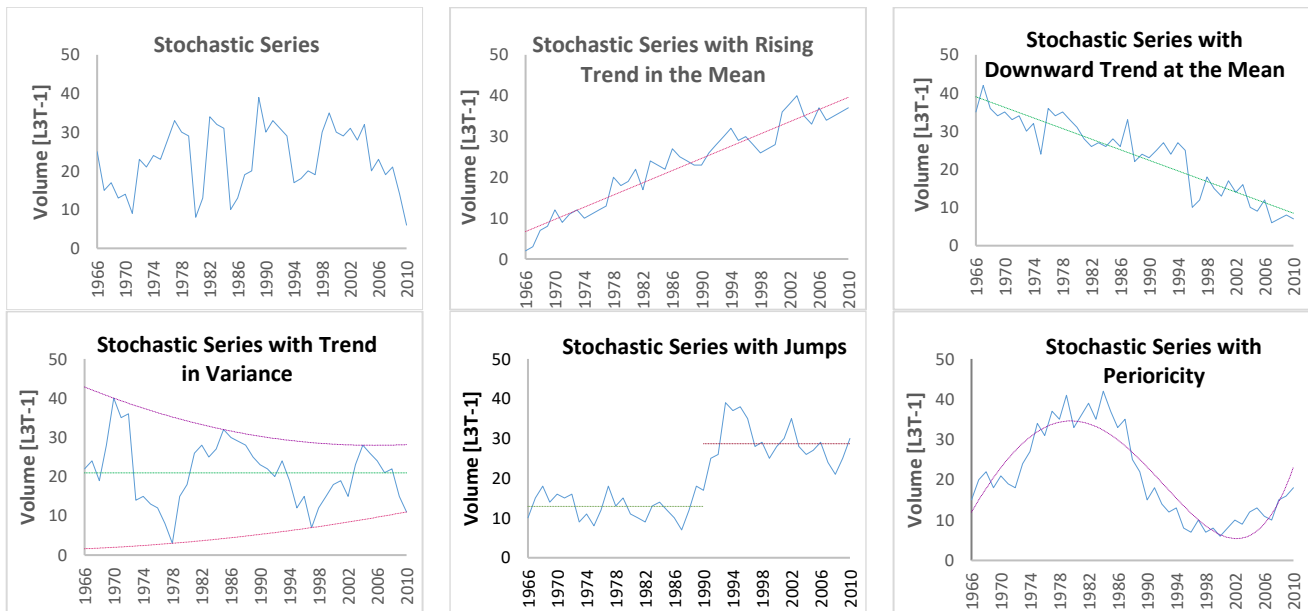
Source: Own elaboration; adapted from Campos (2007).

In general, trends in annual runoff time series can result from changes in the hydrologic environment that produces the series or from alterations that come from natural or human-induced gradual variations. Whether the trend in the time series is due to changes in the watershed or to errors in measurement, the fact is that it causes the series to be labeled as inconsistent. On some occasions, the trend in the mean may be quite obvious, however, in most cases there is some doubt as to whether the suspected systematic error effects are significant or not, which is why numerical tests such as persistence are imperative.

Apart from the trend, sudden changes called jumps can occur, which can be the result of catastrophic natural events such as earthquakes or forest fires, or consequences of hydraulic works built in the basin. In general, the presence of a jump in the series indicates that somehow the homogeneity of the record has been lost, i.e., now the observations that integrate it come from two populations, perhaps statistically different, and therefore, it will be necessary to test whether or not the homogeneity was lost. However, as shown in Graphic 7.7, the series does not show marked jumps over time; in the period from 1977 to 1983, there is a very slight decrease in runoff volume. However, despite the fact that we have old information, it is worth mentioning that there are no control works in the basin, so the stream bed flows without alterations, which indicates that the basin is in a natural regime. In addition, the basin does not receive surface contributions from other basins, which means that the basin under study is a headwater basin.

Graphic 7.7 Annual runoff volumes for hydrometric station 12607 "La Yerbabuena"
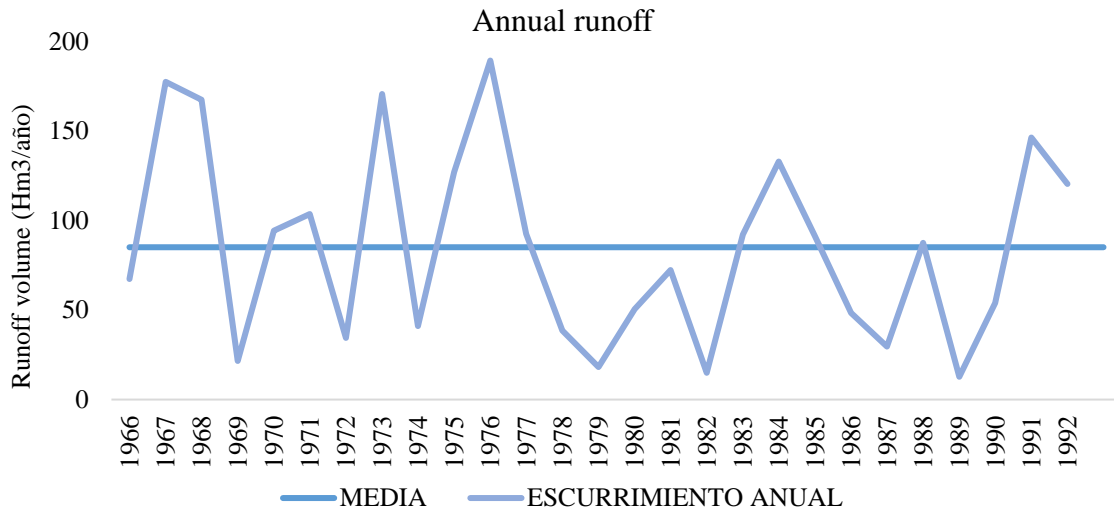
Source: Own elaboration

However, comparing the series shown in Figure 7.7 with the graphs shown in Figure 7.6 the annual volumes of the hydrometric station are representative of a normal stochastic series, with no tendency to rise or fall according to the mean and without significant jumps or periodicity, which indicates that the flow was maintained over time and that there is no significant anthropogenic alteration that could alter the results of future modeling, so it is concluded as part of the visual review that the hydrometric station is suitable for hydrological modeling. Antes de obtener los parámetros que permiten entender la estación In order to determine the hydrometric characteristics with respect to the basin under study (runoff coefficient and relative modulus), the homogeneity (Sequences and Helmert) and persistence (Anderson Limits) tests described above must be performed.

With this, the Helmert and Sequences test procedure (Table 7.25) is shown using the series presented in Table 7.7.

Table 7.25 Sequence and Helmert test for station 14076

Year	PMA	Sequence Testing		Helmert test	
		Comparison	Sequence	COMPARISON	CHANGES
1966	67.40	L	1	L	
1967	177.48	M	2	M	C
1968	167.50	M	2	M	S
1969	21.59	L	3	L	C
1970	94.29	M	4	M	C
1971	103.60	M	4	M	S
1972	34.39	L	5	L	C
1973	170.79	M	6	M	C
1974	41.07	L	7	L	C
1975	127.08	M	8	M	C
1976	189.41	M	8	M	S
1977	92.64	M	8	M	S
1978	38.57	L	9	L	C
1979	18.15	L	9	L	S
1980	50.48	L	9	L	S
1981	72.42	L	9	L	S
1982	15.02	L	9	L	S
1983	92.17	M	10	M	C
1984	133.05	M	10	M	S
1985	91.37	M	10	M	S
1986	48.36	L	11	L	C
1987	29.55	L	11	L	S
1988	87.55	L	11	M	C
1989	12.73	L	11	L	C
1990	54.02	L	11	L	S
1991	146.46	M	12	M	C
1992	120.55	M	12	M	S

Source: Own elaboration

Since the continuous series consists of 27 years (Table 7.24), the comparison value for the sequence test will be the median with a value of 87.55.Hm^3. With this, a total of 12 sequences is obtained and when reviewing Table 4.2 and taking the value for 26 data, it is found that the number of sequences allowed is from 10 to 17 sequences), so, according to the sequences test, it is found that the series is homogeneous.

Similarly, for the Helmert test, the value of the mean is 85.10. Hm^3, this gives a total of 13 changes and 13 sequences, so that when Equation 4.1 is applied, it is shown that the station is homogeneous, with a difference between sequences and changes of zero, as shown below:

$$-\sqrt{27-1} \leq 13 - 13 \leq \sqrt{27-1}$$

$$-5.10 \leq 0 \leq 5.10$$

It is important to mention that the application of this test is only an indicator of what happens in the hydrometric station and serves to understand the behavior of the series in question; however, it is not a limiting factor for the use of the station in question.

On the other hand, since it is a persistence test, the correlogram should be outside the Anderson limits, which indicates the non-independence of the series.

Table 7.26 shows the correlogram results and the limits for the 9 lags generated according to the annual series (Table 7.7).

Table 7.26 Result of the Anderson limit test for hydrometric station 12607

K	X	X²	Y	XY	n
1	2177.14801	256623.771	2230.30216	191939.931	26
2	2030.69198	235174.402	2023.63976	157164.842	25
3	1976.67025	232256.055	1801.05438	159727.409	24
4	1963.9355	232093.881	1816.80983	140810.03	23
5	1876.38378	224428.577	1801.14906	153811.856	22
6	1846.83041	223555.175	1701.36788	142613.568	21
7	1798.46954	221216.402	1728.7964	143600.841	20
8	1707.1015	212868.283	3399.48329	163028.703	20
9	1574.05427	195166.718	3267.04777	143198.67	19
β	σx	σy	r_k	l_r inf	l_r sup
0.07	54.52	54.88	0.07	-0.42	0.34
-0.10	54.09	52.09	-0.11	-0.44	0.36
0.16	54.95	47.83	0.19	-0.47	0.37
-0.22	54.10	47.30	-0.25	-0.49	0.39
0.00	55.37	46.07	0.00	-0.52	0.40
-0.11	55.29	46.98	-0.13	-0.56	0.42
-0.20	55.96	45.21	-0.25	-0.60	0.45
-1.89	57.49	385.38	-0.28	-0.63	0.46
-1.97	58.17	373.86	-0.31	-0.69	0.49

Source: Own elaboration

Graphic 7.7 Correlogram and Anderson Limits for hydrometric station 12607
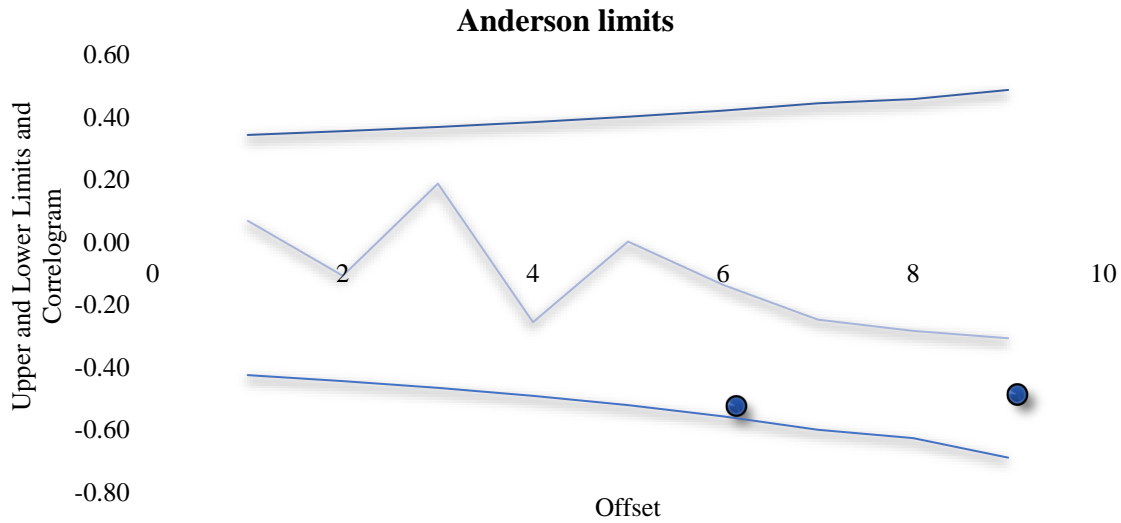
Source: Own elaboration

On the other hand, Figure 5.3 shows the correlogram with the Anderson limits, which is within the Anderson limits; this shows that the station is not persistent (since it is within the limits and not outside), this indicates that greater care should be taken with respect to the simulations; however, this is not an impediment to continue using the information provided by the hydrometric station.

Once the consistency tests are performed at the hydrometric station, the runoff coefficient and relative modulus values are obtained, which require information not only from the station itself, but also from meteorological information and from the basin under study.

Runoff Coefficient

Chow et al. (1994) defined the runoff coefficient as the ratio of direct runoff to the average precipitation intensity of a storm. However, because of the variability of precipitation intensity, this value is difficult to determine using observed information, so it can also be defined as the ratio of the volume of direct runoff to the volume of precipitation in the basin, in a given time period, such that Equation 15 is obtained:

$$Ce = \frac{V_E}{V_P}$$ (15)

Where V_E is the annual volume and V_P is the annual volume precipitated in the area?

The runoff coefficient is an imprecise variable, because it implies a fixed relationship between runoff and rainfall in the basin, which is not actually true. The proportion of total rainfall that will flow as surface runoff depends on the permeability of the soil and the slope of the area.

Another way to understand it is to obtain the parameter K with the relationship between the runoff sheet in mm (E) and the precipitation in mm (P), as shown in Equation 16.

$$K = \frac{E}{P}$$ (16)

For both Ce and K, it must be fulfilled that: K<1 and Ce<1; this is due to the fact that the runoff of a basin must be less than the present precipitation.

For the case of application, we have the information of the annual flow rates presented in Table 7.7, which shows that the average annual flow rate at the hydrometric station is 85.10 Hm³; the value of the surface area of the watershed is also recalled, which is 299.20 km².

The precipitation in the basin is of 903.23 mm, which is obtained by means of a fictitious station at the center of the basin generated by hydrometric station 12607, according to the monthly information obtained from meteorological stations 14076 and 14087.

With the values described in the previous paragraphs, Equation 15 and Equation 16 are developed, which must be identical, since the volume of annual contribution (V_E) and the annual precipitated volume (PV) are the sheets are the runoff sheet and precipitation multiplied by the basin area, such that:

$$V_E = 85.10 \ Hm^3$$

$$V_P = (903.23 \ mm) * (299.20 \ km^2) \quad \rightarrow \quad V_P = 270.26 \ Hm^3$$

$$Ce = \frac{85.10 \ Hm^3}{270.26 \ Hm^3} \quad \rightarrow \quad Ce = 0.3149$$

Likewise, the same is done for the runoff sheets (284.42 mm) and that of precipitation, so that the value of K is obtained.

$$K = \frac{284.42 \ mm}{903.23 \ mm} \quad \rightarrow \quad K = 0.3149$$

It is interesting to note from the above formulation that the runoff coefficient can be obtained as follows (Ce) or the parameter K in either of the two ways. The most important thing is to verify that the runoff volume is less than the precipitated volume. If this is not the case, it is clear that there is a problem in the basin, since it is very likely that it is in an altered regime and has a contribution from an external source.

Modes of Contributions

Sánchez (2017) mentions that different modes can be presented in the gauging data, such as: daily, monthly or annual flows, contribution, equivalent water sheet and specific flow (Figure 5.4). These last two allow relating runoff and precipitation to the study area and that is why, it is used as a parameter for understanding the hydrometric stations under review.

Daily flow rates: which may correspond to the daily reading of a limnimetric scale or correspond to the mean ordinate of the daily graph of a limnigraph.

Monthly or average monthly flows: for a given year, it is the average of all the days of that month. For a series of years, it refers to the average of all October values, all November values, etc. for the entire series studied.

For a given year, the annual or mean annual flow (modulus) is the average of all the days of that year, for the series of years it refers to the average of all the years of the series under consideration.

The contribution is normally referred to a year (annual contribution), although it is sometimes referred to a month (monthly contribution). It is the volume of water contributed by the watercourse at the point considered during a year or a month (Hm^3).

The equivalent sheet of water is the thickness of water that would be obtained by distributing over the entire basin the volume of the annual inflow (en mm). It is obtained by dividing the annual contribution by the surface area of the basin. It is useful especially when we want to compare runoff with precipitation. If the basin is hydrologically closed and the data come from more than 20 years, this value should be similar to the non-evapotranspired precipitation. (P-ETR). The specific flow rate is the flow rate per unit area. It represents the flow rate provided by each km^2 basin. It is calculated by dividing the flow (normally annual average flow by the surface area of the basin or sub-basin considered (liters /seg·km^2); this parameter is also known as relative modulus and as shown in Equation 17 is obtained with the modulus or flow rate (M) in liters per second and with the basin area (S) in km^2.

$$M_r = \frac{M}{S}$$ (17)

The relative module allows comparing the flow of various basins, being their surfaces different (Sanchez, 2017). Mountain areas provide more than 20 liters/sec-km², while, in the lower parts of the same basin only 4 or 5 liters/sec-km2 are generated. Likewise, we know that:

- If the relative modulus is less than 5 liters/sec-km², there is a water shortage.

- If the relative modulus is in the range of 5 to 15 liters/sec-km², it is said to be in average values and if the relative modulus is greater than 15 liters/sec-km², the values are high and it is possible that a parameter is being poorly considered.

Figure 7.6 Report on parameters obtained from gauging in the basins
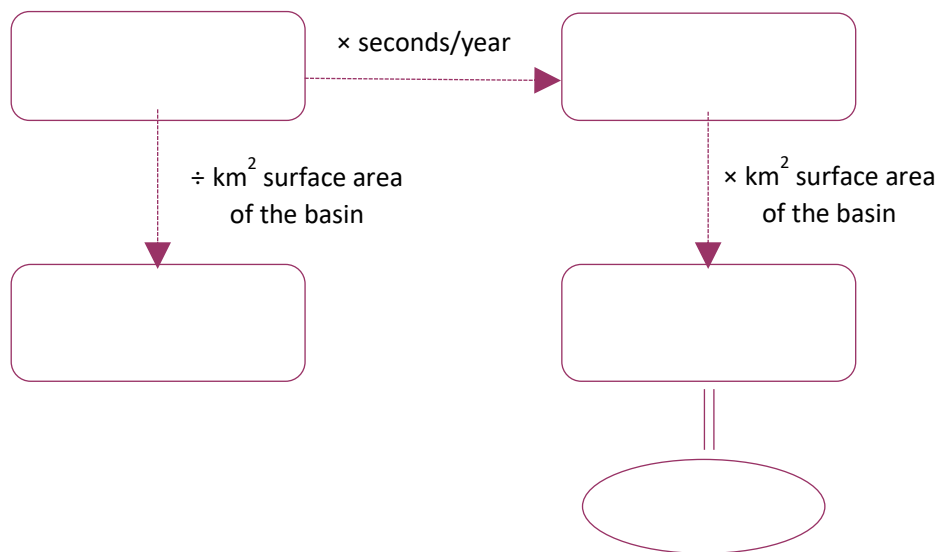
Source: own elaboration; adapted from Sánchez (2017)

Now, the relative modulus of the basin generated from hydrometric station 12607 is obtained, for this purpose, it is convenient to obtain the monthly flow information, so Table 3.8 shows the monthly series of the hydrometric station under study, with which an average monthly value of 7.24 is obtained Hm³.

Thus, Equation 17 is developed, considering that special care must be taken with the change of units; in such a way that it is obtained:

$$M_r = \frac{7.24 \frac{Hm3}{mes}}{299.20 \ km2}$$

$$M_r = 9.34 \frac{l}{s \cdot km2}$$

Thus, the relative modulus is within the range of average values, which does not indicate the scarcity of water or the contribution to the basin from any other external source, which shows that the hydrometric station has not been altered and can be used without problem to be modelled.

Summary of results. Validation of hydrometric stations

Table 7.27 shows the summary results of the consistency tests and basin parameters with respect to the hydrometric series applied to hydrometric station 12607. As can be seen, the station is not persistent, however, it is convenient to remember that this is not an impediment to continue using the station. With respect to the values obtained for the runoff coefficient (parameter K) and the relative modulus, they are within the recommended ranges, since $Ce < 1$ y $5 < M_r < 15$.

Table 7.27 Consistency test results for weather stations 12607

Test	Meteorological Station 12607
Sequences	Homogeneous
Helmert	Homogeneous
Anderson limits	Non Persistent
Ce & K	0.3149
M_r ($l/s \bullet km^2$)	9.34

Source: own elaboration

7.6 Conclusions

The development of this work allowed us to generate a methodology for the treatment of precipitation series and average flows from meteorological and hydrometric stations, as well as to provide reliability to the data so that they can provide certainty in their application for modeling purposes or other objectives.

This work allowed the analysis of a set of tests to evaluate the consistency of precipitation and mean flow series. Although the suggested tests are already existing methods, this work shows a clear procedure for the evaluation of the properties that characterize each type of series, such as homogeneity and independence.

The methodology provides a set of established criteria that allow the selection of the best meteorological and hydrometric stations. The current literature does not reflect criteria that show an established procedure to make such selection, therefore, in this work a complete process has been presented to execute this selection of stations considering specific aspects of each series and compare it with the rest; in this way and through the weighting of such criteria, it was possible to assign a numerical value to each station, compare it with other stations and determine which of the available stations are the best.

Within the framework of the methodology, the procedure for generating monthly and annual precipitation data when there are gaps was also proposed, and the corresponding procedure for generating annual average flow data when there are gaps was also proposed. Criteria were established to consider a data as null, a valuable criterion as a starting point in the treatment of data with an understanding of risk.

There is a complementary contribution to the methodology, and that is the deduction of missing data necessary to complete some gaps identified in the generation. Although data deduction methodologies exist, this work proposes criteria, and based on this proposal, it is possible to be risky or conservative in the deduction of missing data.

7.7 Acknowledgments

7.8 References

Anderson, R. (1941). Distribution of the Serial Correlation Coefficient. The Annals of Mathematical Statistics.

Aparicio Mijares, Francisco J. (1989). Fundamentos de Hidrología Superficial. Ed. Limusa. México D.F.

Campos Aranda, D. F. (1998). Procesos del Ciclo Hidrológico. México: Editorial Universitaria Potosina.

Campos Aranda, D. F. (2007). Estimación y Aprovechamiento del Escurrimiento. México: UNAM.

Cao, L. J., & Yan, Z. W. (2012). Progress in research on homogenization of climate data. Advances in Climate Change Research, 3, 59-67.

Costa, A. C., & Soares, A. (2006). Identification in inhomogeneities in precipitation time series using SUR models and the Ellipse test (pp. 419-428). In: Proceedings of Accuracy 2006. Caetano, M., & Painho, M. (eds.). 7th International Syposium on Spatial Accuracy Assessment in Natural Resources and Environmental Sciences. Instituto Geográfico Portugués. Lisbon.

Chow, V., Maidment, D. R., y Mays, L. (1994). Hidrología aplicada. Colombia: McGraw Hill.

CICESE. (2018, febrero). Base de Datos Climatológica Nacional. CLICOM. http://clicom-mex.cicese.mx/mapa.html

CONAGUA. (2016, 31 julio). Banco Nacional de Datos de Aguas Superficiales. BANDAS. https://app.conagua.gob.mx/bandas/

Cotler Ávalos, H., Galindo Alcántar, A., González Mora, I., Pineda López, R., y Ríos Patrón, E. (2013). Cuencas hidrográficas. Fundamentos para su manejo y gestión. México: Secretaría de Medio Ambiente y Recursos Naturales.

Doorembos, J. (1976). Agro-meteotrological field stations: Vol. Irrigation and Drainage Paper No. 27. Food And Agiculture Organization of the United Nations.

Gobierno del Estado de Jalisco. (2019, 5 enero). Municipios de Jalisco. Jalisco. https://www.jalisco.gob.mx/es/jalisco/municipios

Guajardo-Panes, R. A., Granados-Ramírez, G. R., Sánchez-Cohen, I., Díaz-Padilla, G., & Barbosa-Moreno, F. (2017). Validación espacial de datos climatológicos y pruebas de homogeneidad: Caso Veracruz, México. Tecnologia y Ciencias Del Agua, 8(5), 157–177. https://doi.org/10.24850/j-tyca-2017-05-11

IIEG. Instituto de Información Estadística y Geográfica de Jalisco (IIEG) (2020). Principales Ríos y Cuerpos de Agua en el Estado de Jalisco. Instituto de Información Estadística y Geográfica de Jalisco. https://iieg.gob.mx/ns/wp-content/uploads/2020/04/RIOS.pdf

Lugo Arias, F. T. (2014). Agua y Reservas Hidrológicas. Jalisco, México: Programa Sectorial.

Martínez P.E., Martínez P., & Castaño S. (2006). Fundamentos de Hidrogeología. Ed. Mundi-Prensa, México D.F.

Mather, J.R. 1975: Estimation of areal average precipitation using different network densities and averaging techniques. Publication in Climatology, vol. XXVIII, No. 2, C.W. Thornthwaite Associates, Laboratory of Climatology, Elmer, New Jersey

Mejía, J., Vega Méndez, F., Man Eddin Abou Asaad, S., & Mora, E. (2019). Hidrogeografía de una cuenca de usos múltiples ubicada en la cordillera de la Costa Venezuela. Cuadernos de Geografía: Revista Colombiana de Geografía, 30(1), 217-238.

Merlos Villegas, F., Sánchez Quispe, S. T., y Almanza Campos, J. A. (2014). Creación de un Sistema de Información Hidrológico para el Cálculo de Intensidades Máximas y Gestión de Datos Meteorológicos. Jalisco, México: XXIII Congreso Nacional de Hidráulica.

Salas, J. D., Delleur, J. W., Yevjevich, V., y Lane, W. L. (1980). Applied Modeling of Hydrologic Time Series. Colorado: Water Resources Publications.

Sánchez San Román, F. (2017). Hidrología Superficial y Subterránea. España: Createspace Independent Pub.

Salvador-González, M. C., Canul-Reich, J., & Corona-Ferreira, A. (2018). Análisis del Dataset de CLICOM de precipitaciones del Estado de Tabasco, México. IV Conferencia Internacional en Ciencias Computacionales e Informática.

Sandoval Erazo, W., y Aguilera Ortiz, E. (2014). Determinación de Caudales en cuencas con poca información Hidrológica. Ciencia UNEMI, 100 - 110.

Siegel, S. & TRILLAS, EDITORIAL. (2015). Estadistica No Parametrica (4.a ed.). Trillas.

Solera Solera, A., y Andreu Álvarez, J. (2003). Herramientas y métodos para la ayuda a la decisión en la gestión sistemática de recursos hídricos. Aplicación a las cuencas de los ríos Tajo y Júcar. Valencia, España: Universidad Politécnica de Valencia.

Walker, S. (2000). The value of hydrometric information in water resources management and flood control. Meteorological Applications, 7(4), 387–397. https://doi.org/10.1017/S1350482700001626

World Meteorological Organization (WMO). (1966). Climate change (N.o 79). Secretariat of the WMO.

Chapter 8 Comparative study of inorganic pollutant (Chromo) in a surface body water in frontera, Centla, Tabasco

Capítulo 8 Estudio comparativo del contaminante inorgánico (Cromo) en un cuerpo de agua superficial de frontera, Centla, Tabasco

SUAREZ-GARCÍA, Sandra Manuela†*, ZARATE, Marco Antonio, PÉREZ-DURÁN, Marco Antonio and VÁZQUEZ-AGUILAR, Clotilde

Instituto Tecnológico Superior de Centla, Academic Bodies in Formation Conservation and Preservation of Tropical Natural Resources / Technologies and Sustainable Alternative Energies, Mexico.

ID 1st Author: *Sandra Manuela, Suarez-García* / **ORC ID:** 0000-0002-8573-6409, **CVU CONACYT ID:** 565464

ID 1st Co-author: *Marco Antonio, Zarate* / **ORC ID:** 0000-0002-3977-5394, **CVU CONACYT ID:** 549508

ID 2nd Co-author: *Marco Antonio, Pérez-Durán* / **ORC ID:** 0000-0002-8267-1443, **CVU CONACYT ID:** 497892

ID 3rd Co-author: *Clotilde, Vázquez-Aguilar* / **ORC ID:** 0000-0002-5801-2114, **CVU CONACYT ID:** 549515

S. Suarez, M. Zárate, M. Pérez, C. Vázquez

* suareazgarciasandramanuela@gmail.com

Abstract

Human activity has been increasing, generating more contamination in air, soil and particularly in water, which is the reason for the following work that aims to measure the levels of heavy metal contamination such as chromium, considering other factors of the vital liquid such as pH and Total Suspended Solids (TSS); to know some characteristics of the body of water analyzed. The water body of study is a lagoon called Fonapo I in the city of Frontera, Centla, Tabasco, which has an 80% population around the lagoon, who are influencing the concentration levels of heavy metals, particularly chromium. The work consisted of two rainy season samplings in the lagoon, in September 2019 and September 2020. An increase in chromium concentration was observed in sampling number two in September 2020, with a direct relationship between chromium concentrations in 2019 and 2020, with a confidence level of 95% between both samplings. This statistically demonstrates that there are significant increases of chromium in this water body, and even though they are within the permissible limits of the NOM-001-SEMARNAT-1996 standard, this increase can lead to damage to society, which uses this water body for fish farming, likewise the pH recorded in the first and second samples are bases as indicated in the pH table, the Total Suspended Solids (TSS) in both samples are above what is indicated by the standard.

Heavy metal, Chromium, Physicochemical parameters, Water pollution, Pollutant

Resumen

La actividad humana ha ido en creciente aumento, generando así mayor contaminación de aire, suelo y en particular agua motivo por el cual se realiza el siguiente trabajo que tiene como propósito medir los niveles de contaminación del metal pesado cromo, considerando así otros factores del agua como son pH y solidos suspendidos totales, para conocer algunas características propias del cuerpo de agua analizado, el cuerpo de agua de estudio es una laguna llamada Fonapo I de la cuidad de Frontera, Centla, Tabasco la cual cuenta con un 80% de población al contorno de la laguna, quienes están influyendo en los niveles de concentración de metales pesados en particular cromo, en trabajo consistió en dos muestreos en temporadas de lluvias en la laguna, en el mes de septiembre del 2019 y septiembre 2020. Observándose incremento de la concentración de cromo en el segundo muestreo del 2020, existiendo una relación de incremento de las concentraciones del cromo del año 2019, en relación con el año 2020, con un nivel de confianza del 95% entre ambos muestreos. Lo que demuestra estadísticamente que se tienen incrementos significativos de cromo en dicho cuerpo de agua, y aun que están dentro de los límites permisibles de la norma NOM-001-SEMARNAT-1996, este incremento puede llevarnos a daños a la sociedad, que utiliza dicho cuerpo de agua para cultivos de peces, así mismo el pH registrado en el primer y segundo muestreos son bases como lo indica la tabla de pH, los sólidos suspendidos totales en ambos muestreos están por arriba de lo que indica la norma.

Metal pesado, Cromo, Parámetros fisicoquímicos, Contaminación de agua, Contaminante

8.1 Introduction

The various chromium (Cr) compounds represent a great threat to the environment and to man due to their harmful effects. Intoxications manifest themselves in renal, gastrointestinal, liver, kidney, thyroid gland and bone marrow lesions, and the body's elimination rate is very slow. Porras, A. C. (2010). Considering the above, chromium requires very detailed studies to remove it from water bodies since water is the main recipient of this pollutant and one of the main problems today is contamination by heavy metals, particularly in this project we will work with chromium, compounds or elements that normally would not be without the action of man, or by an increase or decrease in the normal concentration of already existing substances due to human activity (Ramalho, R. S. 2021). Some of the most potentially toxic chemical components are heavy metals, including As, Cu, Hg, Pb, Cr, Zn. The contribution of these metals to the hydrological cycle comes from various sources, one of them being of lithogenic or geochemical origin from minerals that, due to erosion, rainfall, among others, are dragged to the element.

Currently, the greatest concentration is of anthropogenic origin or due to human activity. Mining, industrial processes and domestic waste are an important source of contamination, which contribute metals to the air, water and soil especially. (Londoño, 2016).

In recent decades the world has been showing concern and is trying to solve the problems related to the disposal of liquid effluents from domestic, commercial and industrial use of water supply (Rincón R. D. and Sanabria G. J. 2021). The study of the presence of heavy metals in river waters and sediments is a contribution to the availability of environmental information on these rivers and will contribute to the diagnosis of each of their basins and, consequently, to facilitate decision making, especially of a governmental nature. Heavy metals constitute a serious environmental problem due to their toxicity and physiological repercussions in both humans and animals, as is the case of fish. Research on the presence of heavy metals in certain waters allows us to know the routes of contaminants and their interaction with other substances present in the water. (Contreras, et al, 2004).

The present study consists of evaluating the concentrations of chromium in the Fonapo I lagoon, located in the city of Frontera, Centla, Tabasco (closed body of water), to determine if there is the presence of heavy metals, which can affect the inhabitants of the area who fish and have ponds with fish. If heavy metals are found, measures will be taken to protect the population and avoid future consequences.

8.2 Problem Statement

It is worth mentioning that chromium is found in water bodies in soluble form, can be stable enough to be transported, precipitates rapidly and adsorbs on suspended particles and bottom sediments. It has been found to accumulate in many biotic organisms, especially in bottom-feeding fish such as catfish (Ictalujrusnebulosus), bivalves such as the oyster (Crassostreavirginica), blue mussel (Mytilusedulis) and soft-shell clam, Porras, Á. C. (2010), the aquatic fauna mentioned is mainly used for human consumption, therefore, the ingestion of these species is an effective chain of affectation to human health.

One of the main sources of heavy metal contamination, particularly chromium (Cr), is derived from domestic wastewater (Martínez, et al., 2019). The study area is surrounded by houses that generate the aforementioned water; therefore, it is observed that the inhabitants of the area fish and capture aquatic organisms, and it is also observed that there are fish hatcheries or nurseries in the area; For all of the above reasons, the study of chromium concentrations is considered important in order to propose mitigation and control strategies for the health of the population (Guzmán, et al, 2011).

8.3 Methodology

a) Description of the sampling site

The Fonhapo I lagoon is in the town of Frontera, Municipality of Centla, in the State of Tabasco, Mexico, at the following coordinates: 18° 31' 19" North (N) and 92° 38' 42" West (W) and is adjacent to the Palapa de Chilapa. The predominant climate is hot and humid with abundant rainfall in the summer, with an average annual temperature of 20.5°C (68°F). Its zip code is 86750 and its area code is 993.

Figure 8.1 Location of Fonhapo I lagoon, Frontera, Centla, Tabasco, Mexico

b) Tour of the study area

Prior to the sampling, the Fonapo I Lagoon area was visited, the type of surrounding vegetation was identified, predominantly Sword grass (Typha latifolia) and red (Haematoxylum campechianum), as well as critical points of domestic water discharges to the water body to define the specific sampling points.

It was observed in the field that there are floating cages in the area where fish and other crustaceans are cultivated, and that there are human settlements around Fonapo I lagoon that discharge domestic water into the area.

It is worth mentioning that the surveys were carried out by boat with all the corresponding safety measures.

Design and implementation of the sampling plan

Based on the NMX-AA-121/1-SCFI-2008 standard, a sampling plan was designed to collect water samples based on the criteria and the aforementioned standard and the size of the lagoon, 20 sampling points (20 water samples) were defined. Sampling was carried out on the dates mentioned in the following table.

Table 8.1 Sampling dates

First sampling	Second sampling
September 1, 2019	September 1, 2020

8.4 Collection and processing of water samples

Samples were obtained using sterile 500 ml plastic bottles, placed in a cooler and preserved with ice at 4 °C with their proper label to preserve the physical and chemical characteristics of each of the samples. It is worth mentioning that after the cooler they were placed in a refrigerator with the adjusted temperature.

For site selection, the indications established in the NMX-AA-121/1-SCFI-2008 standard were followed, considering discharge zones and an average distance of 5 meters between sampling points. Site 1 was the first sampling point.

Figure 8.2 Preservation of samples in the refrigerator

Laboratory sample procedure for chromium determination, established by the Official Standard NMX-AA-044-SCFI-2014.

- Bring the samples to room temperature.

- The sample was filtered through a 0.45 µm membrane. Using a portion of sample to rinse the filtration unit, collect the required filtrate volume. The pH was adjusted between 9.3 and 9.7 by adding 1 mL of the buffer solution plus 0.6 mL of the 5 mol/L sodium hydroxide solution per 100 mL of sample to bring the pH in the indicated range.

- For each 100 mL of sample, 0.25 mL (5 drops) of phosphoric acid was added. According to the pH of the sample, sulfuric acid was used, and the pH was adjusted to 2.0 ± 0.5 and mixed.

- Measured 100 mL of sample or a suitable aliquot according to the Cr content in the sample and brought to 100 mL with water, added 2 mL of diphenylcarbazide solution, mixed and let stand for 5 to 10 min for complete color development, after this time, read immediately.

- The wavelength was set on the spectrophotometer at 540 nm and adjusted with the reagent blank to zero absorbance using a cell of 1 cm or greater optical path length of light.

- The absorbance of the samples and reference solutions were measured.

8.5 Data analysis and interpretation

To demonstrate that there is a significant increase in the concentration of chromium in the Fonapo I lagoon, a statistical analysis was performed to compare the chromium deposits between the two years, 2020 and 2019. The following assumptions were applied:

a) The sample size is n = 20.

b) Being a small sample size, the use of the T-Student test statistic was considered.

c) Confidence interval of 95%, and a significance of $\alpha = 0.05$.

d) The difference between the 2020 data minus the 2019 data is taken.

8.6 Results

The following are the results of the sampling carried out in the months of September 2019 and September 2020 (Table 8.2) where the behavior of the concentrations of the heavy metal chromium can be observed, the determination of chromium concentration was analyzed under the NMX-AA-044-SCFI-2014 standard.

Table 8.2 Chromium concentration measurements for the September 2020 versus September 2019 sampling periods of the samples taken in the Fonapo I lagoon supported by the methodology

N	2020 Cromo mg/L (1)	2019 Cromo mg/L (2)	Diferencia
1	0.174	0.19	-0.016
2	0.135	0.046	0.089
3	0.137	0.061	0.076
4	0.245	0.06	0.185
5	0.074	0.096	-0.022
6	0.141	0.086	0.055
7	0.169	0.081	0.088
8	0.082	0.081	0.001
9	0.12	0.073	0.047
10	0.145	0.07	0.075
11	0.255	0.097	0.158
12	0.157	0.075	0.082
13	0.085	0.073	0.012
14	0.118	0.08	0.038
15	0.076	0.074	0.002
16	0.12	0.089	0.031
17	0.08	0.08	0
18	0.158	0.074	0.084
19	0.098	0.089	0.009
20	0.214	0.09	0.124

Table 8.2 shows that in the first sampling the chromium concentrations vary from 0.046 mg/L to 0.109 mg/L, on average the chromium concentrations are 0.07 mg/L. In the second sampling the lowest chromium concentration was 0.074 mg/L and the highest concentration was 0.255 mg/L. On average the chromium concentration is 0.13 mg/L. In both samplings, the concentrations of the heavy metal chromium are below what is established by NOM-001-SEMARNAT-1996, since this standard establishes a maximum permissible limit of 0.5 mg/L.

Table 8.3 Data averages

Medias Muestrales (μ)	μ
2020 Cromo mg/L (1)	0.139
2019 Cromo mg/L (2)	0.083

We proceeded to generate the null hypothesis (H0) and the alternative hypothesis (Ha), which are defined as follows.

H0: $\mu 1 = \mu 2$ or, H0: $\mu Cr\text{-}2020 - \mu Cr2019 = 0$

Ha: $\mu 1 > \mu 2$ or, Ha: $\mu Cr2020 - \mu Cr2019 > 0$

The critical value of tables (T-Student) is found, with a significance $\alpha = 0.05$ and 19 degrees of freedom. As well as the critical value of the test statistic, we found the following results

Critical value of tables = 1.729

Critical value of test = 4.393

The critical values of tables and test statistic are shown in the following graphic 8.1.

Graphic 8.1 Comparison of critical values of tables versus test statistic
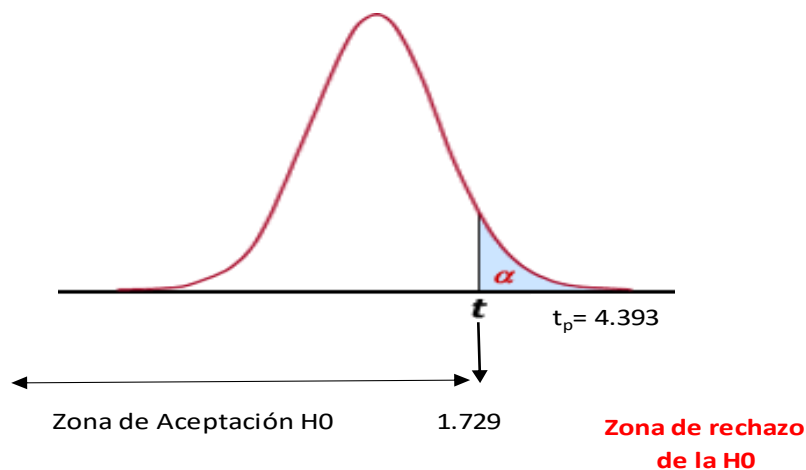
8.7 Conclusion

Based on the results obtained in the samples taken in September 2019 and September 2020, an increase in chromium concentrations from the first to the second sampling of 0.06% can be observed at a glance, indicating that the positive value is given because the test statistic is precisely to the right of the critical value of tables, which shows that the alternative hypothesis is true. This may be due to the fact that the main sources of chromium emissions are wastewater and domestic water, domestic water, agricultural use and livestock activities that are observed in the area surrounding the lagoon where the samples were taken.

The probability associated with the test statistic, p-value: yields the following result:

p-value: $0.000156 < 0.05$.

This shows that the data analyzed are statistically consistent.

According to the results shown in graph 1 and the associated probability p-value, the null hypothesis H0 must be rejected, accepting the alternative hypothesis Ha, concluding that there is a significant increase in the concentration of Chromium for the period 2020, with a significance $\alpha = 0.05$.

8.8 References

Contreras, et al, 2004; Determinación de metales pesados en aguas y sedimentos del rio Haina; ciencia y sociedad, vol.29, N°1, pag.38-71.

Guzmán, et al, 2011; Evaluación de contaminantes en agua y sedimentos del rio San Pedro en el estado de Aguascalientes, Scielo, vol.1, pag.17-32.

Londoño, et al, 2008; Los riesgos de los metales pesados en la salud humana y animal, Biotecnología en el sector agropecuario y agroindustrial, vol.2, pag.145-153.

Martínez, et al, 2019, Remediación de suelos contaminados: Fundamentos y Casos de Estudio, Ediciones EAN, 1era Edición, Bogotá, Pág. 189.

Porras, Á. C. 2010. Descripción de la nocividad del cromo proveniente de la industria curtiembre y de las posibles formas de removerlo. *Revista Ingenierías Universidad de Medellín*, *9*(17), 41-49.

Ramalho, R. S. (2021), Tratamiento de Aguas Residuales, Editorial Reverte S. A. Pág. 696.

Rincón R. D. y Sanabria G. J. 2021, Estudio Comparativo de Evaluación del Ciclo de vida de procesos tratamiento de aguas residuales de una industria textil en Medellín. UNIVERSIDAD CATÓLICA DE COLOMBIA. Tesis 101 Pág.

PROY-NMX-AA-121/1-SCFI-2008 ANÁLISIS DE AGUA - AGUAS NATURALES EPICONTINENTALES, COSTERAS Y MARINAS.

NMX-AA-044-SCFI-2014 ANÁLISIS DE AGUA. - MEDICIÓN DE CROMO HEXAVALENTE EN AGUAS NATURALES, SALINAS, RESIDUALES Y RESIDUALES TRATADAS.

NOM-001-SEMARNAT-1996, QUE ESTABLECE LOS LIMITES MAXIMOS PERMISIBLES DE CONTAMINANTES EN LAS DESCARGAS DE AGUAS RESIDUALES EN BIENES EN AGUAS Y BIENES NACIONALES.

[Title in Times New Roman and Bold Type No. 14 in English and Spanish]

Last Name (IN CAPITAL LETTERS), First Name of 1st Author†*, Last Name (IN CAPITAL LETTERS), First Name of 1st Co-Author, Last Name (IN CAPITAL LETTERS), First Name of 2nd Co-Author and Last Name (IN CAPITAL LETTERS), First Name of 3rd Co-Author.

Author's Institution of Affiliation including dependency (in Times New Roman No.10 and Italics)

International Identification of Science - Technology and Innovation

1st Author ID: (ORC ID - Researcher ID Thomson, arXiv Author ID - PubMed Author ID - Open ID) and CVU 1st Author: (Scholar-PNPC or SNI-CONACYT) (No.10 Times New Roman)

1st Co-author ID: (ORC ID - Researcher ID Thomson, arXiv Author ID - PubMed Author ID - Open ID) and CVU 1st Co-author: (Grantee-PNPC or SNI-CONACYT) (No.10 Times New Roman)

2nd Co-author ID: (ORC ID - Researcher ID Thomson, arXiv Author ID - PubMed Author ID - Open ID) and CVU 2nd Co-author: (Scholar-PNPC or SNI-CONACYT) (No.10 Times New Roman)

3rd Co-author ID: (ORC ID - Researcher ID Thomson, arXiv Author ID - PubMed Author ID - Open ID) and CVU 3rd Co-author: (Grantee-PNPC or SNI-CONACYT) (No.10 Times New Roman)

Instructions for Scientific, Technological and Innovation Publication

Abstract

Text written in Times New Roman No.12, single spaced, in English.

Indicate (3-5) keywords in Times New Roman and Bold No.12.

1 Introduction

Text written in Times New Roman No.12, single spaced.

Explanation of the topic in general and explain why it is important.

What is its added value with respect to other techniques?

Focus clearly on each of its characteristics.

Clearly explain the problem to be solved and the central hypothesis.

Explanation of the sections of the Chapter.

Development of Sections and Sections of the Chapter with subsequent numbering.

[Title in Times New Roman No.12, single space and Bold].

Development of Chapters in Times New Roman No.12, single space.

Inclusion of Graphs, Figures and Tables-Editables

In the content of the Chapter, all graphs, tables and figures must be editable in formats that allow modifying size, type and number of letters, for editing purposes, these must be in high quality, not pixelated and must be noticeable even if the image is reduced to scale.

[Indicating the title in the upper part with Times New Roman No.12 and Bold, indicating the font in the lower part centered with Times New Roman No. 10].
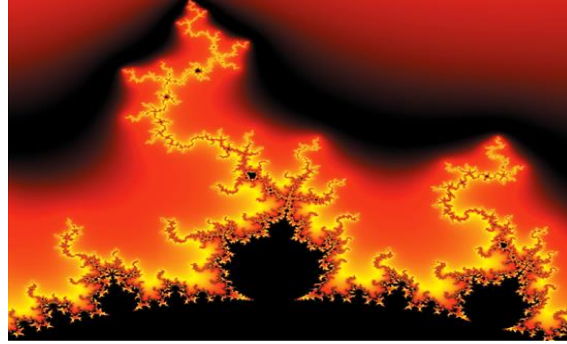
Table 1.1 Title

Variable	Description	Value
P_1	Partition 1	481.00
P_2	Partition 2	487.00
P_3	Partition 3	484.00
P_4	Partition 4	483.50
P_5	Partition 5	484.00
P_6	Partition 6	490.79
P_7	Partition 7	491.61

Source:

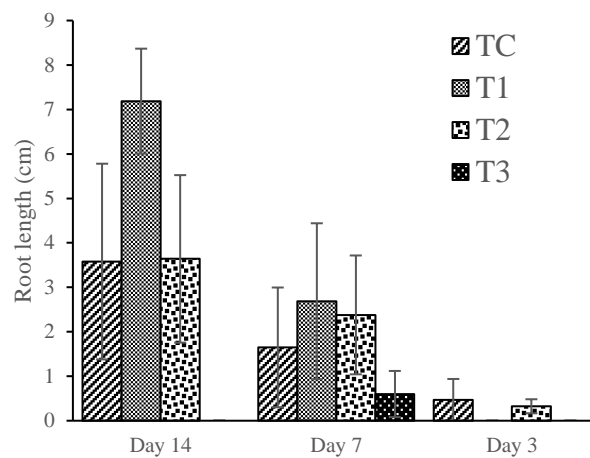(They should not be images, everything should be editable)

Figure 1.1 Title

Source:

(They should not be images, everything should be editable)

Graphic 1.1 Title

Source:

(They should not be images, everything should be editable)

Each Chapter should be presented separately in **3 Folders:** a) Figures, b) Graphs and c) Tables in .JPG format, indicating the number in Bold and the sequential Title.

For the use of Equations, indicate as follows:

$$\int_{lim^{-1}}^{lim^1} = \int \frac{lim^1}{lim^{-1}} = \left[\frac{1\,(-1)}{lim}\right]^2 = \frac{(0)^2}{lim} = \sqrt{lim} = 0 = 0 \rightarrow \propto \tag{1}$$

They should be editable and with numbering aligned on the far right.

Methodology to be developed

Give the meaning of the variables in linear wording and it is important to compare the criteria used.

Results

The results should be per section of the Chapter.

Annexes

Tables and appropriate sources.

Acknowledgements

Indicate if they were financed by any Institution, University or Company.

Conclusions

Clearly explain the results obtained and the possibilities for improvement.

References

Use the APA system. They should not be numbered or bulleted, however, if numbering is necessary, it will be because there is a reference or mention in some part of the Chapter.

Technical Data Sheet

Each Chapter should be presented in a Word document (.docx):

Name of the Handbook
Title of the Chapter
Abstract
Keywords
Sections of the Chapter, e.g:

1.   *Introduction*
2.   *Description of the method*
3.   *Analysis based on demand curve regression*
4.   *Results*
5.   *Acknowledgement*
6.   *Conclusions*
7.   *References*

Name of Author(s)
Correspondence E-mail to Author
References

Intellectual Property Requirements for its edition:

- Author's and co-authors' autographic signature in blue colour of the <u>originality form</u>.

- Author's and co-authors' autgraphic signature in blue colour of the author and co-authors' <u>acceptance form</u>.

Reservation to the Editorial Policy

ECORFAN Handbooks reserves the right to make any editorial changes required to bring the Scientific Work into compliance with the ECORFAN Handbooks Editorial Policy. Once the Scientific Work has been accepted in its final version, ECORFAN Handbooks will send the author the proofs for review. ECORFAN® will only accept the correction of errata and errors or omissions arising from the editing process of the journal, reserving in its entirety the rights of authorship and dissemination of content. Deletions, substitutions or additions that alter the formation of the Scientific Work will not be accepted.

Code of Ethics - Good Practices and Statement of Solution to Editorial Conflicts

Declaration of Originality and unpublished character of the Scientific Work, of Authorship, on the obtaining of data and interpretation of results, Acknowledgements, Conflict of interests, Assignment of rights and distribution.

The Management of ECORFAN-Mexico, S.C. claims to the Authors of the Scientific Work that its content must be original, unpublished and of Scientific, Technological and Innovation content in order to submit it for evaluation.

The Authors signing the Scientific Work must be the same who have contributed to its conception, realization and development, as well as to the obtaining of the data, the interpretation of the results, its writing and revision. The Corresponding Author of the proposed Scientific Work should fill in the following form.

Title of the Scientific Work:

- The submission of a Scientific Paper to ECORFAN Handbooks implies the author's commitment not to submit it simultaneously to the consideration of other serial publications. To do so, he/she must complete the Originality Form for his/her Scientific Paper, unless it is rejected by the Referee Committee, it may be withdrawn.

- None of the data presented in this Scientific Work has been plagiarized or invented. The original data are clearly distinguishable from those already published. And we are aware of the PLAGSCAN test, if a positive plagiarism level is detected, we will not proceed to refereeing.

- The references on which the information contained in the Scientific Work is based are cited, as well as theories and data from other previously published Scientific Works.

- The authors sign the Authorization Form for their Scientific Work to be disseminated by the means that ECORFAN-Mexico, S.C. in its Holding Mexico considers pertinent for the dissemination and diffusion of their Scientific Work, ceding their Scientific Work Rights.

- Consent has been obtained from those who have provided unpublished data obtained through verbal or written communication, and such communication and authorship are properly identified.

- The Author and Co-Authors signing this work have participated in its planning, design and execution, as well as in the interpretation of the results. Likewise, they critically reviewed the work, approved its final version and agree with its publication.

- No signature responsible for the work has been omitted and the criteria for Scientific Authorship have been met.

- The results of this Scientific Work have been interpreted objectively. Any results contrary to the views of the signatories are stated and discussed in the Scientific Work

Copyright and Access

Title of the Scientific Work:

Name and surname(s) of Contact Author and Co-authors	Signature
1.	
2.	
3.	
4.	

Principles of Ethics and Editorial Conflict Resolution Statement

Editor's Responsibilities

The Editor undertakes to guarantee the confidentiality of the evaluation process, and may not reveal the identity of the Authors to the Referees, nor may he/she reveal the identity of the Referees at any time.

The Editor assumes the responsibility of duly informing the Author of the stage of the editorial process in which the submitted text is, as well as of the resolutions of the Double Blind Arbitration.

The Editor must evaluate manuscripts and their intellectual content without distinction of race, gender, sexual orientation, religious beliefs, ethnic origin, nationality, or political philosophy of the Authors.

The Editor and its editorial staff of ECORFAN® Holdings will not disclose any information about the submitted Scientific Work to anyone other than the corresponding Author.

The Editor must make fair and impartial decisions and ensure a fair peer review process.

Responsibilities of the Editorial Board

The description of the peer review process is made known by the Editorial Board so that the Authors are aware of the evaluation criteria and will always be ready to justify any controversy in the evaluation process. In case of Plagiarism Detection to the Scientific Work, the Committee notifies the Authors for Violation of the Right of Scientific, Technological and Innovation Authorship.

Responsibilities of the Referee Committee

The Referees undertake to notify any unethical conduct on the part of the Authors and to point out any information that may be a reason to reject the publication of the Scientific Work. In addition, they must undertake to keep confidential the information related to the Scientific Work they evaluate.

Any manuscript received for refereeing must be treated as a confidential document, not to be shown or discussed with other experts, except with the permission of the Editor.

Referees should conduct themselves in an objective manner; any personal criticism of the Author is inappropriate.

Referees should express their views clearly and with valid arguments that contribute to the Scientific, Technological and Innovation achievements of the Author.

Referees should not evaluate manuscripts in which they have conflicts of interest and which have been notified to the Editor before submitting the Scientific Work for evaluation.

Responsibilities of Authors

Authors must guarantee that their Scientific Works are the product of their original work and that the data have been obtained in an ethical manner.

Authors must guarantee that they have not been previously published or that they are not being considered in another serial publication.

Authors must strictly follow the rules for the publication of Scientific Works defined by the Editorial Board.

Authors should consider that plagiarism in all its forms constitutes unethical editorial conduct and is unacceptable; consequently, any manuscript that incurs in plagiarism will be eliminated and will not be considered for publication.

Authors should cite publications that have been influential in the nature of the Scientific Work submitted for refereeing.

Information Services

Indexing - Bases and Repositories

RESEARCH GATE (Germany)
MENDELEY (Bibliographic Reference Manager)
GOOGLE SCHOLAR (Citation Indexes-Google)
REDIB (Ibero-American Network of Innovation and Scientific Knowledge- CSIC)

Editorial Services

Citation Identification and H Index
Originality and Authorization Format Management
Handbooks Testing with PLAGSCAN
Evaluation of Scientific Work
Issuance of Referee Certificate
Scientific Work Editing
Web Layout
Indexing and Repository
Publication of Scientific Work
Scientific Work Certificate
Invoicing for Publishing Services

Editorial Policy and Administration

ECORFAN®

Advertising and Sponsorship

(ECORFAN® - Mexico – Bolivia – Spain – Ecuador – Cameroon – Colombia - El Salvador – Guatemala – Nicaragua – Peru – Paraguay - Democratic Republic of The Congo - Taiwan), sponsorships@ecorfan.org

Site Licenses

03-2010-032610094200-01-For printed material, 03-2010-031613323600-01-For electronic material, 03-2010-032610105200-01-For photographic material, 03-2010-032610115700-14-For Compilation of Data, 04 -2010-031613323600-01-For its Web page, 19502-For Ibero-American and Caribbean Indexing, 20-281 HB9-For Latin American Indexing in the Social Sciences and Humanities, 671-For Indexing in Electronic Scientific Journals in Spain and Latin America, 7045008-For dissemination and publication in the Ministry of Education and Culture-Spain, 25409-For its repository in the University Library-Madrid, 16258-For its indexing in Dialnet, 20589-For Indexing in the Directory in the countries of Iberoamerica and the Caribbean, 15048-For the international registration of Congresses and Colloquia. financingprograms@ecorfan.org

Management Offices

143 - 50 Itzopan, Ecatepec de Morelos - Mexico.
21 Santa Lucia, CP-5220. Libertadores -Sucre - Bolivia.
38 Matacerquillas, CP-28411. Moralzarzal -Madrid-Spain.
18 Marcial Romero, CP-241550. Avenue, Salinas I - Santa Elena-Ecuador.
1047 Avenida La Raza - Santa Ana, Cusco-Peru.
Boulevard de la Liberté, Immeuble Kassap, CP-5963.Akwa- Douala-Cameroon.
Avenida Suroeste, San Sebastian - León-Nicaragua.
31 Kinshasa 6593- Republique Démocratique du Congo.
Avenida San Quentin, R 1-17 Miralvalle - San Salvador-El Salvador.
16 kilometers, U.S. highway, Terra Alta house, D7 Mixco Zone 1-Guatemala.
105 Alberdi Rivarola Capitán, CP-2060. Luque City- Paraguay.
69 Street YongHe District, Zhongxin. Taipei-Taiwan.
43 Street # 30 -90 B. El Triunfo CP.50001. Bogotá-Colombia.